FRI-UW-8108
March 1981

FISHERIES RESEARCH INSTITUTE
College of Fisheries
University of Washington
Seattle, Washington 98195

SEDIMENT PRODUCTION FROM GRAVEL-SURFACED FOREST ROADS, CLEARWATER BASIN, WASHINGTON[1]

by

Leslie Margaret Reid

Submitted by

C. J. Cederholm and E. O. Salo

FINAL REPORT

This work was sponsored by the
Washington State Department of Natural Resources

---

[1]This report was accepted as a Master of Science thesis at the University of Washington, under the supervision of Professor Thomas Dunne, Department of Geological Sciences.

Approved

Submitted March 30, 1981

Robert L. Burgner, Director

TABLE OF CONTENTS

Page

LIST OF TABLES

LIST OF FIGURES

SEDIMENT PRODUCTION FROM GRAVEL-SURFACED FOREST ROADS, CLEARWATER BASIN, WASHINGTON

By Leslie Margaret Reid

ABSTRACT

Erosion on the surfaces of in-use gravel logging roads is a significant source of fine-grained sediment in logged basins of the Pacific Northwest. Runoff from ten road segments subjected to a variety of traffic levels was monitored during a series of storms in the central Clearwater basin of western Washington. The resulting data allowed the construction both of sediment rating curves for different road-use levels and of unit hydrographs for different road-use levels and of unit hydrographs for different road-surface types. These relationships could then be combined with a continuous rainfall record to calculate an average annual sediment yield from road segments of each use-level. Road segments used by more than 16 trucks per day are seen to contribute 130 times as much sediment as roads not subjected to truck traffic, and 1000 times as much as roads which have been abandoned. Measurements of sediment production on paved roads indicates that paving a heavily-used road will decrease the quantity of sediment reaching streams through road culverts by a factor of 240. These measurements also suggest that sediment production from backcuts is relatively insignificant if roads are in use; backcut erosion is responsible for about 0.4% of the sediment yield from a culvert on a heavily-used road.

Comparison of the calculated sediment production rates from road-surface erosion with those measured for road-related landslides shows landslides to be 2.5 to 4.1 times as important as road surface erosion in a hypothetical 10 km^2, 40% logged basin with a road density of 2.5 km/km^2 and a typical distribution of road-use intensities. Road-surface erosion in such a basin accounts for about 47 $t/km^2/yr$, while road-related landslides are responsible for 115 to 194 $t/km^2/yr$. If only sediment finer than 2 mm is considered, however, the contributions from these two sources are more nearly equal. Erosion induced by this road distribution increases sediment production rate in the basin by a factor of 3.4 to 4.9 over the average reported rate of 82 $t/km^2/yr$ for undisturbed basins in similar areas. Measurements and estimates of sediment production rates from natural sources in the Clearwater area indicate that there is an average background sediment production rate of 79 $t/km^2/yr$; the most important natural sediment sources are bank erosion and landslides.

ACKNOWLEDGMENTS

As is the case with any protracted study, this thesis reflects the efforts, ideas, and influences of many people. I would in particular like to acknowledge the enthusiastic and indispensable aid of Blake Harrison, Patricia Irle, Steven Parsons, and Robert Norris during various phases of field work; enthusiasm left remarkably undampened even in the face of a 3500 mm/yr annual precipitation. The encouragement, interest, and cooperation of Messrs. E .C. Gockerell (Olympic area manager), Benjamin Lonn (Olympic area engineer) and other staff members of the Forks office of the Washington State Department of Natural Resources has proven extremely helpful. I would in addition like to thank Dr. David Wooldridge and Messrs. A. Larson, J. Jacoby, and W. Abercrombie of the College of Forest Resources, University of Washington, for providing hydrologic data for the Clearwater area.

The Washington State Department of Natural Resources provided funding to study the effects of logging road sedimentation on the fisheries resources of the Clearwater River to the Fisheries Research Institute of the University of Washington, which in turn provided funds and logistic support for the present study under the supervision of Dr. E. O. Salo and Mr. C. J. Cederholm. Additional support was provided by a National Science Foundation three-year graduate fellowship. Manuscript preparation has been made possible by the patience and wizardry of the staff of the College of Fisheries Publications Center. Dr. Thomas Dunne, chairman of my advisory committee, and Dr. Richard Reid played important roles in making the content intelligible with their helpful critiques of the manuscript.

Gratitude is due also to Dr. Estella Leopold and Dr. Steven Porter for their suggestions and encouragement as members of my advisory committee, and to M. V. Reid and D. N. Clayton for their suggestions and encouragement as non-members of my advisory committee. Finally, I cannot fully express my indebtedness to William Dietrich, C. Jeff Cederholm, and Dr. Thomas Dunne for the extended discussions during which this research project--and my approach to the field of geomorphology--has taken form.

CHAPTER I. INTRODUCTION

Construction and use of forest roads and the logging which accompanies them affect drainage basin hydrology, slope stability, channel morphology, and many other basin characteristics. Changes in these factors in turn result in a well-documented increase in sediment yield during and after logging, but the source of the sediment is poorly understood. This thesis is directed toward the identification of sediment sources related to forest roads and the measurement of sediment production from each source.

Identification of sediment sources and measurement of sediment production rates are of importance to both the geomorphologist and the land manager. The geomorphologist is interested in landforms and the sediment transport processes which mold them. By determining sediment production rate in an undisturbed area we learn something about the rate at which the land surface is evolving, and by understanding the relative importance of different sediment sources and transport processes we learn something of their relative efficacy in shaping the land surface. In logged basins sediment production and transport are accelerated, and by determining the mechanisms for these changes, the geomorphologist increases her or his understanding of the factors controlling rates of geomorphic processes. In addition, the quantification of sediment production rates provides the basis for understanding other problems of geomorphic interest. Increased sediment production rate may profoundly affect channel morphology, but in order to understand the response of the stream channel to the changing sediment input, we must be able to quantify the sediment input.

The land manager is interested in sediment sources and production rates because of the effect of high sediment loads on other resources. In the Pacific Northwest, high rates of sediment production induced by logging have been implicated in the compromise of water quality and the decrease of anadromous fish production. Increased frequency of landslides and debris flows removes land from lumber production, necessitates costly repairs to roads and bridges, and introduces logs into streams, facilitating the formation of debris jams and sometimes aggravating floods. The land manager is concerned with minimizing any increase in sediment production. In order to do so, she or he must know the sources of sediment and their relative importance. Knowledge of the degree of dependence of the sediment production rates on their controlling variables may be used to plan methods of minimizing sediment production. The need for such measures is growing in importance as the steeper, hitherto less-accessible areas of the Pacific Northwest are being logged, as population increases in the lowlands into which these areas drain, and as the demand increases for the fish and water resources adversely affected by accelerated sediment production.

An additional problem of concern to both geomorphologist and land manager is the nature of medium- and long-term effects of changing

processes and increased sediment production rates. The information necessary to predict medium- and long-term basin responses does not yet exist, but an approach that could eventually solve the problem is the construction of a detailed sediment budget. A sediment budget is an accounting of material transfers between different conceptual or actual parts of a basin. In its most developed form such a budget would include quantifications of soil formation rates, hillslope and fluvial transport rates, rates of transfer from transport to storage, residence times for sediment within different storage units, change of character (as, for example, grain size) of the sediment, and rates of sediment discharge at different points in the basin. Ideally, process rates would be considered mechanistically, with the dependence of process rates on controlling factors and on other process rates quantified.

This thesis represents a first step toward the eventual goal of constructing sediment budgets for both undisturbed and logged basins in western Washington state. Road-related sources of sediment have here been isolated and their rates of production measured. Measurements of production rates from the most significant natural sediment sources then allow evaluation of the importance of sediment production from roads.

CHAPTER II. REVIEW OF LITERATURE

Basin Studies

The importance of roads in generating sediment has long been recognized. Qualitative observations of road-induced impacts gave way to a quantitative proof of their significance in the 1940's and 1950's. Anderson and co-workers regressed basin sediment yield from drainages in western Oregon against basin characteristics such as land use, road density, gradient, soil characteristics, and mean annual runoff. The results of such multiple regressions indicated that if 0.6% of a basin is roaded, suspended sediment yield would increase by 24% over natural conditions (Wallis and Anderson 1965). An earlier study (Anderson 1954) suggested that current logging practices could be expected to increase natural sediment yields by a factor of 4, and that 80% of the increase would be attributable to roads. A similar study of suspended sediment yields after a large storm implicated roads in the prolongation of high suspended sediment loads (Anderson 1970). Cederholm and Salo (1979) used simple regressions to test the significance of such basin characteristics as road area and clearcut area against the proportion of sediment smaller than 0.85 mm in Olympic Peninsula spawning gravels. They found that the relation between percent fine sediment and the proportion of basin area in roads is the most significant of those tested. Although such studies are important in suggesting the significance of roads in generating sediment, the results are limited by the mutual dependence of many of the variables tested: level ground has been most intensively logged, road length correlates directly with clearcut area, and soil character is partially determined by hillslope gradient. The effects of different variables thus can not be completely separated. This type of study is not designed to determine the specific sources of sediment, and thus has limited use in designing sediment control measures.

The recognition of the importance of roads, however, generated a number of studies designed to isolate their effects. These have generally taken the form of paired-basin studies, wherein sediment yields are measured at the mouths of basins undergoing different levels of impact or at the mouth of a basin before and after impact occurs. The differences in yield are then attributed to the differences in disturbance. The earliest such study was reported by Hornbeck and Reinhart (1964) in West Virginia. In this case the effects of roads were not isolated: after a 6-year calibration period four watersheds were logged using different techniques. The road-intensive logging methods were shown to generate the highest suspended sediment concentrations, and the authors suggested that roads constituted the major source of sediment.

Later studies in the western states involved several years' measurement of sediment yields after road-building and before logging. Fredriksen (1965, 1970) reported a 250-fold increase in suspended

sediment concentrations after road construction in an unlogged basin in the Oregon Cascades; immediately before the basin was clearcut 2 years later, sediment yield from the roaded basin remained twice as high as that predicted on the basis of yields from a neighboring unroaded basin. A similar study in the Oregon Coast Range (Brown and Krygier 1971; Beschta 1978) showed no significant increase in sediment yield during the year between road building and logging, but subsequent increases in sediment yields were attributed largely to road-related landslides. Sediment from roads constructed in a northern California coastal basin was monitored for 4 years before logging began (Krammes and Burns 1973; Rice et al. 1979). Suspended sediment yield during the first year after construction was four times that predicted from a control watershed; over the 4-year period the presence of roads was associated with an 80% increase in total suspended sediment yield. These measurements were complicated by the failure of a small dam immediately after roads were constructed.

The paired-basin approach has been applied to two situations in the Idaho Batholith. In one case sediment yields from three basins containing new roads were compared with sediment yields from nearby undisturbed basins (Megahan and Kidd 1972a, 1972b). During the year before logging and the following 5 years the sediment yield per unit area of road (including bearing surface, cut-bank, and fill slope) was 770 times as high as the natural rate; 71% of this increase resulted from a single landslide. Applied to a typical road density of 0.03 km^2/km^2, this rate indicates a 12-fold increase in sediment yield. In the second study, sediment yield from a basin containing a 37-year-old road was shown to be two times that predicted from undisturbed basins (Megahan 1974, 1975).

The paired-basin approach presents the same limitations as does the multiple regression approach: specific sources of sediment can not be identified, and the effects of roads can not be isolated. In four of the described studies the occurrence of landslides in either the study basin or the control greatly complicated the results of the studies. The effect of a landslide can not be isolated from that of other road-related sources, and the number and size of the basins observed in each study are insufficient to evaluate the importance of landsliding. If a landslide occurs during the study the process tends to be over-represented, while if no landslide occurs it is under-represented. The isolation of road-related sediment production from that of other sources is also difficult. To date, paired-basin studies have been designed to isolate only the immediate effects of road construction, while other effects of greater long-term significance can not be addressed. Road-related landslides, for example, may take years to develop as organic material in road fill rots (Beschta 1978) or as repeated saturation by road drainage progressively weakens slope material (Yee and Harr 1977a). In addition, much of the sediment contributed by roads may be generated by the action of traffic on road surfaces, but in the studies described, sediment production from roads is evaluated while the roads are not in

use. Thus, sediment generated by road use is not represented until logging begins, at which time it becomes indistinguishable from sediment produced by logging. Finally, because paired basin studies are expensive to carry out, results are not replicated, and too few basins are used to permit the measurement of sediment yields as a single variable is altered. Because of these limitations, the results of such studies can not be applied quantitatively to predict either sediment yields from other basins or that of the monitored basin under different levels of impact.

Landslides

In order to avoid the problems described above, many studies have been designed to determine the significance of individual erosion processes. The most evident of the road-related sediment sources in the western United States is landsliding, and Swanston and Swanson (1976) provided a discussion of its importance. Several studies have been concerned with the mechanism of slope failure on forested and clearcut slopes. Swanston (1967a, 1970) used an infinite slope model to apply the Mohr-Coulomb failure criterion to debris avalanches in southeast Alaska. He demonstrated the importance of high pore pressures in the soils there, and provided quantitative support for the contribution of tree-root strength to hillslope stability, as postulated by Croft and Adams (1950) and Bishop and Stevens (1964). Measurements of pore pressures during storms in Alaska (Swanston 1967b) and coastal Oregon (Pierson 1977) demonstrated the role of bedrock depressions in concentrating subsurface flow, thus isolating such sites as loci of potential instability. Yee and Harr (1977a) specifically addressed the significance of roads in concentrating surface drainage on slopes, suggesting that the sudden saturation of slope material at the mouths of culverts may lead to destabilization by breaking down soil aggregates (Yee and Harr 1977b).

Gonsior and Gardner (1971) applied a factor-of-safety analysis to three failure sites along logging roads in central Idaho. These analyses again demonstrated the significance of high pore pressures in initiating landslides, but in these cases road design was responsible for the high pressures. The ponding of drainage at the mouths of culverts above road fills and the compaction and weathering of the fill material led to decreased permeability and a raised water table within the fill. Decreasing root strength beneath embankments was also mentioned as a possible mechanism for landslide initiation. In Oregon, Fredriksen (1963) analyzed an isolated road failure, qualitatively associating its intiation with undercutting of road fill by misdirected road drainage.

Other studies have involved surveys of large areas to determine the relative sediment contribution of landslides in undisturbed areas, in clearcuts, and along roads. Dyrness (1967) surveyed the landslides generated by the 1964-1965 storms in the H. J. Andrews Experimental Forest

in the central Oregon Cascades. Of the failures identified, 72% were associated with roads, which covered only 1.8% of the area surveyed. The resulting rates are 31.1 slides/km^2 of road right-of-way 0.96 slides/km^2 of clearcuts, and 0.1 slides/km^2 of undisturbed forest. Of the 47 landslides identified, 12 were initiated in road fill, 5 on backcuts, 6 involved both, 8 were caused by the concentration of road drainage and 3 by culvert failure. Swanson and Dyrness (1975) continued the study over a longer period with aerial photographs and field observations. At the level of development they observed, road-related landslides were transporting sediment at 30 times the background landslide rate, while clearcuts increased the rate by a factor of 2.8; 85% of the landslides entered streams. The authors pointed out, however, that at this time the planned road network was 62.5% complete, while only 28% of the basin area had been clearcut. They further warned that extrapolation of the results would require an understanding of the attenuation of landslide frequency over time as the most unstable areas are depleted. The H. J. Andrews studies also pointed out the extreme importance of bedrock type in controlling landslide initiation: 98% of the slides emanated from the 50% of the area underlain by pyroclastic rock.

Fiksdal (1973, 1974, [no date]) provided a similar survey of landslides in tributary basins of the Clearwater basin in western Washington, the site of the present study. In one 25 km^2 basin he found that road-related landslides occurred at a rate of 13.3 events/yr over the 6-year period since development began, while natural landslides had a rate of 0.3/yr. No landslides were observed in clearcuts, and road rights-of-way accounted for 3% of the basin area. Because the natural landslides observed tended to be larger than those related to roads, road-related landsliding contributed sediment at only 5.5 times the natural rate. Of the road-related landslides, 78% were found to be sidecast failures, 17% originated on backcuts, and 5% were related to road drainage. In this study aerial photographs were used to identify both the natural landslides and those related to roads without adjusting for differences in resolution in logged and forested areas, so landslide frequencies in the two areas are not strictly comparable. In addition, the natural landslide rate was estimated by averaging the total slide volume over the age of the oldest dated landslide; the calculated natural landslide rate of 64 t/km^2-yr is thus only an estimate. Seventy percent of the road-related slides come in contact with streams, but the author estimates that only 63% of the landslide debris in contact with streams is eventually removed.

Gresswell et al. (1979) surveyed landslides triggered by a severe 1975 storm in coastal Oregon. Road-related landslides were triggered at a rate of 2.9 events/km^2 of road right-of-way, while clearcut slides occurred a 0.9 events/km^2. The researchers point out that the estimated rate of 0.04 events/km^2 for slides in undisturbed areas is likely to be low since resolution is poorer in forested areas. Landslides occurring in clearcuts averaged 2.3 times the volume of landslides on forested slopes, while road-related slides were 6.9 times larger than those on

uncut slopes. The relatively low frequency of road-related landslides was attributed to the fact that devastation resulting from an earlier storm had prompted the implementation of a series of protective measures: road standards had changed to emphasize the need for stable road beds and continued maintenance, and ditches were patrolled and kept free of debris during storms.

In an area in coastal British Columbia aerial photo surveys indicated that roads were responsible for the mobilization of 2,076 tons of landslide debris per square kilometer of clearcut over an unknown time period, while clearcuts themselves contributed only 586 t/km^2 over the same period. The production rate from natural areas was 952 t/km^2, but the ages of these landslides are also not known (O'Loughlin 1972).

Studies in Idaho also demonstrated the significance of road-related landslides. Day and Megahan (1975), reviewing damage caused by a single storm, attributed 75% of the 214 landslides identified in Clearwater National Forest to the presence of roads; of these, 32% came in contact with streams. In a separate study, Jensen and Cole (unpublished, quoted in Rice et al. 1972) reported that in the Zena Creek area 90% of the mass movements from a single storm originated on road rights-of-way. Of these, road-fill failures comprised the largest proportion, followed by failures initiated by obstructed road drainage (Megahan 1967, as quoted in Swanston 1974).

Repeated themes in most of the described studies are the importance of roads in triggering landslides, the significance of major storms, and the control exerted by bedrock in determining the location of slope failures. In no case, however, is failure frequency addressed with respect to the age of the roads. Thus data concerning long-term rates of landslide initiation from roads are not directly comparable; any valid comparison would need to consider changes in landslide frequency after roads are constructed.

Road Surface Erosion

Literature pertaining to erosion from logging in the gentler, more deeply weathered Appalachian Mountains rarely mentions landsliding as a source of sediment. Instead, surface erosion from haul roads and skid roads is most commonly addressed. Loggers in the Appalachians make frequent use of road-intensive yarding techniques such as tractor, skidder, and jammer logging, which may result in road densities of 12%, 10%, and 8%, respectively (Kochenderfer 1977; Mitchell and Trimble 1959). The qualitative recognition of the importance of road surface erosion is reported in the eastern United States (Packer 1967; Trimble and Sartz 1957; Kidd and Kochenderfer 1973; Aubertin and Patric 1974; Patric 1976), in Idaho (Haupt 1959a, 1959b, and 1965), and in Australia (Gilmour 1971). In some studies isolated measurements of erosion from road surfaces have

been made, but in no case was the total contribution from this sources calculated.

A study in the Coweeta watershed of North Carolina demonstrated an erosion rate of 339 m^3 per hectare of 17° gradient skid road over a 3-month period (Hoover 1945); revegetation of the road was expected to take 3 years. Repeated measurements of cross-sections on an access road in the same area disclosed an average loss of 0.4 m^3/m of road over a 21-month period (Lieberman and Hoover 1948). In this case no road width was reported, but examination of the accompanying photograph suggests a width of about 3 meters. The resulting erosion rate would amount to 1400 m^3/ha of road surface over 21 months. In a third study in the same area, cross-sections were measured on a 3.7-km road segment over a 4-year period (Hoover 1952). Average loss rate was 1423 m^3/road-km-yr, or approximately 4740 m^3/ha-yr if a 3-meter road width is assumed.

Similar studies have been carried out on the Fernow watershed in West Virignia. Cross-sections on skid roads of four different qualities were surveyed over a 1-year period immediately after logging ceased (Weitzman and Trimble 1952). Erosion varied from 0.048 m^3/m on the highest quality road to 0.085 m^3/m on the poorest. Skid-road widths were not reported. Trimble and Weitzman (1953) and Weitzman and Trimble (1955) later related the rate of erosion on skid roads directly to the intensity of road use. Repeated cross-sections of two heavily-used and three lightly-used skid roads disclosed an average surface lowering of 9.4 cm on heavy-use roads and 2.5 cm on light-use roads during skidding. In the 2-month period following skidding, roads that had been heavily used averaged an additional 1.9 cm of lowering, while lightly-used skid roads lost only 0.5 cm. An additional 3.0 cm and 2.5 cm of surface lowering occurred on heavily- and lightly-used skid roads, respectively, before stabilization was complete. Kidd (1963) reported measurements of rill volumes on skid roads in Idaho, but the areas of the skid roads were not reported.

Most of the reports described above focus on skid roads, which are steep, low-standard roads used briefly by tractors, jammers, or skidders and then abandoned. Such roads are not surfaced and have no counterpart in areas dominated by high-lead and skyline logging, such as are common in the Pacific Northwest. In addition, calculations of surface erosion based on cross-section measurements can not account for compaction and lateral displacement of sediment during road use. This problem was also encountered by Lund (no date) while studying gravel-surfaced haul roads in central Oregon. A multiple regression of cross-section loss against variables describing use, topography, and surfacing material showed road-use level and road gradient to be the most significant variables. The author suggested, however, that much of the elevation loss may have been due to displacement of material to the sides of the road during maintenance and use. These problems may be avoided by direct measurement of sediment in transport.

In North Carolina, Hafley (1975) traced the major sources of stream turbidity to runoff from unpaved roads and from ditches on paved roads. Sixteen isolated concentration measurements provided an average sediment concentration of 1000 mg/l at the mouths of culverts, but data were insufficient to calculate an erosion rate from this source. Wald (1975) used the same approach to estimate sediment yields from heavily-used and idle gravel-surfaced haul roads in the Clearwater basin of western Washington. The 68 measured concentrations on the heavily-used road averaged 1306 mg/l while 56 measurements from the non-used road averaged 100 mg/l. By assuming that these values reflected the annual average, that annual discharge through the road-side ditch is equal to the volume of rain falling on the road surface, and that "actual suspended sediment yield on an annual basis might be two-thirds the [calculated] value," Wald estimated a total yield of 18.4 t/road-km for heavy-use roads and 1.4 t/road-km for non-use roads for the 1973-1974 water year. Culvert discharge was not measured, however, and inspection of the road segments monitored during the the study reveals that a significant component of culvert discharge flows from backcut springs and dilutes the sediment concentration of runoff generated on the road surface.

Wooldridge (1979c) avoided the problem of dilution by using automatic pump samplers to collect water samples in a gauged stream above and below the influx of road drainage. One of the road segments produced no significant effect on sediment concentration; this road surface had been treated with pulping liquors, creating "a cemented road surface." The other monitored stream showed significant increases in suspended sediment during periods of hauling, but a sediment production rate was not calculated.

Wooldridge (1979a) used a similar approach to evaluate the impact of road construction on sediment yield. In this case, too, sediment production rates were not calculated or a net effect computed, although at some time during or after the installation of a culvert in a stream with a discharge of 0.5 l/s, 11.7 kg of sediment was washed away over a 3-hour period. Other measurements were not related to specific activities. A second study using the same format (Wooldridge 1979b) demonstrated the contribution of 3.7 tons of sediment to a 17 l/s stream during 5.5 days of site preparation and culvert installation; two of these days were on a weekend during which no construction occurred.

That logging road surfaces are significant sediment sources is largely a result of their ability to generate surface runoff. Infiltration capacities on compacted road surfaces are lower than those on both undisturbed forest floors and lightly-disturbed clearcut surfaces (see, for example, Hornbeck and Reinhart 1964; Patric and Gorman 1978). Hornbeck and Reinhart further suggested that overland flow resulting from low infiltration capacities on road surfaces may be augmented by surface runoff generated by the interception of subsurface flow in road cuts. Megahan (1972) demonstrated the importance of this phenomenon in central

Idaho: subsurface flow intercepted during snowmelt accounted for an estimated 90% of the annual runoff in roadside ditches.

Backcut Erosion

Erosion from road backcuts has long been of concern, since unvegetated backcut slopes are the most evident sediment source along roads. In Georgia, sediment trapped in sampling tanks below three erosion plots indicated erosion rates of 230 t/ha from northwest-facing cuts over a 2-year period. Similar plots on southeast slopes lost 102 t/ha (Diseker and Richardson 1962). Of the material eroded, 70% was redeposited at the base of the slopes; only 30% was carried beyond the ditch.

Sediment accumulated in troughs at the bases of ten 6- to 7-year-old backcuts in the Oregon Cascades at an average rate of 153 t per hectare of backcut (Wilson 1963). The same study also examined newly excavated backcuts: sediment loss from twelve new backcuts averaged 370 t/ha-yr. Loss rate during dry months was nearly twice that of wet months for the older backcuts, but for the new cuts the winter rate was four times that of the dry season. This difference may be a result of the fact that excavation occurred immediately before the first winter's measurements; data from the two winters unfortunately were not compiled separately. A later study in the same area demonstrated a loss rate of 0.5 cm/yr on bare 5-year-old backcuts over a 7-year period (Dyrness 1970, 1975), while unvegetated 1-year-old slopes were found to lose sediment sediment at a rate of 0.7 cm/yr over a 5-year period. Calculations were based on measurements of surface lowering.

Megahan (1980) used measurements of root exposure on backcuts of a 45-year-old road in central Idaho to determine a long-term loss rate of 1.0 cm/yr for soil and 1.1 cm/yr for the granite bedrock. The discrepancy in rates was attributed to the buttressing effect of roots on the soil.

Surface erosion of road-fill material has also been examined in central Idaho. A trough at the mouth of an unvegetated road-fill plot indicated a loss rate of about 94 t/ha over a 10.5-month period starting in late November (Bethlahmy and Kidd 1966). Megahan (1978) carried out a similar study in the same area. Trough accumulation measurements over a 3.5-year period indicated a loss rate of 12 t/ha-yr on a 12-year-old fill slope, with at least 15% to 52% of the yearly loss due to dry creep. Megahan (1974) used the results of these and other studies to construct a general exponential relation between erosion rate and time after disturbance. Leaf (1974) modified this equation to apply to total erosion induced by roads as measured at the mouths of basins.

Determinations of backcut erosion rates generally have focussed upon measurements at or near the sediment source. As Diseker and Richardson (1962) demonstrated, however, much of the eroded material

becomes redeposited before entering a stream. Megahan (1980) also addressed the problem of sediment delivery from backcut erosion, using a comparison of measured sediment production rate with measurements of basin sediment yields to demonstrate that only 5% of the material leaving the backcut is transported as far as the basin mouth. The measured backcut erosion rates thus do not reflect the rate of sediment production to streams from this source.

Effect of Roads on Hydrology

A much less obvious and rarely considered sediment source is the increased channel erosion induced by basin disturbance. Increases in average peak discharge have been demonstrated statistically to enlarge channels in urbanized areas (Leopold 1968; Hammer 1972). Madej (1978; in press) suggested that an increase in sediment load has caused channel widening and aggradation in a rural western Washington stream with a logged catchment.

The presence of roads in a basin has been demonstrated to increase peak flows in several areas. Hoover (1952) mentioned observations of storm peak flows doubled by the addition of overland flow from road surfaces in North Carolina. In West Virginia, Weitzman and Trimble (1952) also mentioned the importance of road-generated runoff in increasing peak flows and further suggested that this increase may lead to increased channel erosion.

Studies in Oregon have provided measurements of the effect of roads on peak discharges. Harr et al. (1975) reported a 20% increase in peak discharge in a Coast Range basin containing a road density of 12%, while Harr et al. (1979) found increases of up to 35% and 48% in peak discharges in two southern Oregon basins containing compacted areas of 13% and 12% of the total area. A third basin with 15% of its area compacted exhibited peak discharge increases of 11%. In another case, however, peak discharges were reported to have decreased after road construction (Rothacher 1973). Megahan (1972) mentioned the possibility that effective stream piracy caused by the interception and diversion of subsurface flows by roadcuts may lead to increased peak flows and channel erosion in some small basins. Anderson and Hobba (1959) used multiple regression techniques to associate logging and road-building with increased peak discharges in larger basins in Oregon.

Control of Sediment Production from Roads

An extensive body of literature is concerned with methods of preventing road-induced erosion. Burroughs et al. (1975) examined the factors contributing to landsliding from roads in Oregon and described methods of recognizing and avoiding unstable areas. Haupt (1959a, 1959b), Trimble and Sartz (1957), Packer (1967), and Hafley (1975)

discussed the effectiveness of vegetated filter zones below culvert outlets in preventing sediment generated from road surfaces and backcuts from reaching streams. Prevention of erosion on road surfaces and skid roads was addressed by Kidd (1963) and Trimble and Weitzman (1953), each of whom advocated diversion of surface flow off roads at intervals decreasing with increasing road gradient.

Backcut and fill-slope erosion rates have been shown to be decreased significantly by planting and mulching new cuts (Bethlahmy and Kidd 1966; Dyrness 1970, 1975; Megahan 1978). Other recommendations can be found in many of the papers already cited, and are reviewed by Larse (1971).

Comparisons of Sediment Production Rates in Disturbed Areas

As yet few syntheses of sediment contribution from different logging-related sources exist. Models based on multiple regressions provide information on the relative importance of broad categories of sources such as roads and cultivated land (see papers by Anderson), but provide no information on the actual sediment production processes. At the other extreme, although many studies examine the relative importance of various types of landslides, rarely are such compilations compared with sediment production rates from other sources. Dissmeyer (1973, 1976) took a different approach, using a combination of the Universal Soil Loss Equation (Wischmeier and Smith 1965) and the Musgrave formula to calculate surface erosion rates from different kinds of logging-related sources in forests of the southeastern United States.

Effects of Sediment on Fisheries Resources

Concern over increasing stream sediment loads in the Pacific Northwest is generated largely by concern over their impact on fisheries resources. Support for this association is growing (see Gibbons and Salo 1973, for review of relevant literature). High suspended sediment loads have been shown to cause physiological damage to salmonids (see, for example, Noggle 1978) while lower concentrations may both impair feeding efficiency by decreasing visibility (Noggle 1978) and decrease the population of fauna upon which the salmonids prey (Cordone and Kelly 1961), thus decreasing the fitness of the fish. The tolerance of salmonids to high suspended sediment concentrations has been demonstrated to have strong seasonal dependence. During summer the LC50 (concentration causing 50% mortality in a 24-hr period) for coho salmon smolts was found to 1500 mg/l, while during the winter season the LC50 rose to more than 30,000 mg/l (Noggle 1978).

Fine-grained sediment is also detrimental to salmonids when entrained in spawning gravels. Decreased permeability of the spawning substrate may cause egg mortality by restricting the supply of oxygen to the eggs, and once eggs hatch the restricted pore space allows only the

smallest, least fit fry to escape from the gravel (Koski 1975). Experiments in both laboratory and field settings have demonstrated strong relationships between decreasing percentage of eggs surviving to emergence and increasing proportion of fine sediment in spawning gravels (see, for example, Koski 1975; Tagart 1976).

Other studies have related the grain size distribution of stream gravels to basin characteristics. Cederholm et al. (in press) demonstrated a strong relation between the percentage of basin area occupied by roads and the proportion of fine material in spawning gravels in western Washington. In Alaska, Shapley et al. (1965) demonstrated significant increases in fine sediment in spawning gravels after the addition of suspended sediment to the stream.

Sediment Production in Undisturbed Basins

In order to determine the significance of sediment production from roads it is necessary to compare it to natural sediment production rates. The understanding of the relative importance of various sediment sources is more strongly developed with respect to sediment production in undisturbed basins than it is for those undergoing disturbance. A pioneering study by Leopold et al. (1966) set out the framework of a sediment budget: rates of sediment production were measured and compared with rates of channel aggradation and transport in a semi-arid basin in New Mexico. Since then the approach has also been applied to forested basins. Dietrich and Dunne (1978), working in coastal Oregon, constructed a sediment budget based on a balance of bedrock weathering rate, estimated creep rate, and fluvial sediment transport rates. The authors also outlined the process interactions which must be considered in the construction of a more detailed budget. Sediment production rates were considered in more detail by Swanson et al. (in press) in a sediment budget for a small watershed in the Oregon Cascades. Here, long-term measurements of sediment yield, dissolved load, and rates of slope transport processes allowed an accounting of the contributions of the major hillslope transport processes. In coastal California, Lehre (in press) used a comprehensive monitoring program to quantify sediment transport rates and construct a sediment budget.

Necessary considerations in the construction of sediment budgets were outlined by Dietrich et al. (in press), who discussed the necessity of conducting preliminary studies to identify the significant processes, of determining the nature of process interactions, of defining the recurrence intervals for the various processes and measuring process rates over a time frame appropriate for those intervals, and of quantifying rates of material exchange between transport media and storage elements.

Efforts to quantify sediment yield from undisturbed basins have been widely undertaken and are summarized in the final chapter of this report. Individual transport and sediment production processes have

also been widely studied in natural settings. Most of the landslide surveys already cited include data on natural landslide frequencies, and almost all of the referenced studies of surface erosion state that overland flow does not occur in the observed undisturbed forests. Measurements of sediment accumulation in troughs indicated that other forms of surface transport such as dry ravel and needle ice growth account for the contribution of 0.5 t/yr of sediment to a stream draining a 10.2 ha watershed in the Oregon Cascades (Swanson et al., in press).

Imeson (1976) and Imeson and Kwaad (1976) reported that animal burrowing activity and rainsplash transport on the resulting mounds are a major mechanism for hillslope sediment transport in a Luxembourg forest. The two processes together were calculated to provide 1.5 t/km^2-yr of sediment to streams. Thorn (1978) working in an alpine environment in the Colorado Front Range, calculated that pocket gophers are responsible for displacing 3.9 to 5.8 t/ha in favorable habitats. Yair (1974) also mentioned the importance of burrowing animals in making sediment available for transport in arid areas, while Price (1971) described their importance in an arctic environment. None of the studies, however, accounted for the direction of subsurface transport as the burrows are being excavated.

The process of treethrow is also widely recognized. Denny and Goodlett (1956) provided data which permit the calculation of a transport rate of 0.14 cm^3/cm^2-yr from treethrow in a Pennsylvania forest, while Kotarba (1970) calculated the soil transport caused by treethrow during a single windstorm in the Polish Tatra Mountains. In the Oregon Cascades, Swanson et al. (in press) calculated a sediment production rate of 0.1 t/yr from treethrow in a 10.2 ha watershed but do not express the result as a transport rate.

Bank erosion on low-order streams, on the other hand, has rarely been addressed. Imeson and Jungerius (1977) described the importance of bank erosion in an undisturbed Luxembourg catchment but presented no estimate of erosion rate. Carson et al. (1973) suggested that bank scour is the most important source of sediment in an 86 km^2 eastern Canadian catchment. They estimated that this process contributes 2 to 21 tons of sediment per kilometer of low-order stream during the snowmelt period, which is expected to account for 80% of the year's sediment transport. Swanson et al. (in press) approached this process implicitly by applying a measured soil creep rate to the channel perimeter of their 10.2 ha basin to calculate a sediment contribution of 1.1 t/yr by "creep."

In the only detailed compilation of actual field measurements available for forested catchments in the Pacific Northwest, Swanson et al. (in press) combined the measurements already described with an estimated annual production rate for debris avalanches of 6 t/10.2 ha-yr, based on surveys of debris flows in nearby basins, to compute a total production rate of 7.7 t/yr for the 10.2 ha basin. An additional 3 t/yr is lost in solution.

CHAPTER III. APPROACH AND QUALITATIVE ANALYSIS

This study addresses the quantification of logging-enhanced sediment production by isolating specific types of road-related sediment sources and measuring the sediment production rate from each. The dependence of sediment production rate upon external variables can also be measured using this approach if rates are measured under a variety of conditions. In order to do so, measurement sites are not limited to the confines of a single basin but are located in several parts of the Clearwater drainage. Similarly, measurements either must explicitly define the dependence of process rates upon the magnitude of hydrologic events or must represent an average rate over a long enough period of time that the effect of individual storms is not disproportionately large. Measurement techniques include mapping of landslides and other areally discrete sources both in the field and on aerial photographs, and long-term monitoring of more diffuse sources such as backcut erosion.

The measurements of sediment production rates resulting from this study can be combined according to the distribution of the sediment sources to predict sediment yields from roads in the basins studied. Sediment source distribution in other basins may be predicted on the basis of observed dependencies of process rates upon such factors as stream order, hillslope gradient, and the length, location and use intensity of roads. By determining the distribution of these kinds of variables in a basin with bedrock, climate, vegetation, and soils similar to those of the basins studied, the sediment production rate from each source can be adjusted to fit the conditions in the basin and sediment yield can be estimated for that specific basin. This kind of estimate may also be made to evaluate the effects of different management plans on sediment production in a single basin.

In order to understand the relevance of the processes considered in this study and the methods used in their analysis it is first necessary to understand both the nature of the processes themselves and the extent of their interactions. The rest of this chapter is thus devoted to a discussion of the creation and transport of sediment and of the processes which introduce it into streams. As used in this report, sediment production refers to the transfer of material from hillslope to stream.

Sediment Transport and Production in Undisturbed Basins

In order to plan an effective measurement program to evaluate sediment production in a basin, it is first necessary to identify the sources that contribute sediment to streams and to understand their relationship to the hillslope transport processes supplying them and the fluvial processes carrying sediment from them. This step is critical to the selection of effective measurement locations and techniques; it also ensures

that processes acting in series are not treated as though they were acting in parallel. In other words, an understanding of process interactions helps prevent the inadvertent consideration of the same sediment more than once in a sediment budget.

Sediment originates by the chemical weathering and mechanical breakdown of bedrock (see Fig. 1). Groundwater percolating through cracks in the rock dissolves minerals and brings reactive ions into contact with fresh mineral faces, where oxidation, hydrolysis, carbonation and other weathering reactions can proceed. Weathering-induced changes in mineral composition may result in more soluble minerals which can then be removed by the percolating waters, or may change the specific gravity of the material present, propagating cracks and increasing its accessibility to the water. If removal of material in solution proceeds without mechanical disturbance, the more inert or less-weathered residual is left as saprolite, a soil-like material still preserving primary bedrock structure. Solution and weathering of the sediment continues during every subsequent phase of transport and storage.

Mechanical breakdown of fresh bedrock may occur by endogenic processes such as pressure-release expansion when overburden is removed; often, tectonically induced jointing is already present in the rock. If the soil thickness is not too great, exogenic processes like frost riving and prying by root growth may be effective in breaking apart the rock. Saprolite is more easily disturbed; most processes active in hillslope sediment transport may at times extend deeply enough to disrupt saprolite. The mechanical incorporation of saprolite and weathered bedrock into the soil layer has been termed "mixing" (Dietrich and Dunne 1978). Weathering and mixing occur at all points along a hillslope.

Once disrupted, saprolite becomes soil, and if it is located on a hill it becomes subject to a host of processes which transport it downslope. Such processes fall into three major categories. Surface transport is localized on the soil surface and includes processes such as rain splash, treading by animals, overland flow, needle ice growth, dry ravel, and wind transport. A second category has generally been termed creep, and includes transport by plastic flow (if material is not shearing along a definable surface), expansion and contraction by wetting and drying and by freezing and thawing, and biogenically-induced processes such as infill of root holes, transmission of wind stress by trees, and activities of soil organisms. These processes all involve transport of soil to some depth, but although the transport rate generally decreases with depth, there is no well-defined surface of differential transport; strain is distributed through the soil profile. In these cases transport occurs incrementally in space. The third category is that of spatially discontinuous transport processes such as landslides, treethrow, and animal excavations. In each case there is a well-defined surface between material moved and that left in place, and material is displaced a finite distance. The motivation for categorizing slope transport

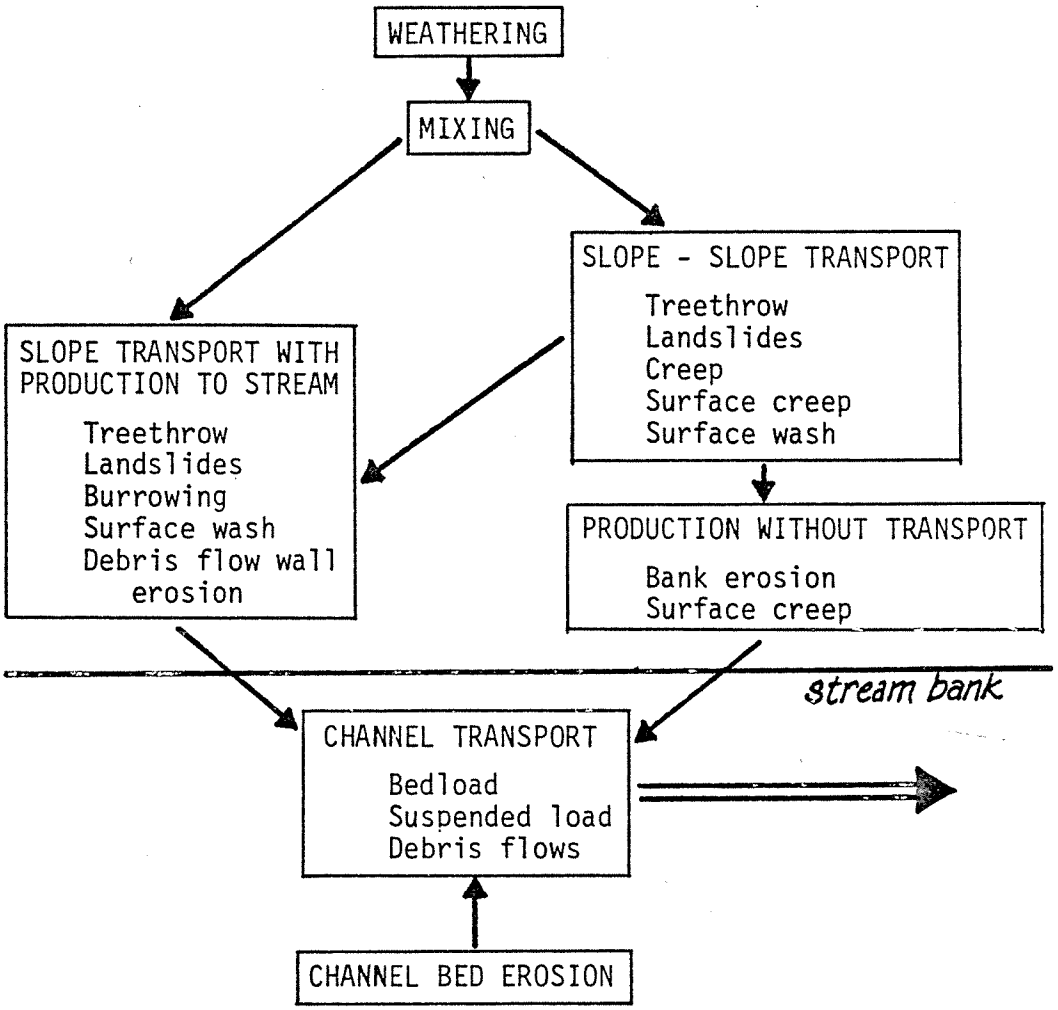

Figure 1. Flowchart of sediment transport and production in undisturbed basins.

processes in this manner is that each category requires a different measurement technique for the analysis of process rates.

Sediment is displaced downslope by one process after another until it is moved close enough to the stream that a final transport episode transfers it from hillslope to stream channel. This final step may involve additional hillslope transport in the case of spatially discontinuous processes such as treethrow, landslides, animal excavations and valley-wall erosion generated by debris flows, or may be a final incremental displacement in the case of erosion of stream banks supplied by creep processes. The material transferred to the stream may include saprolite or weathered rock which has not previously been involved in hillslope transport, such as would be produced by channel erosion. As mentioned above, weathering continues as the sediment is transported downslope. The longer the residence time is of the soil on the slope, the finer the soil texture and the higher the clay content will be by the time the sediment reaches the stream.

Once contributed to the stream system, sediment is transported by an entirely different set of processes whose effectiveness depends largely on the grain-size distribution of the sediment and the discharge of the stream. Fine-grained sediment is transported in suspension, moving through the stream system at nearly the velocity of the water unless it is either deposited in low-velocity ponds and eddies or filtered from water passing through the gravel substrate. Coarse sediment can not be suspended, but moves by traction on the stream bed and is referred to as bedload. Still coarser material must remain in place until reduced in size by further weathering or mechanical breakdown. In steep, low-order channels, an additional form of channel transport is the debris flow: a landslide entering a channel may initiate failure of channel deposits, and the whole mass will move down the valley as a flow competent enough to transport sediment of virtually any size available.

Whether a particular grain size in a stream will move in suspension or as bedload is determined by the tractive force at the base of the flow, which is in turn determined by the depth, slope, and velocity of the flow. Thus material moving as bedload in a first-order stream may be thrown into suspension upon entry into a higher-order stream or during a rise in stream discharge during a storm.

The sediment itself changes character during transport. Gravels are abraded and fractured during motion, and further chemical weathering while the particles are in long-term storage in floodplains may reduce pebbles to fine sediment. These changes in grain-size distribution also affect the relative importance of suspended load and bedload in different stream orders.

The present study is limited to the measurement of the rate of transfer of material from hillslope to stream system; "sediment production" here refers to this transfer, and sediment "sources" are those

which involve the direct transfer of material from slope to stream. This particular step was selected for measurement because 1) most sediment eventually leaving the basin crosses this boundary at some time; 2) it involves material transfer across a definable, recognizable boundary, the stream bank; 3) many of the processes involved in the transfer are easily observed; and 4) increase in transfer rate is evident in logged areas and is of concern to land managers. In many cases stream banks represent a boundary not between hillslope and stream, but between the stream and elements of long-term fluvial storage such as debris fans or floodplains. In such cases transfer across the boundary is not considered; the sediment has entered the stream at some time in the past and so has already been included in other measurements of sediment production rates.

The assumption that the transfer rate of material from storage can be ignored implies that the basin of concern is in an equilibrium state with respect to sediment production, transport, and storage. In other words, there is not net gain of sediment from storage and no net loss of sediment to storage. Over a long period of time there are of course shifts in process rates as basin relief and channel slopes decline, and over a short period the occurrence of storms temporarily shifts the balance between sediment production, transport, and storage. Over a time period that averages out the effects of high-intensity storms, however, this assumption must be approximately valid or else the basin would exhibit extensive fluvial deposits, implying net long-term aggradation.

In the Clearwater basin, however, though modest floodplains can be found on most streams of greater than third order and fans are common at the mouths of first- through third-order basins, bedrock channel segments are present along streams of every order. If the equilibrium assumption is valid, if dissolution is relatively insignificant once sediment leaves the hillslope, and if the amount of sediment contributed by channel erosion is relatively small, then the rate of sediment contribution from hillslope to stream must be approximately equal to the rate at which sediment is being removed from the basin. The measured rate of sediment production within a basin should approximately equal the measured sediment yield at the mouth of the basin.

The equilibrium assumption is also important in calculating sediment production rates. Much of the sediment contributed to streams can not be removed immediately by the stream but remains in temporary storage in the stream channel. If the average process rates have not changed over a long period of time, then the average annual rate at which sediment is being removed from these temporary storage elements must equal the average annual rate at which sediment is being added to them.

Sediment Transport and Production from Roads

Analysis of sediment production becomes far more complex in basins undergoing artificial disturbance, both because more sediment-producing processes are active and because the assumption of equilibrium possible in natural basins is not tenable as rates and processes of sediment production and transport are altered. The presence of roads in a basin locally affects weathering and mixing rates (see Fig. 2), with changes for the most part involving only the ground laid bare by excavation. Perturbations in groundwater drainage down-slope of roads may also lead to changes in local weathering rates.

Hillslope transport rates are profoundly affected by the presence of roads. Threethrow is accelerated along road rights-of-way, and landslide frequency is increased greatly both by direct physical destabilization of slopes above and below the road and by alterations in natural drainage patterns. Excavation of the road bed is also of great significance, and in many cases the excavated material is pushed over the edge of the road and left as sidecast on the slope below. Such material is then subject to accelerated surface creep by dry ravel and needle-ice activity as well as to small-scale sloughing, processes which are also active on road backcuts and on their mantling debris aprons.

During rainstorms the presence of roads increases the drainage density of a basin by the length of road in that basin. Not only does this increased drainage density increase the amount of sediment delivered by such processes as bank erosion, in this case on roadcuts, but it also permits the activity of an erosional process not significant in undisturbed basins. Overland flow generated on near-impervious gravel road surfaces is capable of mobilizing and transporting large quantities of fine sediment brought to the surface by the action of traffic. Runoff generated on a road surface generally flows into a roadside ditch, whence it either enters a stream or is left to seep into a hillslope. In the latter case the sediment load becomes another component of hillslope transport, while in the former it constitutes direct production of sediment from hillslopes into streams. A proportion of the overland flow is diverted from the road surface by topography. On the slope below the road such flow may excavate rills before it either reaches a water-course or infiltrates into a slope.

Other processes of sediment production are also accelerated. Because drainage disturbances caused by the presence of roads play a large role in landslide initiation, a high proportion of the road-induced landslides are in contact with running water and thus contribute sediment directly to streams. In addition, the high incidence of debris flows associated with roads is responsible both for increasing erosion from valley walls and also for increasing the proportion of sediment introduced into stream channels by the landslides initiating the flows.

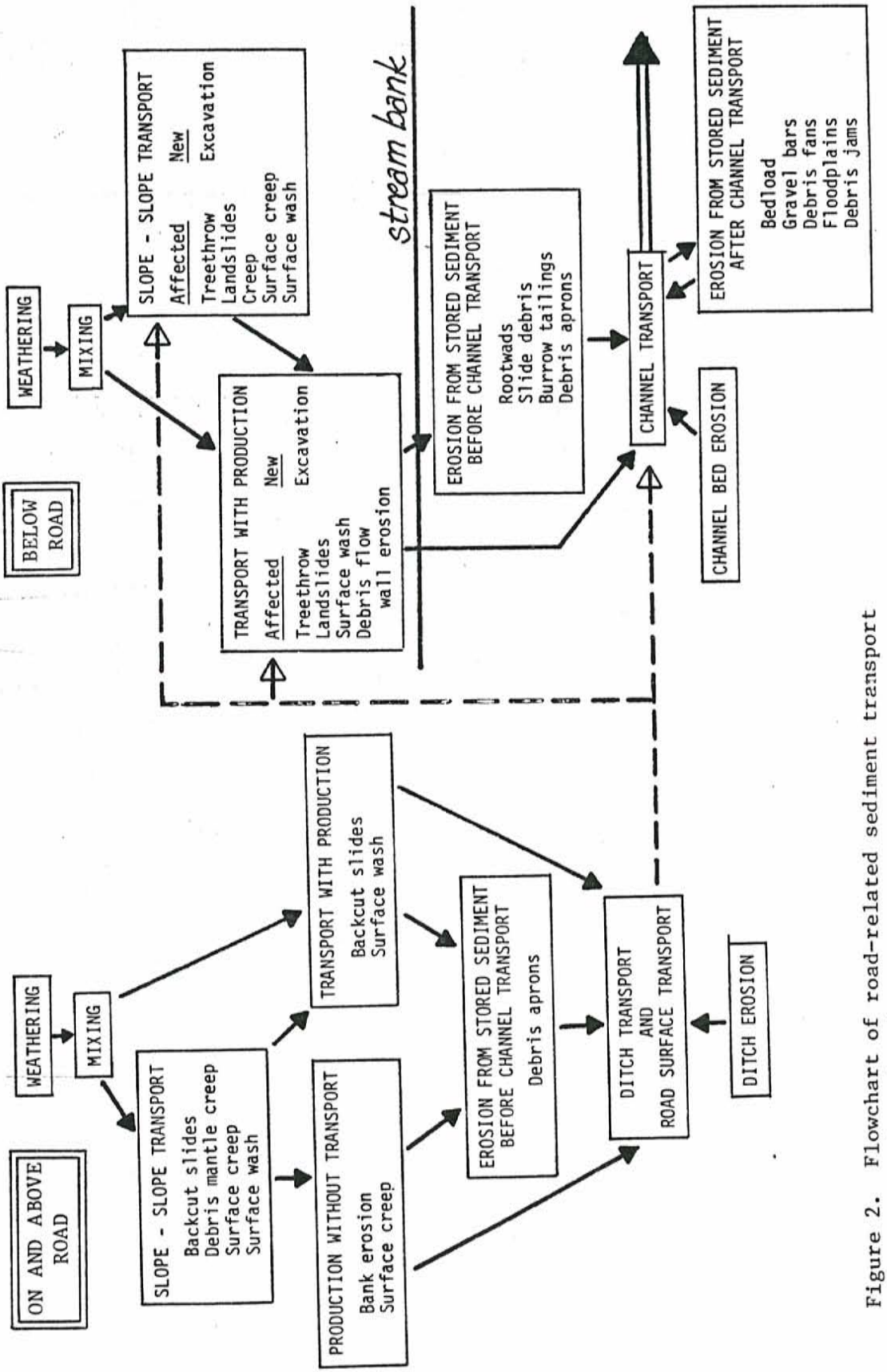

Figure 2. Flowchart of road-related sediment transport and production.

Some effects of the presence of a road may be generated at locations distant from the road itself. The road-related increase of coarse sediment in streams may lead to channel widening, accelerating both stream bank and landslide erosion. In low-order channels, increased peak flows generated by overland flow on road surfaces may also lead to channel destabilization and increased sediment production rates. In some places drainage from a first-order basin is diverted along a roadside ditch into a culvert draining a neighboring low-order basin; in such cases average discharge may be instantly doubled in the second basin, also leading to a downstream destabilization.

In a disturbed basin the average rate of sediment production can no longer be assumed to equal the average sediment yield. The inertia imbued by relatively low transport rates for coarse material, by the presence of sediment in storage, by the long lag-time for response of some processes to changing conditions, and by the complex interactions between weathering, mixing, and sediment transport rates all prevent a speedy reattainment of equilibrium between sediment production and basin sediment yield. Destabilization of channels may cause sediment to be removed from storage in floodplains at a faster rate than that at which it is being replaced. Alternatively, the influx of coarse sediment due to road-related erosion may lead to channel aggradation and a general increase in in-channel storage; coarse sediment may be supplied to a channel at a higher rate than it can be removed. The calculated sediment yield from a basin would then be equal to the difference between the total sediment production rate and the net change in volume of sediment in in-channel storage. Such calculations would thus require the measurement of erosion and accumulation rates of in-channel sediment stored both before and after channel transport. Pre-transport storage elements would include rootwads, slide debris, debris cones from animal burrows, and debris aprons built up against channel banks. After an episode of channel transport, sediment may be stored as bed material or in gravel bars, floodplains, debris fans, or debris jams. The following analysis and discussion is limited to consideration of sediment production rates independent of storage elements. Calculations of sediment yield arising from the analysis should thus be considered only as general indications of the magnitude of expected yield until changes in storage volume are addressed explicitly.

CHAPTER IV. DESCRIPTION OF AREA

Location

Fieldwork was carried out in the central Clearwater basin, a 370 km^2 tributary basin to the Queets River on the western slope of the Olympic Mountains, Washington (see Fig. 3). The basin is 30 km south of Forks and east of Highway 101, and is effectively isolated from the Olympic core by the south fork of the Hoh River to the east. To the north the basin is also bounded by the Hoh River drainage, and to the south by the Queets drainage. Work was concentrated in the Christmas and Miller drainages in the northwest part of the Clearwater basin and in the Stequaleho drainage to the southeast. Access within the basin is good due to the presence of a dense network of logging roads.

Geology

Christmas and Miller basins are carved from the Miocene marine siltstones and sandstones of the Hoh lithic assemblage. Here the assemblage is dominated by siltstone, but units containing thick-bedded sandstones are mapped over 40% of the area, and the siltstones themselves are often interbedded with thin sandstone beds in rhythmite sequences. In this area the unit is broken into fault-bounded blocks; locally the rocks are severely sheared and folded even within the blocks. Bedrock in the Stequaleho basin is also characterized by interbedded sandstones and siltstones, but here sandstones dominate. Rocks in the basin are mapped as an undifferentiated Tertiary marine unit containing less than 40% siltstone and argillite. Although the unit is sheared in places, structure is generally more continuous than that to the northwest (Tabor and Cady 1978).

Quaternary glacial advances affected the northwest and southeast areas in different ways. The most recent advance of the Hoh Valley glacier in the basin immediately north of the Clearwater overtopped the divide and drained melt-water down the southward-flowing Clearwater tributaries (Crandell 1964). The resulting outwash deposits remain as wide terraces in valleys of greater than fourth order. Earlier advances appear to have been even more extensive: weathered outcrops of till atop ridges suggest that at one time much of the basin may have been inundated by ice.

To the southeast the high divide between the upper Clearwater basin and the Queets glacier prevented significant overtopping, though the presence of outwash terraces and till outcrops in some of the eastern valleys suggests that cirque glaciers may have become established in their headwaters. West of Stequaleho basin, the divide between the Queets and Clearwater drainages is itself a lateral moraine, and ridge-top remnants of deeply weathered gravels may represent either

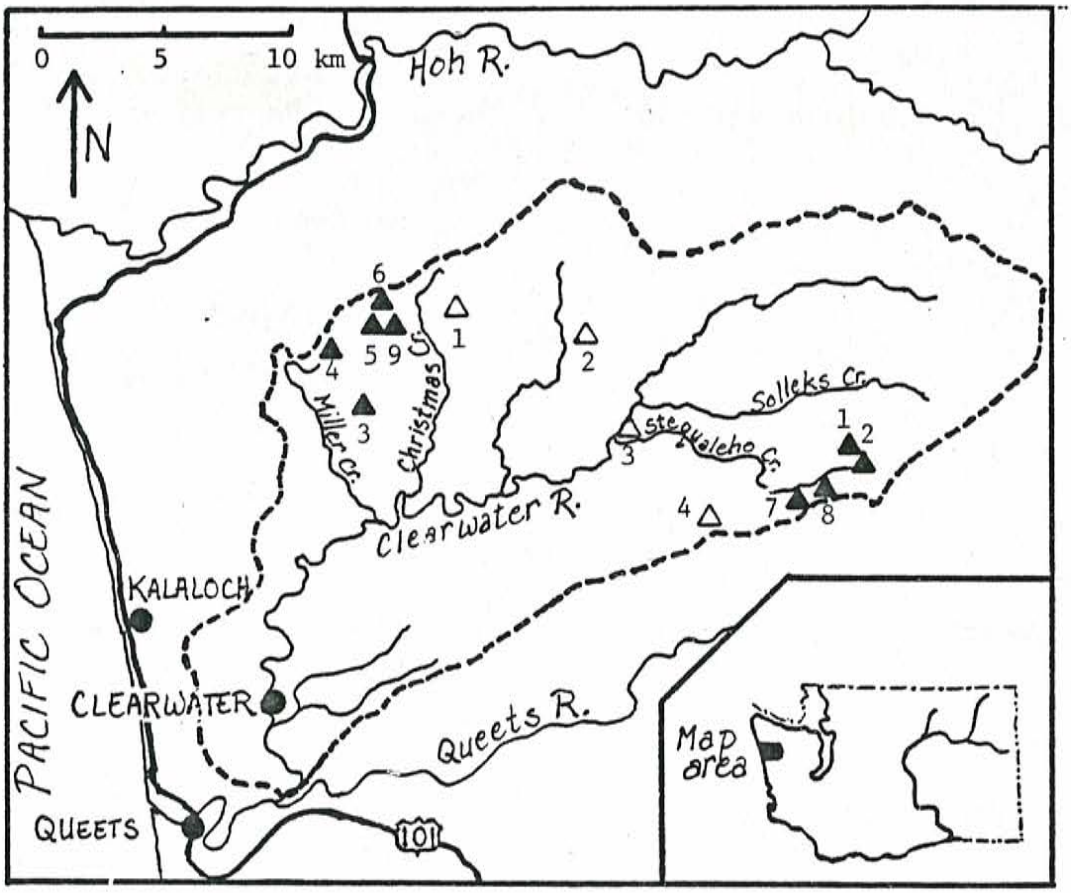

Figure 3. Map of Clearwater basin.

earlier periods of outwash or molasse sediments shed from the Olympic core. Extensive deposits of stratified colluvium immediately east of the Stequaleho basin indicate that periglacial activity may have been important during the Pleistocene, and pollen records from nearby bogs indicate that much of the area was covered by tundra rather than forest during this time (Heusser 1978).

Physiography

The differences in bedrock geology and glacial history between the northwest and the southeast parts of the basin are to some extent reflected in topography. To the north, sideslopes of the higher ridges are slightly concave to straight and average 21°, though hills near the Hoh-Clearwater divide are generally rounded, possibly reflecting the influence of glacial ice. Elevation ranges from 70 m at the basin mouths to 480 meters atop the ridge between Christmas and Miller basins. To the southeast, slopes are straight and steep, averaging 30°, and are generally longer than those to the northwest. Many slopes steepen noticeably at a point halfway down the hill. Elevations in Stequaleho basin range from 110 meters at the mouth to a high point of 1020 meters on the Clearwater-Queets divide.

Drainage density was determined using measurements from both 1:62,500 topographic maps and 1:12,000 aerial photographs. The aerial photographs could be used to map stream courses only in clearcuts and so provided data only in limited areas. These areas, however, were large enough to permit the determination of drainage densities for first- through fourth-order channels. The topographic maps were used to evaluate drainage densities of higher-order channels, but were not of a small-enough scale to allow the discernment of low-order channels. Because aerial photograph resolution is much finer than that of the topographic maps, what would be considered first-order streams on the maps correspond to second- or third-order streams on the aerial photographs. Similarly, the smallest streams printed in blue on the maps represent fourth-order streams on the aerial photos and in the field. The difference in resolution between the two data sources is reconciled by plotting on semi-logarithmic paper the drainage densities for different stream orders as measured by each method and drawing a best-fit line (see Fig. 4). The drainage density calculated by this method is approximately 9.3 km/km^2. Of this value, 5.3 km/km^2 represents first-order streams, which were defined to head at the uppermost extent of channelled surface flow. Unchannelled topographic depressions are also present at a density of 2 km/km^2, and the ability to distinguish the channelled and non-channelled forms using aerial photographs was affirmed by fieldwork.

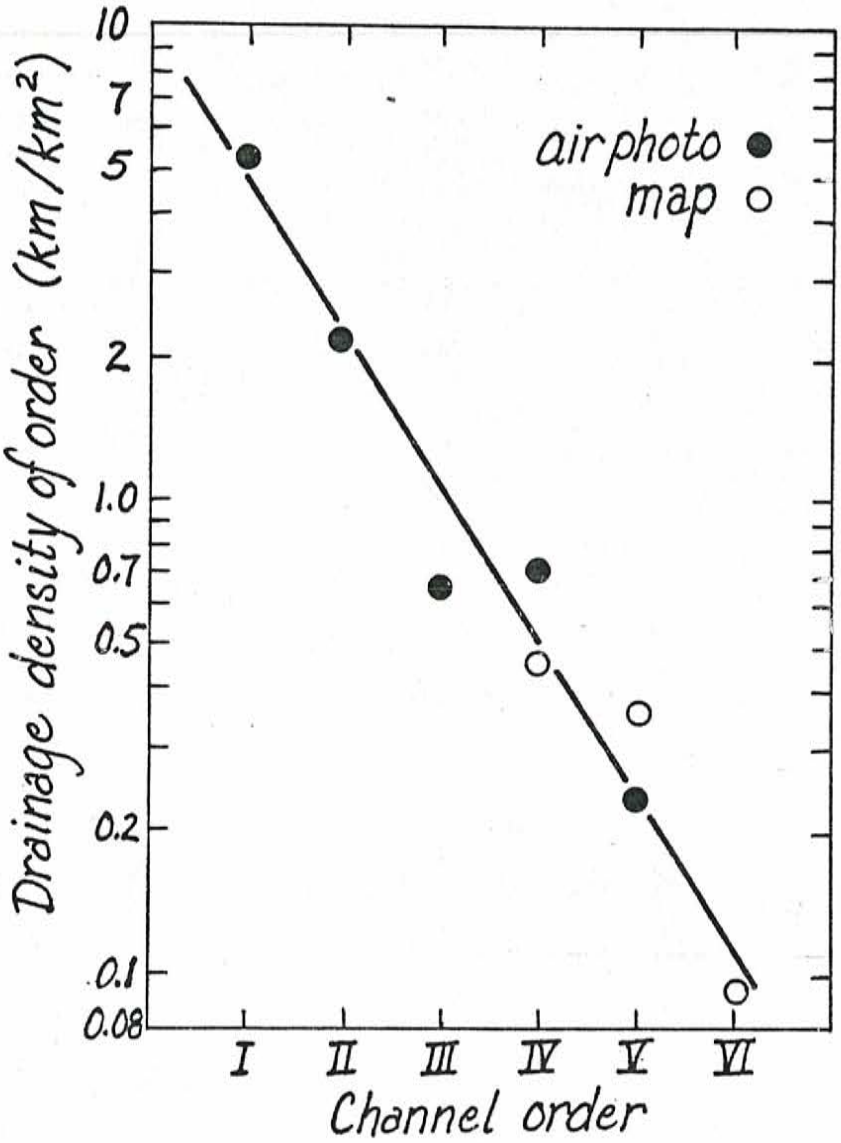

Figure 4. Drainage density of channels of various orders within a sixth-order basin, as measured from aerial photographs and from topographic maps.

Soils

Soils of the Dimal series occupy 40% of the area of Christmas and Miller basins and 85% of Stequaleho (discussion follows material presented by McCreary 1975). This series, classified as a lithic dystrochrept, is represented in the area by the Dimal very flaggy silt clay loam (see Table 1). The soil ranges in thickness between 25 and 50 cm and may be composed of 65% to 90% clasts of greater than 76 mm in diameter (see Fig. 5). My own field observations suggest that locally clasts may not be so abundant. Soils of this series are generally found over well- indurated sandstones and shales on slopes ranging from 30° to 40°.

Table 1. Typical soil profiles in Clearwater area (from McCreary 1975).

Soil	Horizon	Distance from base of 02 (cm)	Description	Percent < 2mm
Dimal very flaggy silt clay loam	01	5 - 2.5		
	02	2.5 - 0		
	A1	0 - 8	very flaggy silt clay loam	45
	B2	8 - 41	" " " " "	75
	R	>41	shale or sandstone bedrock	
Solleks channery silt clay	01	5 - 2.5		
	02	2.5 - 0		
	A1	0 - 13	channery silt clay loam	35
	A3	13 - 43	very channery silt clay loam	55
	B2	43 - 76	" " " " "	55
	C	76 - 107	" " " " "	70
	R	>107		
Hoko gravel silt loam	01	13 - 5		
	02	5 - 0		
	A11	0 - 10	gravel silt loam	30
	A12	10 - 20	" " "	35
	B21	20 - 30	" " "	35
	B22	30 - 41	" " "	35
	B23	41 - 56	gravel silt clay loam	40
	C1	56 - 74	" " "	30
	C2	74 - 102	gravel silt, weakly cemented	30
	C3	>102	very compact gravel silt clay loam, glacial till	

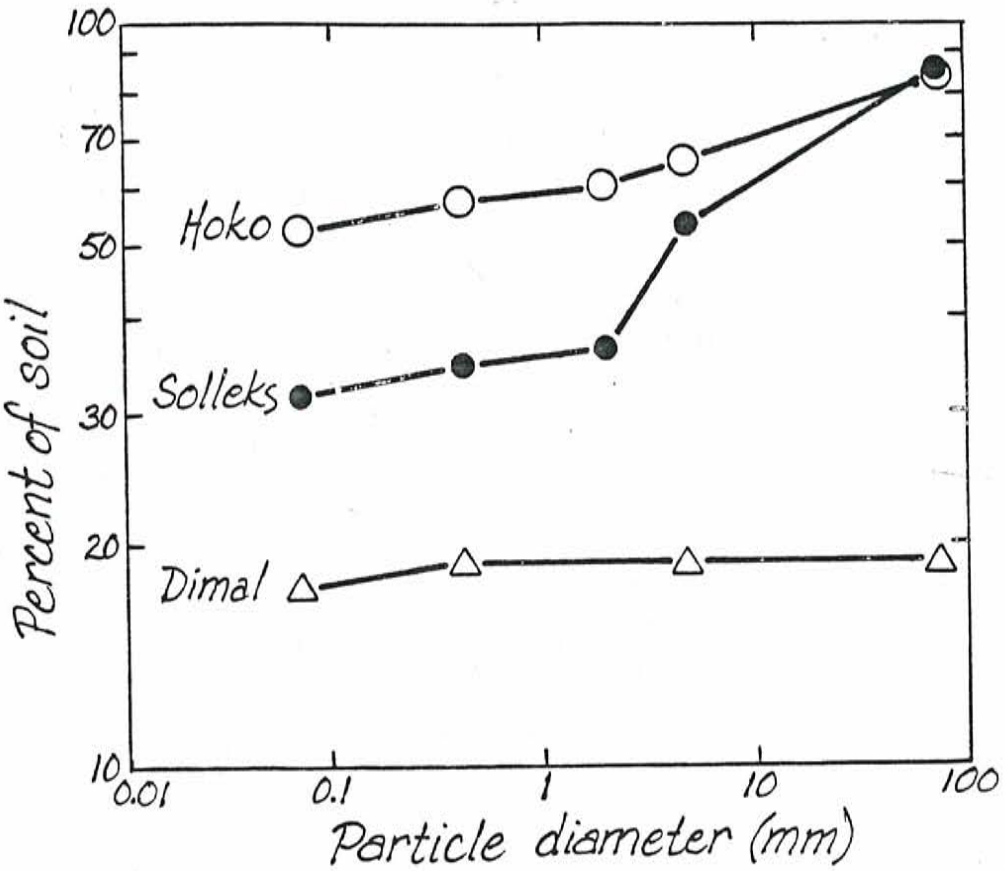

Figure 5. Average soil textures of A, B, and C horizons for selected soils of the Clearwater basin, presented as cumulative curves of soil of particle diameter less than or equal to that given.

The Solleks channery silt clay loams of the Solleks series of typic haplumbrepts occupy an additional 44% of the northwest basins and 12% of the Stequaleho basin. These soils are most common on slopes ranging from 20° to 30°, and they average 100 to 130 cm in thickness. Particles of diameter greater than 76 mm account for as much as 20% of the soil column.

Glacial outwash terraces in both areas support the Hoko gravelly silt loam, a dystric entic durochrept. These soils average 50 to 100 cm in depth and are composed of up to 30% rounded pebbles; up to 20% of the profile may be of clasts larger than 76 mm (see Fig. 5). Horizonation is more developed in these soils than in the others of the area (see Table 1).

Soil thicknesses in the area were also measured directly using observations along roadcuts. As described by Dietrich and Dunne (1978), soil thickness varies systematically with hillslope gradient, irrespective of soil series (see Fig. 6). When the distribution of hillslope gradients in the area is taken into account, this relationship can be used to calculate an average soil thickness of 50 cm for both the northwest and southeast portions of the basin. Areas of anomalously deep soils, termed wedges by Dietrich and Dunne (1978), are found throughout the area; in most cases these colluvial accumulations are located in topographic depressions.

Climate and Hydrology

The Clearwater basin experiences a mild maritime climate with high annual precipitation. Four climatic stations have been maintained in the basin since 1973 (Wooldridge et al. 1975; Larson and Jacoby 1976, 1977; Abercrombie et al. 1978, 1979). A U.S. Weather Service precipitation gauge is also located in the basin (see U.S. Environmental Data Service reference for record). The gauges demonstrate a weak west-to-east gradient in annual precipitation, ranging from an average of 3100 mm/yr near the mouth of the Clearwater (Phillips and Donaldson 1972) to 3800 mm/yr 30 km to the east (see Table 2). No orographic effect is evident.

Most precipitation falls as low-intensity showers from September through May (see Fig. 7), though intensities of 250 mm/24 hrs and 240 mm/24 hrs have been recorded since 1972. Frequencies of 15-min rainfall intensities for 3 years of record at the Queets Ridge gauge are shown in Fig. 8. The highest parts of the basin are snow-covered for up to 12 weeks each year, although at elevations below 300 m snow is rarely present for more than a week. Frost is expected on about 40 days each year, and during infrequent prolonged cold periods, as occurred in January, 1979, ground may be frozen to a depth of 25 cm under open areas such as roads. On non-compacted soil the frost was observed to be of the permeable, honeycomb variety.

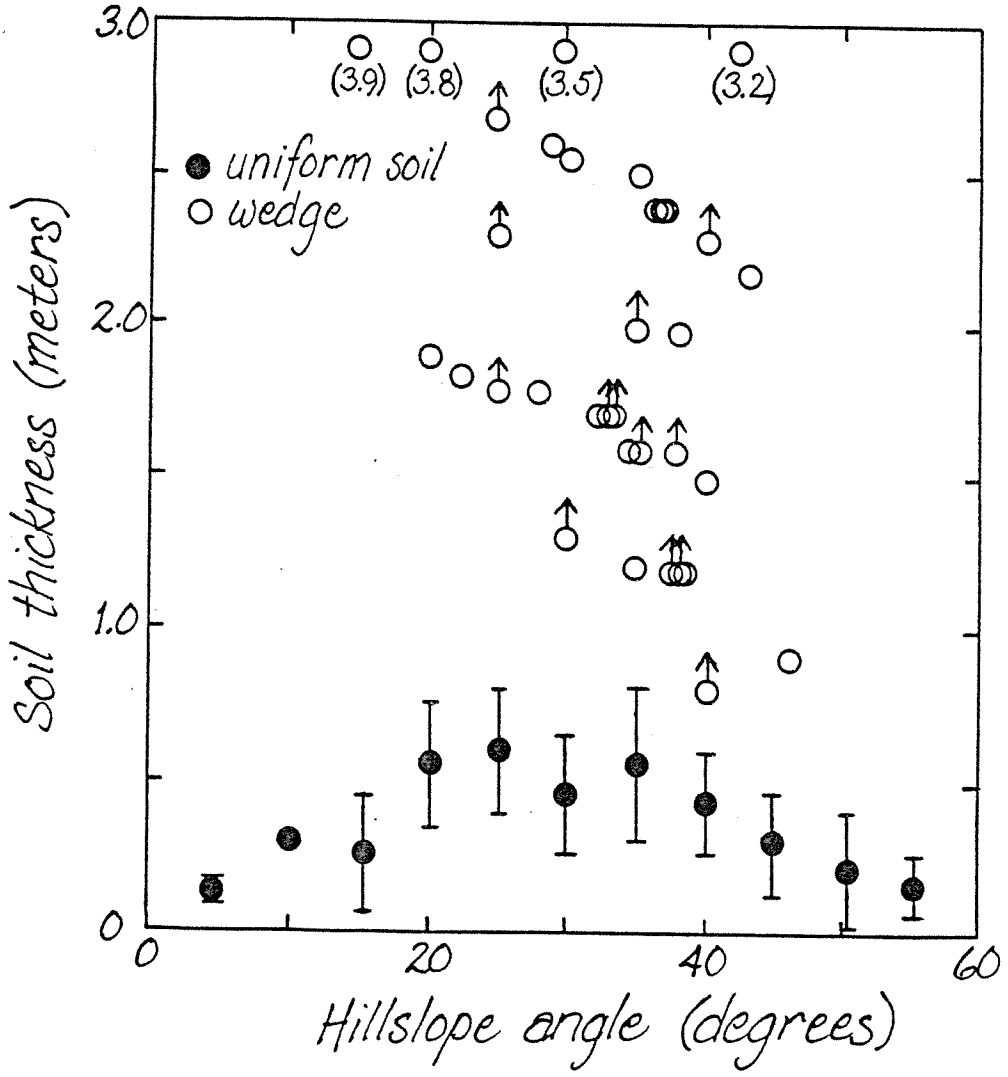

Figure 6. Variation of soil depth with hillslope angle. Solid dots represent averages of measurements from areas of uniform depth (bars indicate standard deviation), and circles indicate individual measurements in areas identified as wedges.

Table 2. Rainfall in Clearwater basin (for gauge locations see Fig. 4), showing recorded precipitation and relationships between gauge maintained by the U.S. Weather Service and those maintained by the University of Washington Forest Hydrology Group.

(A)

Water year	U.S. Weather Service, Clearwater*** (mm)	Honor Camp (mm)	Christmas Ridge (mm)	Stequaleho Stockpile (mm)	Queets Ridge (mm)
1978 - 79	2,519	2,597**	2,827**	2,841**	*
1977 - 78	3,528	3,569	3,573	3,550	3,468
1976 - 77	2,345	2,605	3,028	2,673	2,624
1975 - 76	3,678	4,768	*	5,289	4,784
1974 - 75	2,624	3,012	3,048	3,263	3,555
1973 - 74	3,978	4,679	4,528	4,973	5,201
1972 - 73	2,474	3,201			
1971 - 72	3,729	4,630			
1970 - 71	3,357	4,045			
1969 - 70	2,551	2,849			
1968 - 69	3,349	3,972			
Average	3,103	3,630	(3,401)	(3,765)	(3,926)
Standard error	182	252	(308)	(452)	(469)

(B)

Gauge	Number of years of record	Ratio of record to corresponding record from Clearwater gauge
Honor Camp	11	1.17
Christmas Ridge	5	1.13
Stequaleho Stockpile	6	1.21
Queets Ridge	5	1.22

*Missing record.
**Unpublished data from University of Washington Forest Hydrology Group.
***Average annual precipitation for 1931-1960 is 3,076 mm.

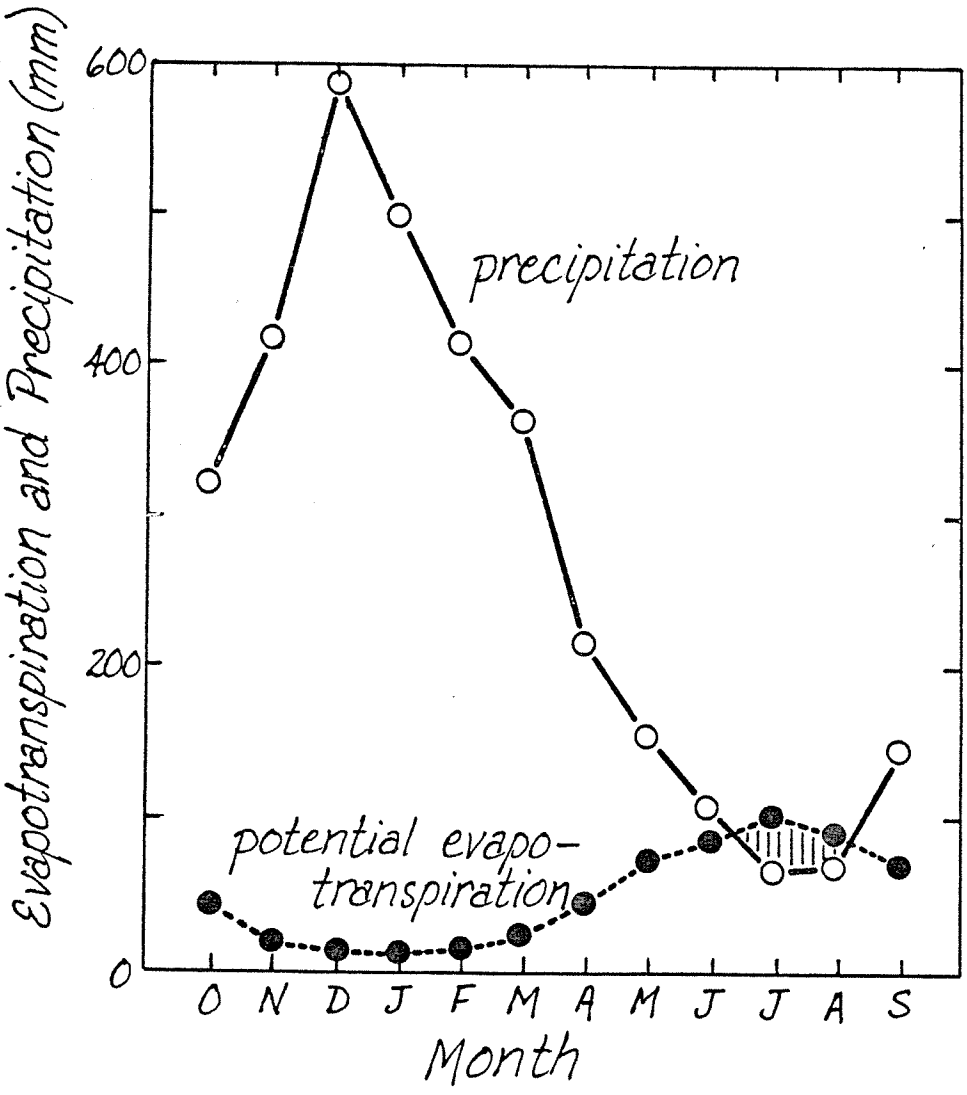

Figure 7. Average monthly precipitation and Thornthwaite potential evapotranspiration for Quinault Ranger Station, Washington. Data represent 69-year averages from U.S. Weather Service stations at Clearwater (precipitation) and Quinault (potential evapotranspiration), as reported in Phillips and Donaldson 1972.

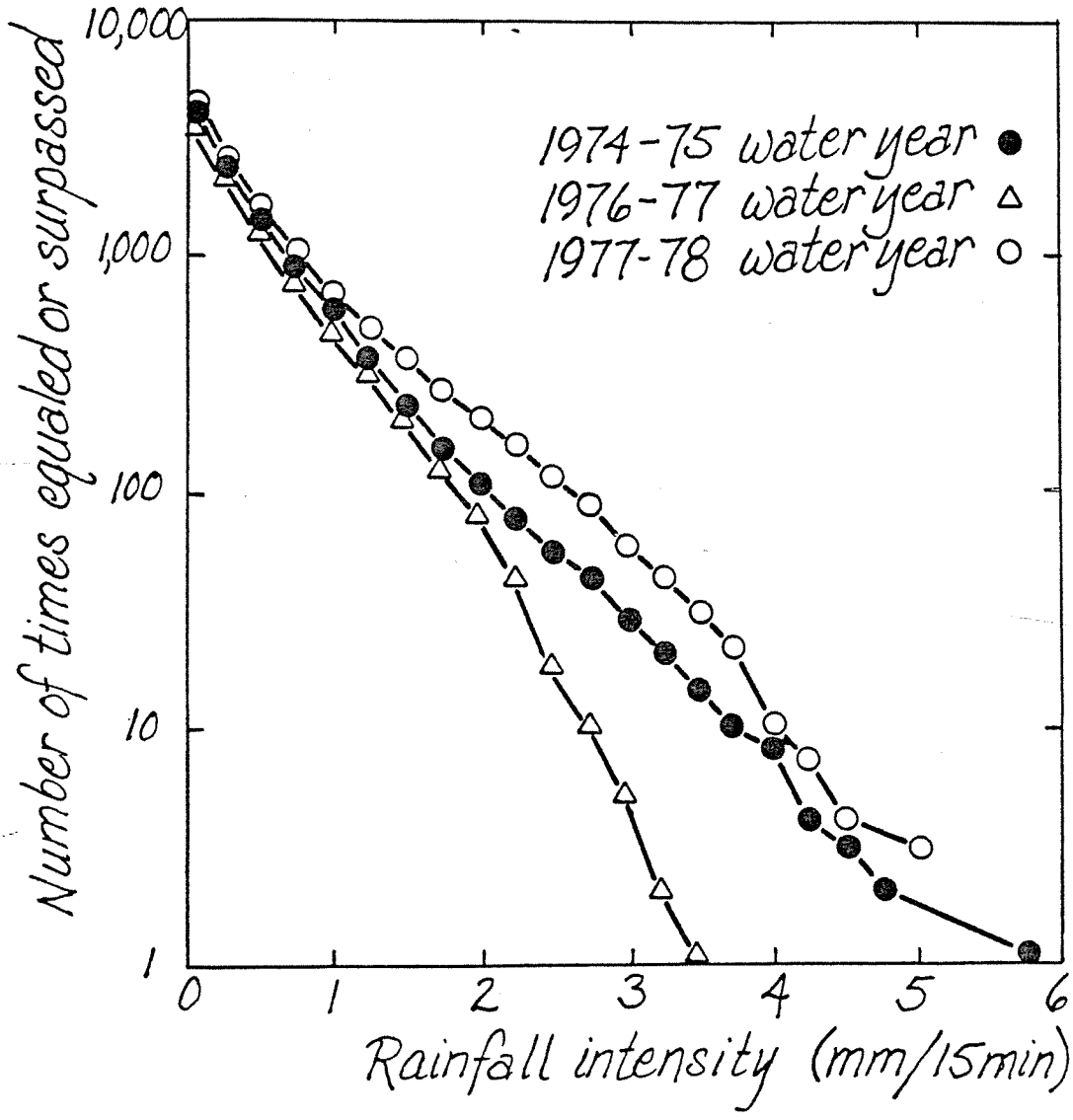

Figure 8. Frequencies of 15-minute rainfall intensities recorded at the Queets Ridge gauge during selected years.

The Clearwater area is also subject to occasional major wind storms during winter or autumn, and wind velocities may reach 150 km/hr. Wind direction is generally from the south during the major storms, though topographic effects result in strong local deviations. Such storms have resulted in major blowdowns at least twice during the last 80 years; during the 1921 storm trees were leveled over nearly 12% of the 15 km^2 upper Christmas basin. Almost every year storms with wind velocities of over 80 km/hr cause localized blow-downs.

Continuous water-stage recorders have been maintained on Christmas, Stequaleho, and Solleks creeks since 1973 (see Wooldridge et al. 1975; etc.). Mean annual runoff during this period was 3550 mm while precipitation averaged 3910 mm/yr. Mean discharge was 0.11 m^3/km^2-s, but discharges varied from a summer minimum of 0.011 m^3/km^2-s to the highest flow of record of 13.9 m^3/km^2-s in a 20 km^2 basin.

Calculation of Thornthwaite potential evapotranspiration from the nearby Quinault basin demonstrates an average net water deficit in July and August (see Fig. 7). Total potential evapotranspiration is 580 mm (Phillips and Donaldson 1972).

Horton overland flow has not been observed on undisturbed land in the area, but saturation overland flow is quite common both in drainage depressions and on stream terraces. Subsurface flow is commonly observed to follow pipes, and seepage often emerges from the floors of bedrock depressions intersected by roadcuts.

Vegetation

The mild, wet climate supports a dense coniferous forest dominated by western hemlock (Tsuga heterophylla) at low elevations and by western hemlock and Pacific silver fir (Abies amabilis) on the higher ridges. Red cedar (Thuja plicata) and Sitka spruce (Picea sitchensis) are locally abundant in more poorly drained areas. Riparian vegetation is dominated by red alder (Alnus rubra), though big-leaf maple (Acer macrophyllum) and black cottonwood (Populus trichocarpa) are common on higher terraces. Undergrowth varies from a sparse cover of herbs and sword ferns (Polystichum sp.) to dense thickets of huckleberry, blueberry (Vaccinium sps.), and salal (Gaultheria shallon). Areas of natural disturbance are quickly colonized by salmonberry (Rubus spectabilis) and by hemlock seedlings if the area is well-drained; alder and devil's club (Oplopanax horridum) are important locally.

Management

Eighty percent of the Clearwater basin is being managed for timber production by the Washington Department of Natural Resources (DNR). Logging proceeds according to a sustained yield plan with a 60- to 80-yr

cutting cycle. Much of the remaining land is owned by ITT-Rayonier and is being managed under a similar plan, so logging practices are relatively uniform throughout the basin. Units of 20 to 130 hectares (average 35 ha) are clearcut, and cables from a high-lead tower drag the logs to a ridge-top platform where the logs are loaded onto trucks. Because an individual tower location has a range of about 600 m (depending upon topography), road density is relatively low compared to that for such techniques as tractor and spar yarding. About 35% of the Clearwater basin has been clearcut; 100% will be cut by the year 2000. Cutting began in upper Christmas basin in 1968 and was 37% complete by 1977 (see Fig. 9a) while 27% of Stequaleho basin was cut by 1977 (see Fig. 9b). Cutting has generally progressed from the level lowlands to the less accessible, steeper highlands, so the eastern parts of the Clearwater basin are less heavily impacted than those to the west.

The majority of the haul roads in use at a given time are 4-m wide gravel-surfaced roads, although 30% to 50% of the roads in any basin are narrow, "logger's choice" spur roads built without specifications to service one or two platforms and then be abandoned until the next cutting cycle. About 100 of the 560 km of road in the Clearwater basin are paved. Road gradients may reach 13^{o} on spur roads but are generally below 9^{o} on roads undergoing more continuous use. Surface drainage is diverted either off the side of the road or into a roadside inboard ditch which drains into a culvert. Culvert spacing averages 200 m but is dependent upon road gradient and the location of natural drainages; 75% of the culverts eventually drain into stream channels while the rest disgorge flow onto hillslopes, where it infiltrates. Flumes are widely used at culvert mouths to prevent gullying.

Road density is now about 1.5 km/km^2 averaged over the entire basin, and a final density of about 2.2 km/km^2 is expected after logging is complete. Christmas basin has a road density of 2.4 km/km^2 with no paving, while Stequaleho basin has a density of 1.8 km/km^2, 5% of which is paved. At any time about 11% of the roads are used for hauling, 39% undergo casual use, and 50% are no longer being maintained.

Road maintenance consists of occasional grading, usually done during a light rain or while the road is wet in order that the surface material can be moved more easily. If the accumulation of fine material on a road surface becomes too deep to allow easy passage, a new layer of gravel is added. For the roads considered in this study the surfacing gravels are mined from outwash deposits in the Clearwater valley, but for unpaved main roads more competent gravel is brought in from neighboring basins.

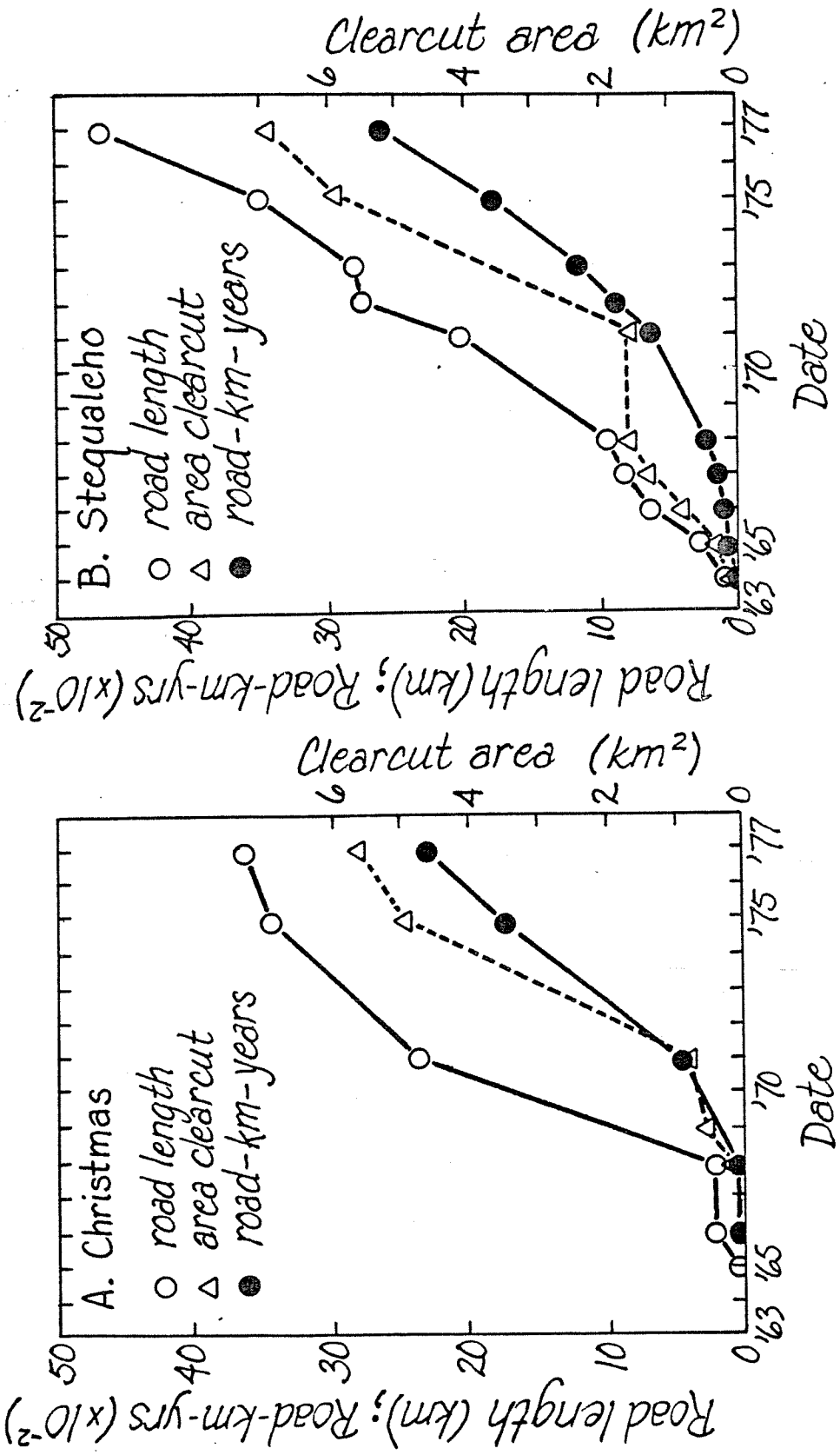

Figure 9. History of road construction and clearcutting in Christmas and Stequaleho basins.

CHAPTER V. SEDIMENT PRODUCTION FROM ROAD SURFACES AND BACKCUTS

Introduction to Chapter

The most visible of the sediment sources related to roads are landslides and debris flows, and the ubiquity and obvious impact of these processes cause them to overshadow the less-evident sources such as backcut erosion and road-surface erosion. In several cases, however, plumes of turbid water in streams were traced directly to the mouths of road culverts, and it became clear that these latter two sources were also contributing significant quantities of sediment to streams. Sediment in the culvert discharge originated by road surface erosion, backcut erosion, and ditch erosion. In the following analysis these sources are initially considered together. Measurements of precipitation, water discharge and sediment concentration at the mouths of selected culverts are used to construct sediment rating curves and unit hydrographs, which can then be combined with rainfall-intensity records to calculate sediment yield from a road segment. Sources are later isolated by independent measurements of backcut erosion and road surface sediment yield.

Measurement of Combined Sources

Processes

Logging road surfaces, other excavated surfaces such as yarding platforms, and recent landslide scars are the only sites in the basin on which Horton overland flow occurs. Saturation overland flow, on the other hand, is quite common in drainage depressions, but such areas have dense covers of moss and herbs and the flow remains relatively free of sediment. On road surfaces, overland flow has access to a source of fine sediment that is continuously renewed by truck traffic. The runoff is quickly channelled into ruts where its transport capacity is increased by channelization and it is in contact with sediment disturbed by passing trucks.

The mechanism of sediment production on road surfaces is not fully understood. The observation that surfacing gravels from different sources have noticeably different wear-lives suggests that breakdown of the gravel may be an effective mechanism for supplying fine-grained sediment to the road surface. In addition, fine-grained sediment may be brought to the surface as the weight of a truck packs the road gravels into the substrate, forcing interstitial fine sediment upward. Close observation of the passage of a pickup truck over a saturated road disclosed a temporary surface compaction quickly replaced by a surficial film of muddy water after the tire passed, while before passage there was no standing water on the surface. Such pumping action may also be effective at depth, and the ITT-Rayonier Company is experimenting with

the use of porous polypropylene fiber mats placed beneath the road ballast to filter out fine sediment pumped up from the substrate.

Road surface erosion is of particular importance because it will continue to be a significant source as long as the road is in use, while the frequency of landslides and debris torrents may decrease after the initially unstable sites have failed. In addition, though road-induced failures on the average introduce a greater volume of sediment into stream channels each year, that produced by road surface erosion is dominantly fine-grained and is fed directly into flowing water, thus having a disproportionately high potential for affecting fisheries resources and water quality.

Backcut erosion is a general term which includes the effects of many different processes. Where a road bench is partially cut into a hillside the excavated wall, or backcut, is left at an angle of 45° to 75°, depending upon the type of material excavated. Revegetation is generally slow or absent, although attempts to establish grass cover by hydro-mulching are locally successful on the more stable slopes. Erosion of material from cut-banks by rainsplash, sheetwash, dry ravel, freeze-thaw activity, wind erosion, and spring-sapping quickly builds up debris aprons composed of sediment finer than 30 mm in diameter. Once on the debris apron, sediment may again move by water erosion, dry ravel, and wind erosion, but it is now also subject to transport by bombardment of particles from above, ice needle growth, dislodgement by animals ranging in size from ant to elk, small-scale mudflows, and small-scale failures triggered by undercutting at the ditch. Occasionally, larger landslides may deposit a portion of both cut-bank and debris apron on the road surface.

As the backcut ages, the debris apron grows, both decreasing the area of cut-bank supplying sediment and encroaching upon the roadside ditch. On roads that have not been abandoned, ditches are kept clear by occasional excavation by graders, which either spread the sediment over the road surface or remove it to nearby dumps. Such activity decreases the stability of the debris slope, but the decreasing rate of sediment production from the receding, increasingly talus-covered cut-bank will eventually decrease the rate of sediment input to the ditch, and the slope may stabilize. Such stabilization is evident on backcuts of abandoned roads: debris aprons often completely fill the ditches and are stable enough to support vegetation of herbs, grasses, hemlock seedlings, and alders.

Primary erosion from roadside ditches, in contrast, is exceedingly uncommon. In general, ditches are partially filled with sediment already eroded from road surface or cut-bank, and only rarely is bedrock exposed after the initial excavation. Even after grading some sediment is generally left in the ditch, shielding the bedrock from channel erosion. The roadside ditches will thus be considered a location of transport and not a sediment source in the following analysis.

Site Selection

Eleven road segments were selected for monitoring of sediment discharge. Each of the nine maintained road segments is drained by a culvert, while drainage is carried from the two abandoned segments by cross-ditches.

Road segments that satisfy the selection criteria are relatively rare. Because road surface drainage was observed to carry more sediment than ditch flow not originating on a road surface, only those road segments which do not contain backcut springs or intercept surface drainage from the hillslope above are considered. This criterion severely limits the possible sites both because of the high drainage density in the area and because culvert placement is often determined by the location of stream crossings.

Average road gradient in the large tributary basins of the Clearwater drainage is about $5.5^{o} \pm 1^{o}$. Because it was not possible to monitor a large number of roads, it was decided to examine roads of approximately the same gradient. Segments were thus selected which have relatively uniform gradients of between 4.5^{o} and 6.5^{o} (see Table 3).

Table 3. Monitored road segments.

Culvert	Road	Basin	Use[2]	Gradient (degrees)	Ditch length (m)	Road length (m)	Basin area (m^2)	Maximum probable area[3] (m^2)	Minimum probable area[3] (m^2)	Area of ditch and road-side (m^2)	Use of segment in analysis[4]
CMI-1	C-2100	Miller	H,W,L	6.6	123	248	690	740	650	210	S,H
CMI-4	C-2100	"	H,L	4.5	173	287	910	960	840	380	S,H
CMI-5	C-2130	"	L	5.7	96	150	-	-	-	-	S
CSQ-1	C-3147	Stequaleho	A	8.0	56	56	-	-	-	-	S
CSQ-2	C-3147	"	A	8.3	63.5	54.5	190	200	185	-	S,H
CSQ-3[1]	C-3100	"	H,M,W	415	138	175	-	-	-	-	S
CSQ-4	C-3100	"	P	5.3	176	-	-	-	-	-	S
CSQ-5	C-3100	"	W,L	5.4	187	266	920	980	885	300	S,H
CSQ-6	C-3100	"	P	5.5	171	204	1005	-	-	300	S,H
CCL-1	C-2820	Willamaud	M,L	4.8	204	186	-	-	-	-	S
CCL-2	C-2820	"	M,L	7.5	132	203	-	-	-	-	S

[1] Road segment is surfaced with different gravels than other sampled roads.
[2] Road-use categories: H - heavy, M - moderate, L - light, W - temporarily non-used, P - paved, A - abandoned.
[3] These areas are calculated using extreme values of measurement uncertainties and are included here to indicate confidence interval of calculated road catchment area.
[4] Data from segment used in evaluation of: S - sediment rating curves, H - unit hydrograph.

Gradients on the abandoned segments are higher, measuring 8.0° and 8.3°. Each of the monitored roads is at least 5 years old.

Roads expected to sustain different levels of use are built to different specifications, which vary in required surface width, ballast thickness, and maximum gradient. At the lowest use level, logging spur roads are built to service one or two platforms and are abandoned after the clearcut unit is burned and planted. These roads have no mandated specifications but are generally built to the same specifications as management-standard roads, although in some locations spur roads expected to be used only during summer months are left without surfacing material. Certain requirements based on projected impacts may be made by DNR area managers upon examination of the written road plan; these changes may include relocating the roads, endhauling excavated material, and revising backcut gradients. After use ends the roads are required to be cross-ditched and blocked to traffic (Washington Forest Practice Board, 1976).

Roads providing access to several clearcut units are built to management-standard specifications, which require a maximum grade less than 12% for loaded trucks and 18% for unloaded, and a ballast depth of at least 30 cm. In the Clearwater basin these roads are surfaced either with Pleistocene glacio-fluvial gravels or with crushed rock, both of which consist mostly of local graywackes, indurated sandstones, and basalts. Road-bed width for the 4-m wide road surface is 6 m to 7.5 m (see Fig. 10). Most of the length of heavily-used road falls into this category, and it was upon these roads that work was concentrated. Within this classification road width and ballast depth may vary according to site characteristics and projected use.

Mainline gravel roads are 6 m in width, have a maximum grade of 6%, and a minimum ballast depth of 45 cm. Surfacing material is selected for durability. Such roads are generally not found in the tributary basins of interest here, and in other parts of the Clearwater basin most have been paved. One of the monitored heavily-used segments was located on such a road to allow comparison with an adjacent paved segment.

The selected road segments fall into five categories of road use intensity. Abandoned roads are those that are no longer maintained and have not been subject to hauling for over a year; traffic is limited to an occasional light truck, and in many cases the roads are physically blocked. Lightly-used roads are those which have experienced no logging truck traffic for at least 3 days prior to monitoring but which are still maintained. In most cases light vehicles continue to use the road infrequently, and in each case the road experienced other levels of use during the study.

Moderately-used roads are those upon which hauling traffic consists of only one to four trucks per day. None of these roads remained in the moderate-use category throughout the study. Hauling traffic of fewer

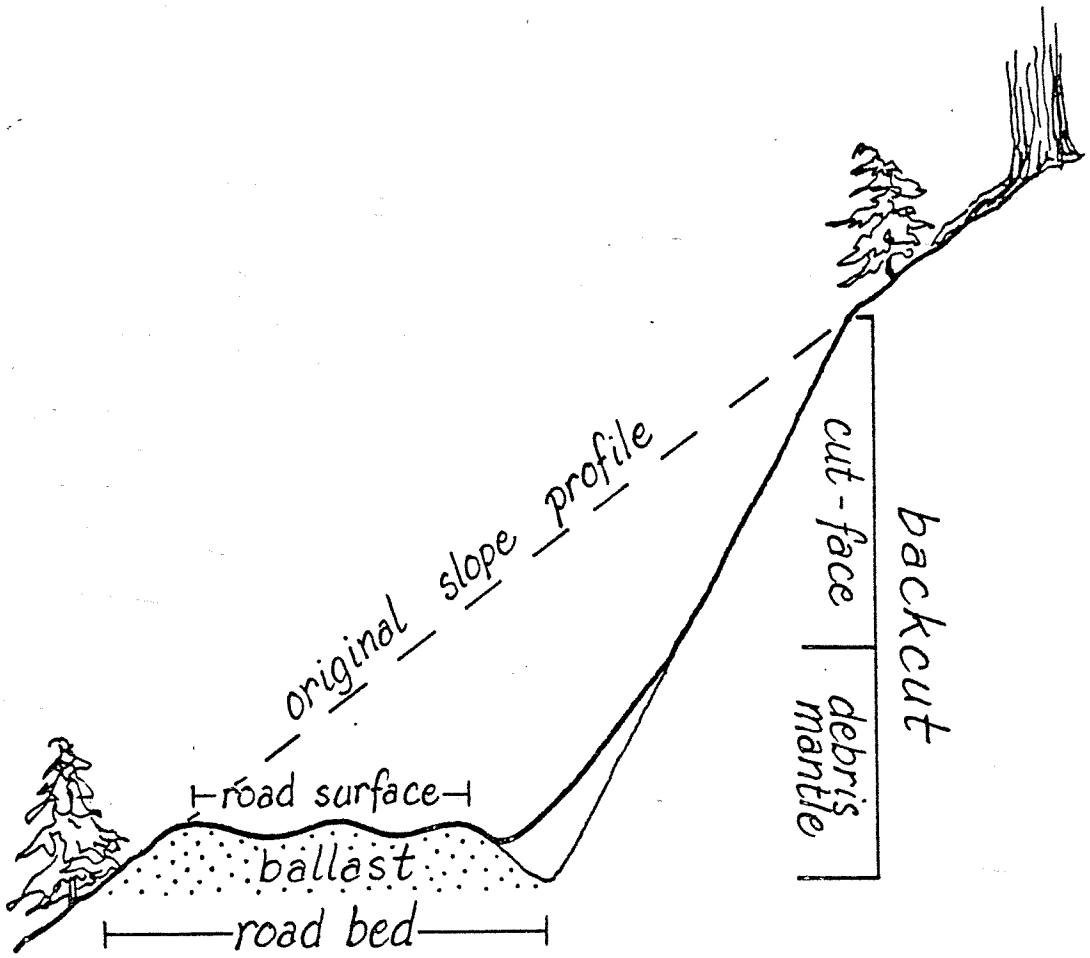

Figure 10. Typical cross-section of a full-bench road.

than four trucks per day generally occurs during the felling of road rights-of-way, and such traffic conditions do not apply to much of the road length in a basin at a given time. Roads that sustain traffic of over four trucks per day are considered heavily used.

Temporarily non-used roads are roads which are otherwise heavily or moderately used but upon which no hauling took place on the day of measurement. Measurements falling into this category are usually those made on weekends.

A sixth category, paved roads, was selected because of the independence of sediment yield from use intensity on these roads. Paved roads were monitored in order to determine the background sediment yield attributable to backcut erosion.

Six of the eleven monitored road segments are 3- to 4-m wide management-standard roads and are surfaced with local glacio-fluvial gravels. A seventh segment (CSQ-3) is an unpaved portion of a mainline road, and was selected to compare with two nearby paved segments of the same road (CSQ-4 and CSQ-6). Surfacing material on the unpaved segment is of the relatively more durable Takoma Creek gravel, so measurements from this segment are not included in the general analysis. The two remaining roads (CSQ-1 and CSQ-2) are adjacent abandoned segments leading to six platform locations, and were constructed using nearly the same specifications as the management-standard roads. Culverts are generally removed from abandoned roads and drainage returned as much as possible to a pre-construction configuration; a road was thus selected which had always had some drainage diverted by surface ditches, and measurements were made at the mouth of a ditch. These segments were the steepest and the shortest of those monitored.

Field Methods

Each of the selected culverts was monitored during several storms between January and September, 1978. Instantaneous water discharge and rainfall intensity were measured at the culvert mouth, and during the later part of the study the number of trucks passing while measurements were being made was counted. Water samples were collected for later filtering and gravimetric determination of sediment concentration. Finally, the drainage pattern on the road surface was mapped during the storm. In some cases discharge measurements were made and water samples taken on the road surface.

Water discharge at the culvert mouths was measured by catching the outflow in a container. The size of the container was selected to provide a sampling period of 4 to 30 seconds, although during periods of very high discharge measurement durations as short as 2 seconds occasionally had to be used. The containers used ranged from a 100 ml graduated cylinder calibrated in milliliters to a 20 liter bucket accurate to the nearest 1/2 liter. Precision in volume measurement was

consistently within ± 5%. Measurement duration was recorded to the nearest 1/2 second, but precision was actually higher because measurements lasting less than 10 seconds were made using fixed time intervals reproducible to ± 0.2 seconds. Most discharge measurements are thus estimated to be accurate to ± 10%.

Precipitation was measured by determining the volume of rainwater in a straight-sided 7-cm deep plastic gauge with a surface area of 74 cm^2. At the beginning of each measurement period the gauge was wetted and emptied. Volumes were read to ± 0.007 mm of rain at 15-min intervals or when major changes in intensity occurred; in several cases measurement intervals decreased to 3 min during intense bursts. A single gauge provided data during most measurement periods, but reproducibility was checked on several occasions by comparing volumes in two gauges. Over a 30-min period two identical gauges agreed to ± 4%, and over a 5-hour period the sum of 20 measurements from one gauge was within 1% of the accumulated volume in a second gauge. A similar comparison over a 2-hour period produced agreement to ± 6%. On this basis rainfall volume is estimated to be precise to within ± 10%. Duration of the measurement period was noted to within 15 sec, producing a minimum precision of ± 8% and an average of ± 3% for the 8.5-min average duration. Rainfall intensities can thus be expected to be precise to within ± 13%.

Water samples for concentration measurements were collected by holding a pint milkbottle to catch the flow at the culvert mouth. Where discharge was too high for the entire flow to be caught, the bottle was moved from side to side to sample every part of the flow. Bottles were immediately sealed with wax-coated caps and stored in darkness to prevent algae growth until the samples were filtered. Flow during the falling limb of high-discharge hydrographs occasionally broke down into pulses when discharge dropped below 150 ml/sec. The pulses had periods of 3 to 10 sec, preventing the sampling of an entire cycle by a single bottle. In these cases the bottle was put briefly into the flow at 3 to 5 sec intervals during three or more pulse cycles.

Initially it was assumed that road use on a given day could be reconstructed from records filed by truck drivers. This was indeed the case for logging trucks, but part way through the season it was learned that no such records exist for gravel trucks. From this time on the trucks were counted directly, but this method produced a record of use only during the measurement period. This record is generally sufficient to categorize the use-level of the sampled road, but it does not allow more detailed consideration of the effect of variations of use within the general categories. Future measurements should make use of automatic traffic counters.

A sketch map of the drainage pattern on each road surface was made during storms of moderate intensity. Distances were paced from landmarks and from markers placed at major forks if the pattern was complex. Road-surface drainage is intricately braided, so the percentage of the

flow following each branch was estimated to ± 10% at each major fork. During the dry season each road segment was mapped using a tape and level, with branch locations either determined directly or reconstructed from paced distances to landmarks. These maps could then be used to calculate effective drainage area.

Discharge could be measured and samples taken directly on the road surface in some places by catching the flow in a plastic bag. A site was chosen where the surface wash was confined to a rut and was cascading over a small rock or lip. The mouth of the bag was held tightly against the base of the rock and all flow channelled into the bag. In cases where the entire flow could not be captured, discharge was estimated by measuring average width, depth, and velocity and dividing the product by an empirically determined factor of 1.39. This factor was calculated by comparing the results of the width-depth-velocity product with actual discharge for eight road surface flows for which discharge could be measured directly (see Table 4). The factor implicitly

Table 4. Empirical discharge factor for surface wash.

Measurement	Measured discharge (ml/s)	Calculated discharge (ml/s)	Average flow depth (mm)	Ratio of calculated to measured discharge
1	34.1	46.6	5	1.37
2	51.4	96.0	8	1.87
3	65.6	89.1	8 and 1*	1.36
4	79.6	86.1	8 and 1*	1.08
5	73.0	85.1	8	1.17
6	34.1	46.6	5	1.37
7	466.5	667	3	1.43
8	1,300	1,913	15	1.47

*Drainage flowed in two strands.

accounts for horizontal and vertical variations in velocity, since the measured velocity is that of the leading edge of a drop of dye placed in the center of the channel. The relative uniformity of the calculated factor reflects the similarity of channel morphology for the measured road surface flows. Calculations of discharge using this method are estimated to have an accuracy of ± 20%.

Laboratory Analysis

Samples collected for concentration measurements were vacuum-filtered through Whatman GF-C glass-fiber filter papers in plastic Buchner

funnels (see Guy 1969, for discussion of technique). If sediment concentration was abnormally high then the sample was first vacuum-filtered through a thin qualitative paper to remove the coarsest particles and decrease the filtering time necessary for the GF-C paper. The filtrate was then passed through the GF-C paper, which has an effective pore size of 1.2 m, and can thus trap colloidal material. If the filtrate was not clear, it was refiltered. Such refilterings were weighed separately in eight instances, and the amount of trapped sediment ranged from 8 mg (5.5% of the total sample) to 252 mg (4% of the sample). Volume of each sample was measured to 1 ml, or $\pm$ 0.25%.

After filtering, the sediment-laden filter papers were air-dried and placed in coin envelopes for transport to Seattle, where they were oven-dried at 110°C to 120°C for 24 hr, cooled in a dessicator, and reweighed to $\pm$ 0.0001 g on the same balance used to measure the tare weight of each filter paper. Two or more unused filter papers of each type were included in each set in order to check for incomplete drying or re-hydration. The 24-hr drying period was selected by repeatedly measuring a drying sample until the weight stabilized, but periods as long as 72 hr were occasionally used for particularly heavy samples. Drying times longer than 100 hr resulted in discoloration of the papers and renewed weight loss. Although the balance could be read to $\pm$ 0.0001 g and reweighing of the 60 papers eventually returned empty demonstrates that measurements are reproducible to $\pm$ 0.0006 g or $\pm$ 0.2%, uncertainties introduced by the possibility of over- or under-drying are estimated to raise the total uncertainty to $\pm$ 5% for concentration values.

Measurement of Road Areas

In order to construct a unit hydrograph for a basin it is necessary to know the area of the basin that contributes runoff. On road surfaces this area is difficult to define because drainage is in the form of anastomosing channels, but the drainage maps and estimated flow branch proportions for runoff on each road surface could be used to divide the surface into blocks defined by the major branches. The proportional flow rates between blocks and out of the system can then be treated as conditional probabilities operating on the area of each block (see Fig. 11). In other words, an area of road surface can be defined for which the downhill limit is the location of a branch in the channelled surface flow, the sides are drainage divides or the roadside ditch, and the up-hill boundary is either a drainage divide or the location of the last major branch. Definition of the proportion of flow following each branch completely defines the outflow from the block if the inflow rate from uphill, the area of the block, and the rainfall intensity are known. A random drop of rain falling in the area thus has a probability of leaving the area via a specific branch equal to the proportion of the flow following that branch, and the proportion of the area effectively contributing runoff to the branch is also equal to the flow proportion. Each possible flow route is traced and the effective

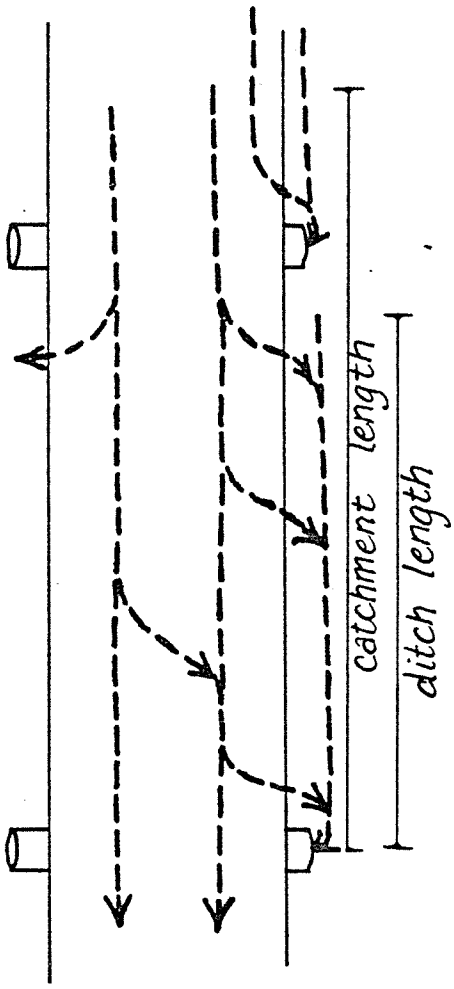

Map of drainage pattern in in road catchment

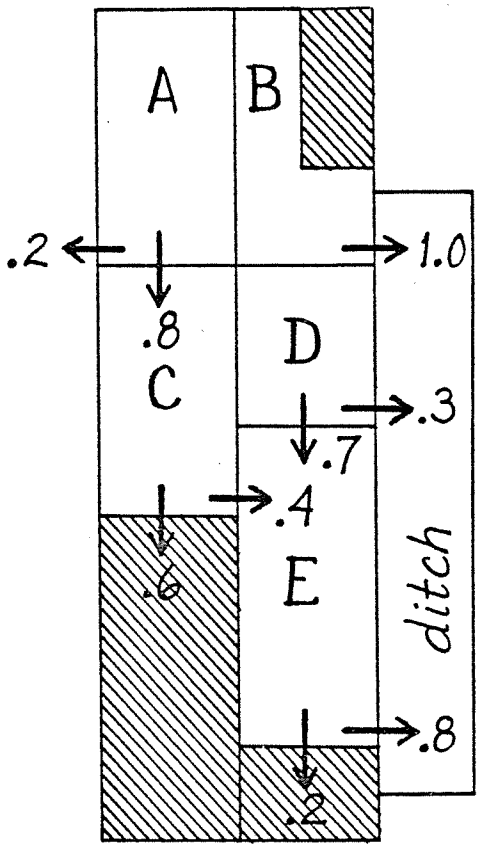

Block diagram of drainage with measured flow branch proportions

Effective area = (0.8 x 0.4 x 0.8) A + (1.0) B + (0.4 x 0.8) C
+ (0.3 + (0.7 x 0.8)) D + (0.8) E + ditch

where A through E represent areas of blocks.

Figure 11. Calculation of road-catchment area.

areas summed. The actual area of each defined block is planimetered from the surveyed road surface maps with the paced drainage pattern superimposed.

Uncertainties in road surface area are computed by assuming an uncertainty of $\pm$ 0.1 for each estimated branch proportion and calculating the resulting maximum and minimum areas. Road surface areas and uncertainties are shown in Table 3.

The calculated area includes road surface, ditch, and the slope between. The area of backcut and of hillslope above the backcut are not included, because the area of importance is considered to be that generating the flow recorded in the hydrograph measurements. Observation of the backcut surfaces during intense rain bursts demonstrates that although overland flow sometimes occurs on the steep cut-faces in the form of a thin film made visible only by the addition of dye, it is completely absorbed by the porous debris aprons growing beneath the cut-faces. Interception of subsurface flow by backcuts, as described by Megahan (1972) during snow-melt, was not observed during a measurement period, although piping was evident on some backcuts during a 1-week storm dropping 70 cm of rain in December 1979.

On paved road segments surface flow is not channelled, so the boundaries of the contributing areas are difficult to determine. In these cases drainage divides were constructed from surveyed contour maps of the road surfaces.

Culvert Discharge and Unit Hydrographs

Discharge and precipitation measurements were plotted against time to construct a hydrograph and hyetograph for each rainstorm monitored. Hydrograph peaks generated by uniform bursts of rain could then be isolated and used to construct unit hydrographs for the road surface catchments.

The use of unit hydrographs is based on the reasoning that the temporal distribution of runoff is determined by the physical characteristics of the contributing area. These characteristics include such factors as basin size and configuration, factors which do not change between storms. All bursts of rain of a given duration will thus generate runoff with the same time distribution; the proportion of the total flow occurring by any time after the beginning of the storm will be the same for each rainfall intensity. Different rainfall intensities will of course generate different volumes of runoff, but it is assumed that these differences are manifested only as differences in the magnitude of discharge at any time, rather than by changes in the speed of the runoff. The characteristic hydrograph form for a storm of given duration is thus a function operating linearly on rainfall intensity to produce a hydrograph for that storm (see Fig. 12a). If the volume of discharge represented by the characteristic hydrograph is that generated by one

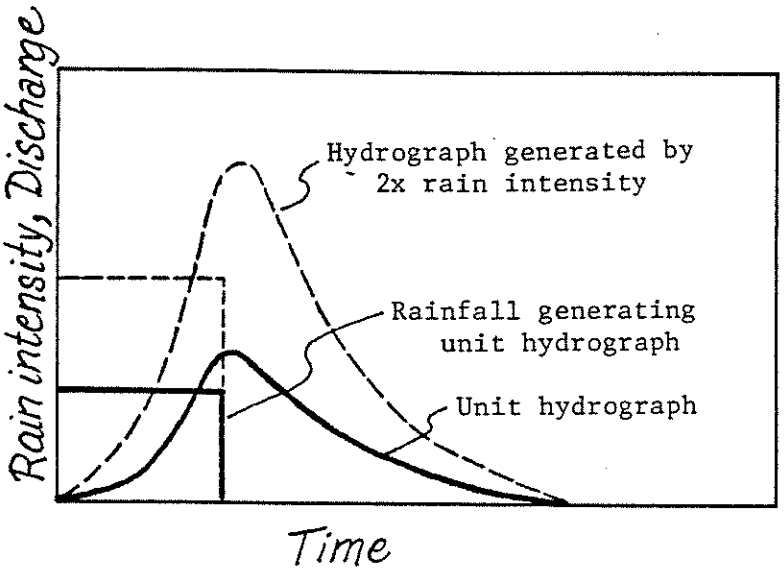

A. Adjustment of hydrograph to reflect intensity of rain.

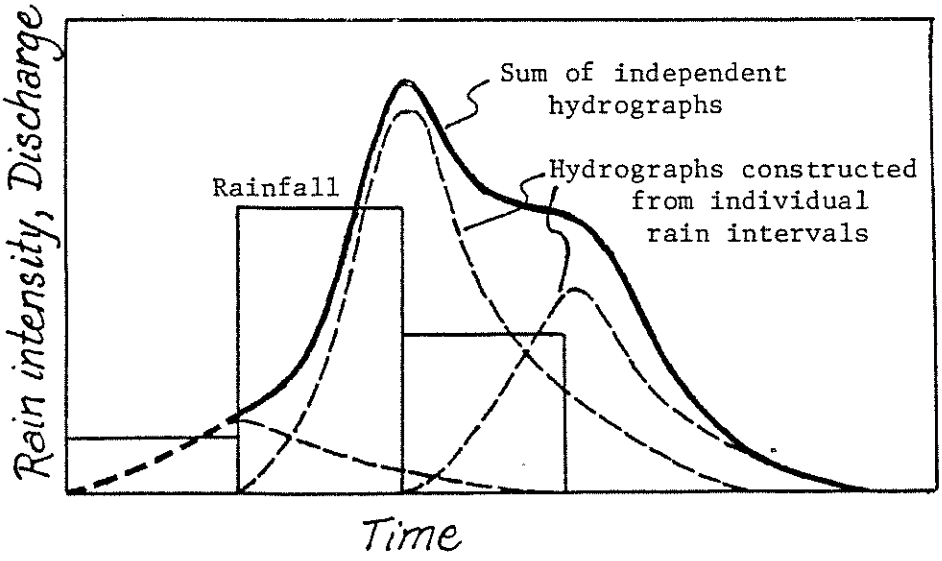

B. Addition of superimposed hydrographs.

Figure 12. Hydrograph manipulations.

unit of excess precipitation (rainfall intensity minus infiltration capacity), then the hydrograph is termed a unit hydrograph, and the hydrograph for any value of excess precipitation over the same duration may be constructed by multiplying the ordinates of the unit hydrograph by the excess precipitation. A hydrograph can then be constructed to reflect any sequence of rainfall intensities by constructing a hydrograph for each intensity, offsetting each to begin at the starting point of its intensity period, and adding the superimposed ordinates (see Fig. 12b; see Chow 1964, for further discussion of unit hydrograph theory).

The unit hydrograph for a specific storm duration can also be used to calculate hydrographs for other durations. The assumption is made that water already on the surface does not affect the time-distribution of runoff generated by rain falling onto the wet surface, and unit hydrographs are offset by the durations of their generating storms and their ordinates added until the sum approaches a constant. The resulting curve, termed an S-hydrograph, is then smoothed. Hydrographs generated by any storm duration can then be constructed by offsetting the S-hydrograph by the length of the desired duration and subtracting (see Fig. 13).

The underlying principles of these hydrograph manipulations are that hydrograph ordinates can be multiplied to reflect different rainfall intensities and that hydrographs can be offset and added to reflect different storm durations. These same principles form the basis for other manipulations.

For example, if the desired time duration is an integer multiple of the duration for which the unit hydrograph was constructed, then the required number of unit hydrographs can be offset and added without using the S-hydrograph. The direct method is more accurate because it does not involve as much smoothing.

Secondly, the temporal additivity of hydrographs can be invoked to motivate the inverse process: a hydrograph generated by a storm of given duration can be broken down into two identical hydrographs, each generated by a storm of intensity equal to that of the original but duration equal to half that of the original. If the transformation for rainfall intensity is combined with the temporal additivity principle, then this technique can be used to separate a hydrograph generated by two periods of rain of different intensities into two hydrographs, each generated by a burst of different but uniform intensity. These separations may be difficult to achieve in practice, and various methods based on these principles have been developed for this purpose. Collins (1939), for example, outlines a method based on iteration around an initial estimate of the unit hydrograph form. Because his technique requires rainfall intensity to be measured over uniform time intervals that are short with respect to the lag to hydrograph peak, his method is difficult to apply to the data available for small basins.

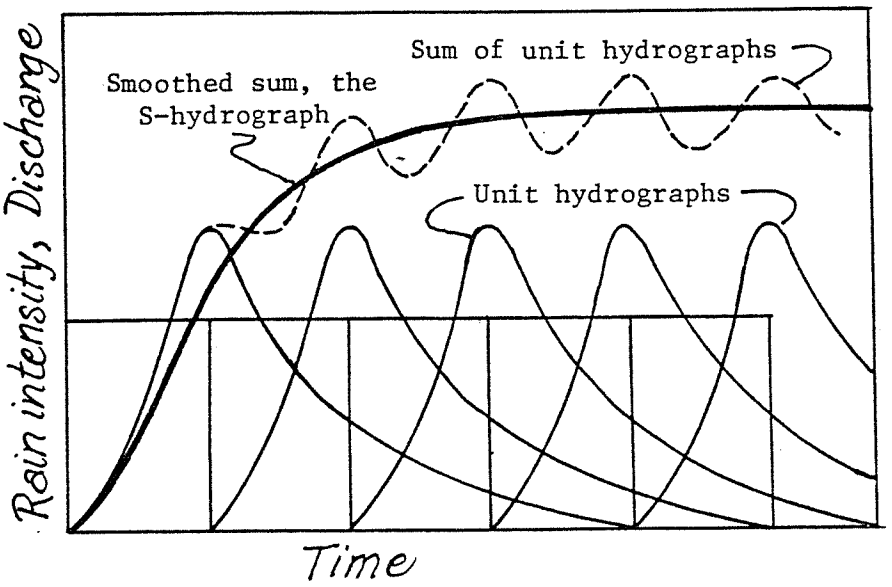

A. Construction of an S-hydrograph.

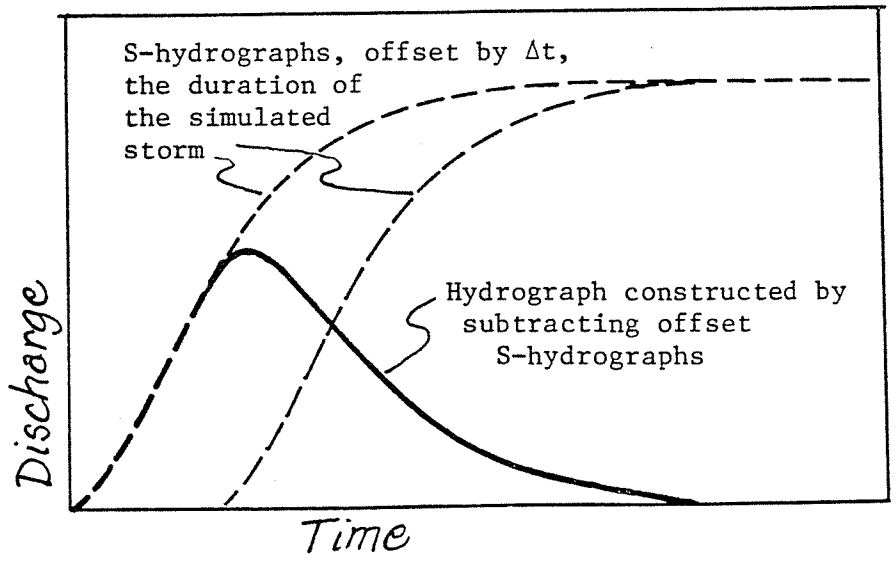

B. Construction of hydrograph from S-hydrographs.

Figure 13. S-hydrograph manipulations.

Unit hydrographs are constructed by selecting several hydrographs generated by storms of the same duration, multiplying their ordinates to make them represent unit volumes of runoff, and superimposing them. The average peak discharge and lag to peak are then calculated, fixing the location of the peak. Average rising and falling limbs are drawn in by eye. The storm duration used varies with the size of the basin, but for basins smaller than 25 km^2 the duration is generally about 25% of the lag to peak. Durations ranging from 7% to 100% of the lag to peak have been used successfully, however, and in practice any duration which provides good results for the basin in question is usable (Dunne and Leopold 1978; for further discussion of unit hydrograph theory see Chow 1964).

The data available for the road catchments do not allow a simple application of this method of unit hydrograph construction. Most of the 57 measured hydrographs are multiple-peaked or were not generated by a well-defined rainfall peak, and those with the least complex peaks were generated by rain periods ranging from 6.5 to 14 min. Twelve hydrographs were selected for which the generating rainfall is well-defined, irrespective of the length of the storm (see Appendix A). It thus became necessary to: 1) isolate the portion of the hydrograph attributable to the rainfall peak if the peak occurred during a period of otherwise low-intensity rainfall or before runoff from a previous burst had ceased; 2) decompose the resulting hydrograph into components reflecting each period of uniform intensity composing the rainfall peak; and 3) construct from each hydrograph a hydrograph of unit runoff volume and standard storm duration. Each of these manipulations is accomplished using the unit hydrograph principles described above.

1) Isolation: Several methods were used to isolate the hydrograph peaks (see Table 5). In one case the storm occurred as an isolated event, so no separation was necessary (see Fig. 14a). In three other cases the rainfall peak occurred as an intense period during an otherwise low intensity rain, and the hydrograph base could be considered to be the equilibrated discharge generated by the uniform background intensity. Effective rainfall intensities generating the peak were then considered to be the differences between the high intensities of the rainfall peak and the background intensity (see Fig. 14b). Two of the cases then required separation from each other by iteration.

The eight remaining hydrographs were isolated by making use of the observations that the falling limb of each hydrograph can be fit quite closely using an exponential curve, and that the exponents for all falling limbs on a given road segment are similar. Four of these hydrographs required only the continuation of their own falling limbs or the subtraction of constructed continuations of preceding falling limbs from the hydrograph peak of interest in order to become isolated. In these cases the rainfall peak was isolated from other rain, and the continuations were constructed by extrapolating the best-fit exponential curve

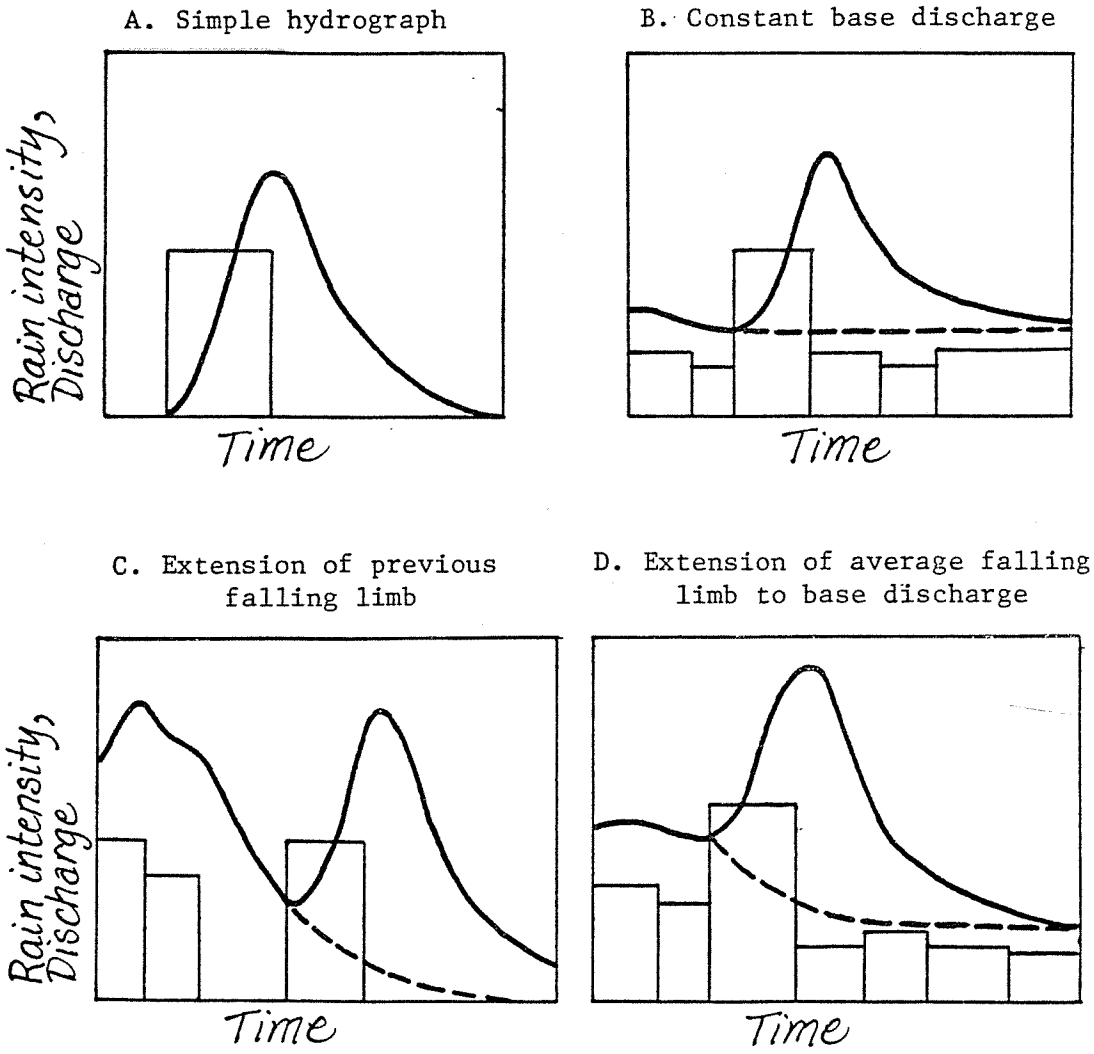

Figure 14. Methods of isolating hydrograph peaks.

Table 5. Hydrograph treatments for the construction of unit hydrographs. See text for discussion of methods.

Culvert	Peak	Maximum discharge (ml/s)	Discharge volume (l)	Duration of rain (min)	Methods of isolation		Decomposition	Time base (min)
					Rising limb	Falling limb		
CMI-1	A	300	320	(14)	zero	zero	simple	(14)
	G	200	210	7	extend previous	extend falling limb	20% from tail	7 + 7
	H	500	240	14	constant base	constant base	simple	14
	J	1,950	1,210	7	extend average	constant base	17% from rise	7 + 7
CMI-4	F	2,800	1,800	8	extend previous	constant base	simple	average to 9.75 split to 4.87
	H	12,500	9,080	11.5	extend previous	zero	simple	9.75 + 4.87
CSQ-5	G	800	520	10	zero	extend falling limb	simple	10 + 10/2
	H	1,350	850	8	extend previous	extend falling limb	29% from rise	8 + 8
CSQ-6	A'	3,240	3,130	13	zero	iterate with A"	10% from tail	*
	A"	1,000	740	6.5	iterate with A'	zero	12% from tail	*
CSQ-2	B	65	120	9	constant base	iterate with C	11% from rise	9 + 9/3 + 9/3
	C	100	160	7	iterate with B	constant base	23% from tail	7 + 7

*The 13-min hydrograph was averaged with a 13-min graph constructed by the addition of two 6.5-min hydrographs. The result was split into eight parts, and the resulting 1.7-min chart was added to the averaged 13-min hydrograph.

defined by discharge measurements on the falling limbs (see Fig. 14c). A fifth case required the extension of the best-fit curve to approach a constant baseflow.

Two of the remaining hydrographs required separation from each other, which was accomplished by the construction of the falling limb separating the two using the average falling limb exponent and iterating until the exponents of the two component falling limbs were equal. This method is described in the following section. In the final case, the intensity before the rainfall peak was greater than that following it, and the average falling limb exponent for the road segment was used to construct a falling limb initiated at the time the rainfall peak began. The equilibrium discharge generated by the post-peak intensity was estimated from records of equilibrium discharge for uniform periods of similar rainfall intensity from the same road. The falling limb of the hydrograph generated before the rainfall peak was then constructed to approach the equilibrium discharge asymptotically. This discharge was considered to be the base for the hydrograph generated by the rainfall peak, and the effective intensities were considered to be the differences between the measured peak rainfall intensities and the background rainfall intensity (see Fig. 14d). In no case was the intensity after the rainfall peak greater than that before the peak.

These methods resulted in the isolation of twelve hydrographs, including at least two examples from each of five road segments.

2) Hydrograph decomposition: Most of the isolated hydrographs were generated by rainfall peaks of multiple intensity, but in four of these cases the minor intensity accounted for less than 10% of the volume of runoff and so was ignored.

As mentioned earlier, the standard method of hydrograph decomposition, as outlined by Collins (1939), was difficult to apply. Instead, an iterative technique was developed that was based on the runoff characteristics of the road surfaces. The method follows from the observation that on the monitored road segments all measured falling limbs can be fitted by exponential curves. Any exponential curve can be decomposed into two exponential curves which have the same coefficient in the exponent, which is also the same coefficient as that in the exponent of the original curve (see Fig. 15):

$$Q_t = Q_o\, e^{-kt} \tag{1}$$

but Q_t is the sum of discharges at time t on two independent falling limbs:

$$Q_t = Q_{oa}\, e^{-k_1(\Delta t+t)} + Q_{ob}\, e^{-k_2 t} \tag{2}$$

and Q_o is the sum of the discharge at Δt on the first falling limb and that at t=0 on the second:

$$Q_o = Q_{oa}\, e^{-k_1 \Delta t} + Q_{ob} \tag{3}$$

Combining equations (1), (2), and (3):

$$Q_{oa}\, e^{-k_1(\Delta t+t)} + Q_{ob}\, e^{-k_2 t} = (Q_{oa}\, e^{-k_1 \Delta t} + Q_{ob})\, e^{-kt}$$

and combining like terms:

$$Q_{oa}\, e^{-k_1 \Delta t}\, (e^{-k_1 t} - e^{-kt}) = Q_{ob}\, (e^{-kt} - e^{-k_2 t}) \tag{4}$$

The falling limb for the first component may be selected to have any value of k_1. If k_1 is chosen to equal k, and k is replaced in expression (4) by k_1,

$$Q_{oa}\, e^{-k_1 \Delta t}\, (e^{-k_1 t} - e^{-k_1 t}) = Q_{ob}\, (e^{-k_1 t} - e^{-k_2 t})$$

$$0 = Q_{ob}\, (e^{-k_1 t} - e^{-k_2 t}) \tag{5}$$

$$e^{-k_1 t} = e^{-k_2 t}$$

$$k_1 = k_2 = k$$

where Q_t is the discharge at time t after rainfall ends, Q_o is the discharge at the end of the rainfall, k, k_1, and k_2 are empirical coefficients, Δt is the time difference between initiation of falling limbs a and b, and Q_{oa} and Q_{ob} are the initial discharges of components a and b. Differences in rainfall intensity are thus manifested as differences between Q_{oa} and Q_{ob}; k remains constant. By selecting a Q_{oa} on the original

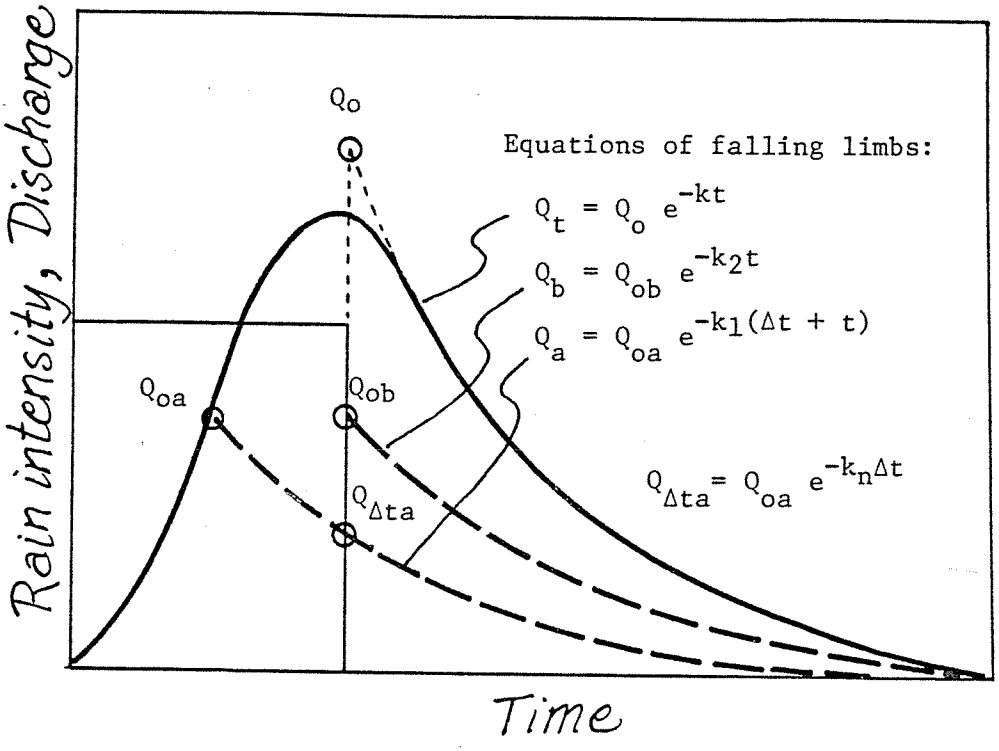

Figure 15. Decomposition of falling limb.

hydrograph and constructing a falling limb using the expression

$$Q_a = Q_{oa}\, e^{-kt} \qquad (6)$$

where k is measured from the falling limb of the original hydrograph, it is possible to decompose the hydrograph into two components. The first component is defined directly by the original rising limb up to the selected point Q_{oa} and by equation (6) for the falling limb; the second is constructed by subtracting the first component from the original hydrograph. The area of each component is then measured and their ratio compared with the ratio of total excess precipitations generating the components. If the ratios do not agree to within the tolerance limit, a new Q_{oa} is selected and the procedure repeated. The final result may be checked directly if the time bases of the rain periods are identical. The two components are transformed to the same total runoff by multiplying their ordinates in the same manner as for a unit hydrograph. The initial point of the second component is defined by the starting time of the second rainfall intensity period. The hydrographs are then superimposed, starting at the same initial point. The results may be checked by comparing peak discharges, lags to peak, and forms of the rising limb, which effectively provide three criteria for goodness-of-fit which are independent of the decomposition technique.

Application of this decomposition procedure to the complex hydrographs succeeded in isolating seven simple peaks in addition to the five that were originally non-complex.

3) Adjustment of time-base: The twelve isolated single-intensity hydrographs were generated by storm periods ranging from 6.5 to 14 min. In order to be used in calculations, the hydrographs had to be adjusted to a uniform time base. The duration selected was 15 min because this corresponded to the resolution of rainfall intensity periods measured at the continuously recording rain gauges in the basin. Because lag to peak is generally about 7 to 8 min for the road basin, it was realized that the actual unit hydrographs should have a time-base of less than 8 min (see Dunne and Leopold 1978, compilation on pg. 332). The 15-min hydrograph could then be constructed by the offset and addition of two 7- to 8-min unit hydrographs. In practice, however, 14-min hydrographs constructed by the addition of two 7-min hydrographs agreed quite closely with 14-min hydrographs constructed from a single 14-min duration storm (see Appendix Fig. B-1), so the selected time base does not appear to be of critical importance.

Although the measured rainfall intensities provide accurate records of average intensities for 3- to 15-min periods, actual intensity may vary significantly during each measurement period. This uncertainty was partially offset by noting rainfall volumes at the time of noticeable intensity changes, and also by recording qualitative descriptions of intensity changes on a five-point scale (very light-light-moderate-heavy-torrent). Uncertainty in the timing of intensity changes is estimated to be $\pm$ 1 min; constructed time bases range from 14 to 15.5 min,

with a mean of 14.7 min. This variation in time base is expected to be within the measurement uncertainty.

Time base adjustments were accomplished using the techniques described above. If the actual storm duration fell between 13.5 and 16.5 min the hydrograph was used without modification. If the time base was between 7 and 8 min, the hydrograph was offset by that duration, added to itself, and smoothed, forming a hydrograph with an effective 14- to 16-min time base. Other combinations required the decomposition of the original hydrograph into equal parts, one of which could then be offset by the original time base and added to the original hydrograph. A 10-min storm hydrograph, for example, was decomposed into two 5-min hydrographs, and the 10-min and 5-min hydrographs added with a 10-min offset. Similarly, a 9-min hydrograph was divided into three 3-min ones, and the 9-min and two 3-min charts were offset and added to form a 15-min hydrograph. In each case the decompositions were checked by superimposing the resulting components, and in each case agreement was quite close (see Fig. 16).

These methods provided two or more independently constructed hydrographs for 14- to 16-min storm durations for three of the roads. For each road the peak discharges and lags to peak were averaged to fix the location of the unit hydrograph peak. The hydrographs for the road segment were then superimposed by aligning the peak discharges according to the average lag to peak, and the rising and falling limbs constructed by averaging the superimposed limbs by eye (see Appendix Figs. B-1, B-3, and B-5). Ordinarily, the averaged limbs are not constructed by aligning peaks, but the forms of the individual hydrographs were similar enough to suggest that differences in lags to peak were generated by inaccuracies in defining the timing of intensity changes.

Data from two other roads required a slightly different approach. In one case two hydrographs were available, one with a time base of 13 min and the other of 6.5. The 6.5-min hydrograph was offset 6.5 min and added to itself to form a second 13-min hydrograph, which was adjusted to the same runoff as the first. The hydrographs were averaged at this point, and the resultant hydrograph split four times to generate a 1.7-min hydrograph; components agreed quite closely at each split. The 1.7-min hydrograph was then offset 13 min, added to the 13-min hydrograph, and smoothed, resulting in a 14.7-min hydrograph (see Appendix Fig. B-4).

The final road was represented by 8-min and 11.5-min hydrographs. These hydrographs were averaged to provide an estimate of a 9.75-min hydrograph, which could then be divided in two, offset, and added to construct a 14.6-min hydrograph (see Appendix Fig. B-2).

The methods outlined above allow the construction of characteristic hydrographs for five of the eleven monitored roads, including three roads

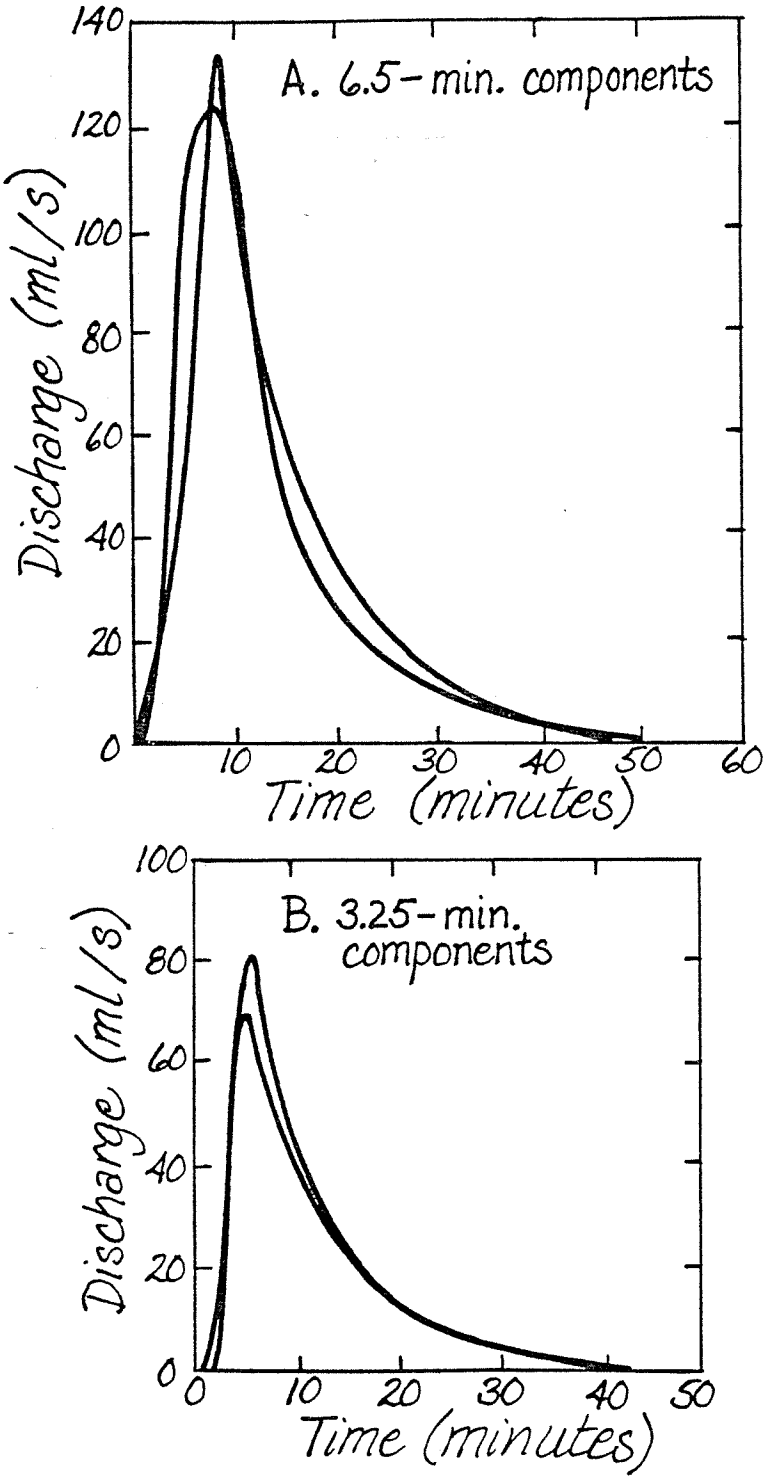

Figure 16. Hydrograph components constructed by successive splits of hydrograph CSQ-6 A'.

which were at different times heavily-, moderately-, and temporarily non-a paved road, and an abandoned road. On the basis of the complexity of the generating rainstorms and the necessity of separating component hydrographs from one another, the hydrographs for the paved and abandoned roads are considered the least well-defined of those constructed. Each constructed hydrograph may be transformed to a unit hydrograph by calculating the volume of runoff contributed by 1 mm of excess precipitation over the area of the road segment and multiplying the ordinate of the constructed hydrograph by the ratio between the calculated volume and the volume as drawn.

If the unit hydrographs are normalized by area and superimposed, the similarity of form of all but that from the abandoned road is quite striking (see Fig. 17). The unexpected correspondence of hydrograph form between the relatively smooth paved road and the rough gravel-surfaced roads may reflect the short distance that runoff must travel as sheet flow before it is constricted into channelled flow in roadside ditches and, in the case of the gravel roads, road surface ruts. The forms of the hydrograph would in this case be controlled by the hydraulic characters of the ditches and ruts, which are similar to each other. Alternatively, the difference in appearance of the two kinds of road surfaces may belie an actual similarity in the hydraulic roughnesses of the surfaces. Qualitatively this is made easier to believe if the surfaces are observed at close range. The smooth paved surface is seen to consist of closely-packed irregularities of the same scale as the expected surface flow depth, 1 to 2 mm. The rough gravel road, on the other hand, is surfaced with pebbles protruding from a less-noticeable, but areally significant, smooth-surfaced silt matrix.

Surface roughness on the two road types was compared by use of Moody diagrams. A Moody diagram is a plot of the Darcy-Weisbach friction factor against Reynolds number for a flow, illustrating the change of energy-loss due to boundary roughness as the flow becomes increasingly turbulent. For laminar flows, hydraulic theory predicts that the relation will have a slope of -1.0. Relatively smooth surfaces (those with ratios of roughness height to flow depth of less than 0.05) are further constrained by theory to fit the relation (see Streeter and Wylie 1975):

$$f = 6 / R_e \qquad (7)$$

where R_e is the Reynolds number:

$$R_e = \frac{uh}{\nu}$$

and f is the Darcy-Weisbach friction factor for sheet flow (see Dunne and Dietrich 1980):

$$f = \frac{2gsh}{u^2}$$

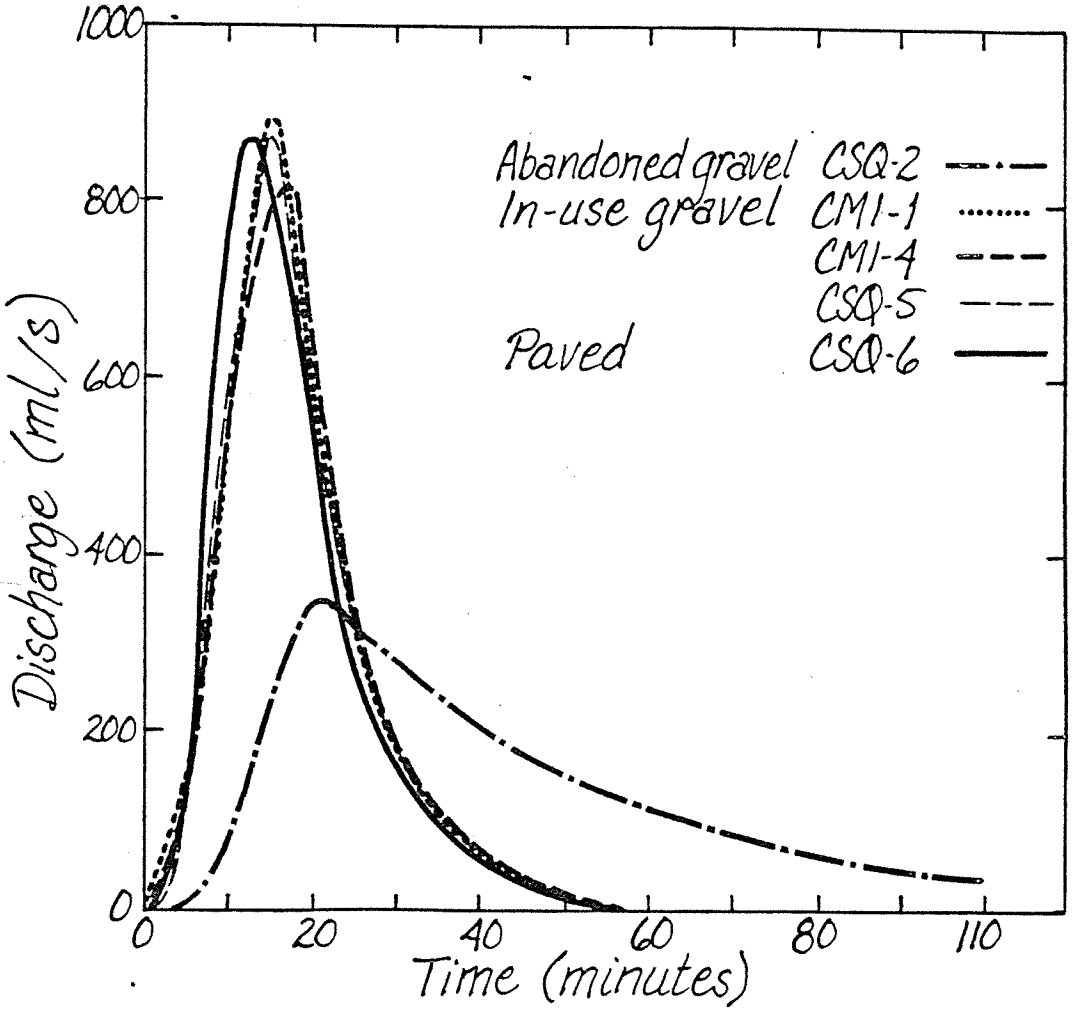

Figure 17. Unit hydrographs from each road type, normalized by area of catchment equal to 850 m^2.

The average flow velocity is represented by u, h is the average flow depth, s the gradient, g the acceleration due to gravity, and ν the kinematic viscosity of the fluid. The coefficient of 6 in equation (7) is a result of the derivation of the equation for sheet flow; the equation is generally presented with a coefficient of 16, valid for pipe flow. This relation provides a minimum value for effective roughness on the road surfaces. For surfaces with roughness elements of the same order as the depth of flow, however, the y-intercept of the relation has been shown empirically to vary with the density of roughness elements (Dunne and Dietrich 1980) and thus the coefficient in equation (7) provides an index of hydraulic roughness for a surface. Moody diagrams were plotted from depth and velocity measurements of flow on twelve gravel-surfaced logging roads; flow depth had been measured using a thin millimeter rule and velocity by determining the transit time of a drop of dye added to the flow. Data from three heavily-used roads, though widely scattered, indicate the relation:

$$f = 65/R_e$$

The coefficient has increased by a factor of 11 over the value predicted for smooth surfaces.

Several flow measurements were made on paved road surfaces. Although these measurements fall within the field defined by heavy-use road data they plot midway between the theoretical minimum roughness line and the gravel road regression line (see Fig. 18). A log-log regression of the three data points with slope constrained to equal -1.0 produces the relationship:

$$f = 23/R_e$$

These data are of course insufficient to define the relation, but they do suggest that invoking a similarity in surface roughness to explain the similarity in form of paved and gravel road hydrographs may be difficult to support.

The abandoned-road hydrograph exhibits a different anomaly: although the abandoned surface is superficially more similar in appearance than the paved surface to that of other gravel roads, the hydrograph form is profoundly different from both paved- and gravel-road hydrographs. In this case differences both in surface roughness and in the morphology of the flow may be important. A plot of flow measurements from three abandoned road surfaces (see Fig. 18) results in the regressed relationship:

$$f = 235/R_e$$

The gravel lag which produces the high roughness value on the abandoned road surface also protects the surface from the formation of ruts;

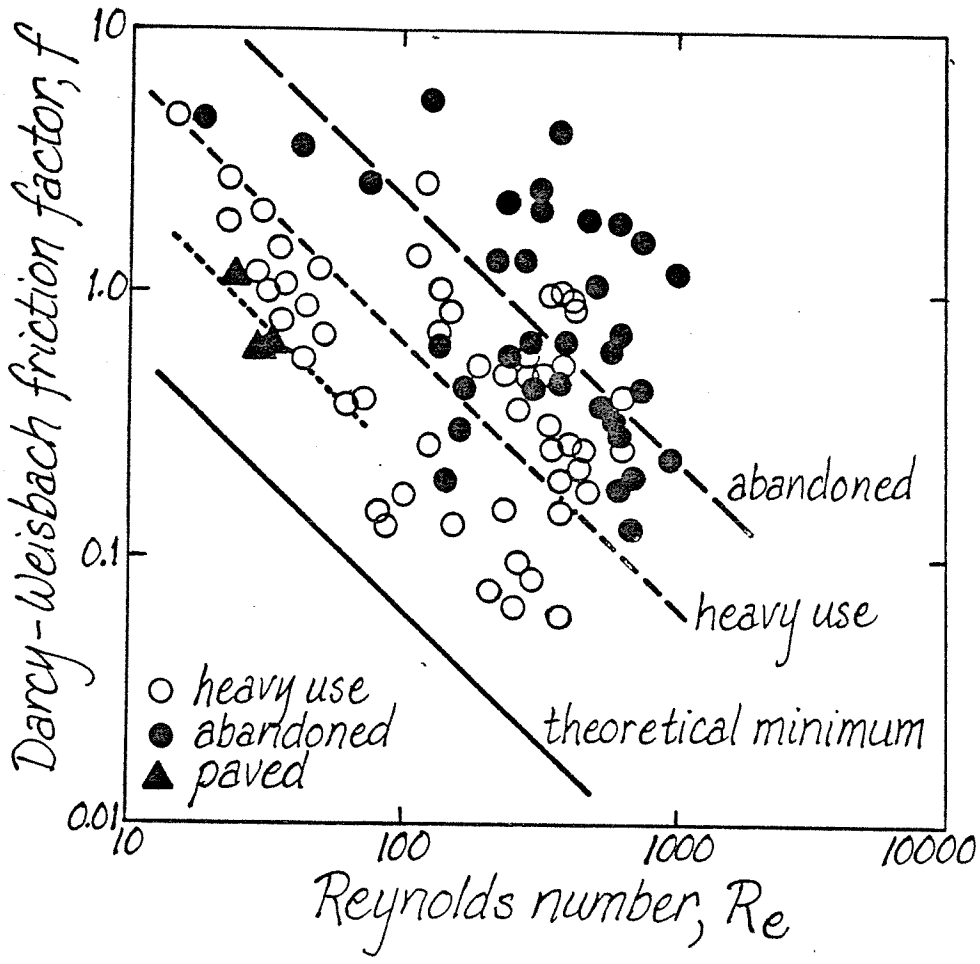

Figure 18. Moody diagram for paved road and for abandoned and heavy-use gravel roads.

thus runoff is more likely to flow as a sheet rather than being channelled on the road surface. In addition, little of the flow on the monitored road segment is diverted into the roadside ditch until immediately above the measurement point, so a high proportion of the run-off flows as a dispersed sheet over most of the road length. As would be expected under such conditions, the hydrograph peak is depressed and attenuated with respect to hydrographs measured on the maintained roads.

Because the variation between the forms of the unit hydrographs of the three in-use gravel roads and of the paved road is less than the variation between the hydrographs used to construct any one of them, these forms are averaged. The resulting unit hydrograph is applied to heavily-, moderately-, lightly-, and temporarily non-used roads and to paved roads in the following calculations. The abandoned-road hydrograph is used only in calculations of sediment yield from abandoned road segments.

Infiltration

In order to use a unit hydrograph to construct a hydrograph from a rainfall intensity record, it is necessary to calculate excess precipitation. In the absence of significant depression storage, excess precipitation is the amount of water that runs off a surface, and is thus equal to the difference between the total volume of rain falling on the surface and the volume of water lost by such processes as infiltration and evaporation. In the context of road surface hydrology, only loss to infiltration need be considered since conditions immediately after rain ceases are not conducive to significant evaporation.

Three methods were used to provide estimates of infiltration capacity on gravel-surfaced roads. As a first estimate, the maximum rainfall intensity that did not generate runoff was compared with the minimum intensities for which runoff occurred (see Fig. 19a). Only those storms beginning while no flow was present at the culvert mouth were considered. All of the storms with intensity greater than or equal to 0.5 mm/hr generated runoff, while five of the six storms with intensity less than 0.5 mm/hr did not. This method may reflect only the infiltration capacity of the ditch and the slope between road surface and ditch, but before runoff begins the slope material and porous ditch sediment are expected to have higher infiltration rates than the well-compacted road surface.

A second estimate may be made by observing the runoff rate that has equilibrated with a prolonged period of uniform-intensity rain. Eleven such periods could be identified; those occurring after several hours of continuous rainfall were avoided because it was suspected that the baseflow component from the backcut and hillslope could become significant under such conditions. Calculated infiltration capacities from these

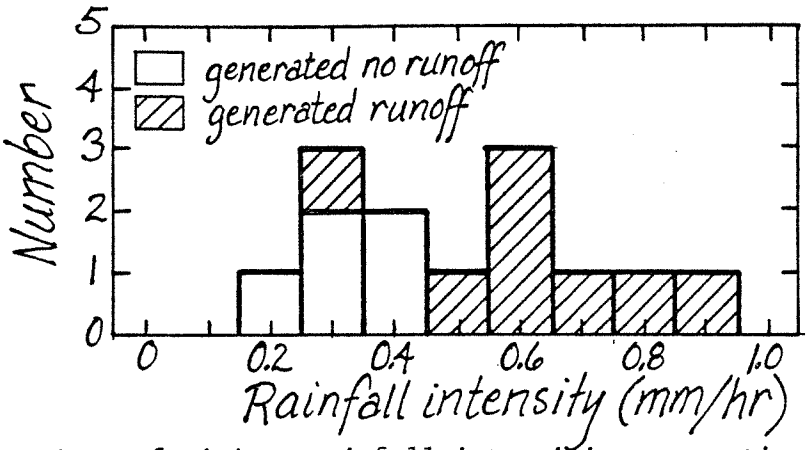

A. Comparison of minimum rainfall intensities generating runoff and maximum intensities generating no runoff.

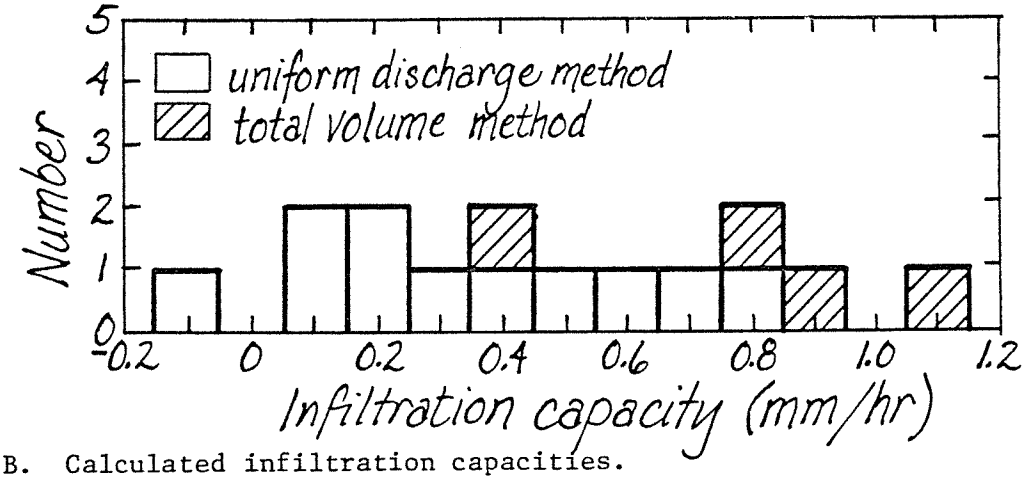

B. Calculated infiltration capacities.

Figure 19. Determination of infiltration capacities on gravel-surfaced roads.

eleven storms ranged between -0.1 and 0.8 mm/hr, with a mean of 0.3 (± 0.1)[2] mm/hr (see Table 6 and Fig. 19b). These calculations are

Table 6. Infiltration capacities calculated from uniform rainfall periods.

Culvert	Date	Time	Rainfall (mm/hr)	Discharge (ml/s)	Discharge (mm/hr)	Infiltration (mm/hr)
CMI-1	4-15	1240	1.5	140	0.74	.8
	4-15	1350	0.65	50	0.26	.4
	4-15	1440	1.0	95	0.50	.5
	4-15	1740	1.0	75	0.39	.6
	8-23	1750	1.3	270	1.42	-.1
	8-23	1815	3.2	480	2.53	.7
CMI-4	9-1	945	3.4	800	3.23	.2
	9-13	850	1.35	300	1.21	.1
CSQ-5	5-13	1515	1.4	300	1.17	.2
	5-27	1520	0.3	55	0.21	.1
	5-27	1610	0.55	70	0.27	.3

dependent upon drainage area; uncertainties in area may introduce an error of up to 8% in the calculated infiltration rate.

A third method is to subtract total volume of runoff in a hydrograph from total volume of precipitation generating it. This difference, when divided by basin area and by duration of runoff, is the average infiltration rate. Four naturally isolated hydrographs from three of the road segments provided data for the calculation. Calculated infiltration rates range from 0.2 to 0.6 mm/hr, with an average of 0.4 (± 0.1) mm/hr (see Table 7). This value is expected to be low because infiltration is averaged over the duration of the hydrograph, while the surface area available for infiltration decreases as flow is increasingly confined to channels after rainfall ends. This effect was estimated in a second calculation in which infiltration after rainfall ended was averaged over the 16.6% of the road catchment area covered by channels. Interfluves were estimated to drain over a 3-min period. This calculation indicates an infiltration rate of 0.8 (± 0.1) mm/hr.

These lines of evidence suggest that an infiltration rate of 0.5 mm/hr is a reasonable spatial average for a moderately- to heavily-used gravel road surface, roadside ditch, and intervening slope.

It may be expected that the less-compacted surfaces of abandoned roads would have higher infiltration capacities. A one-hour, 1.0 mm/ hr

[2] An error range within parentheses indicates the standard error of the mean throughout this report.

Table 7. Infiltration capacities calculated from total hydrograph volumes.

Culvert	Peak	Runoff volume (l)	Rainfall volume (l)	Rainfall duration (min)	Rainfall and runoff duration (min)	Derived duration** (min)	Infiltration calculated from duration of: Rainfall (mm/hr)	Rainfall and runoff (mm/hr)	Derived (mm/hr)
CMI-1	E	177	405	40	105	53	.5	.2	.4
	F + G	734	1,330	41	114	56	1.3	.5	.9
CMI-4	K	390	684	13	75	26	1.5	.3	.8
CSQ-5	G + H*	1,368	2,362	45	110	58	1.4	.6	1.1

*The falling limb of H was extended independently of the following hydrograph by extrapolating the exponential curve defined by points on the falling limb.

**Derived duration = t_{pp} + 3 min + 0.166 (t_{pp} - 3 min) (see text for explanation)

where t_{pp} = rainfall duration

t_{pp+ro} = duration of rainfall plus runoff.

storm resulted in ponding and surface flow on the road, but the rainfall intensity had reached 2.4 mm/hr before the condition of the surface was observed. Maximum infiltration capacity must therefore be less than 2.4 mm/hr and is probably less than or equal to 1.0 mm/hr. Comparison of total precipitation and total runoff over a 7.5-hour period indicates an average infiltration rate of 0.7 mm/hr, and an infiltration capacity of 1.0 mm/hr is selected for use in calculations.

Sediment Load

Field observations of culvert discharge provide qualitative evidence that runoff from heavily-used roads is more turbid than that from lightly-used roads. This relation was quantified by using measurements of sediment concentration in runoff from ten road segments to construct sediment rating curves for different intensities of road use. In the following analysis rating curves are first derived as relations between sediment concentration and water discharge in order to facilitate statistical analysis and are later transformed to the conventional plots of sediment discharge versus water discharge.

As explained above, roads were divided into six categories depending upon current and antecedent use-intensity and surface type: heavy use, temporary non-use, moderate use, light use, abandoned, and paved. None of the roads selected to represent heavy-, moderate-, and light-use conditions remained in the same category throughout the study. Two

of the six road segments built to management standards provided data during heavy use, two during temporary non-use, two during moderate use, and five during light use. In addition, two segments provided abandoned road data and two were paved. An additional segment provided measurements during various use levels on a road built with more competent surfacing gravel than that used on management-standard roads.

Sediment concentration was first plotted against water discharge for each road segment, and the results were examined on a storm-by-storm basis. In 16 of the 18 cases for which more than six measurements were made, the slope of the linear regression on log-log paper was found to be significant at the 0.05 level. Points representing different use levels on a single road plotted in different fields, and those representing the same use levels on different roads plotted in similar fields. On this basis measurements from the same use category on different roads were pooled to characterize that use level.

Several sources of variation are inherent in the data, and pooling of the data introduces several others. The amount of sediment carried by a given discharge is highly dependent upon the supply of sediment of size small enough to be entrained by that discharge. On a road surface this supply is largely generated by traffic, and concentration will thus vary to some extent according to the time lag between truck passage and sample collection. In Fig. 20, sediment concentration measured in a wheel rut on the road surface is plotted against time. Surface discharge and rainfall intensity remain relatively constant, but concentration increases from 4,500 to 31,000 mg/l immediately after the passage of a loaded truck and requires a 15-min period to regain its pre-disturbance level.

Antecedent moisture and traffic condition are also important. One of the mechanisms of surface sediment production is the upward pumping of fine interstitial sediment by compaction of gravels into the saturated substrate. Supply might thus be expected to be low at the beginning of the rain season before the road substrate has become wet, and during the first few days of traffic on a wet road. Variation is also present during a single hydrograph peak. Runoff from road catchments may exhibit pronounced hystereses in time-sequence plots of concentration against discharge. The peak concentration tends to occur before the peak discharge, making concentration higher for a given discharge on the rising hydrograph limb than on the falling limb. This effect has been variously attributed to the quick removal of the most readily entrained sediment, the enhanced influence of raindrop impact in entraining sediment while depth of flow is low and its absence on the falling limb, and the increased importance of relatively clean baseflow on the falling limb. Whatever the cause, the hysteresis may be expected to increase scatter, although its effect will be averaged out for a random sample.

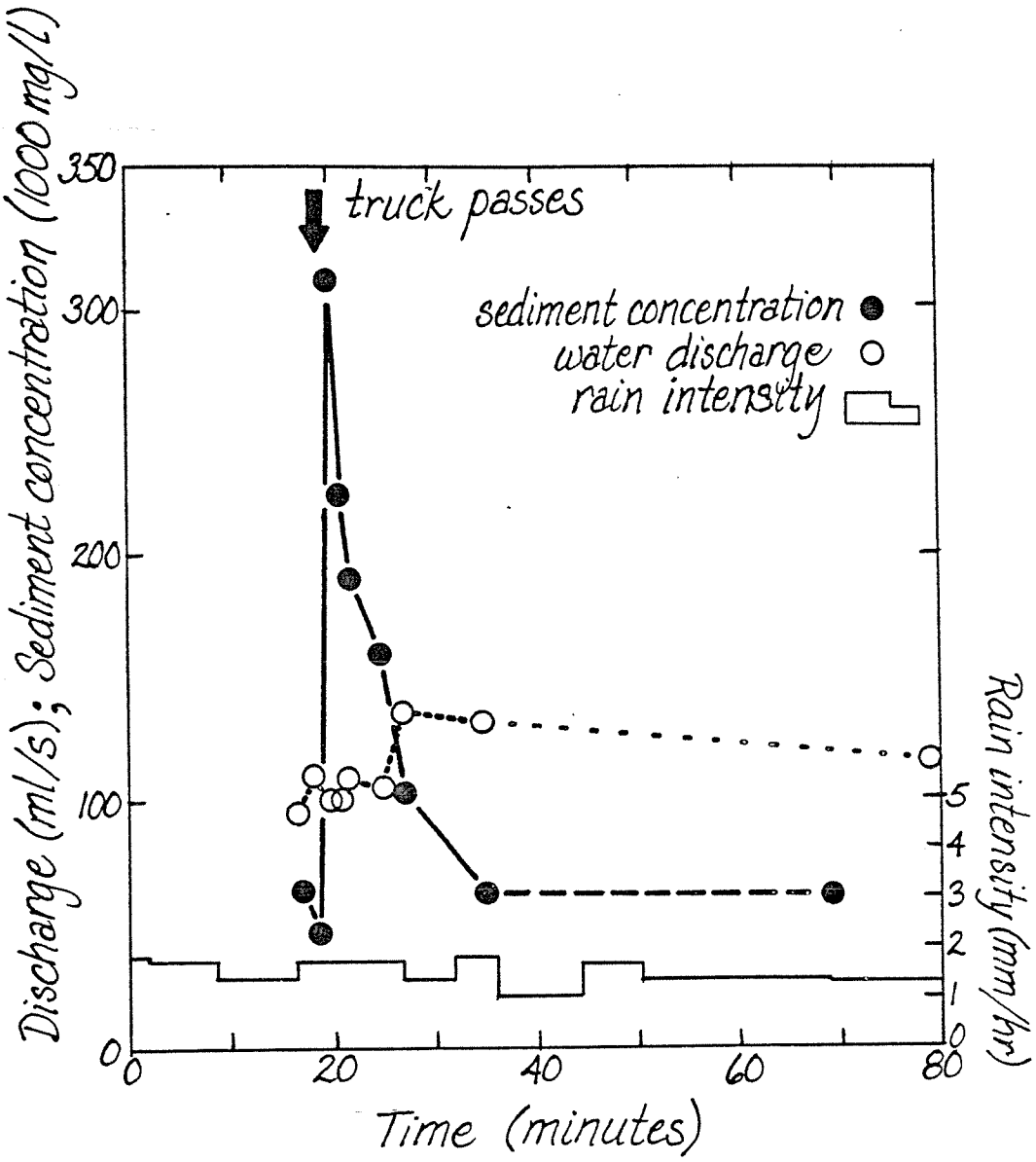

Figure 20. Short-term effect of truck traffic on sediment concentration in road-surface flow.

Finally, the nature of the categorization allows a relatively large variation in conditions within any one category. The heavy-use category, for example, includes roads bearing from 16 to 32 trucks per day, along with an undetermined number of light vehicles.

Despite the sources of variation, the slopes of the regression lines for different measurement sets on the same road types agree relatively closely, although, as expected, the positions of the lines differ. Direct regression of the pooled data, however, does not consistently reflect the slopes expected from the results of the single-storm regressions. Closer examination demonstrates that this is largely an artifact: the relatively broad category definitions and the relatively small range of discharges sampled during some measurement days combine to distort the plotted field and produce a pooled regression such as the dashed line shown in Fig. 21a from individual storm regressions shown in solid lines. This problem was avoided by determining the center of mass for the measurements from each storm and replotting all measurements with the centers of mass from the various storms superimposed (see Fig. 21b). A least squares regression is performed on the resulting field in order to compute an average slope, and the coefficient of determination is calculated. This coefficient is then compared with that calculated for the direct regression of the pooled data, and the regression method which produces the highest coefficient of variation is used to calculate the slope of the rating curve.

The averaged-slope method provided increased significance only for the heavily- and temporarily non-used roads (see Table 8). These roads contribute the most sediment and have the lowest initial variation in rating-curve slopes, and, because of the breadth of the heavy-use category, are expected to have the highest inherent variation in sediment concentration. The pooled data for these roads, including both isolated measurements and multiple measurements from single storms, were then regressed with slope constrained to equal the calculated average. Insufficient data exist for the averaged-slope method to be used on either moderately-used or abandoned roads, and sediment rating curves for abandoned, light-use, and paved roads were regressed directly from the pooled data for each road type. The result of these analyses is a regression line relating sediment concentration to water discharge for each of the 6 defined road-types (see Fig. 22).

The regression for the heavy-use roads is based on 54 measurements, all but two from a single road (see Appendix Fig. C-1). Eleven measurement days are represented, and 50 of the measurements were used to construct the average slope. Measurement days spanned the period January-May; during this time the roads also contributed data to temporary non-use and light-use categories. The concentration-discharge curve from this category plots the highest of those measured and has a slope of 0.76 ± 0.14, determined by averaging slopes of regressions of measurements from single storms, as described above. The indicated range is

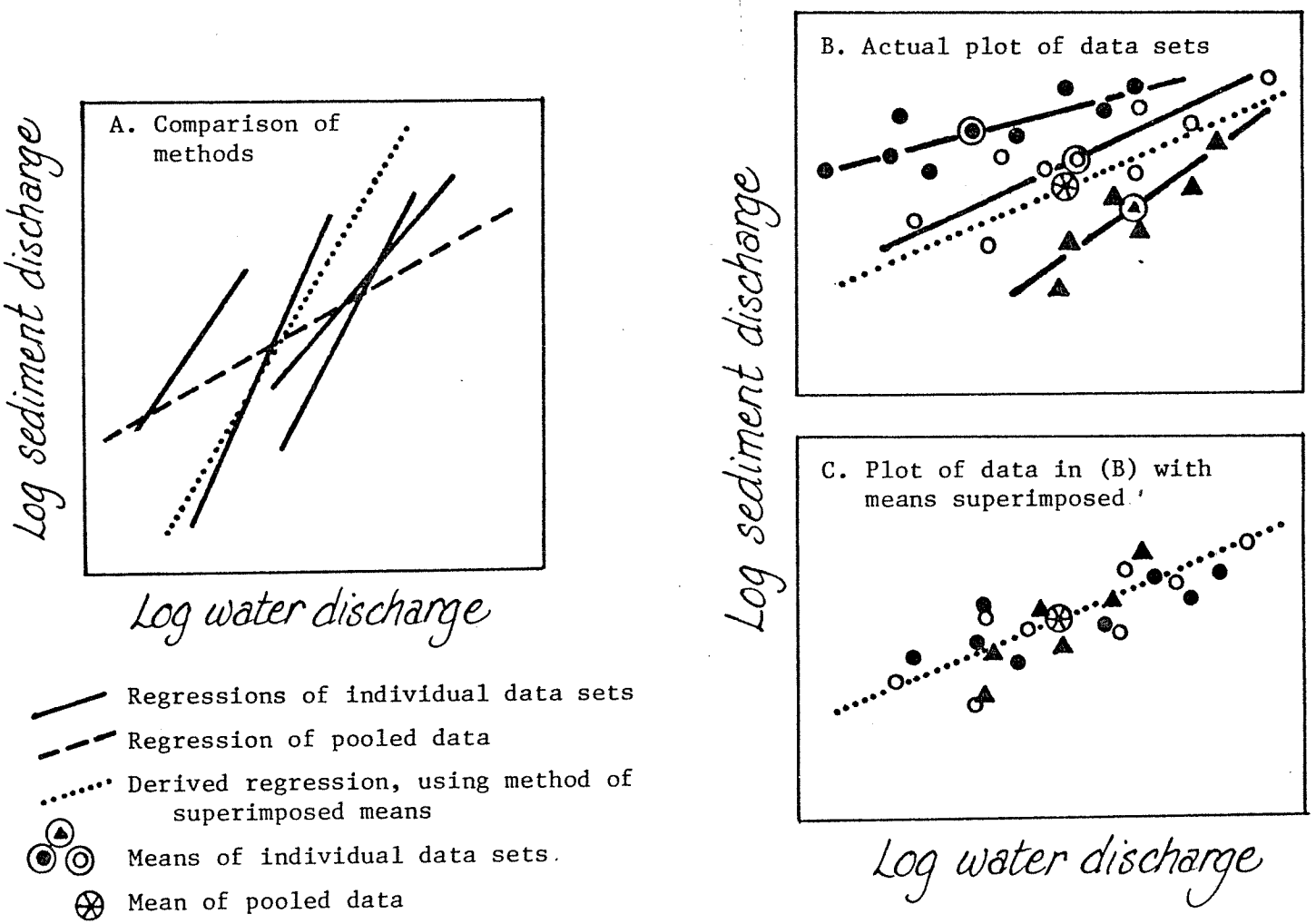

Figure 21. A comparison of individual regressions, pooled regression, and derived regression for hypothetical sediment rating curves, and method of construction of derived regression.

Table 8. Sediment concentration versus water discharge equations for various road use levels.

Road type	Type of regression	Number of samples	Number of roads	Number of measurement days	Coefficient	Exponent	95% confidence interval for exponent	r^2	Number of samples for derived slope
Heavy	standard	54	2	11	293	.63	±.25	.33	-
	averaged slope	54	2	11	161	.76	.14		50
Moderate	standard	13	2	3	3.3	1.01	.71	.48	-
	constrained slope	13	2	3	13	.76			-
Temporary non-use	standard	54	2	5	11	.90	.15	.74	-
	averaged slope	54	2	5	18	.78	.12		52
Light	standard	41	5	15	12	.44	.23	.23	-
	averaged slope	41	5	15	13	.42	.39		34
Abandoned	standard	29	2	17	70	-.10	.21	.04	-
Paved	standard	50	2	10	.83	.72	.21	.48	-
	averaged slope	50	2	10	1.5	.59	.24		46

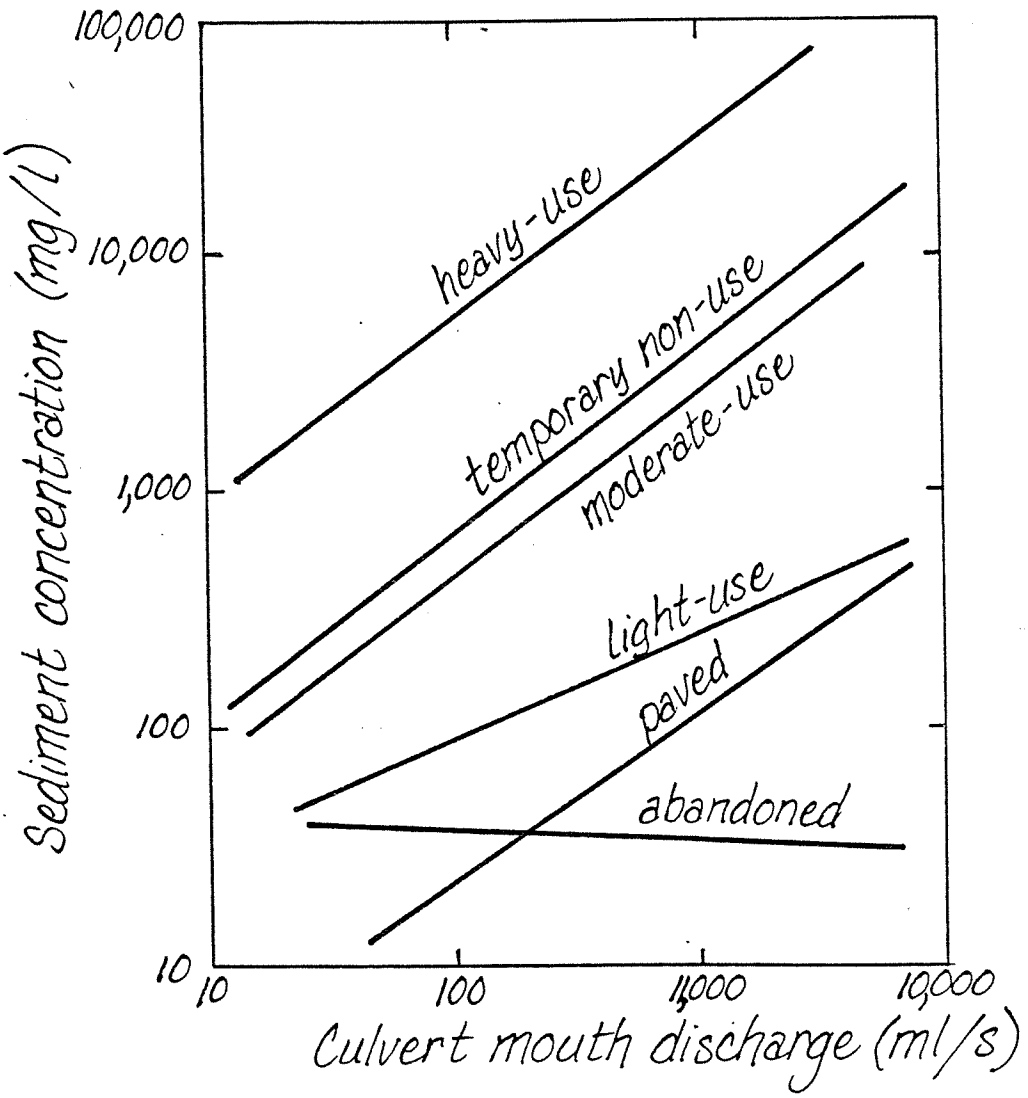

Figure 22. Concentration versus discharge curves for six road types.

that of the 95% confidence interval. Traffic on the measurement days varied between 16 and 32 trucks.

The slope of the concentration-discharge curve for heavy-use roads agrees quite closely with that of 0.78 ± 0.12 calculated for temporary non-use roads using the same technique, although the levels of the lines differ by nearly an order of magnitude. Fifty-four measurements from five days on two road segments were used to construct the rating curve for the weekend roads; 52 of these also contributed to the slope determination (see Appendix Fig. C-2). Traffic preceding the days of measurement varied from 36 trucks the previous day to 4 trucks two days before, but the two extremes plot in the same field. Twenty-four of the measurements were from the road which provided most of the heavy-use road measurements; 23 of these were taken within two days of heavy-use measurements, and a comparison of sediment rating curves for weekdays (heavy-use) and weekends (temporary non-use) directly illustrates the contrast (see Fig. 23). That the measurements are relatively insensitive to the traffic level on the preceding day and that the weekday-weekend difference exists at all imply that the road surface cleans up relatively quickly after use is discontinued; research on Weyerhaeuser roads suggests that the period necessary for clean-up may be as short as 6 hours (Kate Sullivan, Weyerhaeuser Co., personal communication). The prompt cleansing probably reflects the importance of traffic both in maintaining sediment supply and in actively entraining it by the shearing action of tires in the road-surface channels.

Few data were collected for moderate-use roads because the condition applied so infrequently; as one logger explained, "either they're haulin' or they ain't." The sparse data and small range of sampled discharges result in an imprecise though significant determination of the concentration-discharge curve slope and preclude use of the superimposed-mean method of slope averaging. Moderately-used roads are expected to reflect a condition intermediate to heavily-used and temporarily non-used roads because the supply of sediment continues to be renewed but the infrequent traffic makes it probable that some hours of depletion have occurred prior to a measurement. Slopes of the regression lines for heavy-use and temporary non-use roads agree to within 5%. On this basis, data from the moderate-use roads were used to establish the level of the regression line and were regressed with slope constrained to equal that of the heavy-use roads; the adopted slope is well within the confidence interval of the slope obtained by a standard regression of the pooled moderate-use data. The resulting curve is nearly colinear with but slightly lower than the temporary non-use curve. Two road segments contributed 13 measurements to this category from a total of three measurement days, and traffic load was one to two trucks per day (see Appendix Fig. C-3).

Light-use roads, on the other hand, are well-represented. Each of the five road segments contributing data also contributed to other categories. The scatter of data is much wider than in the cases already

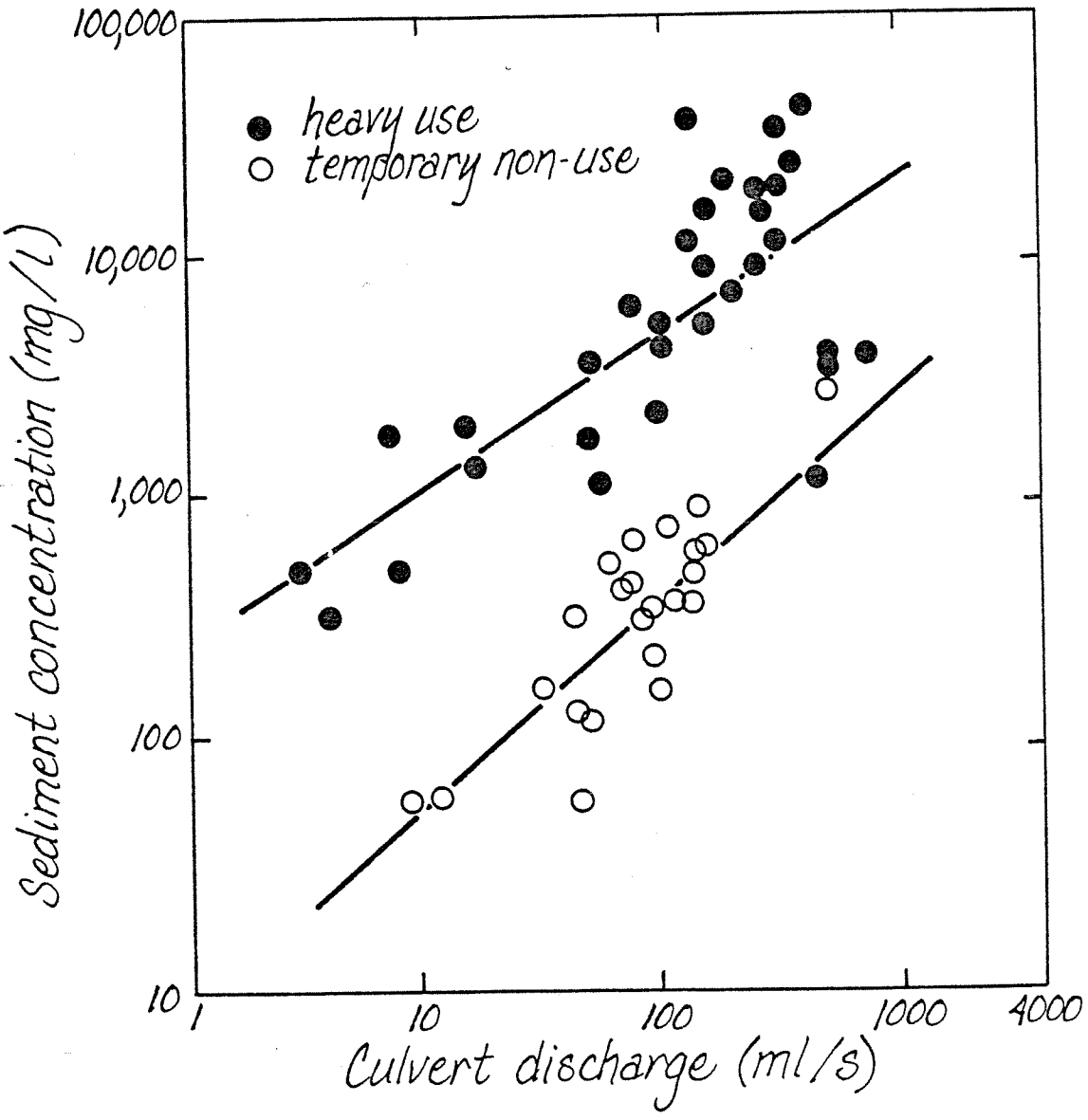

Figure 23. Sediment concentration versus discharge curves for a single road segment on adjacent heavy-use and temporary non-use days.

described (see Appendix Fig. C-4), as is the variation between the slopes defined by data-sets from individual storms. The overall slope is substantially lower, as might be expected if fine sediment were available but in short supply. Low flows on the rising limb of the hydrograph could carry off the major portion of the fine sediment contributed by occasional vehicles, leaving the high flows relatively depleted in fines. The slope of the concentration-discharge curve would thus be lower than if fines were available to all discharges. This situation would also lead to a more pronounced hysteresis in a time-sequence plot of concentration versus discharge, which would lead to increased scatter. The concentration-discharge curve for this road-type is constructed from a standard regression of 41 samples from 15 measurement days. The slope-averaging technique resulted in a lower regression coefficient than the standard regression of the pooled measurements, reflecting the high variation in component slopes.

Two paved road segments provided 50 samples on 10 measurement days and resulted in a concentration-discharge curve with slope quite similar to that of heavy-use and temporary non-use segments (see Appendix Fig. C-5), but with a level two orders of magnitude lower than that of the heavy-use road. Unlike the other road types, the paved road has no sediment source which provides dominantly fine material, so the concentration-discharge curve represents transport from a single source-type, backcut material. In this sense the situation is similar to that of the heavy-use road, where a single source-type also dominates. Efforts to determine an average slope using 46 of the measurements resulted in a lower coefficient of determination than that from a standard regression of the pooled data, so the latter method was used to calculate the slope of the concentration-discharge curve.

The abandoned-road category was the only one for which the concentration versus discharge slope was not significantly different from zero at the 0.05 level. The 29 measurements represented 17 measurement days on two road segments, so there were not enough measurements during individual storm periods to permit slope averaging. Direct regression of the pooled data resulted in a relation with a slope of -0.10 ± 0.21 (see Appendix Fig. C-6). A portion of the variation may be due to imprecision in the determination of discharge, since both road segments had been built without culverts and measurements were made in shallow ditches. This situation is typical for abandoned roads: they are either built without culverts or the culverts are removed when the roads are abandoned. Half of the discharge (Q_w) values were computed from the relation:

$$Q_w = \frac{wdu}{1.39}$$

where w is average width of flow, d average flow depth, u average flow velocity, and 1.39 an empirical coefficient determined from comparisons of calculated and measured discharges in these and similar channels (see Table 4). In the remaining cases it was possible to measure discharge

directly by capturing the flow in a plastic bag. Regressions of sediment concentration versus water discharge for direct discharge measurements and for calculated discharges are nearly identical:

$$C = 89.1\ Q_w^{-.16\pm.37}$$ for 15 data points with measured discharges

$$C = 78.7\ Q_w^{-.11\pm.35}$$ for 16 points with calculated discharges

where C is concentration in mg/l and Q_w is discharge in ml/sec.

The low exponent calculated for abandoned roads would be that expected if stored sediment capable of being transported were in very short supply or if sediment production rate were low and relatively constant through time. In the first case, low flows on the rising limb might deplete the sediment reservoir enough that there would be little left for higher flows to carry, particularly if the sediment produced were dominantly fine-grained. In the second case, if production rate were low and relatively constant through time, and if the sediment produced were dominantly fine-grained, then virtually any discharge would be competent enough to transport the sediment provided. The sediment discharge would thus remain constant, and the concentration would decrease with increasing water discharge. The extreme of either case requires that the supply of transportable sediment be low and that the size of newly available sediment be such that even low discharges would be capable of transporting much of it. If a wide range of sizes were available, then the depletion effect would not be as marked, since low flows would be incapable of removing much of the sediment. In this case sediment yield could increase with discharge because the larger sizes would become transportable with higher discharges.

Sediment smaller than 1 mm is noticeably absent on the abandoned road surface, which instead shows a well-developed armor layer of coarser pebbles. The ditch is armored with even coarser material, and the backcut is short, eroded back to a low angle, and partially vegetated. Because of the low height of the cut it has not penetrated bedrock, and thus the debris apron is composed dominantly of soil-derived silts. Moderate and high flows in the past have removed the transportable coarse material from its only source, the road surface, and new sediment is dominantly fine material derived from the backcut.

A gravel-surfaced mainline road segment had been selected for monitoring but was not included with other gravel-surfaced segments because of the difference in surfacing material. This road is wider than the other roads, averaging 4.4 m as opposed to 4.0 m, but the lengths of the segments are comparable. The road was built to sustain consistently heavy traffic loads, and competent surfacing gravels were imported from the Takoma Creek basin. Takoma gravels have an L.A. wear test percentage breakdown of 21% after 500 revolutions compared to an average of 33%

for the Clearwater gravels used on the other studied roads (for description of procedure, see American Association of State Highway Officials, 1966).

Forty-two samples were collected on two days with road use of 56 and 68 trucks per day (see Appendix Fig. C-7). Six additional measurements were made on two temporary non-use days, and five others on two days of moderate use. Measurement days were too few to justify determination of average slope, and a standard regression of pooled data produced no significant relation. Examination of the time sequence of measurements revealed the most pronounced hysteresis observed on any road. Independent regression of rising limb and falling limb data produced two curves whose slopes are highly significant and which do not differ significantly from each other, but whose regression constants differ by $10^{1.5}$. For these regressions and for that of the combined data, calculated slopes are substantially lower than that calculated for heavily-used management-standard roads, and the data plot in a slightly lower field.

Measurements from the mainline raod during temporary non-use periods, also plot in a field lower than that of the corresponding field for management-standard gravel roads, and the trends, though poorly defined in the case of the mainline road, are quite similar. The relation for moderate-use periods is even more poorly defined. Although the moderate-use fields overlap for the mainline and management-standard roads, the slope of the mainline data is not significantly different from zero and in fact appears to be negative.

In each case relationships for the mainline road are ill-defined and represent few data from few days of measurement, but they suggest that sediment concentration is likely to be lower for a given discharge and road use condition on the mainline road than on the management-standard roads. No final conclusions should be drawn, however, until measurements are made on other roads of the same character.

On each road all measurements that were made during the first month of the storm season were analyzed separately. Samples collected on four roads on a total of five measurement days during the first three weeks of the 1978-1979 storm season suggest that sediment yield is substantially less before the road substrate is saturated than during the wet winter months. Further work is necessary to define the differences in sediment yield between saturated and nonsaturated roads and to determine directly the cause of these differences. In addition it will be necessary to determine the amount of antecedent precipitation necessary for the surface to attain its full production rate. After the road has been saturated, however, temporary breaks in rainfall appear to have little effect: measurements made during storms after one-week dry periods in the winter do not differ significantly from those made during periods of continuous rain.

Prediction of Sediment Yield from Roads

The measured unit hydrographs for the road segments can be used to generate a continuous culvert hydrograph from a record of rainfall intensity at 15-min intervals. In order to facilitate calculations, the relationships between sediment concentration and water discharge for the six road types are transformed to sediment rating curves by plotting sediment discharge against water discharge. Water discharge can then be read from the hydrograph at intervals and the corresponding sediment discharge computed from the sediment rating curve for a specific road-use intensity. If these values are summed, the result is the total sediment yield at the culvert mouth.

Because the variation between standardized hydrographs for the heavily-used, moderately-used, and paved roads is less than the variation between the hydrographs averaged to construct each, these four hydrographs were averaged. An average road catchment area of 850 m^2, composed of surface, ditch, and intervening slope, was calculated by averaging the surveyed areas. This average agrees reasonably well with the area estimated from the overall average culvert spacing of 200 m (calculated from a count of culverts along 16 km of secondary gravel roads), the average road width of 4.0 m, and a slope plus ditch width of 2 m (both values from road specifications), since on the surveyed segments it was found that an average of 16% of the road surface drains off of the side of the road and generally infiltrates before reaching the stream system. These numbers result in an estimated culvert drainage area of about 1,000 m^2.

Sediment contribution from the abandoned road segment was expected to be more difficult to analyze satisfactorily, since roads built to be abandoned may be built to different specifications and occur in different kinds of terrain than the other roads considered. These roads are usually short, since they are built only to connect platforms with more permanent roads, and are often located on ridgetops, which provide frequent opportunities to divert water off the road surface. Average culvert drainage area is thus smaller than on permanent roads. In addition, the constructed hydrograph from the abandoned road is one of the least well-defined of the unit hydrographs. Because the concentration-discharge curve for abandoned roads is horizontal, however, the calculated sediment yield is sensitive neither to average area nor to hydrograph form, but instead depends most heavily on total runoff. In other words, the sum of the sediment yields from two short segments would nearly equal that from a single segment of twice the length. Poor definition of infiltration capacity on abandoned surfaces is thus an important source of uncertainty in the sediment yield calculations. In order to determine the sensitivity of the calculated sediment yield to possible uncertainties in hydrograph form and infiltration capacity, sediment yields from abandoned roads were calculated for both of the unit hydrograph forms derived from Fig. 17, and for two values of infiltration capacity.

Non-channelled flow disappears within minutes of the end of precipitation, and the area over which infiltration may occur is reduced to the area of the road surface channels and roadside ditch, which amounts to only 16.6% of the average 850 m^2 road catchment. Infiltration is thus considered to take place only during the period of precipitation. Because most rain falls as part of a continuous sequence (rain fell during 5,450 15-min periods during the 1977-1978 water year in the Clearwater basin, but runoff ceased only 649 times), the assumption is not critical. The additional infiltration at the ends of the 649 storms amounts to less than 160 mm of the year's total rainfall of 3,460 mm, which is close to the level of accuracy expected for the tipping-bucket rain gauges in the basin. Infiltration capacity on the paved road segments is estimated by applying a capacity of 0.0 mm/hr to the 69% of the road catchment area that is paved and a rate of 0.5 mm/hr to the rest of the area, resulting in an average infiltration capacity of 0.16 mm/hr.

Calculation of sediment yield during the 1977-1978 water year was performed by computer for road segments of each type. The precipitation record used is that from the Queets Ridge tipping-bucket gauge, maintained by the University of Washington Forest Hydrology Group under contract to the Washington State Department of Natural Resources. The gauge records a time-sequence of 0.01-in precipitation units on a strip chart. One-half hour time intervals are marked, and 15-min intervals can be easily interpolated. The gauge is located on the southern ridge of the basin and records annual rainfalls typical of the central part of the basin. During the 1977-1978 year, however, Queets Ridge precipitation totalled 3,468 mm, slightly less than the average annual precipitation of 3,630 mm in the central part of the basin (see Table 2). During the second half of December and the first half of January the gauge stopped working, and a record from the Stequaleho Stockpile gauge at a lower elevation was substituted. This record is marked in 2-hr intervals, but a separate scale was used to read this record, too, to 15-min intervals.

A consecutive listing of 15-min averaged rainfall intensities was loaded onto the computer along with the ordinates of the unit hydrographs and the coefficient and exponent of the sediment rating curves for each road type. The computer generated a hydrograph for each 15-min period, added the overlapping parts to construct the continuous hydrograph, and then calculated sediment discharge from water discharge at 1-min intervals. Sediment yield for each road type was then totalled by storm period and summed over the year. These values can be adjusted to reflect sediment yield in terms of road kilometers by using an average spacing of six culverts per kilometer for the 5.5° gradient.

The results of the calculation show that during the 1977-1978 water year a road in continual heavy use is expected to have produced about 439 tons of sediment per kilometer of road, or 130 times that produced from a road not undergoing hauling (see Table 9). Production is decreased by a factor of 7.5 during temporary non-use periods such as

Table 9. Calculated sediment yield from 850 m^2 segments of various road types for the 1977-1978 water year (road segments are described below).

Road type	Infiltration capacity (mm/hr)	Hydrograph type*	Sediment yield (t/yr)	Minimum** sediment yield (t/yr)	Maximum** sediment yield (t/yr)	Sediment yield per road kilometer (t/yr)
Heavy use	.5	I	73	51	107	439
Temporary non-use	.5	I	9.75	7.1	13.5	58
Moderate use	.5	I	6.1	-	-	36
Light use	.5	I	.56	.40	.81	3.4
Paved	.16	I	.31	.19	.54	1.9
Paved[1]	.5	I	.27	.16	.47	1.6
Abandoned[2]	.5	I	.085	.055	.137	.51
Abandoned[3]	.5	II	.087	.059	.136	.52
Abandoned[4]	1.0	II	.065	.043	.103	.39

Area 850 m^2

Gradient 5.5^{o}

Length of road surface 250 m

Culverts/kilometer 6

Width 4.0 m

Length of ditch 160 m

* I: In-use gravel road and paved road unit hydrograph.
II: Abandoned road unit hydrograph.

** Values calculated from extremes of 95% confidence interval for rating curve slope

1 Paved road rating curve used with gravel road infiltration capacity to estimate backcut erosion on gravel road

2 Included as test of sensitivity of abandoned road yield to hydrograph form

3 Included as test of sensitivity of abandoned road yield to infiltration rate

4 Best estimate of abandoned road characteristics.

weekends. Paving of a heavy-use road decreases sediment production to 0.4% of its original value, and complete abandonment of the road reduces sediment yield by three orders of magnitude from the heavy-use value.

That abandoned road contribution is less than that from paved roads is a function of three major factors: 1) paved roads produce more run-off since they are impervious; 2) roadside ditches are maintained on paved roads, while those of abandoned segments are partially filled in, allowing the backcut to revegetate and thus decreasing backcut erosion; and 3) paved roads are wider than roads built to be abandoned, resulting in a larger average backcut area.

In a drainage basin the contribution from each type of road depends upon the length of each road type in the basin, which in turn depends upon the stage of development of the basin. The length of road undergoing each level of use during the winter of 1978 was measured in Christmas and Stequaleho basins and the proportions were used to calculate total sediment yield from the road catchments for each basin (see Table 10). Variations in road gradient also affect the sediment yield and will be discussed in a later section. The present calculations are based on the assumption that sediment yields calculated for the average road gradient approximate the average of sediment yields calculated for the actual distribution of road gradients.

Not all sediment leaving the culvert mouth is transported as far as the stream system: a survey of 80 culverts indicates that 25% pour out water onto a slope, where it is left to infiltrate and the sediment is deposited. On the other hand, additional sediment may be contributed from the proportion of the road surface which does not drain into culverts but which does contribute drainage to the stream system. The road surface maps indicate that this component may be as much as 5% of the road surface, but any generalizations require a larger sample set.

In both basins the proportion of road length sustaining heavy use is less than one-third, but these roads contribute over 92% of the sediment, while the areally dominant abandoned roads contribute the least. Contributions from the other road types are also comparatively minor.

These calculations are based upon rainfall data from a single year, albeit a typical one. Their major value is thus in making evident the relative importance of various sources, and they should not be taken to indicate long-term averages. Because sediment concentration is dependent upon water discharge raised to a positive power, the influence of a few high intensity storms or of abnormally wet years will be large. These factors will be discussed in a later section.

The method outlined is also useful in assessing the importance of particular storm events and in examining the influence of certain design parameters on sediment yield. But before doing so, it is necessary to

Table 10. Sediment yield from road surface and backcut in Christmas (15.2 km^2) and Stequaleho (25.2 km^2) basins during the 1977-1978 water year. Totals subject to rounding error.

Road type	Road length (km)	Percent total length	Percent time in category*	Sediment yield per 850 m^2 road segment (t/yr)	Sediment yield from average-use road (t/km/yr)	Sediment yielded to stream per km^2 of basin** ($t/km^2/yr$)
Christmas						
Heavy	6.5	17	48	73	36	68
Temporary non-use	6.5	17	52	9.75	5.2	9.8
Light	8.5	23	100	0.56	0.8	1.4
Abandoned	22.7	60	100	0.065	0.2	0.4
Total	37.7				42	79
Stequaleho						
Heavy	12.5	26	48	73	56	78
Temporary non-use	12.5	26	52	9.75	8.0	11
Light	5.2	11	100	0.56	0.4	0.5
Abandoned	21.3	45	100	0.065	0.2	0.2
Moderate	5.9	12	100	6.1	4.5	6.4
Paved	2.5	5	100	0.31	0.1	0.1
Total	47.4				69	97

*A haul road is heavily used on 5/7 of total days, and assuming a 6-hour clean-up period, during 16/24 of the hours in each day. The rest of the time the road is considered temporarily non-used.

**Only 75% of culverts contribute flow to streams.

distinguish the effects of the two major sources contributing sediment to culvert effluent.

Separation of Road Surface and Backcut Erosion

As mentioned above, both road surface and backcut erosion contribute to the sediment load measured at the mouths of culverts. The relative importance of these sources was determined by independent measurements of sediment production from each source.

Road Surface Erosion

Water samples were collected from flow channelled into ruts on the surfaces of four of the monitored road segments and analyzed using the same methods as for culvert wash. Two of the measurement sets provided a wide-enough distribution of sampled discharges taken during periods of uniform traffic use to allow regression of sediment concentration against road surface discharge (see Appendix Figs. D-1 and D-2); in both of the cases the regressions are significant at the 0.05 level. Concentration versus discharge fields could be plotted for summer light-use, summer heavy-use, and winter moderate-use roads, and isolated samples were collected for summer heavy-use, winter temporary non-use, and winter light-use conditions (see Appendix Figs. D-3, D-4, and D-5). Scatter was expected to be considerably greater for the surface wash relationships than for the culvert discharge measurements for several reasons: 1) surface discharge is more difficult to measure and is accurate only to $\pm$ 20%; 2) traction load is more difficult to capture unless the measurement point is carefully selected; and 3) the road surface is extremely sensitive to short-term variations in use (see Fig. 20). Despite the high scatter and low significance of the regression, the slopes of the curves for surface and culvert flow on the moderate-use road in winter agree to within 10%. In the case of the summer light-use road agreement is poorer, but the 95% confidence intervals for the slopes overlap.

The small number of samples, few replications of the same use category on different roads, and few days of measurement make comparisons of regression lines tenuous, but in five cases the surface measurements can be compared directly to culvert mouth samples collected at the same time (see Appendix D). In each case the surface measurements plot one-half to two orders of magnitude above the corresponding culvert mouth measurements.

The relatively higher sediment load for road surface flow is to be expected if the dominant sediment source for culvert wash is the road surface. Not only would flow generated in the ditch and on the roadside dilute the concentration, but also the road surface flow generally occurs in two or more parallel or anastomosing strands. Thus, even if the flow were not diluted, sediment discharge for a given water discharge at the culvert mouth would not be that calculated directly from that discharge using the road-surface sediment rating curve

$$Q_s = a\, Q_w^{\,b}$$

where Q_s is sediment discharge at the culvert mouth, Q_w the corresponding water discharge and a and b empirically determined constants for given road conditions. Instead, if the road surface wash is channelled into n equal streams which join immediately above the culvert, and the roadside ditch is dry, sediment yield at the culvert mouth would be calculated from the relation:

$$Q_s = n\, a \left(\frac{Q_w}{n}\right)^b \qquad \text{or}$$

$$Q_s = n^{(1-b)}\, a\, Q_w{}^b$$

where (1-b) is less than 0 for all cases measured except that of the abandoned road. This effect is enhanced because surface wash generally enters the ditch at several points, further decreasing maximum road surface discharge for a given culvert discharge.

If the surface measurements are regressed with slopes constrained to equal those of the corresponding concentration-discharge curves measured at culvert mouths, then the above relationship may be used in conjunction with road-surface drainage maps to construct concentration-discharge curves for culvert flow for each of the six road conditions. These curves will reflect only the component of sediment derived from the road surface. The constrained-slope regression is used for road surface flow because sparse data in most cases make pooled regressions non-significant. Surface drainage maps are used to determine the length of the major surface channels on each of the four sampled road segments, and discharge in each channel is assumed to be proportional to the length of the channel. The component of discharge originating in the roadside ditch is considered to be proportional to the length of the ditch but is assumed to have no sediment load, and sediment is assumed to be neither lost to nor gained from the roadside ditch after surface flow enters the ditch. Any culvert discharge may thus be partitioned according to the length of each contributing channel. For each road segment:

$$Q_s = \sum_{i=1}^{n} \left[k_i\, a \left(\frac{L_i \cdot Q_t}{\sum_{i=1}^{n} k_i\, L_i} \right)^b \right] \qquad \text{or}$$

$$= a \left[\frac{Q_t}{\sum_{i=1}^{n} (k_i\, L_i)} \right]^b \sum_{i=1}^{n} \left[k_i\, (L_i)^b \right]$$

where a is the coefficient and b the exponent of the road surface sediment rating curve, L_i is the length of the i^{th} of n surface channels, k_i is the proportion of the flow from channel i that eventually enters the ditch, Q_t is the resulting discharge at the culvert mouth, and Q_s is the sediment discharge at the culvert mouth resulting from the observed road surface sediment transport (see Fig. 24).

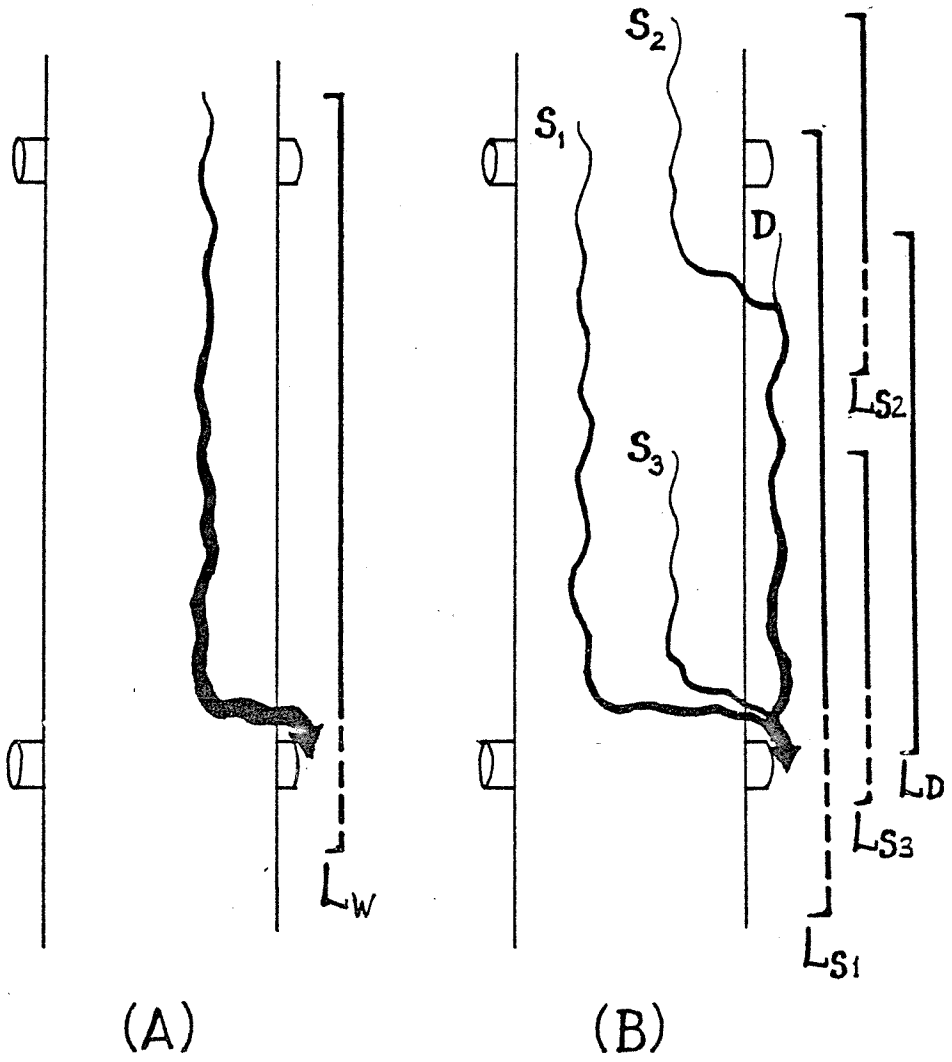

If Q_w is proportional to L and $Q_s = a\,Q_w^b$, where Q_w is culvert water discharge, Q_s culvert sediment discharge, and L the length of a strand of surface flow, then:

in case (A): Q_s is proportional to L_w^b

in case (B): Q_s is proportional to $(L_{s1} + L_{s2} + L_{s3})^b$

Figure 24. Effect of multiple road-surface channels on culvert sediment yield.

In three of the cases the concentration-discharge curve calculated for culvert flow from road surface data is within one-quarter of an order of magnitude of the level of the measured curve (see Appendix Figs. D-3, D-4, and D-5). In most cases the calculated curve is higher than that measured, possibly because of either the presence of an additional drainage component composed of clean baseflow during the sampled storms, the disregard of smaller road surface channels, or because some of the sediment load is being lost en route. In any case, the calculations demonstrate that the sediment load measured in road surface flow is sufficient to account for most of the sediment yield at the culvert mouths. In fact, calculations based on surface sediment measurements tend to overestimate culvert mouth yields.

Backcut Erosion

Sediment production from backcuts was evaluated using two different techniques. First, 36 networks containing a total of 230 erosion pins were located on backcuts and in roadside ditches throughout the central portion of the basin. In addition, paving a road surface effectively isolates the backcut as a source, so the above calculations of sediment production from a paved road segment provide an estimate of sediment yield from this source.

The backcut is composed of two major elements (see Fig. 10). At the top is a portion of the original cut-face, planed to an angle of 45° for unconsolidated material and 70° for hard rock. As material is lost from this face it accumulates on a debris apron of lower gradient which builds both outward, encroaching upon the roadside ditch, and upward, increasingly covering the free-face sediment source. Undercutting of the debris aprons by ditch flow and by ditch maintenance oversteepens the base of the apron, initiating small-scale debris failures and maintaining the effectiveness of the backcut as a sediment source. Erosion pin networks were located both on the free faces of the backcuts and on the debris aprons, and were measured at intervals over periods of up to 18 months. The erosion pins unfortunately were prone to such fates as being graded out, stepped upon by elk, fallen upon by trees, and pulled out by vandals; as a result only 67 pins survived long enough to provide a year's record. Measurements from pins surviving less than a year are used to examine seasonal variation in erosion rate.

The erosion pins used in this study are 25-cm galvanized wire spikes which are pounded perpendicularly into a slope. In areas where sediment accumulation was expected the nails were left protruding as much as 10 cm, but with rare exceptions they were pounded in beyond the depth at which the substrate becomes firm. Pedestals often formed around the pins where the nail heads effectively sheltered the ground surface from direct raindrop impact, but such pedestals were removed before the measurement of erosion. Observations were made at irregular intervals.

Of the 32 pins originally placed in 55° to 70° cut-banks, 17 survived longer than 11 months. These produced an average retreat rate of 16 mm/yr (± 3 mm/yr) perpendicular to the surface, with individual values ranging from 2 mm of aggradation to 40 mm of erosion (see Table 11). Measurement periods ranged from 350 to 381 days but averaged

Table 11. Yearly erosion pin data (A = aggradation; no symbol = erosion).

	Debris mantles below:			
Cut-face (mm)	0-1 m face (mm)	1-3 m face (mm)	3-5 m face (mm)	Thalweg of ditch (mm)
28.6	A 14.4	A 77.3	12.3	17.2
0	A 24.0	A 22.4	17.6	35.5
A 1.5	10.6	A 62.0	5.7	2.9
0.5	27.5	A 43.7	8	A 53.7
25.4	A 13.3	A 29.5	4.0	27.8
32.0	A 8.6	A 18.5	2.8	10.5
29.5	A 9.6	A 10.9	9.1	
40.2	3.8	A 21.7	7.9	
A 2.0	5.3	A 14.1	11.3	
16.8	10.6	A 16.3	31.2	
0	10.2	60.5	37.4	
11.0		3.7		
13.6		0		
4.8		44.8		
26.8		A 1.8		
25.9		A 89.5		
28.5		A 71.2		
		A 5.1		
		A 85.4		
		A 73.2		
		A 50.8		
		A 10.9		
Number of samples: 17	11	22	11	6
Mean: 16.5	A 0.2	A 27.1	13.4	6.7
Standard error: 3.4	4.5	8.4	3.4	13.0

362; values are thus normalized to 365 days by dividing each measured value by the proportion of a year represented by the measurement duration. Normalization is likely to introduce an error because the erosion rate varies through the year, but this effect is expected to be small over the periods considered.

Steep headwalls of recent slides provide an environment nearly identical to that of cut-banks. Slope angle and material are virtually identical, as are the processes active on the faces. Seven erosion pins sited on a landslide headwall were measured over a 13-month period; when the resulting measurements are normalized to a 12-month period they produce an average retreat rate of 16 mm (± 4 mm) for a year. Neither result is conclusive, but their agreement suggests that the values are of the right order.

An independent confirmation of the order of magnitude of the calculated loss rate over a longer period of time is provided by measurements of root exposure of plants growing on the 55° to 70° cut-faces. Sixteen measurements from plants ranging in age from 5 to approximately 15 years provide an average erosion rate of 15 mm/yr (± 2 mm/yr), agreeing closely with the measurements discussed above (see Table 12).

Table 12. Measurements of root exposure on cut-faces.

Species	Age (yrs)	Exposure (mm)	Erosion rate (mm/yr)
Salmonberry	5	73-121	15-24
"	5	150	30
Hemlock	13-16	180	14-11
"	13-16	142	11-9
"	7-12	105	15-9
"	7-12	180	26-15
"	12	140	12
"	13	230	18
"	13	300	23
"	9	138	15
"	9	93	10
"	6-9	120	20-13
"	7	57	8
"	8	79	10
"	9	80	9
"	9	180	20
mean			15 (±2)

An additional 83 erosion pin measurements were made over durations ranging from 1 to 4 months. Each measurement is divided by duration to compute average loss per month and then tabulated by month. In this case, too, normalization introduces errors, and the results should be taken to indicate seasonal trends rather than isolated monthly values. This approach is necessary because measurement durations were not uniform. The resulting tabulation then allows the calculation of average loss rate by month (see Fig. 25 and Appendix Table E-1). The wide scatter of the data points makes the significance of the calculated averages quite low, but the seasonal pattern is clear: erosion rates are highest during late spring and early summer and are relatively uniform through the rest of the year. This pattern is nearly the opposite of the pattern of rainfall distribution during the year of measurement (see Fig. 25); maximum erosion rate coincides with minimum monthly precipitation.

The same kinds of calculations may be made to evaluate aggradation rates on debris mantles at the base of backcuts. The observation that debris mantles of all sizes show identical, uniform gradients of 40^{o} to 45^{o} indicates that the rate of debris accumulation is uniform along the slope. The erosion pin networks are thus divided into three groups on the basis of the height of the free cut-face supplying them without regard to their location on the slope; accumulation rate was expected to reflect most strongly the size of the sediment-contributing face.

Four networks containing a total of 11 pins provided measurements of accumulation beneath cut-faces of 1 m or less in height. All of the pins survived for a year, but the high variation in measurements precludes any significance for the average aggradation of 0.2 mm/yr ($\pm$ 4.5 mm/yr), and not enough shorter-term measurements exist to examine seasonal differences (see Table 11).

Results from the five networks located beneath 1- to 3-m high cut-faces are more meaningful. Twenty-two pins survived for longer than a year (see Table 11) and indicate an average accumulation of 27 mm/yr ($\pm$ 8 mm/yr). Short-term measurements provide data only for the 6-month period between December and May, but there is an apparent trend of increasing accumulation rate from December through March (see Fig. 26 a and Appendix Table E-2). Interpretation of the March record is complicated by the presence of two extreme values; both points are excluded from the analysis.

Networks located on debris mantles beneath 3- to 5-meter cut-faces also produced statistically significant results, but the average accumulation rate is unexpectedly negative. Eleven pins in location for a year (see Table 11) show a net erosion of 13 mm ($\pm$ 3 mm). All surviving pins are located along a single heavily-used road segment, and ditch maintenance had taken place during the later part of the year; the net loss may have been due to undercutting by the grader. Monthly summaries of short-term measurements disclose a period of net erosion between

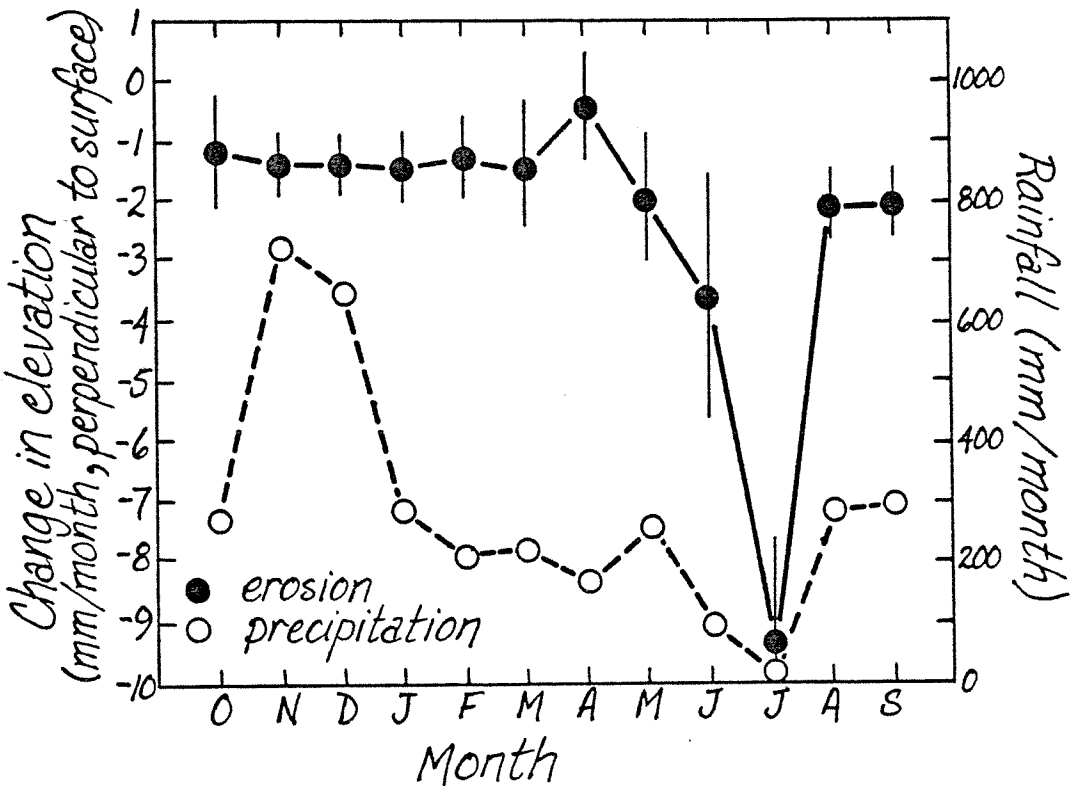

Figure 25. Monthly rainfall and cut-face erosion rate during the 1977-1978 water year. Error bars indicate standard error.

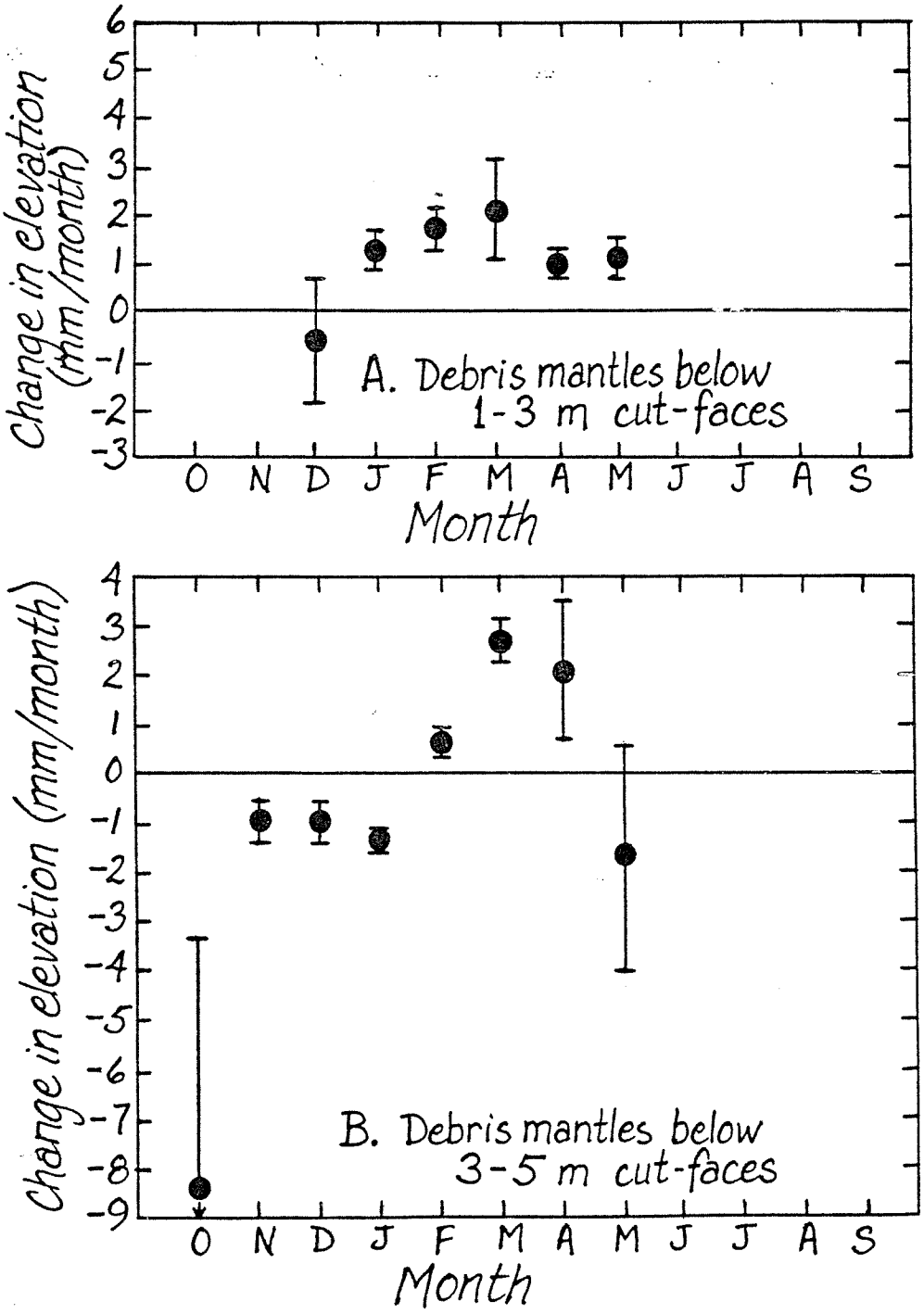

Figure 26. Monthly erosion pin measurements from debris mantles below 1-3 m and 3-5 m cut-faces. Bars indicate standard error. Measurements are made perpendicular to debris mantle surface.

October, when rains began, and January. As in the case of the networks below 1- to 3-m cut-faces, data from the early spring months show an increase in aggradation rate with a relative maximum in March. The May average is once again negative, but data consist of only four measurements and significance is quite low (see Fig. 26b and Appendix Table E-3).

Erosion pins located within 50 cm of a roadside ditch were put into a separate category. Along with pins in the ditches themselves, the toe-slope pins are quite vulnerable to disturbance by grading and none survived for an entire year. Three networks under 3- to 5-m cut-faces do provide short-term data for the months of February through August, however, and all demonstrate significant aggradation. The highest accumulation rates are once again in late winter and early spring, but no early winter measurements exist for comparison (see Fig. 27 and Appendix Table E-4).

The final set of 46 pins was installed in roadside ditches. Six of the pins survived for a year (see Table 11) and indicate an average of 7 mm erosion, but significance of the result is quite low and all pins are located under short cut-faces. Consideration of individual measurements by month for networks below moderate-height and long cut-faces discloses consistent net aggradation from February through August (see Appendix Tables E-5 and E-6). Most of the pins were eventually lost during ditch maintenance in the fall. Observation of ditches on abandoned roads demonstrates that such maintenance is necessary to keep ditches free of backcut debris; ditches would otherwise be sites of net deposition. No measurements could be made of volume of sediment removed from the ditches during maintenance since it was in most cases graded out onto the road surface.

The high erosion rate from cut-faces during summer months and relatively low winter erosion rate suggest that the most intensive backcut erosion is by such dry-season processes as dry ravel, rather than wet-season rainsplash or sheetwash. This pattern is to some extent reflected in debris mantle measurements. The highest accumulation rates on debris slopes are in spring, while winter measurements show net erosion. Winter processes such as rainsplash and needle-ice activity are observed to be important in transporting sediment down debris slopes, and high winter ditch flows repeatedly undercut the slopes, causing accelerated erosion of the debris. Dry ravel, on the other hand, has only limited effectiveness in initiating transport on a slope which is already at the angle of repose.

The importance of dry ravel in removing sediment from cut-faces is supported by measurements from a toe-slope erosion pin network below a 6-m cut-face. A network of four pins showed an average of 3 mm aggradation in a 24-hr period during the first prolonged sunny period after a

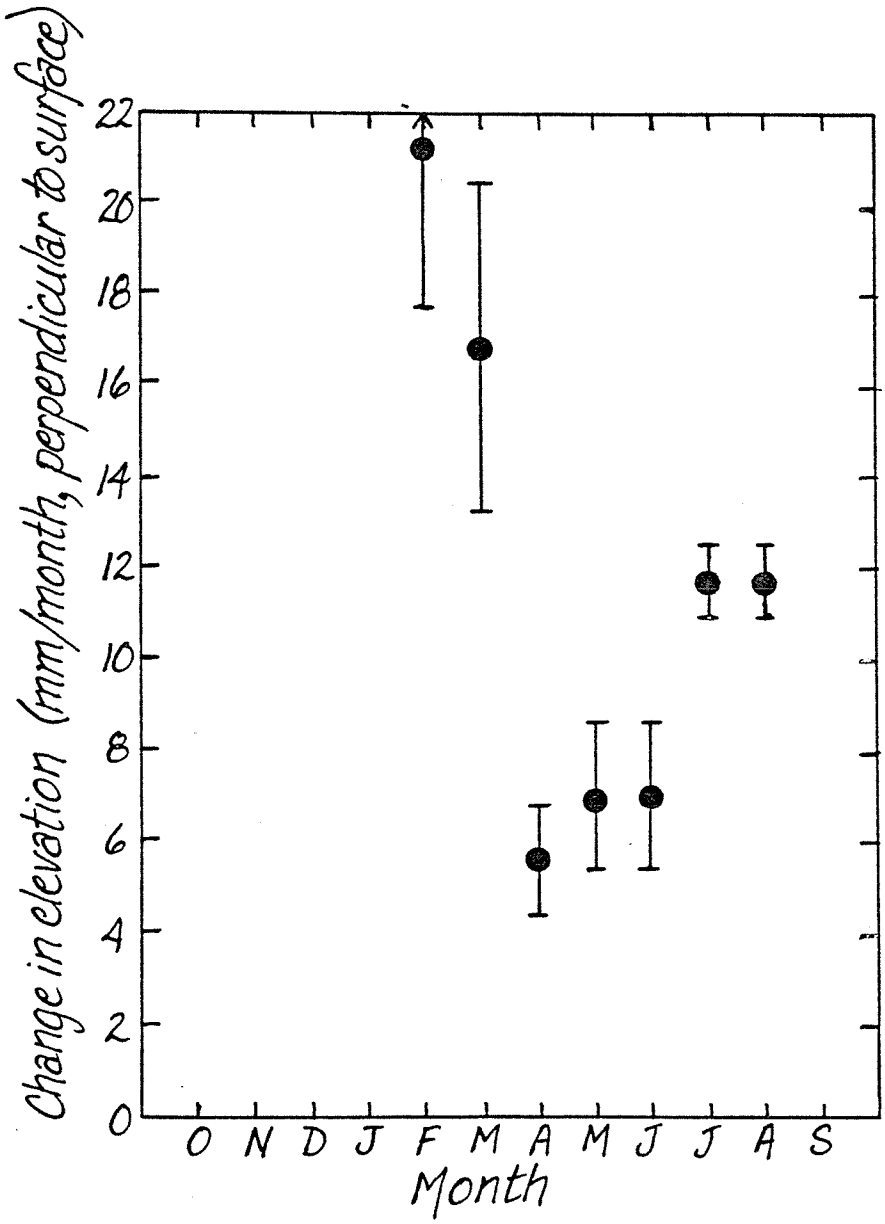

Figure 27. Averages of monthly erosion pin measurements from toe-slopes of debris mantles. Bars indicate standard error.

storm. Observations during this period suggest that much of the material was mobilized directly from the cut-face, where the sediment had been held in storage in small-scale depressions and rills.

Given the area of backcut on a road segment, the measured cut-face retreat rate can be used to provide an estimate of the maximum possible annual sediment contribution from backcut erosion, while measurements of accumulation rates on debris mantles allow an estimate of sediment delivery ratio from backcut to ditch. Cut-face and debris mantle heights measured at points along the surveyed road segments were used as a basis for estimating heights of cut-faces and debris mantles on aerial photographs. Mapping of estimated heights along 12 km of road provides an average cut-face area of 960 m^2/road-km. Associated with the cut-face is an additional 2,450 m^2/road-km of debris mantle surface. Applying the average cut-face retreat rate of 16 ($\pm$ 3) mm/yr to the average area of cut-face results in an estimated sediment production of 16 $\pm$ 8 m^3/road km-yr, where the reported range is that of the 95% confidence interval. The lengths of road having cut-faces of different heights were tabulated separately, allowing debris accumulation rates to be computed according to the rates measured below cut-faces of different heights. This procedure results in a calculated accumulation rate of 46 $\pm$ 38 m^3/road-km-yr on debris mantles beneath an average distribution of cut-face heights. Slopes under 1-m to 3-m cut-faces account for 72% of the area of debris mantle, so the relatively poor measurements of accumulation rate on shorter and longer slopes have little effect on the calculated average. Three measurements of the bulk density of debris accumulations provide an average of 0.71 ($\pm$ 0.02) g/cm^3, indicating an increase in pore space by 29% over that present in the cut-face soils, which have an average bulk density of 1.00 ($\pm$ 0.01) g/cm^3. Even when this increase in pore space is considered, the debris mantle accumulation rate of 33 $\pm$ 27 t/road-km-yr is seen to be more than sufficient to account for the 16 $\pm$ 8 t/road-km-yr of sediment removed from cut-faces. This apparent discrepancy probably reflects the high uncertainty associated with the calculation.

Finally, as mentioned in the previous section, the sediment yield from a paved road segment is derived from the backcut alone. Thus the calculation of sediment yield by the method outlined in that section should represent the sediment yield of the isolated backcut if the infiltration rate of 0.5 mm/hr measured on gravel roads is used in conjunction with the sediment rating curve for paved roads. Such a calculation produces an annual sediment yield of 1.6 m^3/road-km from the backcut alone, supporting the contention that the amount of sediment produced from the cut-bank may be very nearly balanced by the amount of sediment entering storage on debris slopes and in the roadside ditch. As mentioned above, the production rate from cut-faces changes with time. Net production from the cut-face will decrease as the debris mantle increasingly covers the free face. However, the debris apron may eventually stop growing when ditch maintenance at its toe prevents the apron from extending further into the ditch. At this point the mantle will cease

to aggrade and will act merely as a transport slope; all of the material lost from the cut-face will then be made directly available to ditch transport. If maintenance ceases, as in the case of the abandoned roads, the toe of the debris mantle generally encroaches upon and fills in the ditch, allowing further aggradation upslope and a continued decrease in contributing cut-face area.

Applications

Surface Erosion per Unit Area

The separation of backcut and surface sources makes possible the calculation of surface sediment production per unit area of road surface. As explained in the previous section, the component of sediment generated by backcut erosion is estimated by calculating sediment yield from a road segment using the sediment rating curve measured from paved roads and the infiltration rate from in-use gravel-surfaced roads. This value may then be subtracted from the sediment yield of 73.1 t/year for a heavily-used gravel road segment to calculate a sediment production rate of 72.8 t/road-segment-yr from the road surface alone for the 1977-1978 water year. Of the 850 m^2 road catchment area, 564 m^2 is road surface area and the remainder is ditch or road-ditch slope, the contribution of which has been subtracted out as described above. Averaging the remaining sediment production rate over the road surface area results in a production rate of 1,290 t/ha-yr of road surface. This is equivalent to 520 t/road-km-yr for a 4.0 m wide road, but about 37% of this area, as calculated from surveyed maps of road surface drainage patterns and observations of culvert outflow paths, does not contribute runoff or sediment to streams. The same calculations may be carried out for temporarily non-used and lightly-used roads, and are listed in Table 13.

Comparison with Universal Soil Loss Equation Yields

The Universal Soil Loss Equation (USLE) was developed by Wischmeier and Smith (1965) to calculate soil loss from agricultural land and has been used by Farmer and Fletcher (1977) to estimate sediment yields from highway construction sites. Calibration of the equation was based on many years of data on sediment yields from experimental plots of different character and undergoing different treatments. Soil loss (A, in tons/acre) can be calculated from a rainfall erosivity index (R), a soil erodibility index (K), a hillslope length index (L), a hillslope gradient index (S), an index of crop-management practice (C, essentially a land-use index), and an index of erosion control practice (P):

$$A = R\ K\ L\ S\ C\ P$$

Table 13. Sediment yield per average road segment and per unit area of road surface for 1977-1978 water year.

Road type*	Total erosion per road segment (t)	Road surface erosion per segment (t)	Yield per unit area of road surface (t/ha)	Sediment delivered to stream (t/road-surface-ha)
Heavy use	73	73	1300	810
Temporary non-use	9.75	9.5	170	110
Moderate use	6.1	5.8	100	65
Light	.56	.29	5.1	3.2

*Abandoned roads are not included since separation method requires that backcuts be similar to those on paved roads; abandoned backcuts are generally vegetated.

The R factor may be calculated directly for the Clearwater basin by using a technique described by Ateshian (1974). West of the Cascades the factor has been found to be closely approximated by:

$$R = 27.00\ I^{2.2}$$

where I is the 2-yr, 6-hr rainfall depth in inches. In the Clearwater area this intensity is approximately 2.7 in/6 hr (NOAA 1973) and the resulting value of R is 240.

The K factor was evaluated for four road types from point-count measurements of grain size on the road surfaces. This method yields at best only an approximation of size distribution. These data could then be used in the nomograph presented in Wischmeier et al. (1971) to calculate K as a function of percent silt and fine sand, percent sand, percent organic matter (equal to zero for the surfacing material), soil structure (considered to be massive), and permeability (very low). The coarse and fine sand fractions could not be distinguished using the point count data, so the results are presented as a range. Slope length is set to equal 250 m, the expected length of the 850 m^2 road segment considered in the previous section, and the gradient is the average slope of 5.5^{o} for that segment. The S and L factors are evaluated together using the chart given in U.S.S.C.S (1972). The erosion control practice index, P, can be considered to be equal to 1.0, since erosion control procedures generally involve changes in other factors such as

slope length (culvert spacing) or material character (surfacing material).

The remaining factor, C, is more difficult to evaluate. On agricultural land the value of C is influenced by the kind of crop being grown, its stage of growth, the kind of tilling used, and the amount and type of mulch applied. On a gravel road surface the presence of a pebble armor layer provides an analogue to an agricultural mulch; such armor layers have in fact been applied artificially as mulch on agricultural land. The effects of armoring have not been fully quantified in the context of the Universal Soil Loss Equation, although some measurements of sediment yields from armored and non-armored plots have been made (see Meyer et al. 1972, Wischmeier and Meyer 1973, and see Fig. 28). As an approximation C is here considered to be the proportion of the ground surface that is not covered by the armor layer. The point counts of grain size on the road surface may now be used to estimate a C value for the different use-level roads, assuming that all grains larger than 4 mm participate in the armor layer. This size was selected because it was the smallest size defining a measurement boundary that was not found in road-surface channel deposits, implying that particles larger than 4 mm are not commonly mobilized on the road surface.

The USLE may thus be used to calculate sediment yield from each of the four road types for which surface textures were measured, and these values may be compared to those computed from measurements of sediment discharge (see Table 14). Predicted and measured values for the heavily-used and temporarily non-used roads are seen to be of the same order,

Table 14. Universal Soil Loss Equation calculations.

Road type	R	K*	LS	C	USLE sediment yield** (t/ha)	Sediment yield computed from measurements (t/ha)
Heavy-use	240	0.475 ±.075	3.6	0.80	730 ±120	1300
Temporary non-use	240	0.24 ±.07	3.6	0.64	300 ± 90	170
Light-use	240	0.20 ±.03	3.6	0.67	260 ± 40	5
Abandoned	240	0.155 ±.005	3.6	0.46	140 ± 4	<1.1

*Boundaries of range reported for K are the values calculated by considering all of the sand fraction to be fine (maximum) and all to be coarse (minimum).

**Range shown is that resulting from uncertainty in value for K.

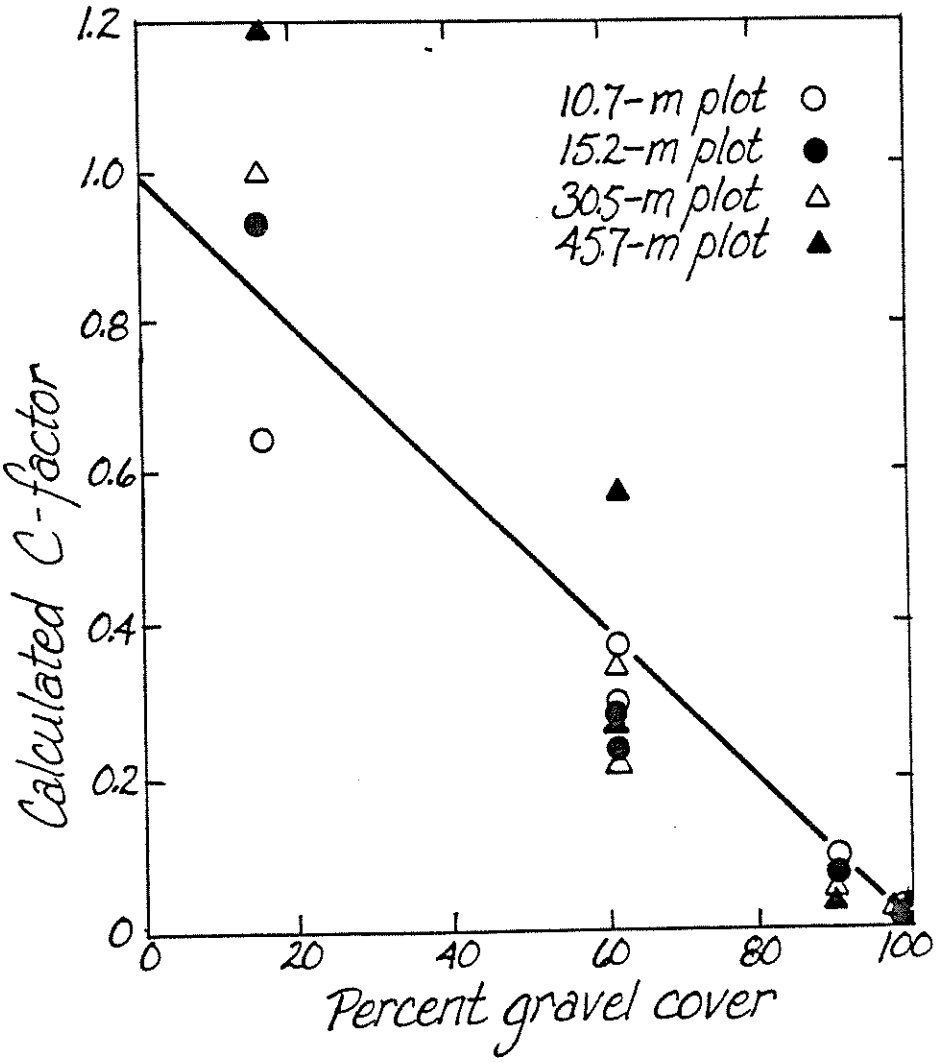

Figure 28. Universal Soil Loss Equation C-factors calculated from erosion plot data reported in Meyer et al. 1972 and Wischmeier and Meyer 1973.

while the USLE greatly overestimates production from lightly-used and abandoned roads. The increasing overestimation for the more heavily armored roads is probably an indication of the complexity of the armoring problem: the effectiveness of the armor layer is dependent not only upon the percentage of the surface covered but also upon the size-distribution of the material present. Particles of a specific size may be trapped by a coarser-grained armor layer and thus be considered a part of that layer, while in the absence of the coarser material particles of that size may be easily transported by the relatively higher-velocity surface wash.

Culvert Spacing

The effect of altering culvert spacing can be examined by computing sediment yields for different sized basins, using the method developed in the previous section. This method provides only an approximation, since the form of the unit hydrograph will change as the length of the basin changes: decreased basin length should decrease the lag-to-peak of the hydrograph and increase its peakedness, though the magnitudes of the ordinates of the unit hydrograph will decrease to accommodate the decrease in drainage area. The fact that ditches on the monitored road segments ranging in length from 123 m to 187 m produced hydrographs with virtually identical forms indicates that the effect on hydrograph form is within the imprecision of measurement for this range of lengths. Ditch length (in meters) for the four monitored non-abandoned roads averages 0.19 times the basin area (in square meters), with a range of 0.17 to 0.20. The 850 m^2 basin used as an average would thus represent a ditch length of 162 m and a culvert density of 6/km. A 200-m ditch length corresponds to a 1,050 m^2 basin, and a 110-m length would be expected for a 580 m^2 basin; these values were selected for examination in order to remain near to the range of road areas for which hydrographs had been measured.

The unit hydrograph used in the calculations for non-abandoned roads of the previous section was adjusted to reflect each of these areas by multiplying each ordinate by the ratio between the new area of interest and the 850 m^2 area previously used. The previously described computer program was then used to compute sediment yield for the 1977-1978 year under the new conditions for road segments of each use type. Sediment yield per road kilometer could then be calculated from the new culvert densities of 4.8/km for the 1,050 m^2 catchments and 8.7/km for the 580 m^2 basins, with the proportion of culverts emptying into the stream system assumed to be the same as in the previous calculations. The resulting estimates of sediment yield are shown in Fig. 29 and Table 15. For this range of lengths, sediment yield is seen to increase approximately as the 0.8 power of ditch length. It should be noted that the culvert densities would represent an average spacing for 4.5° to 6.5° road gradients; individual spacings on this gradient indeed already vary over this range for the present average culvert density. The road lengths used in these calculations represent the length of road surface

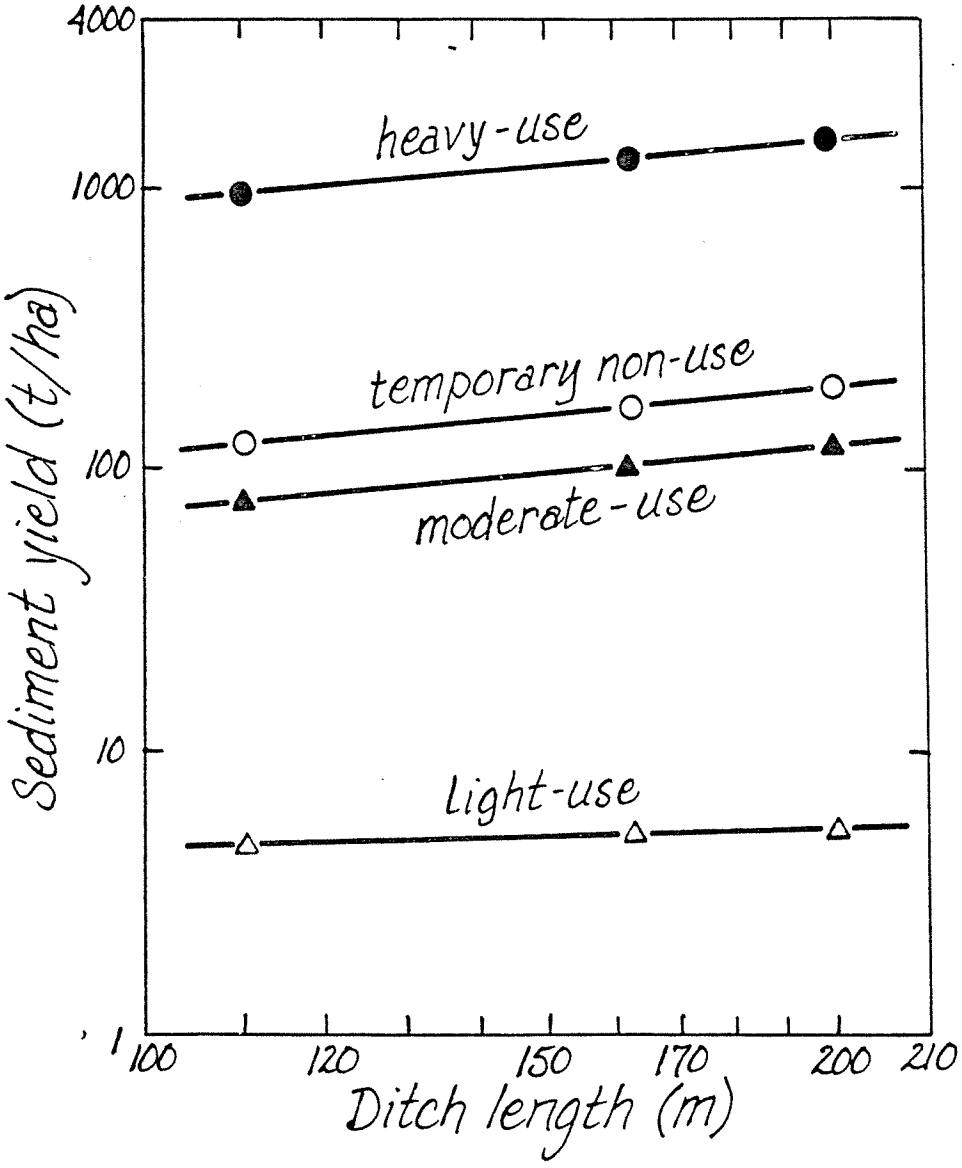

Figure 29. Sediment yield per unit road surface area from roads of various culvert spacings.

Table 15. Sediment yields for road segments of various culvert spacings.

Road catchment area (m^2)	580	850	1,050
Road surface area (m^2)	385	564	696
Ditch length (m)	110	162	200
Culvert density (per km)	8.7	6.0	4.8
Road surface length (m)	170	250	309
Sediment yields (t/ha):			
Heavy use	970	1,300	1,500
Temporary non-use	120	170	200
Moderate use	77	100	120
Light use	4.7	5.1	5.2

flow expected for the given ditch lengths, based on data from the surveyed road segments. Because the location of drainage divides on a road surface is not constrained by the location of the culverts in the roadside ditch, the length of road surface flow on a road segment may be much longer than the ditch length (see Fig. 11).

Transverse Road Slopes

Sloping the road surface in order to remove drainage from the bearing surface as quickly as possible is gaining popularity in some districts. By sloping the road surface outward it is possible to almost completely prevent road-surface sediment from entering the stream system, since the major portion of the runoff is left to infiltrate on the slopes below the road. The transverse gradient is designed to be large enough that the off-road drainage is well-dispersed in order to avoid initiating landslides by concentrating drainage. Such plans, however, have met some resistance from truckers, who claim that out-sloping presents a hazard to driving. Construction of a road-surface slope toward the backcut has therefore been more widely implemented. Drainage on these roads, too, is removed from the bearing surface over a short distance, but runoff is concentrated in ditches and channelled through a conventional culvert system.

The effect of an inward road-surface slope may be examined on the monitored roads by applying sediment rating curves for road surfaces to the appropriate components of the measured unit hydrographs. Concentration-discharge curves were constructed directly from measurements on two

roads (see Appendix Figs. D-1 and D-2), but one of the data sets represents measurements during dry-season storms and so does not characterize the road-surface conditions considered during this study. Flow measurements on road surfaces during winter storms were otherwise too few to allow the direct construction of concentration-discharge curves, and road-surface curves were instead calculated from the measured culvert-mouth curves. The method used is the inverse of that used to reconstruct culvert-mouth concentration-discharge curves from surface flow measurements on roads, as described in the previous section. During the discussion of these previous calculations, however, it was noted that road-surface curves tend to overestimate the level of the culvert-mouth curves, and the difference was attributed to uncertainty about the importance of a baseflow component and the disregard of low-discharge rivulets draining small areas of the road surface. This component, estimated by averaging the differences in level between measured and reconstructed culvert-mouth concentration-discharge curves on summer roads, must now be added to the calculated surface curves for the winter roads. It should be noted that the road-surface curves constructed method provides only an estimate of the relationship for wet-season roads.

The spacing of road surface channels on different in-slope gradients was estimated using measurements of channel spacing on banked curves on the surveyed road segments. A plot of channel spacing against maximum gradient (see Fig. 30) suggests an inverse relation between the two parameters. The data points recorded as open circles are those for which most of the flow proceeded along the road surface ruts, and the transverse channels were fed only by breaches from the rut. The envelope curve is thus expected to be more characteristic of non-rutted conditions.

Transverse gradients of 3^{o}, 5^{o}, and 7^{o} were selected for evaluation on the 5.5^{o} road segment examined in the previous calculations. For each case the magnitude and direction of the maximum gradient was calculated and used to estimate channel spacing (see Table 16). Channel lengths could then be calculated by assuming that the flow would follow the maximum gradient; in reality some channelization occurs for short distances along road ruts, but this effect is not considered. The inward surface slope is expected to restrict the length of road surface contributing to culvert drainage by diverting all flow above the neighboring up-road culvert into that culvert. The lost area is compensated for by the addition of both the portion of the road surface that is located above the culvert in question but which would have drained into the culvert beyond, and the portion which would have drained off of the outer edge of the road (see Fig. 31). Average culvert drainage area is thus expected to increase by about 16%, as determined from road surveys. The number of surface channels is calculated by dividing the average

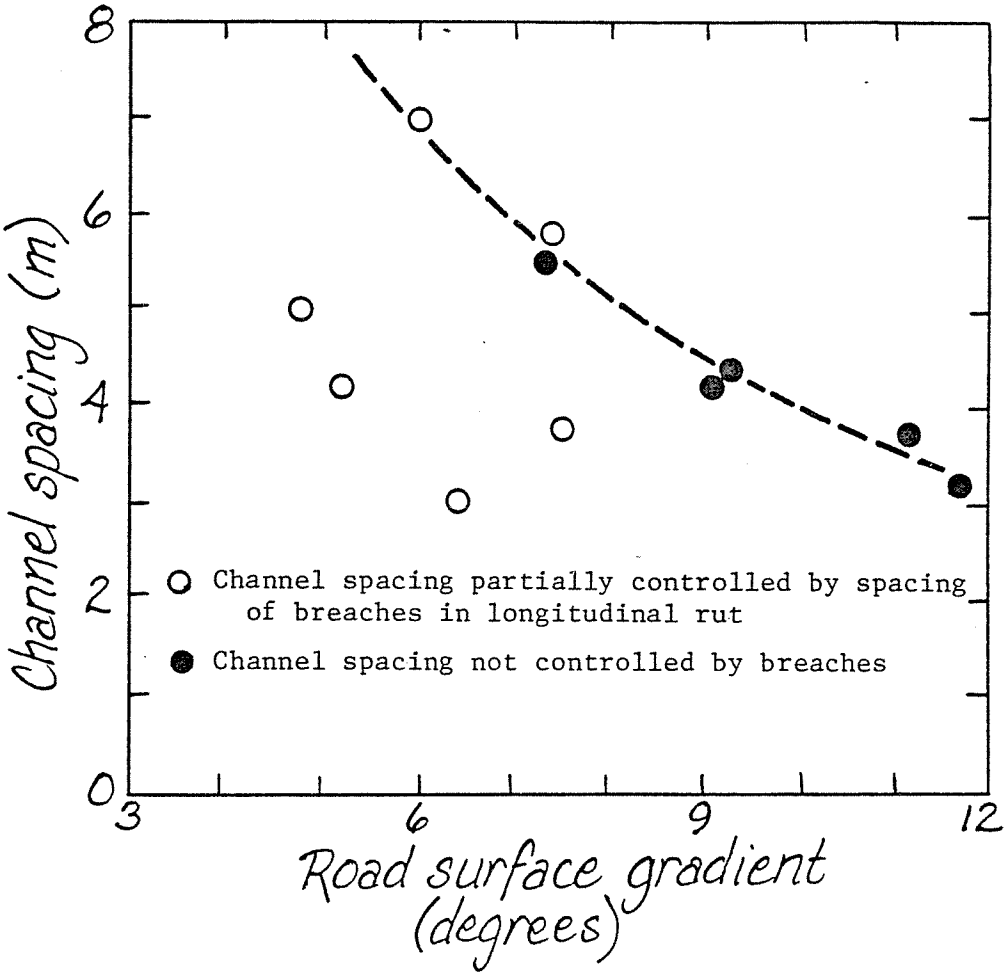

Figure 30. Road surface channel spacing as a function of road surface gradient (as calculated from measurements of down-road and transverse gradients). The indicated envelope curve is fitted by eye.

Table 16. Analysis of transverse slopes and calculation of sediment yield from 167-m in-sloped road segments with 5.5° down-road gradients.

Transverse gradient (degrees)	Maximum gradient (degrees)	Channel spacing (m)	Channel length (m)	Number of channels in road segment	Sediment yield computed from measurements (t/yr)	USLE sediment yield (t/yr)
3	6.3	6.8	7.3	24.6	23	12
5	7.4	5.7	5.2	29.3	17	10
7	8.9	4.7	4.4	35.5	15	9

ditch length of 167 m by the estimated channel spacing. These results may then be used in the equation:

$$Q_s = n\, a \left(\frac{L_r}{nL_r + L_d} Q_w \right)^b$$

to construct a culvert-mouth sediment rating curve for in-sloped roads from that for road surface wash. Here Q_s is the culvert-mouth sediment discharge at a water discharge of Q_w, a and b are the coefficient and exponent of the road-surface sediment rating curve, n is the number of road-surface channels, L_r is the length of each road-surface channel, L_d is the ditch length, and $L_r/(nL_r+L_d)$ is the proportion of the total discharge from each of the road surface channels.

The resulting rating curves (see Fig. 32) can then be used to compute a year's sediment yield for the in-sloped roads. The unit hydrograph ordinates are adjusted to reflect the 16% increase in area, but the form of the hydrograph is assumed to remain the same.

Although uncertainties in hydrograph and sediment rating curve forms make these results only approximate, the calculated sediment yields of 23, 17, and 15 t/road-segment-yr for 3°, 5°, and 7° transverse slopes (see Table 16) represent a decrease in sediment yield by a factor of 3.0 to 4.5 when compared to conventionally sloped roads. The order of this decrease is supported by computations using the Universal Soil Loss Equation. The length-slope factor is computed for each of the in-slope gradients by using the channel lengths and maximum gradients already calculated; all other parameters remain as before. Results are listed in Table 16, and are seen to reflect a decrease by a factor of 3.3 to 4.3,

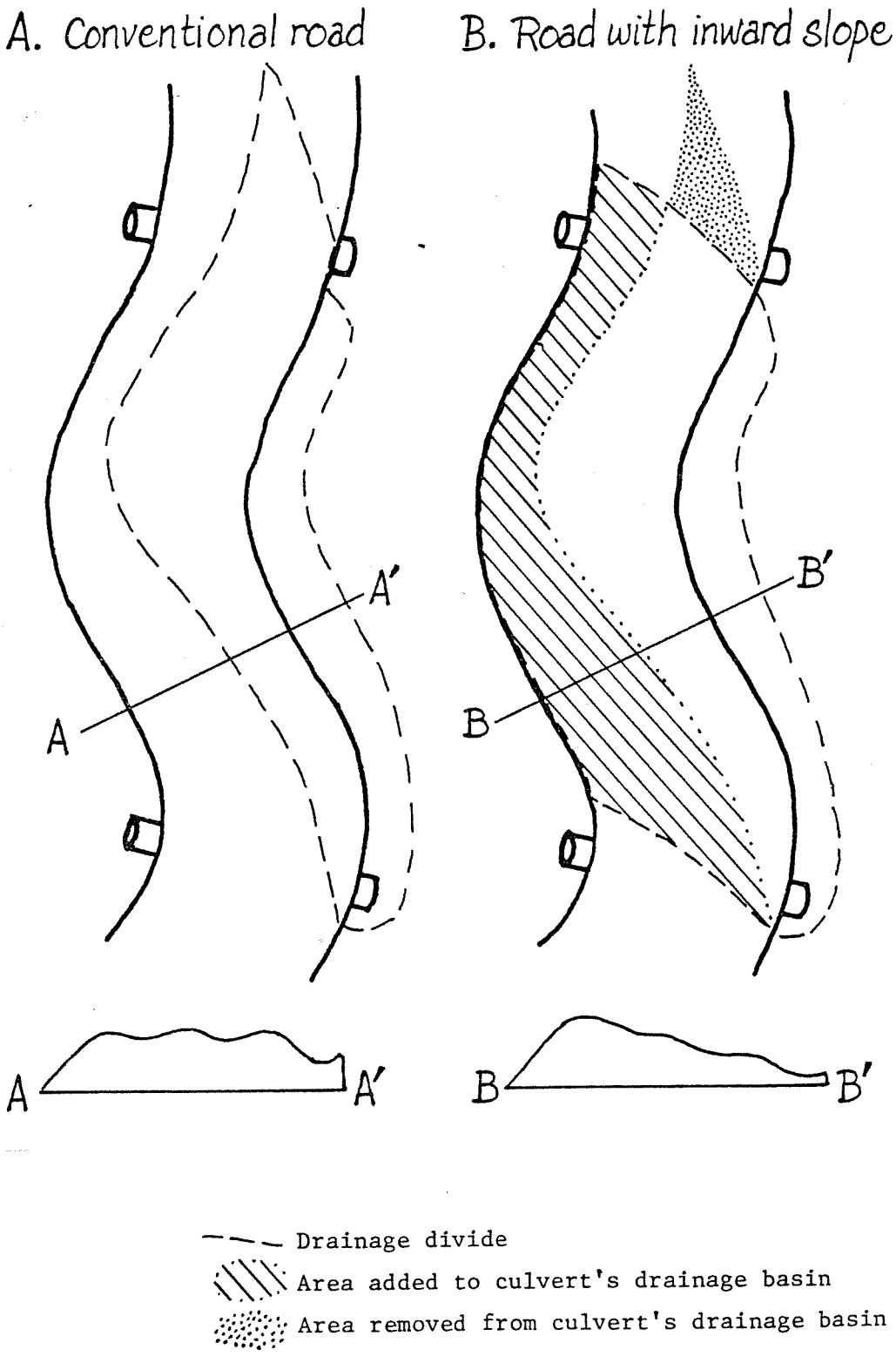

Figure 31. Drainage divides on conventional and inward-sloped road surfaces.

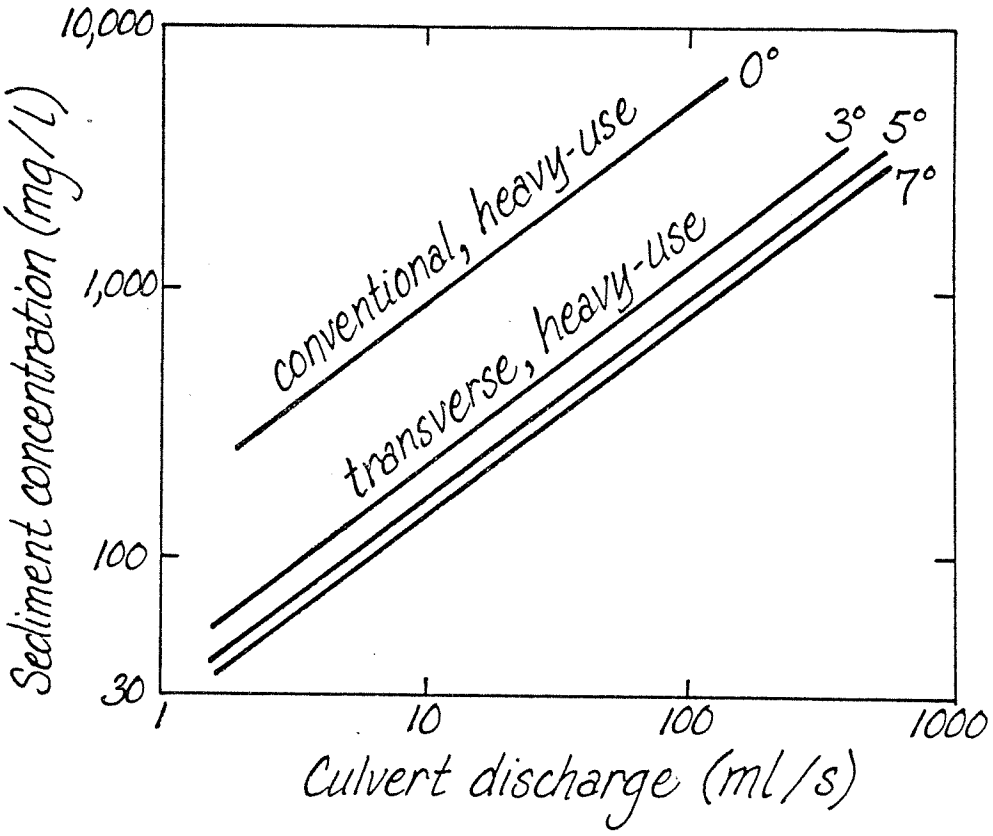

Figure 32. Constructed concentration versus discharge curves for roads with transverse slopes.

agreeing quite closely with that indicated by the values computed above. These calculations do not take into account a possible change in the value of K brought about by the decreased transport capacity and competence of the road-surface drainage.

Road Gradients

The monitoring program did not provide data on roads of different overall gradients, but the Universal Soil Loss Equation can be used to estimate the effect of varying gradient. Although the equation will not give results that are directly applicable to the roads in question, the proportional changes in sediment yield generated by changes in the LS index are expected to be reasonably accurate. Studies of sheet erosion rate versus gradient and slope length have produced well-defined relationships (see Wischmeier and Smith 1965) which are the basis for LS index in the present equation. It is accepted practice to decrease culvert spacing on gravel-surfaced roads as gradient increases in order to compensate for the increased sediment-transporting competence and capacity of the flow. Washington Forest Practice Board guidelines (1976) require a culvert spacing of less than 305 m for roads with 0^{o} to 4.6^{o} slopes, less than 245 m for 4.6^{o} to 8.5^{o} roads, and less than 185 m for those with slopes greater than 8.5^{o}. Calculations using the USLE indicate that on a heavily-used road, sediment yield from a 305-m long, 1^{o} slope would average 73 t/ha, or 10% of that of the 5.5^{o}, 250-m long slope; and a 185-m 10^{o} slope would contribute 2,000 t/ha, or 270% of that for the average slope (see Fig. 33). In these calculations, as before, slope length is considered to be the maximum length of the road surface catchment, and is calculated from the ditch length using the empirical relation:

$$L_r = 1.46\ L_d$$

where L_r is the catchment length and L_d the length of the ditch (see Fig. 11).

Had the culvert spacing not varied with gradient, the variation of yield with gradient would be greater. Sediment yield calculations using the USLE were carried out for 250 m heavy-use road segments with different surface gradients; results are plotted in Fig. 33.

In order for decreasing culvert spacing to exactly compensate for increasing surface gradient, the Universal Soil Loss Equation requires:

$$L_d = -2.82\ \ln S + B$$

where L_d is the length of the ditch in meters and S is the road surface gradient in percent slope. The selection of the constant B depends on the value of the desired sediment yield.

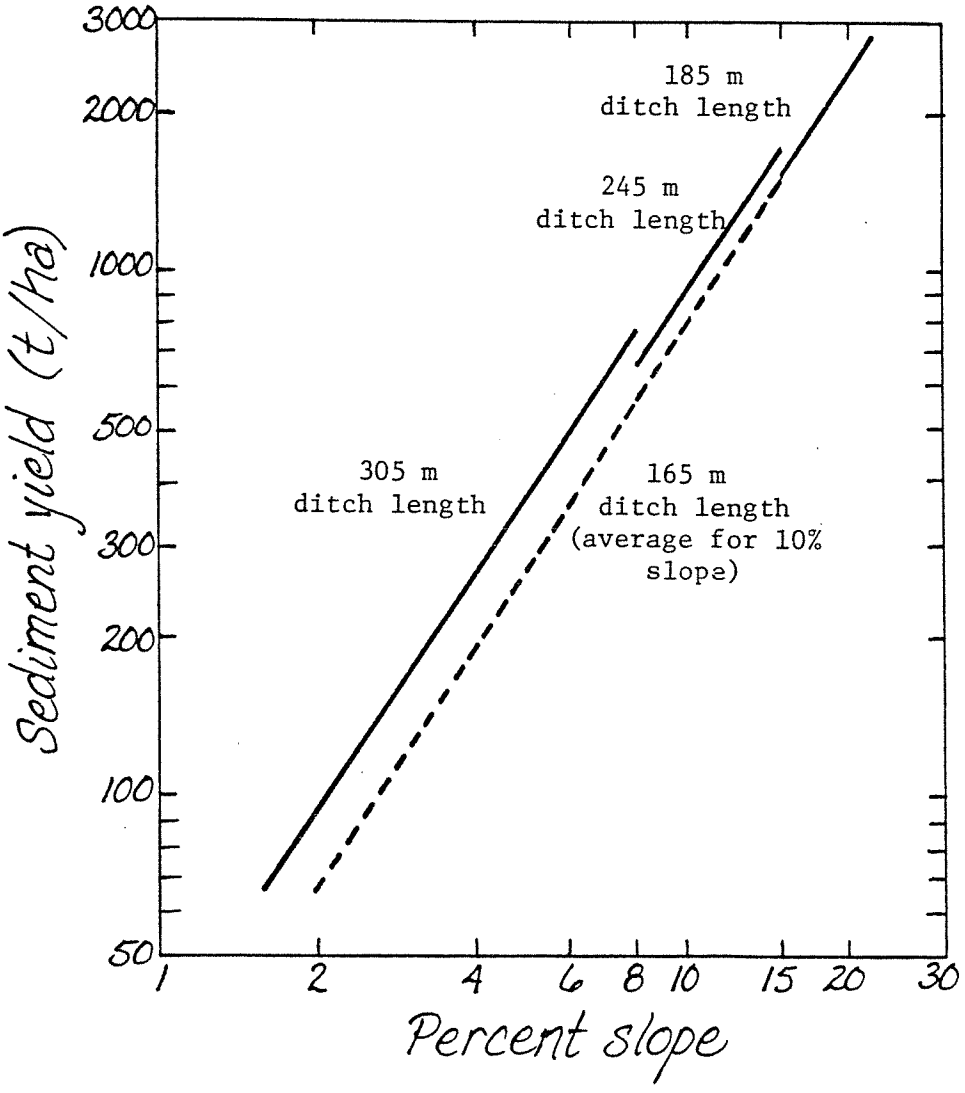

Figure 33. Sediment yield from road surface versus slope for various culvert spacings on a heavily-used road.

Average Annual Sediment Yield from Road Surface and Backcut

Calculations have thus far been made using only a single year's rainfall record. To provide a basis for estimation of year-to-year variation, calculated sediment yields for individual storms on a heavily-used road segment were plotted against total storm precipitation (see Fig. 34), "storm" being defined as a period of rain bounded by days with no precipitation. The resulting relationship may then be used to calculate sediment yield from records of daily precipitation totals for the Clearwater area, again assuming that sediment rating curves for the wet and dry seasons are similar. The high coefficient of determination reflects the uniform nature of the storms and the strong relation between the total storm precipitation and the average intensity. It was expected that a seasonal difference in storm character would be most evident in comparisons of summer and winter storms. Those storms occurring in May, June, and July were thus indicated by open circles in Fig. 34, but it is apparent from the figure that no such difference exists. The variation of average rainfall intensity with total storm precipitation is also well-defined. If no such relationship existed, sediment yield would be directly proportional to the total storm precipitation. The regression, however, demonstrates that sediment yield is proportional to storm precipitation raised to the 1.43 ± 0.05 power, where the range indicated is that of the 95% confidence interval.

Individual storms were identified and sediment yields calculated from this relationship for the period 1973-1978 using the Queets ridge precipitation record. In order to extend the length of the record, calculations were also carried out for eleven years' record from the NOAA weather station in the town of Clearwater. Not only do these calculations provide a basis for estimating an average sediment yield from the heavily-used road, but when the calculated annual sediment yields are plotted against total annual precipitation on log-log paper they define a relation which permits an estimation of sediment yield from annual rainfall (see Fig. 35). If this relationship is used in conjunction with the relation between Queets Ridge precipitation and Clearwater precipitation (see Table 2), an 11-year record for Queets Ridge rainfall and sediment yield may be reconstructed (see Table 17). Average annual sediment yield from an 850 m^2 heavily-used gravel road segment over the 11-year period is approximately 81 tons near the town of Clearwater and 111 tons in the Queets Ridge area; average annual precipitation over this period is 6% higher than the 43-year average in the town of Clearwater.

Because the unit hydrographs used for the moderately- and temporarily non-used roads are the same as that of the heavily-used road, and because the exponents of the sediment rating curves for the three road types are virtually identical, the ratio between their calculated and average sediment yields will be the same. The other three road types contribute relatively insignificant amounts of sediment, and errors in the ratio between calculated and average sediment yield will thus make

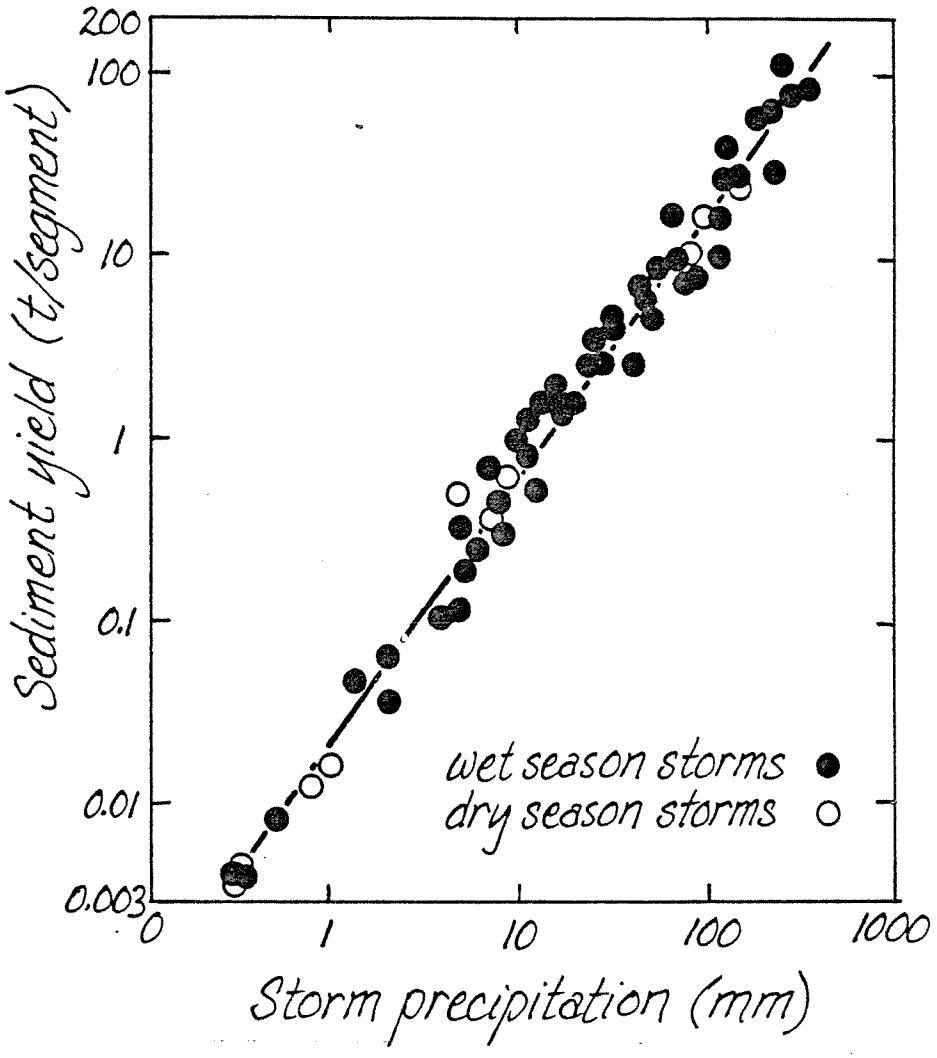

Figure 34. Sediment yield during storms versus corresponding storm precipitation for a heavily-used 850 m^2 road segment.

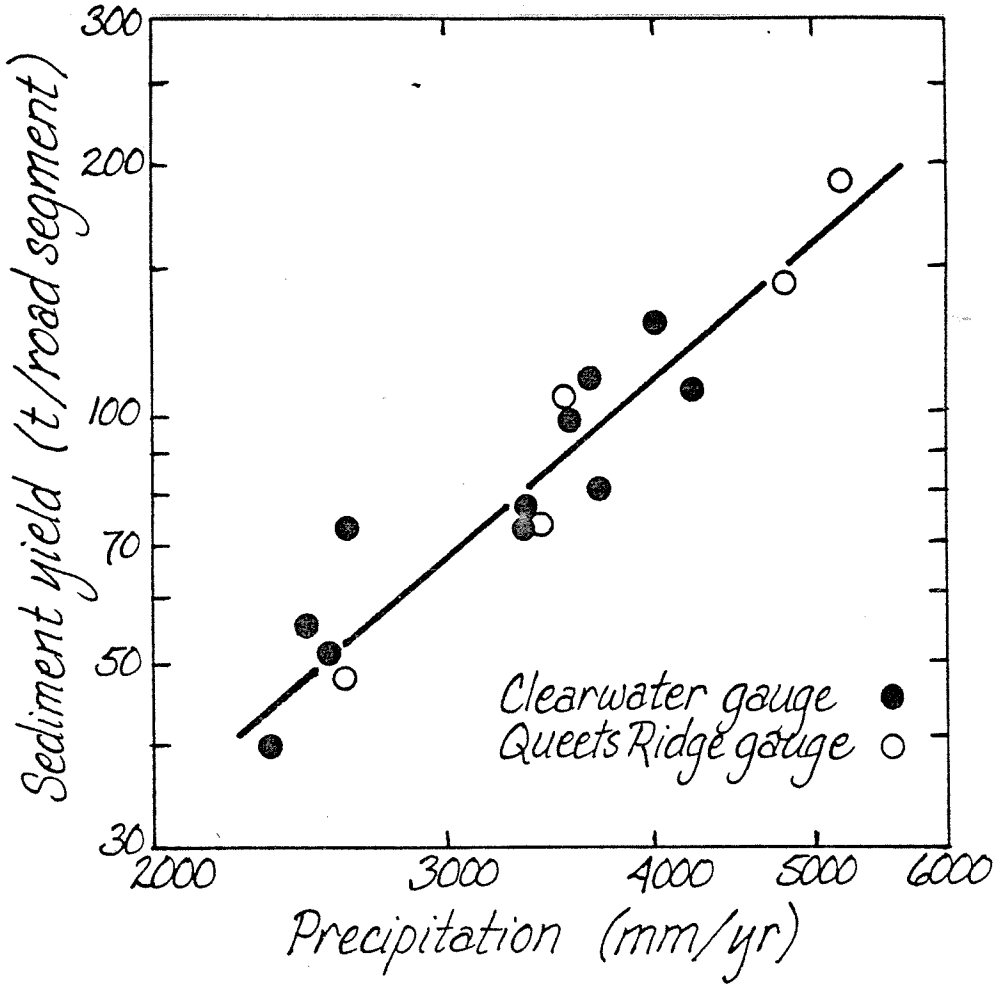

Figure 35. Calculated sediment yield versus total annual precipitation for heavily-used road segments.

Table 17. Annual sediment yields for heavy-use road segments in Clearwater and Queets Ridge areas, as calculated from annual precipitation records.

Year	Clearwater gauge		Queets Ridge gauge		Reconstructed Queets Ridge*	
	Rainfall (mm)	Sediment yield (t/segment)	Rainfall (mm)	Sediment yield (t/segment)	Rainfall (mm)	Sediment yield (t/segment)
1977-1978	3528	98	3464	73	4269	123**
1976-1977	2345	40	2624	48	2837	62**
1975-1976	3678	110	4784	142	4451	132**
1974-1975	2624	72	3555	101	3175	75**
1973-1974	3978	129	5201	189	4814	151**
1972-1973	2474	56			2994	68
1971-1972	3729	81			4512	135
1970-1971	3357	73			4062	113
1969-1970	2551	51			3087	71
1968-1969	3349	76			4054	113
1967-1968	4185	107			5064	164
Average	3254	81	3926	110***	3938	110

Eleven-year average sediment yield calculated using 1973-1978 Queets Ridge precipitation record and 1967-1973 reconstruction = 111 t/segment.

*
**Reconstruction method described in text.

***For comparison; not included in calculations.

Subject to rounding error.

little difference to the net sediment yield. If an increase in calculated rates proportional to that for the heavily-used roads is assumed for average annual sediment yields from other road types, an expected annual sediment yield from roads may be calculated. As in the case of Table 10, the road-use distribution observed in the winter of 1977-1978 is assumed, and roads are assumed to be of average length and gradient. Results are shown in Table 18.

Table 18. Average annual sediment yield from road surface and backcut in Christmas (15 km^2) and Stequaleho (25.2 km^2) basins based on 1977-1978 road-use distribution. Totals subject to rounding error.

Road type	Road length (km)	Percent total length	Percent time in category*	Sediment yield per 850 m^2 road segment (t/yr)	Sediment yield from average-use road (t/km/yr)	Sediment yielded to stream per km^2 of basin** ($t/km^2/yr$)
Christmas						
Heavy	6.5	17	48	111	55	102
Temporary non-use	6.5	17	52	14.8	8.0	15
Light	8.5	23	100	0.85	1.1	2.1
Abandoned	22.7	60	100	0.10	0.4	0.7
Total	37.7				64	120
Stequaleho						
Heavy	12.5	26	48	111	83	119
Temporary non-use	12.5	26	52	14.8	12	17
Light	5.2	11	100	0.85	0.6	0.8
Abandoned	21.3	45	100	0.10	0.3	0.4
Moderate	5.9	12	100	9.2	6.8	9.7
Paved	2.5	5	100	0.47	0.1	0.2
Total	47.4				103	147

*A haul road is heavily used on 5/7 of total days, and assuming a 6-hour clean-up period, during 16/24 of the hours in each day. The rest of the time the road is considered temporarily non-used.

**Only 75% of culverts contribute flow to streams.

CHAPTER VI. MASS MOVEMENTS FROM ROADS

Landslides and debris flows triggered by roads are widely recognized as major sources of sediment in logged areas, and the Clearwater basin contains abundant evidence of their activity. Sediment production from these sources is evaluated quantitatively in this chapter, as is production from gullying and sidecast erosion.

Landslides

Description

Landslides triggered by the presence of roads take several forms. Of relatively minor importance are backcut failures, which may deposit a portion of both excavated cut-face and accumulated debris mantle into the roadside ditch. Such failures, however, are infrequent, and where they occur the ditches are soon cleaned out by grading and the debris removed from contact with running water.

Larger and more common are failures occurring below the road, caused either by direct destabilization of the slope or by the alteration of drainage which then leads to destabilization. Direct destabilization may be caused by the excess load provided by road-fill material or may be brought about by changes in the strength of either the underlying soil or the fill material. Older roads are particularly susceptible to fill failures as organic material incorporated into the fill begins to decompose (Beschta 1978), thus decreasing the material's angle of internal friction, but forest practice laws now prohibit the burial of stumps and logging debris in road-fill and such failures are expected to decrease in frequency. Decay of roots in the soil underlying the road-fill may also induce failure by decreasing the effective cohesion of the soil (Gonsior and Gardner 1971).

The practice of side-casting excavated material onto steep slopes also provides a ready source of sediment. The deposits of disaggregated, cohesionless sediment are inherently unstable on slopes of greater than about 45^{o}, and the material may fail as shallow sloughs. The debris can also continue to ravel for over a decade without initiation of a discrete failure, and the resulting scars are often difficult to distinguish from shallow landslides incorporating sidecast debris. The importance of sidecast material as a sediment source is also expected to decrease in the future; material excavated from steep slopes is now generally hauled to stable dump-sites.

A third type of direct destabilization may occur where roads are built across the toes of relict slumps. In the Clearwater basin these forms are large, measuring up to 180 m by 120 m, and relatively common,

found at a frequency of nearly two per square kilometer in the northern part of the basin. The slumps are visible only as topographic anomalies except in the rare cases that road construction or stream-bank erosion have reactivated them. No active slumps were found in the mapped portion of Christmas basin.

Many slope failures appear to be caused by changes in local hydrology, and in most cases debris from such landslides enters streams directly. These failures often include fill or sidecast material, so a rigid distinction between failure types is rarely possible. Destabilization may be caused in several ways. Drainage diverted from a road surface may be concentrated onto a hillslope or into a drainage depression or first-order channel, allowing abnormally high pore pressures to build up in the hillslope or channel debris. The slope then fails immediately below the point at which the road drainage enters, but the failure may propagate headward and consume the road bed. In other cases water may become ponded at the culvert mouth either because inadequate culvert size allows hydraulic damming or because the entrance becomes plugged with debris. In such cases the ponded water may flow over and gully the road surface or saturate the road fill, often triggering a failure.

Redirected road drainage may also be responsible for triggering slope failures at some distance from the road, but a causal relationship in such situations is difficult or impossible to demonstrate. In low-order basins the increased peak discharges due to the concentration of overland flow from road surfaces may cause widening of channels and undercutting of previously stable slopes. Increased sediment load in roaded basins may also induce channel widening.

In this section only those landslides, gullies, and sidecast sloughs immediately adjacent to roads will be considered. The destabilization of channels due to the presence of roads will not be addressed.

Methods

Landslides adjacent to roads in the 15.2 km^2 upper Christmas basin were mapped on three sets of aerial photographs. The photographs taken in 1971 and 1977 are black and white and have a scale of 1:12,000; the set from 1975 is in color at a scale of 1:24,000. Landslides were first located on the 1977 photographs (see Appendix Fig. F-1 and Appendix Table F-1), which were then compared to the earlier photographs in order to bracket the dates of the slides. In addition, the earlier photographs were examined in order to identify landslides no longer recognizable in the 1977 set. The horizontal projection of the surface area removed by each slide was measured on the 1977 photograph with a millimeter rule. The mirror stereoscope used in the analysis is equipped with 3-power auxiliary oculars which allow estimation of length to the nearest 0.2 mm, equivalent to 2.5 m on the ground. The average measured slide area is 1.9 mm^2, so this uncertainty results in an average uncertainty of $\pm$ 15% for landslide areas. The hillslope gradient at each failure site

was then measured from a 1:24,000 orthophotographic map with a 40-ft contour interval, and the measured area multiplied by the secant of the hillslope angle to calculated the actual area of surface removed.

It is possible to distinguish two general types of disturbances by using the aerial photographs. In the first case, no change in hillslope contour is evident, and the affected area is visible only as a light-toned unvegetated area. In each case such areas are associated with sidecast material, and in most instances disturbance caused by continuous ravelling of sidecast material could not be distinguished from actual sidecast failures. The second type of failure is recognized by the presence of a distinct scarp, showing that material was lost to an appreciable depth over a well-defined area. In most such cases the head-wall scarp is evident as a scallop on the outer edge of the road bed.

Aerial photograph interpretation also allowed a qualitative assessment of the proportion of the landslide debris delivered to the nearest channel. This evaluation was based on a four-point scale: none (failure was not included as a sediment source), low (little evidence for delivery, but proximity to channel would allow some delivery by rill transport), moderate (sediment evident adjacent to channel), and high (generally refers to landslides occurring in or immediately adjacent to low-order stream channels).

Forty-two of the landslides identified on the aerial photographs were examined in the field to determine the accuracy of the aerial photograph measurements, to determine landslide depths, and to calibrate the qualitative sediment delivery categories. Gradient was measured with a clinometer, and the major dimensions of each landslide were paced where possible and estimated where the terrain prohibited pacing. The depth of material removed was measured perpendicular to the slope at sites around the margin of the landslide if the scarp were identifiable, but in many cases the original scarp faces were obscured by back-wasting and debris accumulation, necessitating an estimated reconstruction of the original ground surface in order to determine failure depth. Where debris deposits were still relatively unobscured by vegetation their extent could be paced and their thickness estimated, but in most cases analysis of delivery ratio was restricted to a visual estimate of whether less than 25%, between 25% and 50%, between 50% and 75%, or more than 75% of the original debris remained in storage in unchannelled depressions or on the hillslopes.

Erosion pin networks were placed on the scarps and accumulation areas of three road-related landslides and on a landslide located in a clearcut in order to provide data on long-term modification of landslide scars. In addition, four rills were monitored using erosion pins. Only one of the rill systems was located on a landslide scar, but the three monitored backcut rills are expected to behave in much the same fashion as those on landslide scars.

Landslides were also mapped using aerial photographs in Stequaleho basin in order to provide a second data set for comparison with the Christmas Creek data. These data will be discussed in the final part of this section.

Results

Resolution. Seventy-four road-related landslides which showed evidence of supplying sediment to streams were measured on aerial photographs. All of the landslides visible in the 1971 photographs were also visible in the 1977 set, but in two cases it was not evident from the later set that sediment had once reached the stream. The agreement between photo sets indicates a slow rate of healing of the landslide scars. Road construction began in the basin in 1966, only five years before the first photographs were taken, so loss of resolution due to the healing of scars is assumed to be insignificant. All landslides mapped in the field were visible on the aerial photographs, although in ten cases fieldwork allowed the subdivision of a recognized disturbed area into failures of different types. It is thus expected that virtually all significant road-related landslides in the basin have been identified.

Verification of Measurements from Aerial Photographs. Comparison of aerial photograph and field measurements demonstrates close agreement for most parameters. Thirty-one landslide scars were used to compare gradients. The average difference between hillslopes measured from maps and those measured on the ground is 5.7^{o} ($\pm$ 0.9^{o}), but the error is not systematic.

Three years had elapsed between the date of the photographs and that of the fieldwork. In several cases it was evident that vegetation had encroached upon the affected surface, obscuring the original outline, but in other cases failures had enlarged by recent sloughing. In addition, areas of deposition were in some cases difficult to distinguish on aerial photographs from the actual landslide scars. Despite these potential sources of variation, the average ratio of landslide area measured on the ground to that measured on photographs is 1.02 ($\pm$ .12).

The two categories of landslides defined during aerial photograph interpretation correspond directly to differences in the depth of material affected. Shallow failures in sidecast material average 0.28 m ($\pm$ 0.02 m) in depth as measured perpendicular to the ground surface, while those landslides revealing distinct scarps on the aerial photographs have an average depth of 0.84 m ($\pm$ 0.09 m) (see Table 19). In most cases examination of the headwall scarps of the deeper failures reveals the incorporation of road-fill debris. Scarps of the shallow landslides, on the other hand, are generally not evident even on the ground, so areas of continuous ravel could rarely be distinguished from discrete sloughs. The correspondence between the measured slide depth and the landslide category defined from the aerial photographs allows the uniform application of the average depth for each category to the

Table 19. Thickness of material removed by deep and shallow landslides in upper Christmas basin (catalog of landslides appears in Appendix F).

Deep failures				Shallow failures			
Slide	Thickness (m)	Area (m^2)	Volume (m^3)	Slide	Thickness (m)	Area (m^2)	Volume (m^3)
1	.4	255	100	3	.25	255	77
4	.75	2,420	1,810	5	.25	590	150
13	.4	38	15	6	.3	700	210
15a	1.35	300	405	8	.3	100	30
20c	1.0	140	140	9	.2	280	56
20d	.5	60	30	10	.3	650	200
20e	1.5	155	240	11	.3	320	95
20f	.6	50	30	14	.25	200	40
35	1.25	76	88	16	.2	73	15
36	.5	350	170	17	.2	96	19
38b	.3	35	10	21a	.25	26	6
39b	.85	45	39	21d	.25	14	4
44b	1.0	16	16	38a	.25	510	130
45	1.0	365	365	39a	.5	30	15
63a	.75	40	30	42	.4	105	37
64	.75	300	220	43	.3	49	15
65b	.5	24	12	63b	.3	330	99
66	.75	405	200				
67	1.0	12	12				
69	1.7	810	1,220				
20	avg=.8	5,900	5,250	17	avg=.3	4,330	1,200

mapped area of that landslide type in order to calculate the volume of material displaced.

Measurements of delivery ratio were possible for twenty-five of the landslides observed in the field, but the difficulty of estimating the thickness of deposits introduces an estimated uncertainty of ± 25% into the measurements. The proportion of landslide debris removed was estimated by quartile in ten other cases. The 35 values were then tabulated by the qualitative delivery category recognized from the aerial photographs, and the values averaged for each (see Table 20). Seven of the landslides identified on aerial photographs were discovered not to have introduced sediment into a stream, although post-failure rilling did so in three of these cases. Table 20 presents arithmetic averages for delivery ratios; a volume-weighted average is also included because large landslides appear to dominate landslide-related sediment production and because the size of the landslide is expected to influence the delivery ratio. For the same reason, characteristic landslide thicknesses are also calculated as volume-weighted averages; average thicknesses used in subsequent calculations are thus 0.9 m for deep landslides and 0.3 m for the shallow slides.

Calculation of Landslide Volumes. The volumes of sediment introduced into streams by landslides observed in the field are calculated directly from field measurements, while volumes of those landslides observed only on aerial photographs and those obviously modified since the photographs were taken are calculated from averages of parameters measured in the field. In these cases, the surface area of the landslide, as measured from the aerial photographs, is multiplied by the secant of the hillslope angle, measured from a 1:24,000 topographic map, to calculate the actual area of the landslide. An average depth of 0.3 m or 0.9 m is then assigned to the disturbance on the basis of the identification of landslide type, as described in the previous section. The product of surface area and average depth is then multiplied by the delivery factor corresponding to the qualitative estimate of delivery classification for that landslide. The calculated values are listed in Appendix Table F-1.

Field measurements of landslide volume are expected to be accurate to within 25%, as are field estimates of delivery ratio. The law of propagating errors thus produces an expected accuracy of ± 35% for calculation of landslide sediment delivery based on field measurements. Measurement errors are expected to be non-systematic.

Calculations of sediment delivery for the disturbances mapped on aerial photographs involve an average uncertainty of ± 15% in surface area of a single slide, ± 5% in slope, ± 25% in landslide depth, and ± 25% in estimated delivery ratio. The law of propagating uncertainties indicates an average uncertainty of ± 39% for calculated volumes of delivered sediment from specific landslides. In this case, too, errors

Table 20. Calibration of qualitative sediment delivery categories for road-related landslides.

Low			Moderate			High		
Delivery ratio	Volume (m^3)	Volume delivered to stream (m^3)	Delivery ratio	Volume (m^3)	Volume delivered to stream (m^3)	Delivery ratio	Volume (m^3)	Volume delivered to stream (m^3)
0-.25	65	8	0.4	150	55	0.5	100	51
0	77	0	0.5	210	105	0.75	15	11
0-.25	30	4	0.75	130	99	0.8	405	330
0	15	0	0	56	0	0.4	140	51
0.02	440	15	0.6	19	12	0.5	37	20
0	17	0	.5-.75	200	120	0.2	15	3
0-.25	160	20	0-.25	40	5	0.3	32	10
0	35	0	0.8	88	69	1.0	12	12
0	92	0	0.5	1,220	610			
0-.25	170	22	0-.25	45	6			
0.1	365	36	0.65	330	210			
			.25-.5	130	49			
			0	81	0			
			0.5	54	27			
			0-.25	300	38			
			.5-.75	56	35			
Total:	1,470	105		3,110	1,440		760	490
Delivery ratio average:	0.06	0.07		0.42	0.46		0.56	0.65

are random, and the accuracy of the sum of delivered sediment is expected to be higher than that for individual landslides.

These procedures result in a calculated total volume of 23,810 m^3 $\pm$ 6,630 m^3 of sediment displaced by road-related landslides which contributed sediment to streams in the upper Christmas Creek basin between 1966 and 1977. The indicated range is that calculated from the average uncertainty. Of this volume, 12,370 m^3 $\pm$ 4660 m^3 was introduced into the stream system. This material has been in various proportions transported out of the basin, incorporated into short-term storage elements between episodes of active transport, and redeposited in long-term fluvial storage elements such as floodplains, terraces, debris fans, and log jams.

Relative Importance of Disturbance Types. Although shallow failures are slightly more common than deep failures they account for only 23% of the total volume of sediment displaced by the identified landslides, while the 41% of the landslides classified as deep account for 77% of the sediment moved. The average delivery ratio is higher for the deeper slides: 84% of the sediment delivered to streams is from deep landslides, while 16% is from shallower disturbances.

Field verification allowed more accurate determination of the type of disturbance at forty-two of the locations identified as landslide scars from the aerial photographs. Portions of three of the sites classified as deep failures were found to be gullies cut by culvert drainage. The gullies together accounted for only 57 m^3 of displaced material, of which 32 m^3 was delivered to the stream system. This value represents 0.8% of the total volume delivered to streams by the landslides evaluated in the field. The gullies are all relatively small, the largest measuring 25 m in length, 2 m in width, and up to 0.6 m in depth. In each case the gully is associated with landsliding, but causal relationships between the two disturbances are unclear. It is possible that the growth of the gullies caused the undercutting of adjacent slopes, but in one case the occurrence of a landslide at the mouth of a culvert evidently left the ground surface unprotected, allowing the initiation of the gully. In each case the installation of flumes at the mouths of the culverts, a practice adhered to through most of the basin, would probably have prevented both gully formation and slope failure.

In the case of the shallow, side-cast related failures, the difficulty in distinguishing areas of gradual surface erosion from those of discrete failure has been described. Of the 35 shallow disturbances observed in the field, three were seen to involve only gradual erosion processes, while discrete slope failures were recognized on sixteen of the sites. The remaining sixteen sites were indeterminate, but probably involved some landsliding. If the proportions of the shallow landslide material displaced by gradual erosion and by discrete failures observed in the field are applied to the total volume of material moved by shallow disturbances, as determined from both field and aerial photographic mapping, then the relative importance of the various disturbances may be

determined for the whole basin. The results of these calculations are listed in Table 21. Deep landslides are thus seen to account for most of the sediment introduced into streams by road-induced mass movements.

Significance of Large Landslides. A histogram of the frequency of landslides of various volumes plotted on semi-logarithmic paper reveals a modal value of 147 m^3 for shallow failures (see Fig. 36). The distribution for deep landslides is bimodal, with peak frequencies at 15 m^3 and 316 m^3. While the distribution of shallow failures is strongly right-skewed, the primary mode of deep failures shows a nearly normal distribution on semi-logarithmic paper.

Cumulative frequency curves of total sediment delivery to streams from landslides was then plotted on log-log paper in order to determine the relative significance of landslides of various sizes (see Fig. 37). The diagram demonstrates that 36% of the total sediment delivery by landslides resulted from a single large failure, and that an additional 18% was from the other two landslides with total volumes of greater than 1,000 m^3. Half of the 75 landslides were smaller than 132 m^3, and they accounted for only 8% of the total volume of sediment delivered to streams by road-related landslides. The overwhelming importance of a few large landslides serves to emphasize both the care that must be taken in laying out roads to avoid the most unstable areas and the effort that must be put into determining exactly what constitutes a potentially unstable slope.

Each of the three largest landslides was associated with a debris flow, and in each case some of the sediment was redeposited downstream behind log jams. A direct comparison of the volumes of sediment removed by the slope failures and the volumes deposited in the jams is not possible because the debris flows each mobilized additional volumes of sediment between the failure site and the site of deposition. The deposited debris will be eroded out gradually, prolonging the impact of the slope failure on stream sediment load.

Variation through Time. The temporal distribution of road-related landslides is influenced by several important factors: 1) landslide initiation depends to some extent on the occurrence of large storms, 2) fill failures--largely corresponding to the deep failures identified in Table 21--are expected to increase in frequency as the organic debris incorporated into the road fill decomposes, 3) a rash of landslides is expected soon after road construction is completed, as marginally stable sites irrevocably destabilized by road-construction are subjected to their first storms, 4) as road building practices improve, failures will decrease in frequency, and 5) as logging progresses in a basin the less accessible, more rugged terrain is left until last, and landsliding is expected to be more frequent in such areas. Therefore, one would not expect a single temporal pattern of landslide occurrence, and none is evident in the data (see Fig. 38).

Table 21. Sediment production from various kinds of landslide-related disturbances.

Landslide category, from air photo	Source type	Field mapped			Photo mapped		Both data sets		
		Displaced volume (m^3)	Delivered volume (m^3)	Percent of delivered volume	Displaced volume (m^3)	Delivered volume (m^3)	Displaced volume (m^3)	Delivered volume (m^3)	Percent of total
Deep	landslide	6,090	3,080	99		7,130		10,210	83
	gully	57	32	1		72		100	1
	Subtotal*	6,150	3,110	100	12,260	7,200	18,410	10,310	84
Shallow	sidecast surface erosion	200	100	10		100		210	2
	indeterm.	1,110	400	39		400		800	6
	landslide	1,450	530	51		520		1,050	8
	Subtotal*	2,760	1,030	100	2,640	1,020	5,400	2,060	16
Total							23,810	12,370	100

*Subject to rounding error.

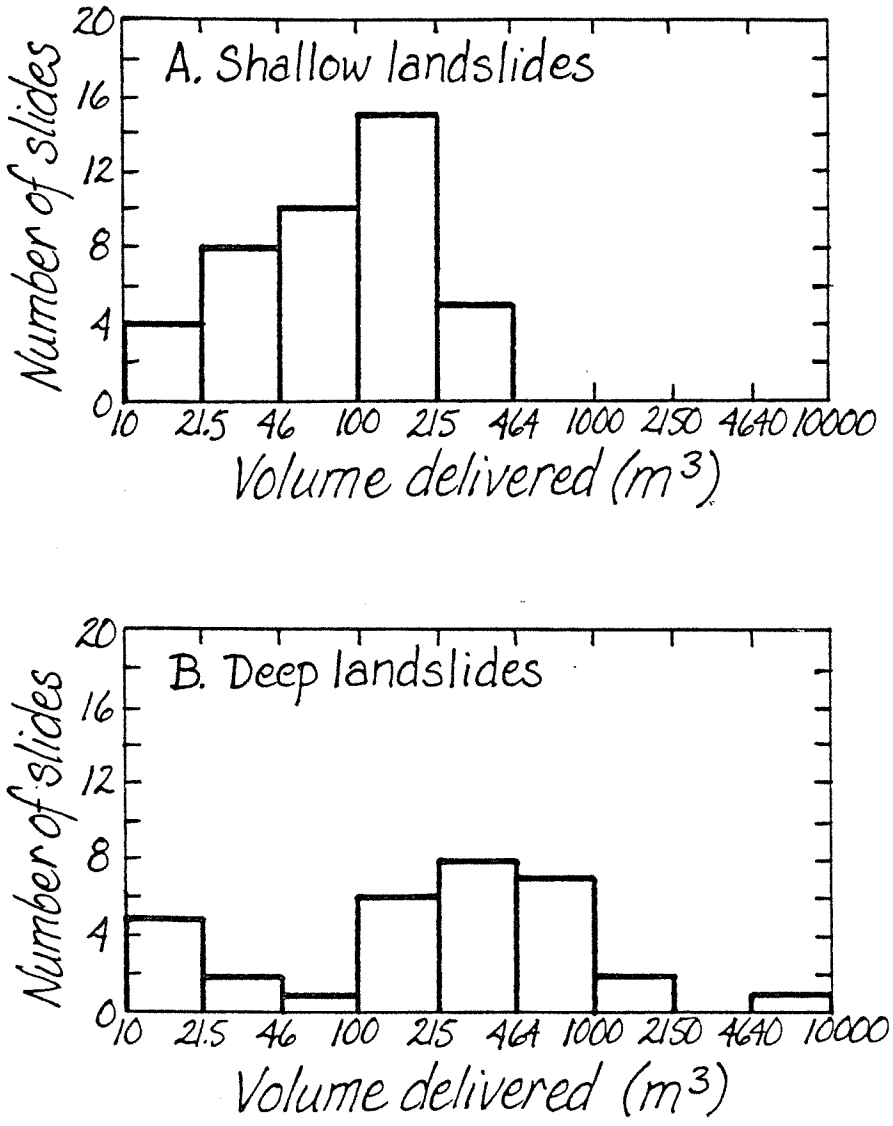

Figure 36. Frequency distribution of volumes of sediment delivered to streams by road-related landslides in Christmas Creek basin. Note semi-logarithmic scale.

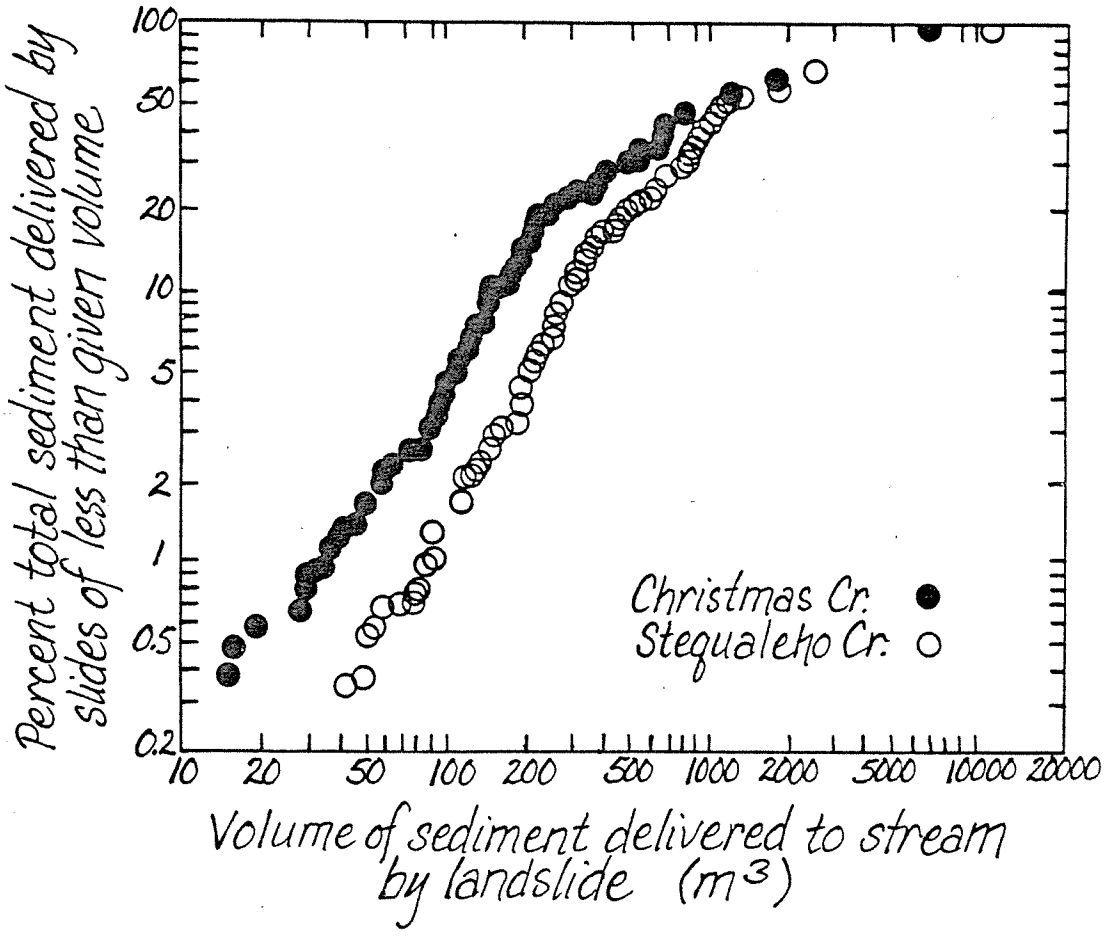

Figure 37. Cumulative volume curve for road-related landslides in Christmas and Stequaleho basins.

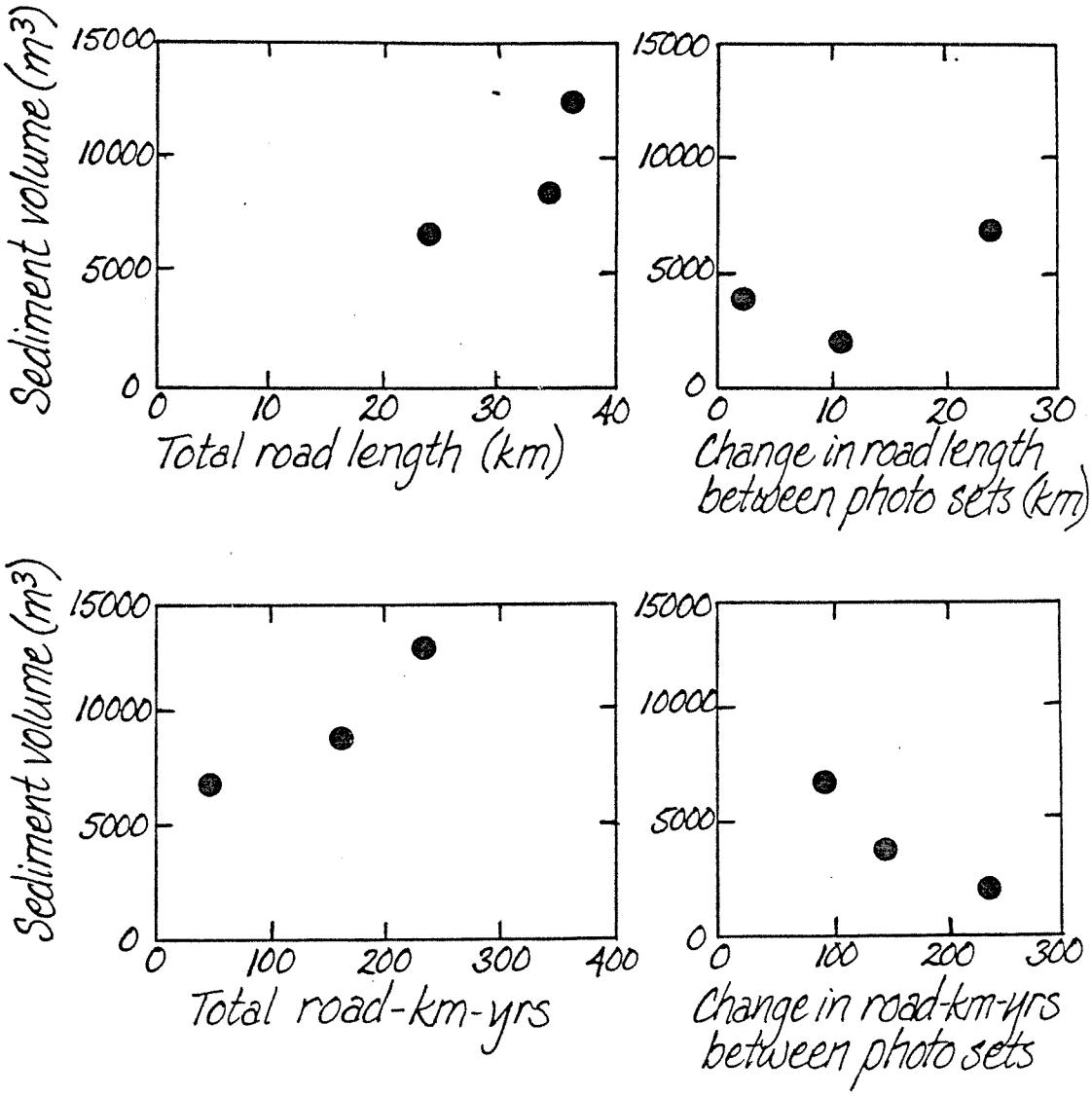

Figure 38. Volume of sediment delivered to streams by road-related landslides in Christmas basin versus changing basin parameters.

Sediment production from a single landslide may also vary through time. Sediment displaced by a slope failure may remain for many years in temporary storage on the landslide scar, in a drainage depression, or adjacent to a stream before it is finally carried into the stream by running water. Even then, redeposition on the valley floor is common; work in Oregon indicates that thousands of years may pass before all mobilized landslide debris from the headwaters of a 16.2 km^2 basin reaches the basin's mouth (Dietrich and Dunne 1978).

Finally, variation in production rate through time may come about by erosional modification of the landslide scar by secondary processes such as dry ravel, rainsplash, sheetwash, and rilling. The past progress of all such processes except rilling has been implicitly accounted for in the measurements of landslide volumes, since volumes of sediment removed by different processes can not be distinguished. The present rate of these secondary processes is evaluated in the following section.

Secondary Modification of Landslide Scars. Landslide scars generally undergo some modification after the failure occurs. The denuded slope is exposed to rainsplash, sheetwash, and dry ravel; in some cases rilling may occur. The combined effects of rainsplash, sheetwash, and ravel were monitored using erosion pins, while the volumes of rills were measured directly.

Nine erosion pins in two networks survived for periods of over a year. A third network was lost due to the whim of elk, a fourth to the occurrence of a secondary failure, and a fifth, having shown little change over a four-month period, eventually disappeared under a thick mat of new grass. Seven erosion pins located on scarp faces showed net erosion amounting to 16 mm/yr (± 4 mm/yr) over a 13-month period (see Table 22). These seven pins survived an additional 18 months, including

Table 22. Erosion pin measurements on landslide scars.

Erosion pin network	Surface loss (mm) over period: 12/77-2/79 406 days	2/79-6/80 536 days
MI-5	2.5	41.0
	19.5	38.0
	33.5	37.5
	18.5	41.5
	7.5	35.0
MI-6	27.5	47.5
	26.5	26.0
Average	17.9	38.1
Standard error	4.0	2.5
Erosion/365 days	16.1	25.9

two wet seasons, with an average retreat of 38 mm (± 3 mm), but this value is not directly comparable to that from the first year since seasonal differences in loss rate are expected. The value of 16 (± 4) mm/yr is not significantly different from that of 16 (± 3) mm/yr measured on road backcuts. The active processes and environments are very similar for both populations, so the close agreement is expected.

The remaining two erosion pins were located on the floors of landslide scars and demonstrated aggradation. Observation of erosion and accumulation zones within the field-mapped landslide scars indicates that secondary erosion processes such as ravel and rainsplash are effective in transporting sediment to the stream only in cases where the landslide scar is directly adjacent to a stream or where the eroding material can fall into rills. The length of time over which these processes are active after a slide occurs is poorly defined. Most of the scars visible in the 1975 aerial photographs are still barren of vegetation five years later and thus are still subject to surface erosion, yet vegetation on a three-year-old scar recovered enough in a four-month period to cause the loss of an erosion pin network.

A maximum possible value for sediment production to streams from secondary erosion processes on landslide scars may be estimated by applying the average lowering rate of 16 mm/yr to the area of those landslides either containing rills or which have scarps adjoining a stream. Accumulation generally occurs on roughly half of the surface area of a landslide. If all of the material eroded from the remaining half of the landslide area enters the channel, the resulting production rate is 129 m^3 for the 1977-1978 water year. If this volume is divided by the road length present at that time, the result is an estimated production rate of 3.1 t/yr per road kilometer. This value represents a maximum possible rate, since even on a rilled scar much of the eroded debris will not enter the rills.

Erosion due to rilling of landslide scars was evaluated by direct measurement of rill volumes. Observation of four erosion pin networks located in rills on backcuts and landslide scars indicates that the rills occasionally fill with debris, though the filling may have been accelerated to some extent by the presence of the nails. In two cases the rills reformed later and were offset several centimeters, partially avoiding the erosion pins. In a third case filling was never completed and the rill remained in the same location. The final case was that of a rill system newly removed from its source of drainage by the opening of tension cracks above the headwall of the slide. In this case the rills filled with debris and never emptied. The volume of sediment eroded by rilling over the history of a landslide may thus be more than that of the rills seen on a scar at a specific time, but the excess volume is filled in by material eroded by more dispersed secondary processes.

Rills were present on the scars of 24 of the 55 road-related landslides that were mapped in the field (see Appendix Table F-3). At 22 of these sites road-surface drainage emptied directly onto the landslide scar; 36 of the 51 mapped rills headed exactly at points that surface drainage entered the scar. In each case the path of the drainage was not intentionally engineered, but banked turns and low points on berms allowed drainage to leave the road surface through unprotected channels. Such misdirection of drainage may have been a factor in the initial destabilization of these sites.

The observed rills have a total volume of 94.9 m^3, or 5.9 x 10^{-3} m^3/m^2 of field-mapped landslide surface. If this rate is applied over the total mapped landslide area in the basin, the estimated total production is 225 m^3 over the period since road-building began. Only the rate for sediment production from rills is directly additive to the production rate from landslides themselves; the value for dispersed surface erosion processes represents a subdivision of the landslide value, since the effects of surface erosion could not be distinguished from those of the original failure when the landslide depths were measured.

Evidence of secondary failures is present on many of the landslide scars in the form of blocks of debris deposited on the floor of failure or arcuate breaks in an otherwise even scarp. In several other cases, tension cracks at the heads of scarps suggest that further failures will occur. In most cases, however, evidence that the smaller failures postdated the major one is not conclusive, and the volume of material removed by all such failures is included in the total volume of the landslide.

Total Sediment Production from Road-Related Landslides. For the purpose of comparison with other basins, temporal and spatial variation in landslide rates within the upper Christmas basin may be ignored and average sediment production rates calculated for various landslide-related processes for the basin as a whole. A useful unit for this comparison is the road-kilometer-year. The length of time road segments have been in existence can be multiplied by the lengths of the segments and summed to yield the total number of road-kilometer-years in a basin (see Fig. 9). For upper Christmas basin, this value is 245. If the total volume of sediment delivered to streams by road-related landslides is divided by this value, the result is the expected production rate per road-kilometer-year. This approach assumes that the time-distribution of landslides after a road is constructed is essentially random; the rate of landslide initiation on an older road will thus be the same as that on a younger one. The same calculation may be performed to compute the corresponding rates for the other processes considered. Because the measured landslide volumes included sediment lost by secondary erosion, the calculated rate of surface erosion on landslide scars is subtracted from the rate of sediment production from landslides to calculate a production rate for the initial failures. The results of these calculations are shown in Table 23. Together these sources produce an average of

Table 23. Sediment production from road-related landslides and associated sediment sources in Christmas and Stequaleho basins (totals subject to rounding error).

Source	Sediment production (m^3/road-km-yr) Christmas	Stequaleho
Deep landslides (fill)	40	69
Shallow landslides (sidecast)	5.8 - 3.0	9.0 - 4.7
Culvert-mouth gullies	0.4	0.7
Sidecast ravel, alone	0.9 - 4.1	1.3 - 6.5
Surface erosion from scars*	3.4 - 2.9	5.6 - 4.7
Rilling	0.9	1.7
Total	51	87

*The value indicated is that resulting from secondary surface erosion of landslide scars and gullies. "Sidecast ravel" represents the sediment production rate of the surface erosion processes in cases where no discrete failure has occurred. The ranges reported are those calculated by including shallow disturbances of indeterminate origin first with the shallow landslide category and then with the sidecast ravel category.

51 $\pm$ 19 m^3/road-kilometer of sediment each year; at the 1977 level of development of the basin, this would be equivalent to 130 m^3/km^2 of basin. The landslides themselves account for 85% to 90% of this volume. The indicated error range is that resulting from the average estimated uncertainty of $\pm$ 38% for sediment delivery from landslides.

Comparison with Stequaleho Basin. A similar analysis was carried out for landslides in Stequaleho basin, although in this case no field verification was carried out (see Appendix Fig. F-2 and Appendix Table F-2). Road-related landslides and related disturbances in the 25.2 km^2 basin yielded a total of 23500 m^3 $\pm$ 9160 m^3 of sediment to streams over the period 1963-1977. As of 1977 Steqaleho had experienced a total of 276 road-km-years (see Fig. 9b), so the total production rate is equivalent to 85 $\pm$ 33 m^3/rd-km-yr, 1.7 times that of Christmas basin. This difference in sediment production rates may reflect differences in topography, climate, and bedrock between the two basins. Hillslopes are generally steeper in the Stequaleho area, averaging 30° compared to the mean of 21° for the Christmas Creek area, and Stequaleho receives about 8% more rain than Christmas basin. Finally, graywacke and indurated

sandstones are relatively more prevalent in Stequaleho basin than in the more shale-rich Christmas basin. The difference in the character of the terrain is also expected to influence delivery ratios and failure depths for the landslides, though for the present calculations these values are assumed to be equivalent to those measured in Christmas basin.

Shallow and deep disturbances could again be distinguished on the photographs, and the relative importance of various types of disturbances could be estimated by assuming the same proportions of gully erosion to deep landslide erosion and sidecast ravel to shallow failures as were measured in Christmas basin (see Table 23). Sediment production from surface erosion and rilling were calculated directly from measured surface area of landslides, using rates measured in Christmas basin, and the surface erosion value was subtracted from the measured landslide contribution, as before. Total sediment production rate from road-related landslides and associated sediment sources is 92 $\pm$ 33 m^3.road-km-yr in Stequaleho basin.

The Stequaleho landslides tend to be larger than those in Christmas basin, having a median volume of 231 m^3 (see Fig. 39) compared with 132 m^3 for Christmas basin, although the shapes of the distributions are similar. As with Christmas basin, the majority of the sediment delivered is from a few large slides. In Stequaleho basin 60% of the delivered sediment is from eight landslides with total volumes of greater than 1000 m^3, and 34% is from a single large failure (see Fig. 37). Half of the 96 landslides mapped were smaller than 231 m^3 in total volume, but these accounted for less than 7% of the volume of sediment delivered. For Christmas basin the equivalent value is 8%.

Debris Flows

Description

Debris from 29 of the road-related landslides mapped in Christmas and Stequaleho basins remained mobile upon entering low-order stream channels. The debris flowed down-channel, scouring sediment and organic material stored in the channel and in places stripping channel and valley walls to bedrock. Such debris flows may travel for distances of up to 0.5 km before being trapped behind debris jams or being deposited upon low-gradient fans. Mobilization of a flow appears to require a steep channel gradient, saturated material, and an opportunity to mix water into the sliding debris; the observed debris flow tracks all headed in bedrock depressions partially filled with debris, forms which correspond to the wedges defined by Dietrich and Dunne (1978). The flows for which precise dates could be established all occurred during periods of heavy rain. These conditions are precisely those which can be aggravated by the presence of roads. Most drainage on midslope roads

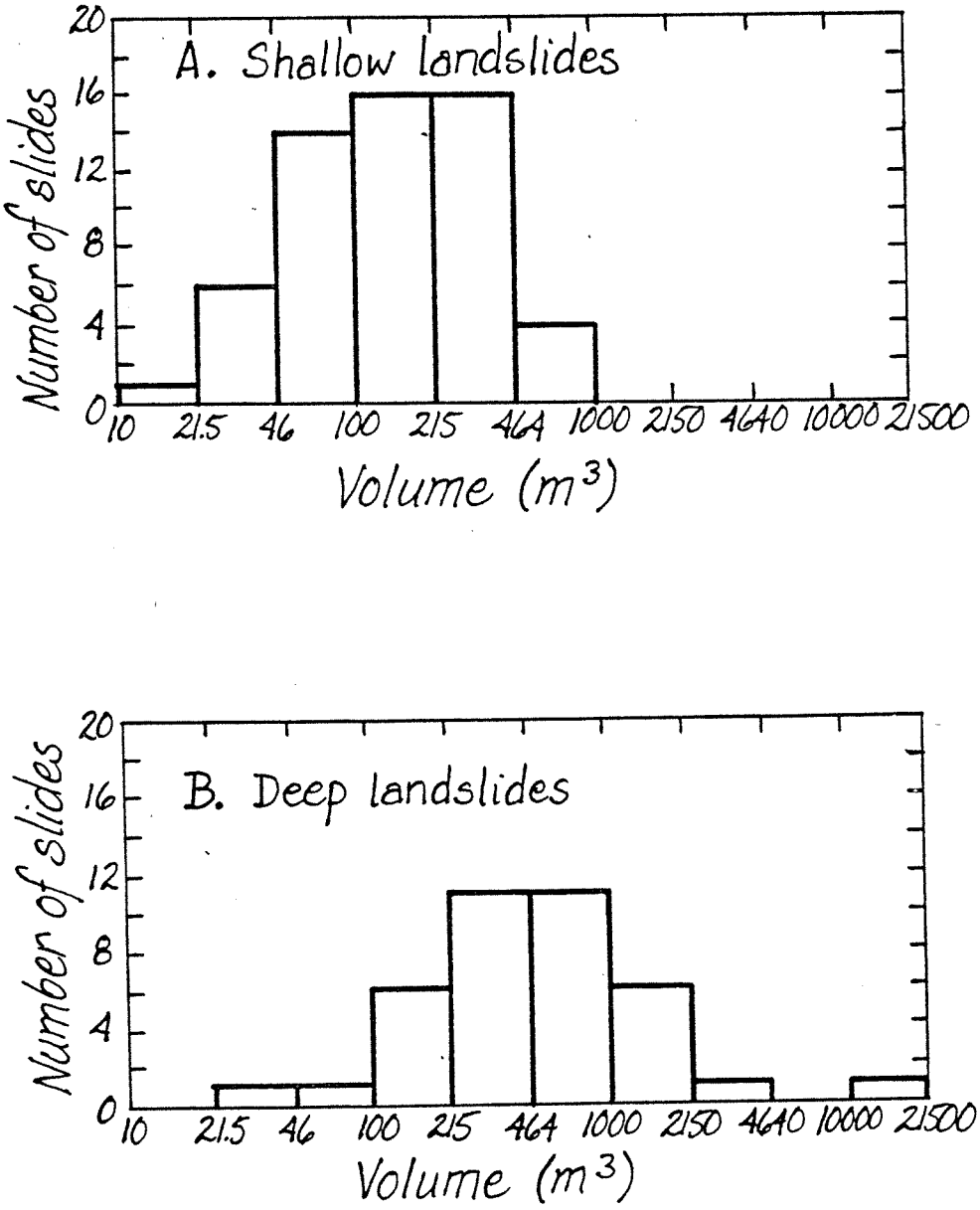

Figure 39. Frequency distribution of volumes of sediment delivered to streams by road-related landslides in Stequaleho basin. Note semi-logarithmic scale.

is diverted into steep drainage depressions and low-order channels, effectively decreasing the recurrence interval for saturation in the channel deposits, and these are the most common locations for the construction of potentially unstable road fills.

The mobilized sediment in such flows is derived from three sources: 1) the original slope failure which triggered the flow, 2) storage elements such as bed material, floodplains and rootwads in the valley bottoms, and 3) soil and bedrock scoured from the valley walls. The first source has been considered in the previous section, and the second constitutes mere remobilization of sediment already produced from other sources. Only the third source can be considered a primary source of sediment produced by debris flows.

Methods of Analysis

The methods used in evaluating sediment production from debris flows are much the same was those used in the landslide analyses. Debris flow tracks in both Christmas and Stequaleho basins were mapped from aerial photographs and their lengths and widths measured. Channel gradient was then measured from a topographic map.

Eight debris flow tracks were observed in the field in order to determine average valley-wall slopes and the thickness of soil removed from the walls. Thickness was evident at 33 sites where the loss of valley wall material left distinct scarps. In most cases material was removed down to bedrock, but there was little evidence that the bedrock itself had been eroded.

Results

Sediment Production Rates from Debris Flows. Twenty-five measurements of valley-wall gradients in debris-flow tracks indicate an average slope of 51° (± 2°). This high value is consistent with field observations: first- and second-order channels in the area generally flow in the bottom of steep-walled, V-shaped canyons cut 2 to 5 m into otherwise smooth slopes of lower gradient. Sixteen additional measurements of low-order valley-wall gradients not affected by debris flows provide an average of 49° (± 2°), and the combined average is 50° (± 2°) (see Fig. 40a).

The thirty-three measurements of the depth of wall erosion measured perpendicular to the slope provide an average of 17.5 cm (± 2.1 cm) (see Fig. 40b). This value is consistent with the measured average valley-wall slope; the relationship between hillslope angle and soil depth measured from roadcuts, as discussed in Chapter 4, predicts an average depth of 20 cm for a 50° slope (see Fig. 6).

Valley bottoms on first- and second-order tributaries average 2.5 m in width, so this value was subtracted from the widths of debris-flow

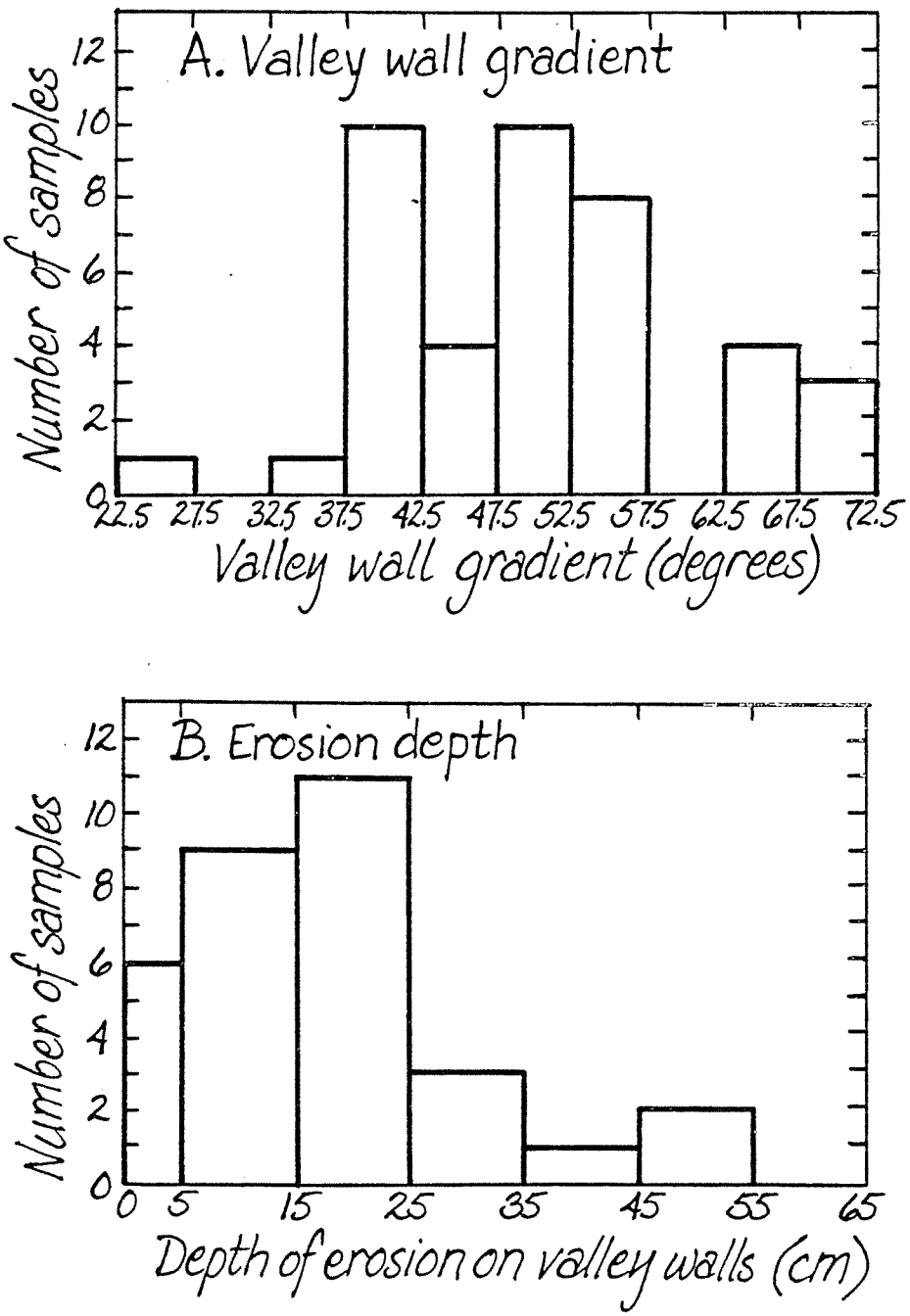

Figure 40. Frequency distribution of field measurements of valley-wall gradients and erosion depth on debris flow tracks.

tracks measured on the aerial photographs. The resulting track width is then multiplied by the secant of the 50° average valley-wall gradient and by the horizontal projection of the channel length, as measured directly from the aerial photographs, in order to calculate the area of valley wall scoured by the flow. The area is then multipled by the average depth of soil removed to calculate the volume of material eroded (see Appendix Table F-4).

These calculations result in a total of 1100 m^3, or 4.5 m^3/road-km-yr, of sediment removed from valley walls by debris flows in Christmas basin between 1965 and 1977. For Stequaleho the volume of sediment eroded is 4490 m^3, or 16.3 m^3/road-km-yr. The difference in production rates between the two basins is paralleled by differences in the character of the flows. The nine flows mapped in Christmas basin have an average overall gradient of 23° (± 1°) and an average length of 66 (± 9) meters, while gradients of the 20 flows mapped in Stequaleho basin average 28° (± 1°) and lengths average 146 (± 25) meters. Volumes of sediment removed from valley walls in Stequaleho basin average 224 m^3 per flow, 1.8 times the average volume removed by flows in Christmas basin (see Fig. 41). These differences probably reflect the differences in topography and bedrock between the two basins, as discussed in the previous section.

As is the case with landslides, a few large failures provided most of the sediment contributed by debris flows in both basins (see Fig. 42). In Christmas basin a single debris flow accounted for 25% of the valley-wall erosion, while in Stequaleho a single flow is responsible for 29% of the calculated total.

Significance of Debris Flows. Although the amount of sediment produced as a direct result of debris flow activity is small relative to that contributed by landslides, debris flows prove to be exceedingly important to sediment production in general. Of the twenty-three largest road-related landslides mapped in Christmas basin (those in the five largest histogram categories in Fig. 36), nine triggered debris flows, and it was largely because of the occurrence of the flows that delivery of sediment to the stream system was consistently high, averaging 67%. Of the fourteen large landslides not resulting in flows, seven had delivery ratios falling in the low category, and average delivery was 34%. Landslides resulting in debris flows accounted for 71% of the total sediment production due to road-related landslides in Christmas basin. If landslides had not evolved into debris flows and the delivery ratio is adjusted to conform to that of the other large landslides, sediment production by road-related mass movements would decrease to 66% of the calculated value, or to 30 m^3/road-km-yr.

The same pattern is evident in Stequaleho basin. Here 77% of the landslide sediment production was from landslides triggering debris flows. In this case, too, twenty-three landslides fall into the five largest histogram categories of Fig. 39. Fifteen of these landslides

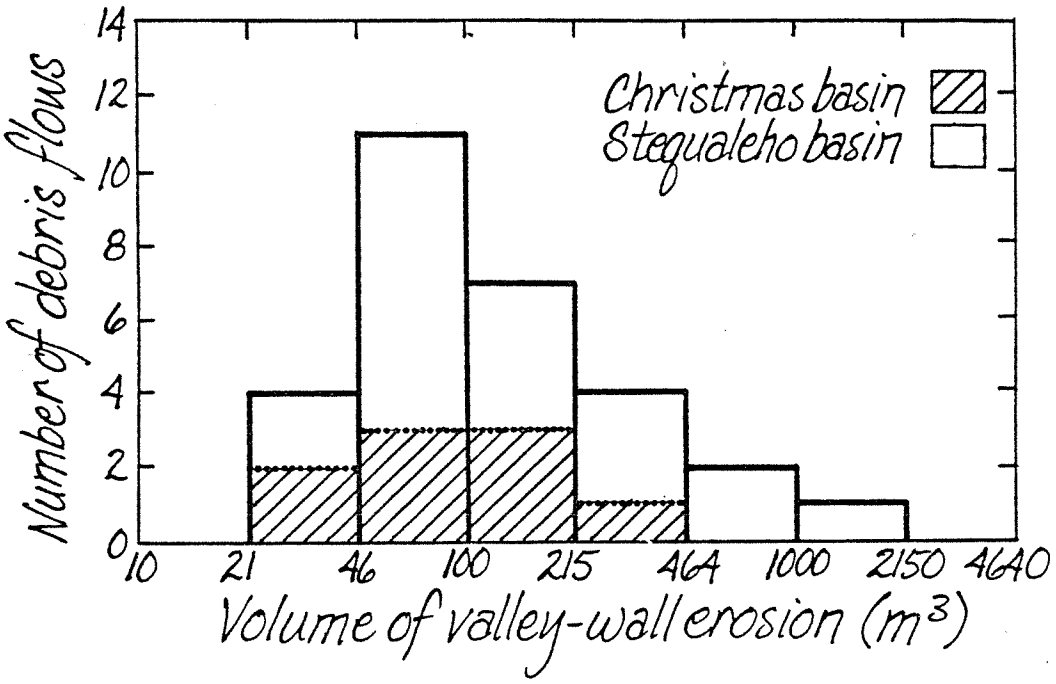

Figure 41. Frequency distribution of volumes of valley-wall erosion caused by debris flows.

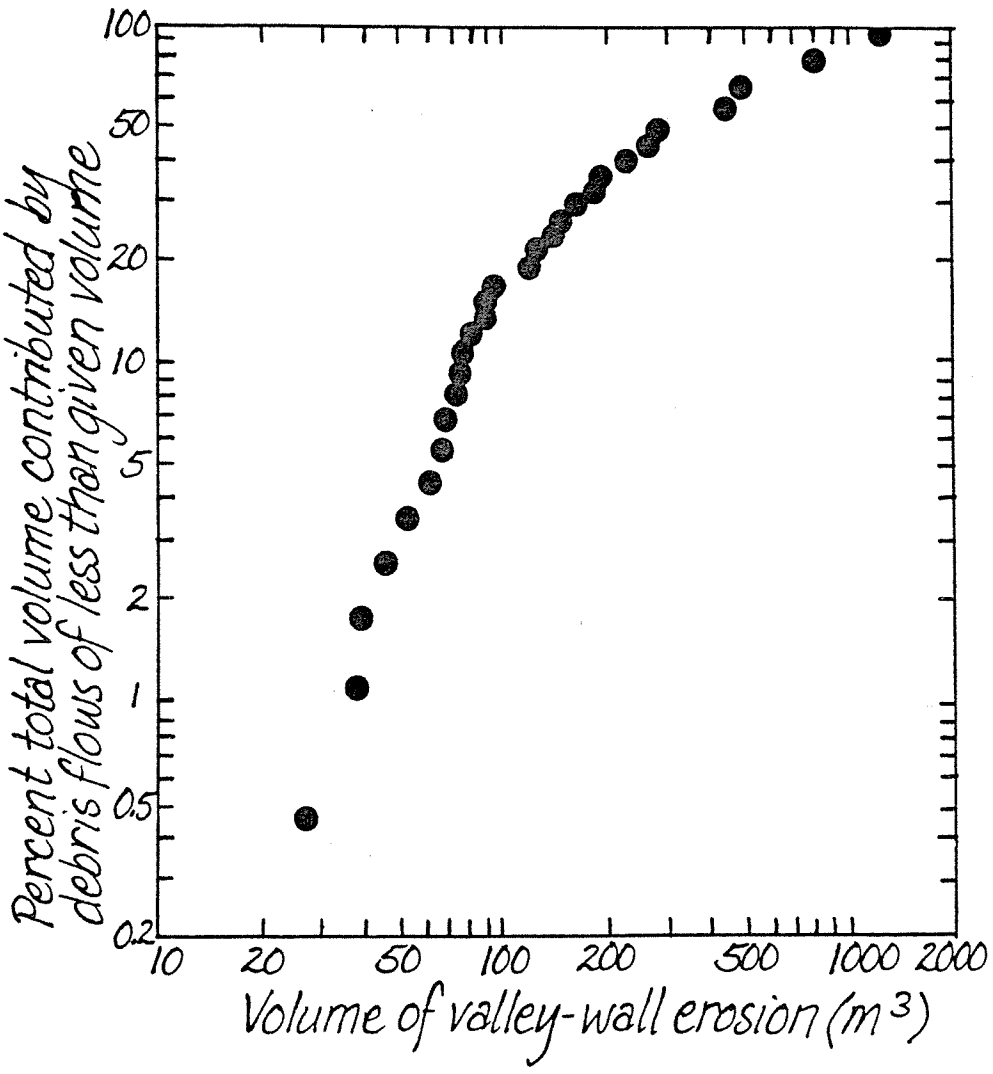

Figure 42. Cumulative volume curve for road-related debris flows in Christmas and Stequaleho basins.

resulted in debris flows and had an average delivery ratio of 0.62. Of the remaining eight landslides four had low delivery ratios, and average delivery for all eight was 35%. A recalculation of production rate assuming delivery ratios based on slides unaffected by debris flows results in a decrease to 67% of the calculated value, or to 52 m^3/road-km-yr.

CHAPTER VII. RELATIVE IMPORTANCE OF SEDIMENT PRODUCTION FROM ROADS

Measurements of sediment production rates from specific sources mean little unless they either are fitted into the context of sediment production in the basin as a whole, are compared to natural rates of basin-wide sediment production, or are compared to natural sediment production rates from the same sources. This chapter describes measurements of sediment production rates from natural sources and compares the calculated sediment production from road-related sources in the Clearwater basin to measurements of sediment yield in similar basins. Calculated sediment production from road-related sources is first put into a form which allows comparison with other measurements, and production rates of suspendible sediment are calculated.

Total Sediment Production from Road-Related Sources

This study has resulted in the quantification of sediment production rates from road surface erosion, backcut erosion, road-related landslides, diffuse surface erosion from sidecast material and road-related landslide scars, gullying by road drainage, and rilling on road-related landslide scars. Other sources of sediment from roads such as increased tree-throw along road rights-of-way, the effects of the actual construction of roads, and the triggering of remote failures and destabilization of channel banks by road-related changes in basin hydrology have not been considered and will not be included in the calculated sediment production rates.

Rates of sediment production from roads and locations of sediment sources in a basin are constantly changing as new roads are built, old ones are abandoned, and road use patterns are changed. Total production rate from the sources considered will thus be calculated for different stages in the development of Christmas and Stequaleho basins. In each case the actual weather patterns and precise distribution of road use are not considered, but averages are used; fluctuations in these parameters will significantly affect the actual sediment production rate for any given year. This approach is necessary because past road-use patterns are poorly defined, because sediment production from sources such as landslides was not measured with respect to weather patterns but was dealt with as a long-term average, and because temporary storage of sediment in streams attenuates the effects of any particular erosional event.

The history of road use in Stequaleho basin was reconstructed by using known dates of clearcutting, making possible the identification of general trends in use patterns with the development of the basin. Over 92% of the basin is under management by the Washington State Department of Natural Resources, and the history of state involvement with each clearcut unit is thus available. The dates of slashburning and planting

were used to estimate the year that each unit was clearcut, and the length of road sustaining hauling from each unit was considered to have fallen into the heavy-use category for 3 months of that year. This method does not account for heavy use due to gravel-truck traffic during road construction, but moderate use by logging trucks during construction is considered. The length of road constructed each year was assumed to equal the length of road necessary for access to the clearcut units logged during that year. In several cases logging activity ceased for a year or more, and the length of new road necessary to access clearcuts logged during the following year was averaged over that year and those intervening. One-half the length of new road and the length of road joining it to the basin entrance was considered to be moderately used over a period of time that varies with the length of road constructed: hauling of logs from road rights-of-way is estimated to proceed at a rate of 200 m of road cleared per week. Roads were considered to be lightly used during the year following clearcutting; after a year in the light-use category the road was considered to be non-used, corresponding in sediment yield to the category of abandoned roads in Chapter V. Through-roads and roads providing the only access to neighboring basins were never considered to be less than lightly used.

In Christmas basin the reconstruction is less detailed. A high proportion of the basin is owned by ITT-Rayonier, and records of development on private land were not seen. The progress of clearcutting and road-building was thus reconstructed from aerial photographs, and the proportion of road length falling into each use category at the time of each set of photographs was assumed to be representative of the road-use distribution for that year. An average-sized clearcut unit is logged and yarded over a 4- to 6-month period. Any indication of logging activity was taken to imply recent or impending hauling, so the resulting values for heavy-use, temporary non-use, and moderate-use sediment production from road surfaces were divided by 2 to account for the time that a clearcut is active without the occurrence of hauling. The earliest phases of clearcutting did occur on state land, allowing more detailed reconstruction of the first year. It is evident that these estimated reconstruction of basin development can result only in calculations of general trends of sediment production. In both basins the most evident change recognized is the increasing percentage of road length abandoned. Results of the calculations of road-related sediment production through time for each basin are shown in Fig. 43 and in Appendix Tables G-1 and G-2. As in previous calculations, sediment production is calculated for roads of average gradient and culvert spacing.

Published analyses of grain-size distribution in the soils of the Clearwater basin (McCreary, 1975; and see Fig. 5) may be used to estimate the production rate of suspendible sediment from landslides, debris flows, and gully erosion. The volumes of sediment produced by these disturbances on each soil type are multiplied by the proportion of soil weight composed of particles of less than 2 mm in diameter for that

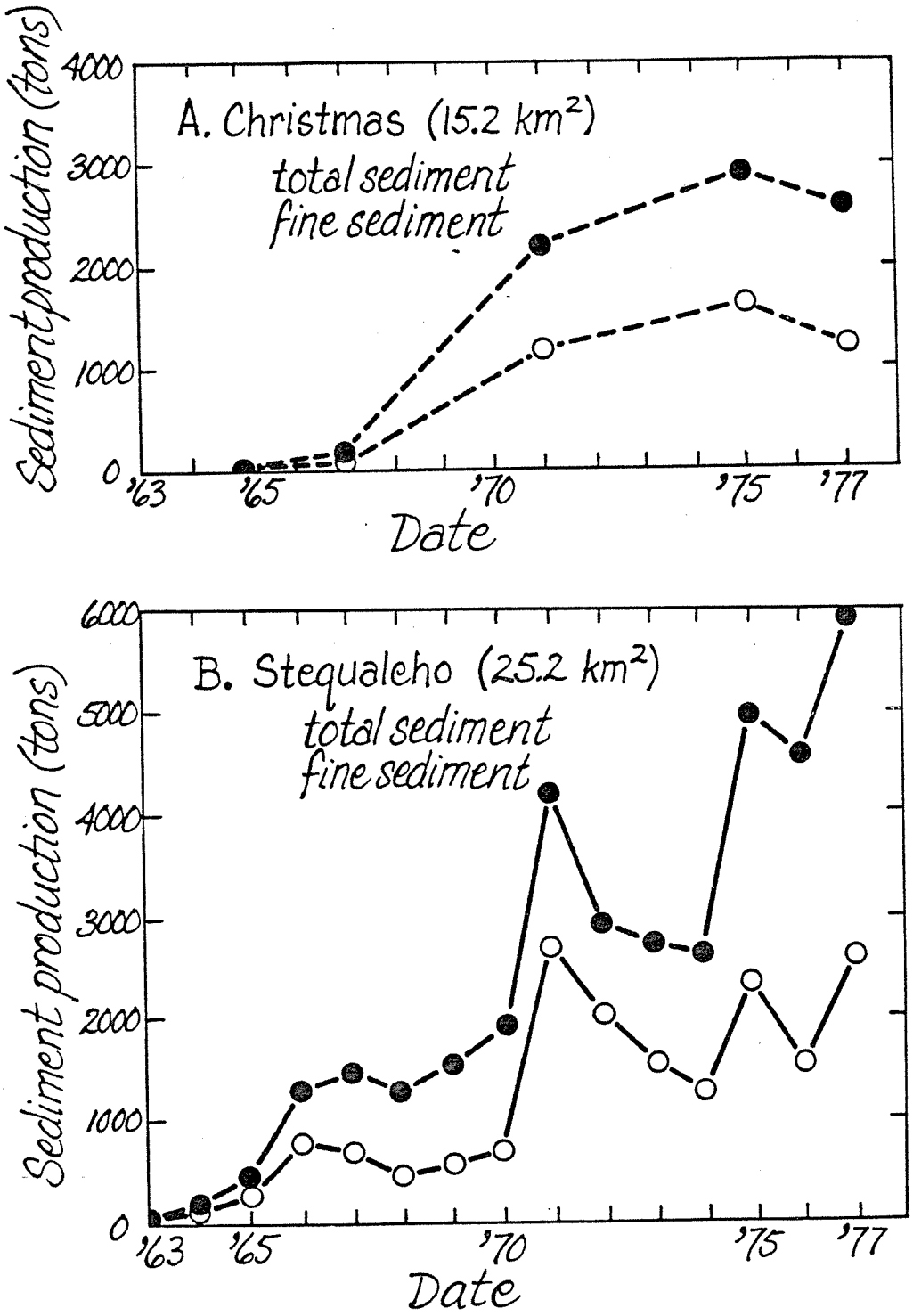

Figure 43. Sediment production from road-related sources through time in Christmas and Stequaleho basins.

soil, and the resulting rates are summed over soil type for each disturbance to calculate the production rate of fine sediment from each type of disturbance. The 2 mm diameter was selected as a maximum grain size for suspended sediment because 2 mm represents the largest particle to be sampled more than once by an automatic suspended sediment sampler located in Stequaleho Creek. The intake for the sampler was positioned 10 cm above the bed at the thalweg, and samples were collected over a 4-month period which included the fifth highest flood period of the water year. In the case of Christmas basin 27.9% of the soil mass involved in landsliding comprises clasts of less than 2 mm in diameter; the corresponding value in Stequaleho basin is 24.5%.

Sediment delivered to streams from road surfaces and backcuts is almost uniformly fine-grained. On only three occasions during the sampling of culvert wash were grains larger than sand-sized collected in sampling bottles. Rilling and surface erosion from landslide scars represent an intermediate ground: some rills and landslide scars show extensive armoring by large clasts while others are evidently capable of transporting any grain size available. These two sources, however, account for less than 6% of the total road-related sediment production during the years evaluated, so the distinction is not critical. For the purpose of the calculations, rills and surface erosion on landslide scars will be assumed to contribute only fine sediment. Four soil samples analyzed for bulk density ranged in value from 0.8 to 1.3 but averaged 1.0 g/cm^3. A value of 1.0 g/cm^3 is thus assumed for soil density in the following calculations.

Calculated production rates for fine sediment are listed in Appendix Tables G-3 and G-4 and are shown in Fig. 43. Production rates can not be related directly to suspended sediment yields, however, because a high proportion of the sediment originating as bedload-sized material is abraded or fractured during transport and eventually leaves the basin as suspended sediment. The importance of particle breakdown is demonstrated by stones composing a gravel bar on a fifth-order stream in a basin adjacent to Christmas Creek: approximately 15% of the pebbles larger than 4 cm in diameter had shattered in place to particles of less than 1 cm in diameter.

Because of the short period of record, the importance of large hydrologic events, and the lack of understanding of long-term trends in sediment production rates from road-related mass movements, these results should not be construed as an indication of long-term trends. They do indicate, however, that during the years for which Christmas basin is analyzed 46% of the suspendible sediment introduced to streams by the road-related sediment sources considered has been derived by erosion from road surfaces. The comparable value in Stequaleho basin is 41%. Breakdown of coarse sediment produced by other sources, however, will increase their significance over time.

The total amount of fine-grained sediment produced by road-related sources in Christmas basin may also be calculated by using a technique similar to that used for Stequaleho basin. The length of road accessing each clearcut unit is assumed to have been heavily used for a 3-month period at some time since 1966, and each heavy-use period is followed by a year of light-use. The moderate-use component is calculated by applying a yarding rate of 200 m of right-of-way cleared per week to the length of road present in the basin in 1978. The lengths of road having undergone heavy, light, and moderate use are then multiplied by the duration of each use-level and the results summed; the difference between this value and the total number of road-kilometer-years in the basin is the number of road-kilometer-years represented by non-use periods. Each of these values is then multiplied by the corresponding sediment production rate in order to calculate total sediment production from surfaces of each road type over the history of the basin (see Table 24). This method results in a calculated total of 4900 t of fine-grained sediment produced from logging road surfaces (the value for backcut erosion has been subtracted), while total production of fine-grained sediment from other road-related sources amounts to 5100 t. Road surfaces are thus estimated to account for 49% of the production of fine-grained sediment from road-related sources in Christmas basin. Again, breakdown of coarse sediment during transport will increase the significance of other road-related sources. If the same method is used to calculate total production from Stequaleho basin, road surfaces are seen to contribute 43% of the fine-grained sediment.

Sediment Production in Undisturbed Basins

As described in an earlier chapter, fieldwork in undisturbed areas of the Clearwater basin disclosed five major sources of sediment to streams: landslides, bank erosion, treethrow, debris flows, and animal burrows. Sediment production by landslides and treethrow are here considered in detail, while sparser data collected for the other sources allow estimation of process rates.

Methods

Ten basins ranging in size from 2 to 17 hectares and representing as wide a variety of conditions as possible were selected for detailed mapping (see Fig. 3 and Table 25). Because the presence of a road anywhere in a basin may affect the downstream hydrology, in only one case was a basin selected which contained any length of road. A 75-m length of ridge-top in the Collapse Creek basin (basin designations are informal) was only several months old when mapped and thus was assumed not to have exerted much influence on erosion processes. Few completely undisturbed basins are left in the central Clearwater basin, so those sampled were constrained both in size and location. No undisturbed basins of greater than fourth order were found, and the smaller basins were largely limited to the highland perimeter of the Clearwater basin.

Table 24. Total sediment production from road-related sources in Christmas and Stequaleho basins (values in metric tons).

	Christmas		Stequaleho	
Source	Total	<2 mm	Total	<2 mm
Landslides*	11,200	3,100	21,400	5,200
Debris flows	1,100	310	4,900	1,200
Gullies	90	25	180	40
Sidecast erosion	210	210	370	370
Secondary erosion	830	830	1,500	1,500
Rills	230	230	470	470
Backcut erosion**	(390)	(390)	(440)	(440)
Road surface and backcut				
Heavy use	3,800	3,800	5,300	5,300
Temporary non-use	560	560	760	760
Moderate use	420	420	720	720
Light use	460	460	550	550
Paved	-	-	10	10
Non-use	50	50	50	50
	19,000	10,000	36,700	16,200

*Shallow disturbances of indeterminate origin are included in landslide value.

**Backcut contribution is included with road-surface production but is listed separately here to allow comparison.

Table 25. Undisturbed basins mapped during study.

Name***	Map no.*	Basin	Area (ha)	Channel length by order (km) 1	2	3	4	Number of links by order 1	2	3	4	Sources mapped: Slides	Tree-throw	Bank erosion
Blacktarp	1	Stequaleho	12	.62	.49			7	1			x		
Green	2	Stequaleho	11	.53	.52			7	2			x		
Collapse	3	Miller	8	.41	.24	.11		4	2	1		x		
Nick	4	Miller	16	1.35	.46	.37		21	3	1		x	x	x
Creak I	5	Christmas	12	1.12	.57	.15		15	4	2		x	x	
Palm	6	Christmas	17	1.35	.49	.21		17	4	1		x	x	
Arm	6	Christmas	2**				.27				1	x	x	x
Creak II	5	Christmas	5	.47			.20	3			1	x		x
Verti	7	Stequaleho	8	.85	.22			5	2			x	x	
Vertitoo I	8	Stequaleho	2		.09	.24			1	1		x	x	
Vertitoo II	8	Stequaleho	2**				.44				1	x		
Tree	9	Christmas	10	.30	1.03	.21		2	2	1		x	x	
			107	7.0	4.1	1.3	.9	81	21	7	3			

*Numbers keyed to locations in Figure 4.
**Area mapped adjacent to channel.
***Informal field designation

Segments of two fourth-order channels in basins containing minor lengths of road were thus mapped in order that some record of processes along higher-order channels be made. It is assumed that because the roads are located on ridge-tops and are 0.7 and 1.8 km from the channel segments studied, their impact would be relatively minor.

Fieldwork consisted of drawing a sketch map of each channel in a basin and locating and describing those sources which contributed sediment directly to the stream or left sediment where it would be in contact with the stream during high flows. The volume of sediment removed from each source was measured if still evident, and the length of time since the sediment was removed was estimated by dating vegetation growing on the resulting scar. The volume of sediment produced from each type of source over a known time interval is then used to calculate the rate of sediment production from that source.

Treethrow into Streams

A high proportion of tree mortality in the Clearwater area is either due to uprooting by wind or is followed by uprooting. If the uprooted trees are adjacent to stream channels or are on steep valley walls above the stream the uprooted mass of roots and soil frequently slides into the stream or into a location where soil eroded from the rootwad will fall into the stream. If the root-mass lands in the stream, the running water removes the sediment quite efficiently. Otherwise, more gradual processes such as rainsplash, dry ravel, and small-scale sloughing both on the rootwad and on the original scar contribute sediment more slowly.

Detailed mapping of 9.2 km of first- through fourth-order channels in undisturbed areas resulted in the location of 59 rootwads that had fallen into stream channels and an additional 131 immediately adjacent to channels (see Appendix Table H-1). In each case sediment trapped by the tree roots was being introduced directly into the streams. A total of 166 other rootwads were mapped which could have contributed some sediment to the stream from further away, but in each case this volume of sediment was small. A minimum age was determined for 54 of the treefalls by measuring the age of vegetation growing in the scar or on the rootwad itself, and these dated falls provided calibration for a qualitative dating system based on the progress of decay in the fallen trees (see Table 26). Five decay classes were defined using characteristics of bark and wood, as described in Table 27. The lengths of time that trees in the older categories had been on the ground were measured by one of the following techniques: 1) counting annual growth rings from hemlocks growing in the treethrow scar or on the underside or side of the rootwad itself and adding one year for seeding and germination and one year for attaining the 20-cm height at which measurements were made, as determined from field observations, or 2) measuring the diameter of the hemlock at 20 cm above ground level and using this value to determine the age from a regressed curve of diameter versus age measured from

Table 26. Minimum lengths of time that streamside treefalls of various decay classes have lain on the ground.

Dating method**	Class II young	Class III middle	Class IV old	Class V relict
Hemlock	22	29	46	107
	11	32	27*	119
	17	37	79	107
	5	34	40	52*
	16	20*	20*	112
	13	28*	44	52*
	5	34	40	137
	12	29	72	34*
			53	75
				59
				117
				177
Shelf fungus	11			
	9			
	12			
	7			
	11			
	9			
	10			
Salmonberry	5			
Number of samples	16	8	9	12
Average age (yrs)	11	30	47	96
Standard error (yrs)	1	2	6	12

*Youngest 25% of decay class; not used in calculation of class boundaries.

**Methods used in dating falls:

Hemlock--number of growth rings at 20 cm above ground surface; add two years for establishment.

Shelf fungus--number of major ridges; add four years for establishment (see Figure 45b).

Salmonberry--number of orders of branching; add one year for establishment (see Figure 45a).

Table 27. Characteristics of decay classes for fallen hemlock and fir trees.

Decay class	Age (yrs)	Firmness of bark and wood	Description of tree
1: New	0 - 2	Firm	Tree still has needles; bark not mossy
2: Young	2 - 25	Difficult to pierce bark with hammer	Bark intact but mossy
3: Middle	25 - 39	Hammer easily pierces bark	Bark starting to slough
4: Old	39 - 75	Hammer easily pierces wood	
5: Relict	75	Foot easily pierces wood	Wood breaking up into chunks

hemlocks in similar environments (see Fig. 44). Definition of the age of younger decay classes made use of additional techniques such as counting annual rings on shelf fungi growing on the downed trees and counting the order of branching of salmonberry bushes growing on the scar (see notes, Table 25, and Fig. 45). Because vegetation may have become established on the fallen tree at any time since the fall occurred, ages of falls based on vegetation necessarily represent minimum ages. The youngest 25% of the treefalls in each decay class were thus excluded from the calculation of age boundaries for decay classes. If the ranges in ages of dated treefalls in adjacent decay classes did not overlap, then the mutual boundary was taken as the average of the ages of the most recent treefall in the older class and the oldest treefall of the younger class. In the case of decay classes IV and V, however, the ranges overlapped, and ages of falls in each category were plotted against the percentage of trees in the same category of that age of younger. The boundary between the classes was taken as the age at which the percentage overlap of the two classes was equal (see Fig. 46).

Because a single microenvironment, the banks of low-order streams, is considered, decay rates are assumed to be relatively uniform throughout the area. Such rates do of course depend on the size and species of tree, but virtually all of the fallen trees mapped were either hemlock or Pacific silver fir, which decay in similar manners.

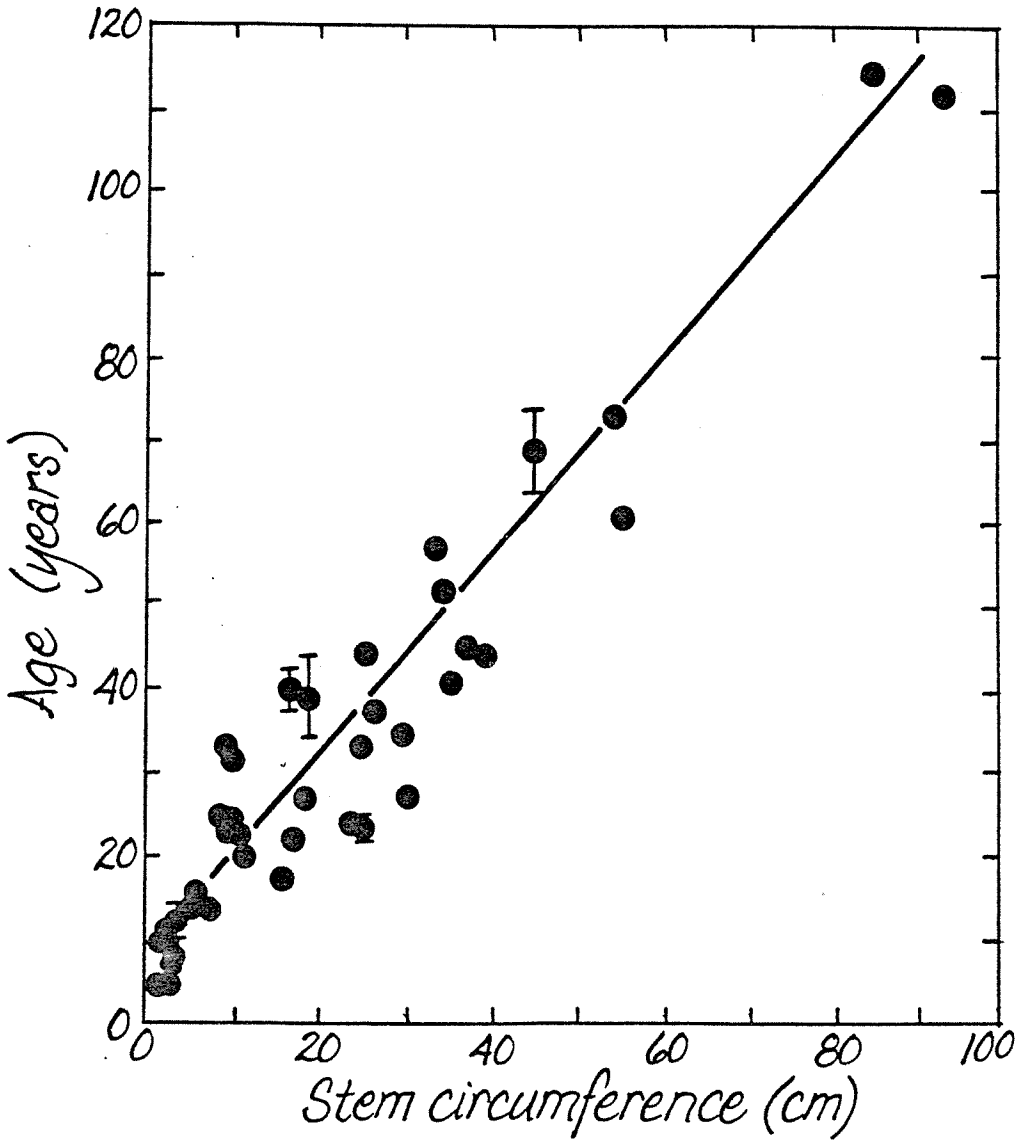

Figure 44. Age versus stem circumference at 20 cm above ground level for seedling hemlocks.

A. Five-year-old salmonberry (Rubus spectabilis) with branching orders indicated.

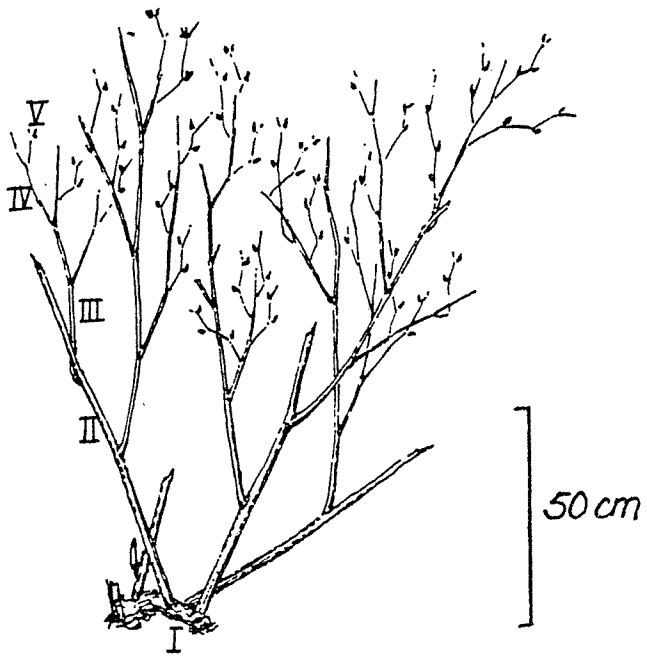

B. Eight-year-old shelf fungus fruiting body.

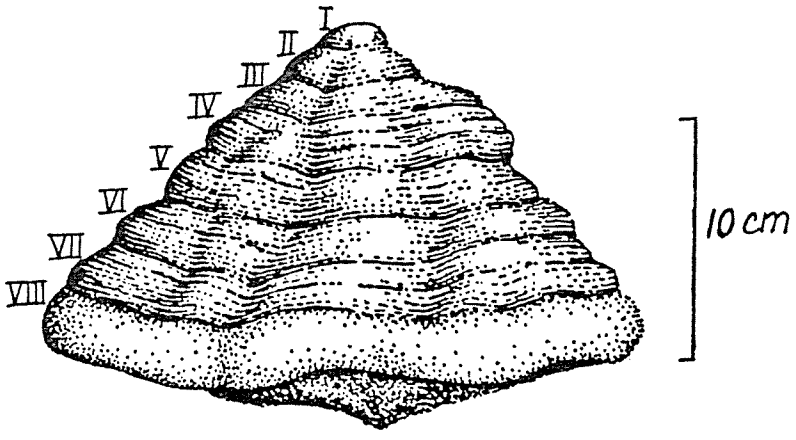

Figure 45. Dating techniques for vegetation.

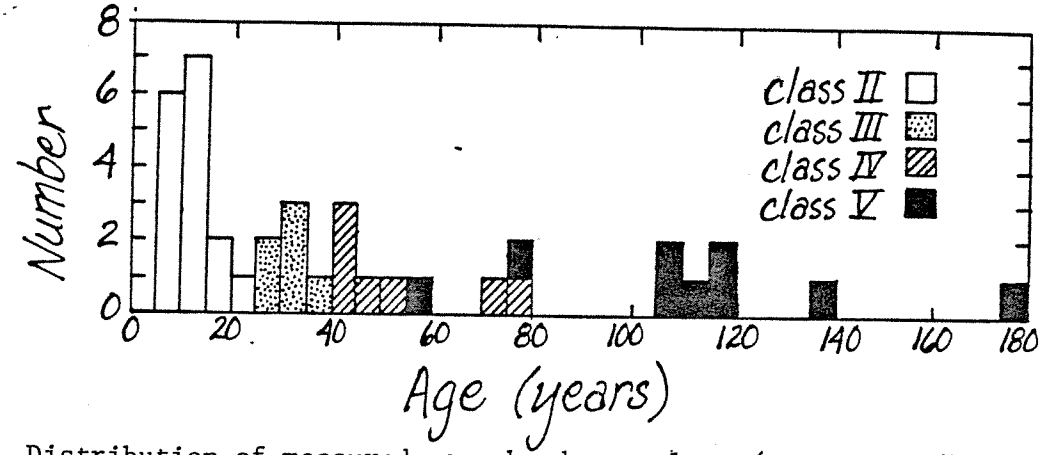

A. Distribution of measured ages by decay class (youngest 25% of each class deleted).

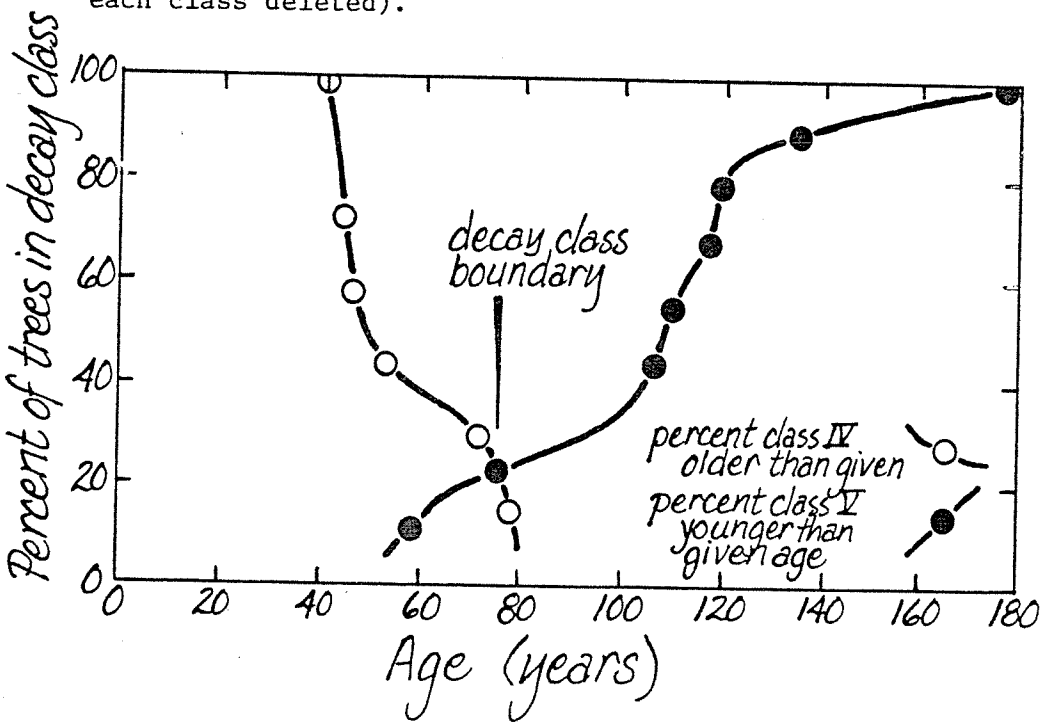

B. Method of determining decay class boundary between classes IV and V.

Figure 46. Determination of age ranges of decay classes of fallen trees.

For the present study only an average fall rate is required. Because fallen trees become unrecognizable during decay class V and because the boundary between classes IV and V is easily recognized in the field, the 25 mapped trees of decay class V were not included in the final calculations, and fall rates were calculated over the 75-year period encompassing decay classes I through IV. The average fall rate into or adjacent to streams as determined by this method is 18 trees per kilometer of channel over the 75-year period. No significant differences in fall rate are evident either between basins or between stream orders, although within basins falls tend to occur in groups.

Rootwad width, height, and thickness, and the circumference of the tree involved (see Fig. 47) were measured on 39 trees which had fallen during the past 5 years; most of these treefalls are located along clear-cut margins. The treefalls mapped in undisturbed basins could not be used since the number of mapped falls younger than 5 years was too small to provide an average; rootwad height and thickness change rapidly as erosion progresses, so older falls were avoided. These measurements allowed the regression of rootwad height versus width (see Fig. 48a), rootwad width versus tree circumference (see Fig. 48b), and rootwad thickness versus tree circumference (see Fig. 48c), which in turn allowed the reconstruction of height, thickness, and circumference from rootwad width for twelve mapped falls of decay classes I and II and for four additional falls outside the map area. Rootwad volumes could then be calculated for these 55 treefalls from rootwad width, height, and thickness measurements by using a model of a cylinder with a segment missing (see Fig. 47). Older falls were not used because original rootwad widths were no longer evident, and tree circumferences had not been measured.

The volume of roots in the rootwad was calculated from tree diameter using the following equation, originally established for Douglas firs but shown to be similar for other conifers (Santantonio 1977):

$$\log_{10} (\text{root weight, kg}) = 2.5309 \log_{10} (\text{stem diameter, cm}) - 1.6393$$

A bulk density of 0.44 for hemlock wood was used to translate root weights to volume. Three samples reported in the same paper indicated that an average of 9.3% of the tree's roots are left in the ground after blowdown. In addition to this value, the proportion of the root-mass in the missing segment of the rootwad cylinder was subtracted from the total volume of roots, which was then subtracted from the total volume of the rootwad to calculate the volume of sediment transported.

The 55 calculated volumes average 4.0 m^3 (see Fig. 49), and this value is then considered the average volume for the mapped rootwads. Since an average of 18 trees fall per channel kilometer over a 75-year period, this is equivalent to a sediment production rate of 0.96 m^3/channel-km/yr for first- through fourth-order channels. Of this volume 31% enters the stream directly, while 69% is washed in gradually from

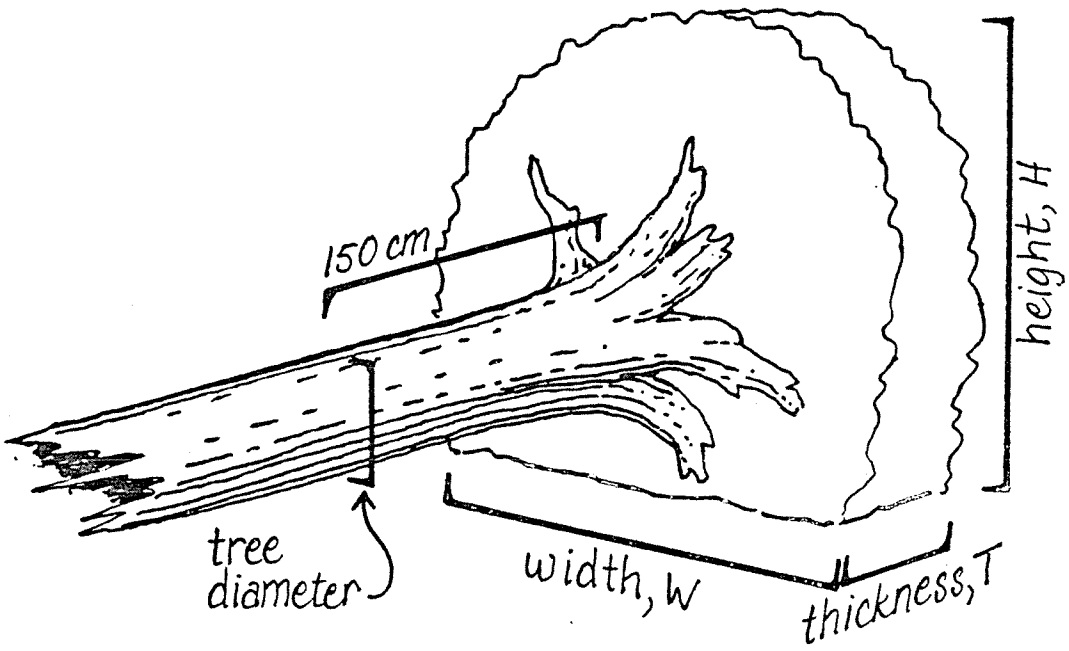

$$\text{rootwad volume} = T \times \left\{ \pi (W/2)^2 - \left[(W/2)^2 \cos^{-1} \left(1 - \frac{(W-H)}{(W/2)} \right) - \right. \right.$$

$$\left. \left. - [(W/2) - (W-H)] \sqrt{(W^2-HW) - (W-H)^2} \right] \right\}$$

Figure 47. Definition of rootwad dimensions.

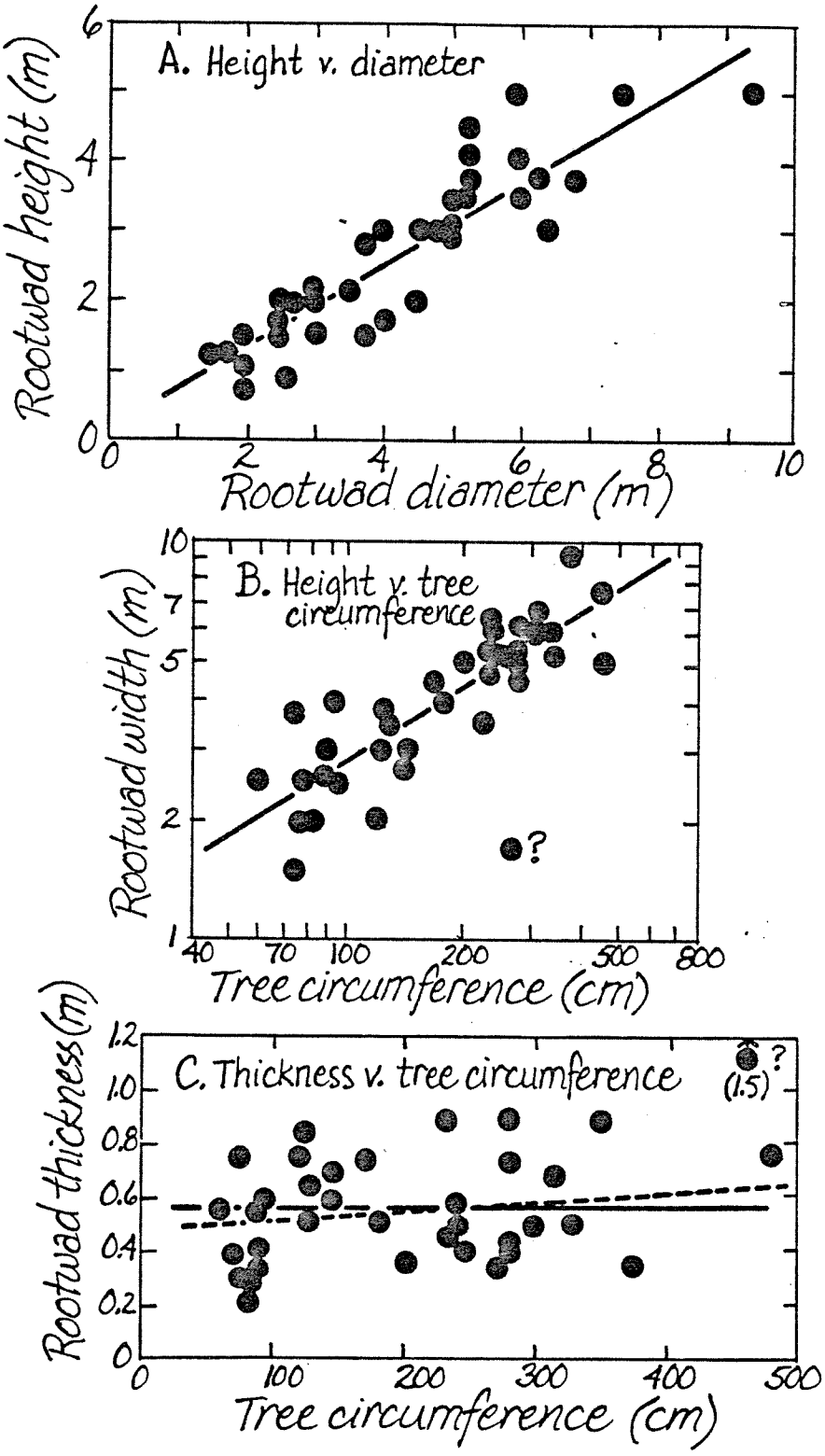

Figure 48. Measured relationships between rootwad dimensions.

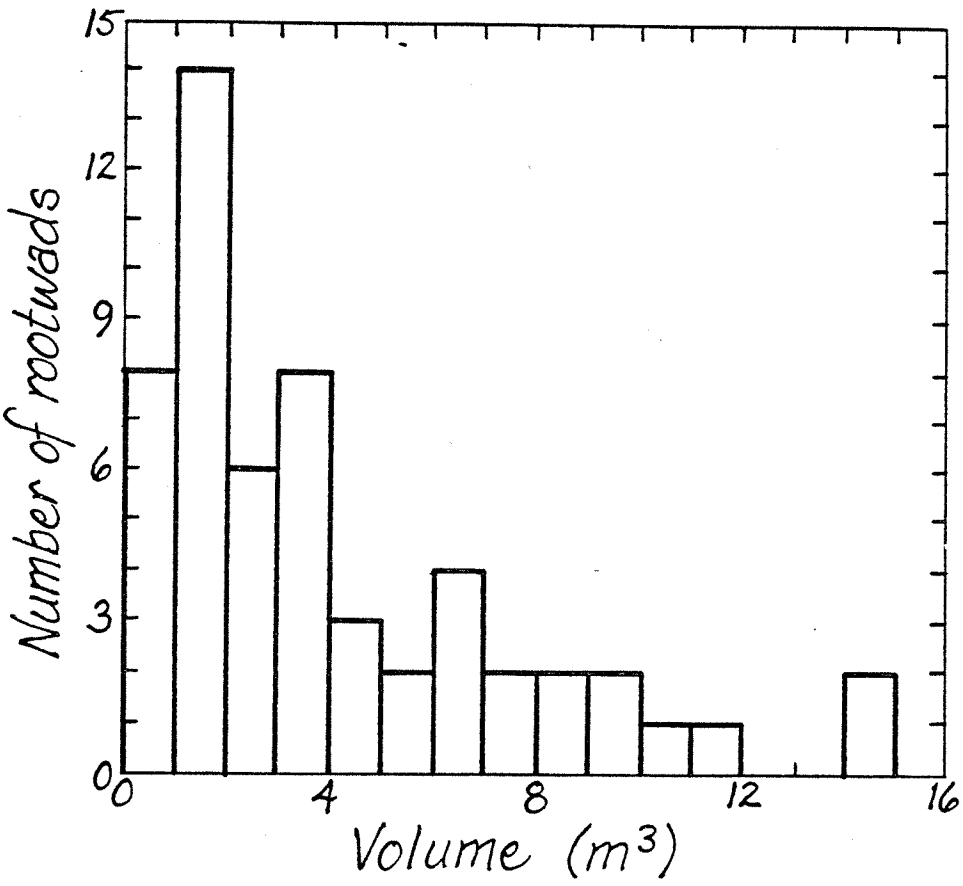

Figure 49. Frequency distribution of measured rootwad volumes.

rootwads that remain on the banks. If it is assumed that none of the sediment left on the banks is retained in permanent storage but eventually finds its way to the stream by the processes mentioned earlier, and that the fall rate has been relatively uniform through time, then this value is equal to the average amount of sediment from rootwads entering the stream each year. In other words, even though it may take 50 years for an individual rootwad to relinquish all of its sediment to a stream, treefalls that have occurred during the previous 50 years are all still contributing. In this stable system the average annual contribution to the stream from rootwads of all ages must equal the average annual influx of rootwads that will eventually contribute sediment. Estimated uncertainty in these calculations is $\pm$ 35%.

Blowdown rates along streams of orders greater than four were not investigated during this study because higher-order stream basins that were free of disturbance could not be found in the central Clearwater basin, so the effects are necessarily based only upon conjecture. As stream order increases both the character of the riparian vegetation and the morphology of the stream banks change: conifers give way to shorter-lived, smaller deciduous trees such as alders, and streams enter broader valleys with well-developed alluvial terraces separating the stream from the hillslopes. In addition, because of their higher discharges, the streams are increasingly capable of undermining the unconsolidated banks. Thus, though the incidence of blowdown probably increases, the sizes of the individual falls and the area contributing falls are both decreased. The rates calculated for first-through fourth-order channels therefore can not necessarily be extended to channels of higher orders; whether those rates are higher or lower will be known only after observations are made of higher-order undisturbed streams. Because higher-order channels account for only 3% of the drainage network in a sixth-order basin, however, differences in sediment production rate along high-order streams will have little effect on a calculated production rate based on measurements from lower-order basins.

Landslides

Landslides contributing sediment to streams were located and described in ten undisturbed basins (see Table 25), four in the southeast portion of the basin and six in the northwest. In addition, the two basins containing minor lengths of road were included in order to increase the length of fourth-order channels sampled. In both cases the roads were 3 to 7 years old, postdating all but one of the ten landslides mapped in the basins.

A total of 82 landslides contributing sediment to streams were identified (see Appendix Fig. H-2). In each case the landslide's major dimensions were measured, and the thickness of material removed was measured at points around the circumference; the volume of material removed was calculated from these measurements.

The ages of landslides were more difficult to determine than those of treefalls, although in many places the same techniques could be used. Hemlocks usually colonize the larger landslide scars and so could provide minimum ages through ring-counts; occasionally fir, spruce, or alder was present instead and could be dated the same way. In many other cases only salmonberry was present. Salmonberries grow a new order of canes each year, so their ages were estimated by counting the number of orders present and adding a year for establishment (see Fig. 45a). Some landslides were associated directly with treefalls and so could be dated using the decay classification described in the previous section; in other cases logs falling into the scar after the failure could be dated using the same techniques to give a minimum age.

Small landslides, especially those related directly to stream undercutting and those in areas that remain saturated, may develop no vegetation more complex than mosses and ferns. In these cases precise dating is not possible, but the sword fern provides a convenient 4- to 5-year time-line. This fern usually does not begin to grow its characteristic leathery dark green fronds until its fourth or fifth year. Before then the fronds are chartreuse and tender, and two or three recognizably different age classes can be observed, suggesting that two to three years' growth is represented. After the leathery fronds develop, two to three years' fronds may be recognized on a single plant. Landslides colonized by ferns can thus generally be separated into those less than or greater than 5 years of age (allowing for one year's establishment time).

Generally those landslides of 8 m^3 or larger provide more precise dating methods; ages of 25 of the 47 landslides larger than 8 m^3 could be dated accurately. In any case, dating of landslides by measuring the age of associated vegetation can provide only minimum ages for the slides; the calculated landslide frequencies are thus maximum frequencies.

Large landslides remain recognizable for a longer period than smaller slides. These resolution periods must be determined so that an appropriate time-scale may be used in landslide frequency calculations: if the age range of the dated landslides used in the calculation is too short, the calculated frequency may reflect only the effects of a few hih-intensity storms, while if the range is too long, the calculated rate may be low because some of the slides that were present within the age range could no longer be recognized. Resolution periods for landslides of different size classes (8-15 m^3, 15-40 m^3, and 40-200 m^3) were determined by plotting the cumulative number of landslides younger than a given age against that age (see Fig. 50). Flattening of such a curve with increasing landslide age would indicate that older landslides are found at a decreasing rate; this is the pattern expected if old landslide scars become increasingly difficult to recognize. In the case of both the 8-15 m^3 and the 15-40 m^3 landslides, the cumulative curves begin to flatten noticeably at an age of about 20 years, although there appears to be a relatively high rate of landsliding between 0 and 5 years. This high rate may reflect the influence of a series of high-intensity

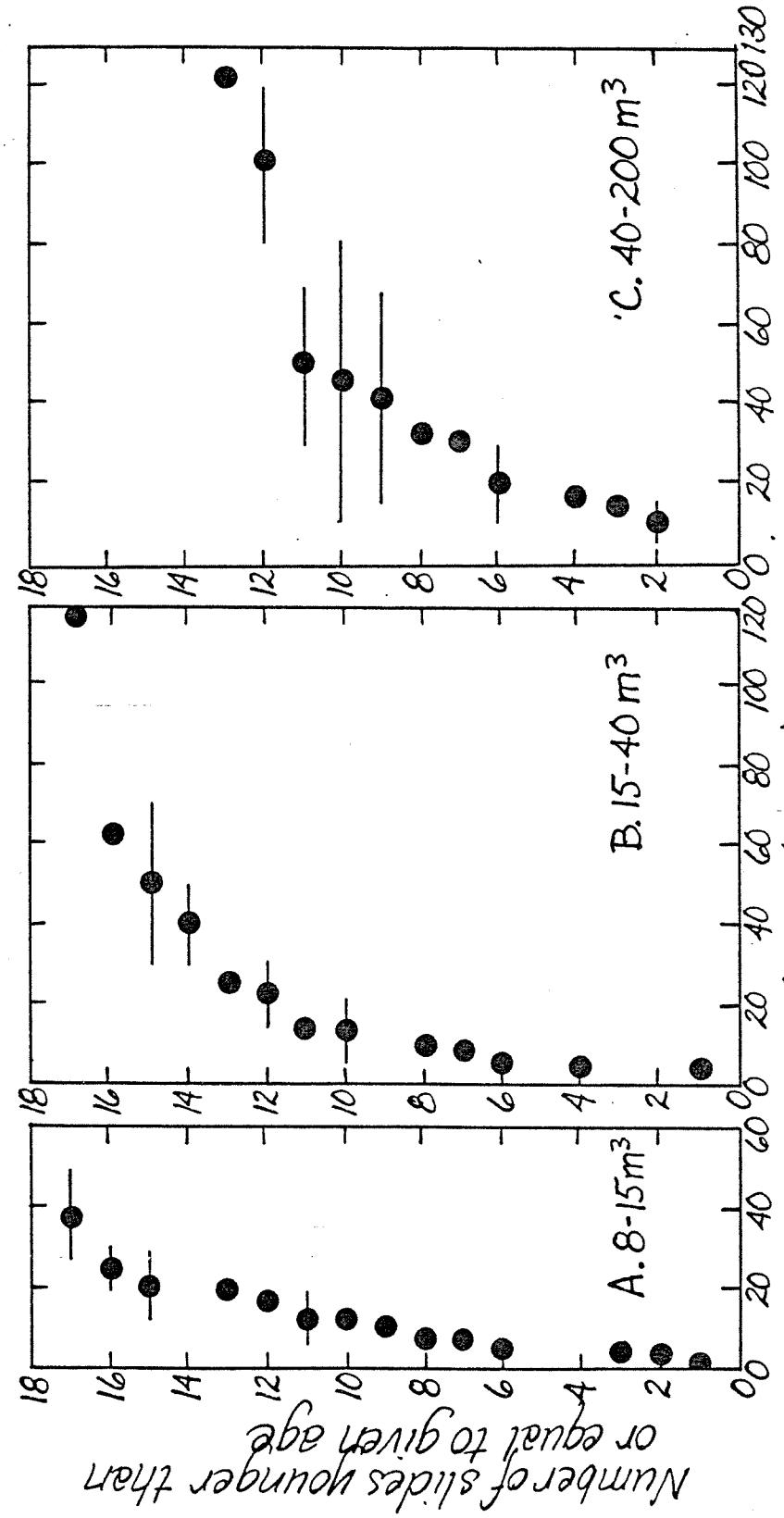

Figure 50. Cumulative number of landslides in undisturbed basins versus age for various size classes.

storms in 1974, 1975, and 1977. Alternatively, the rate may mean that the assumed colonization time of one year, based on observations of revegetation of landslides in clearcuts and of roadcuts of known age, is too low for certain kinds of slides, such as those periodically reactivated by steam undercutting. The flattening of the curves suggests resolution periods of 20 years, and only those 8-40 m^3 landslides younger than 20 years are considered in the following calculations. For landslides with volumes greater than 40 m^3 the cumulative curves remain relatively linear for a 50-year period, although the uncertainty in dating of the five slides older than 30 years is quite high. A 50-year resolution period is assumed for these landslides.

The occurrence of landslides is dependent upon the occurrence of major storms; high pore pressures in a soil mass decrease friction along a potential failure surface at the same time that the increasing moisture content increases the downhill component of force. As implied above, this dependence could control the form of the cumulative landslide curves: the high landslide rate between 0 and 5 years could reflect the frequency of large storms during that period, and the decrease in frequency at 20 years could be a result of a decreased storm frequency at that time. This dependence was tested by plotting for given years the cumulative number of dated 8-15 m^3 landslides occurring against the cumulative number of storms dropping more than 250 mm in four day (see Fig. 51) at the U.S. Weather Service precipitation gauge located in the town of Clearwater near the mouth of the Clearwater basin. This gauge was used because 48 years of data exist from it; average precipitation in the mapped basins is about 1.2 times that at Clearwater (see Table 2). The selected intensity thus becomes greater than 300 mm/4 days in the areas of the mapped landslides. This intensity was chosen because individual high-intensity storms generally last from 3 to 5 days, and 250 mm/ 4 days represents a recurrence interval of about 2.5 years. The smallest size interval of dateable slides, 8-15 m^3, was used because it was suspected that large slides would be less sensitive to individual storm intensities and might depend more upon protracted wet periods of lower intensity storms. The resulting plot is linear for the first 20 years and intercepts the origin, suggesting that the time distribution of high-intensity storms may indeed explain the high landslide frequency between 0 and 5 years. The slope of the curve decreases after a point corresponding to about 20 years, indicating that on average fewer landslides have been recorded per high-intensity storm. This pattern supports the 20-year resolution period assumed above. The sharply defined break-in-slope at 20 years is misleading: the ordinates of all points above it are defined using the single 8-15 m^3 landslide dated that was older than 20 years.

The number of 8-15 m^3 landslides during 5-year periods was also plotted directly against the number of high intensity storms during the same periods, and additional plots were made for other size categories.

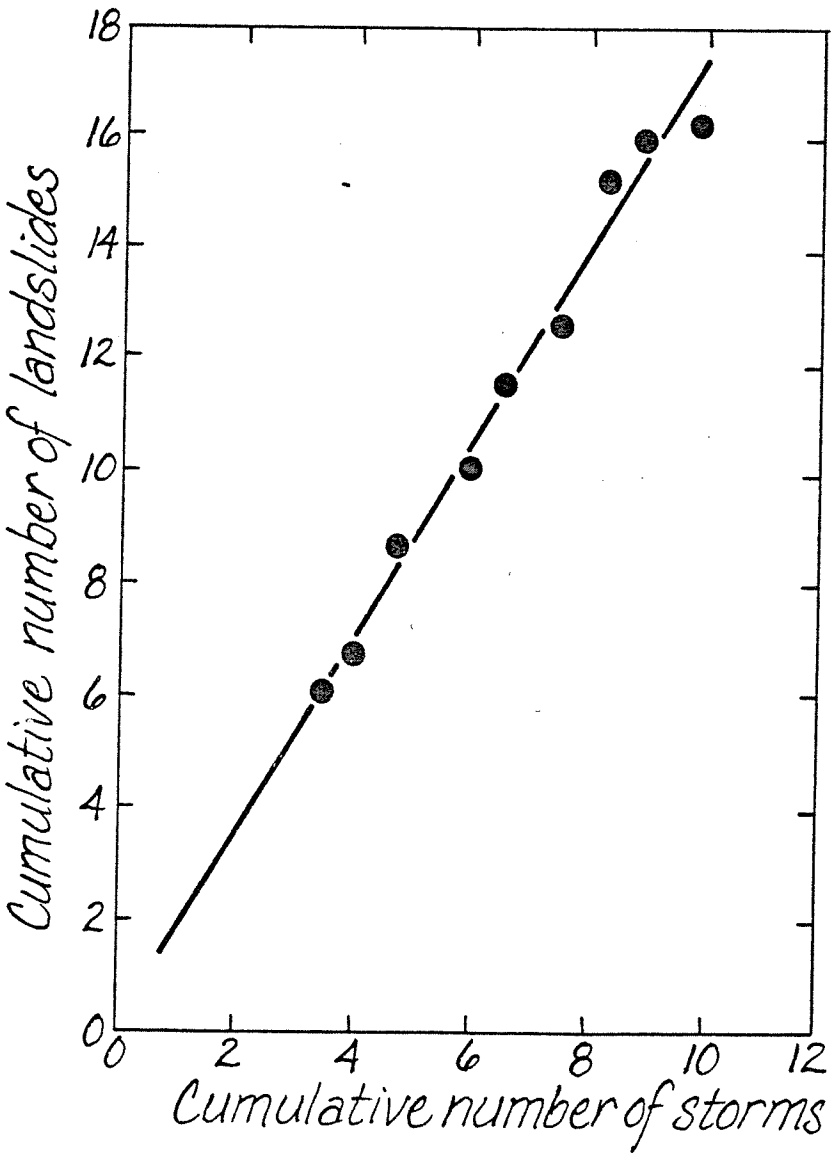

Figure 51. Cumulative number of natural landslides of 8 to 15 m^3 versus cumulative number of storms of intensity greater than 250 mm/4 days. Values are interpolated from cumulative curves for each factor.

In the case of the small landslides the relationship is quite well-defined, while for larger slides the relation becomes increasingly random (see Fig. 52).

Because landslides smaller than 8 m^3 rarely provide dateable vegetation other than ferns, they are considered over a time range of only 5 years, as determined by the approximate age at which the sword fern begins to grow dark green leathery fronds. The resulting calculated frequency therefore will not reflect a long-term average and will probably be high, both because of the frequency of high intensity storms between 1973 and 1978 and because of the increased significance of the possible variation in colonization time.

The spatial distribution of landslides and their average size are both dependent upon hillslope gradient, bedrock type, soil type and thickness, local groundwater hydrology, and the presence of external triggering mechanisms such as undercutting by streams. Thus frequencies differ according to the stream order with which the slides are associated, the type of site in which they occur (e.g., streambank or drainage depression), and which part of the basin--northwest or southeast--they occur in.

Difference in location within the Clearwater basin integrates to some extent all of the other factors because of the distribution of topographic, bedrock, and climatic differences, so results are compiled separately for the northwestern and southeastern basins. Within each of these regions landslide frequency varies greatly between individual basins, both because the basin sizes are small and the slide frequency low and because the landslides often occur in groups. Landslide occurrence is further broken down by stream order to detect differences in frequency based on order-related differences in streamside morphology and channel activity (see Table 28), but possibly because sample sets are small, no patterns are evident. Size classes are treated separately because their resolution periods are different, though resolution periods are assumed to be the same for a given size class in either part of the basin.

Sediment production rates from landsliding are calculated for each size class by averaging the volume of landslides younger than the determined resolution period over that resolution period (see Table 28). Combination of estimated $\pm$ 20% uncertainties in landslide volumes and ages results in an estimated net uncertainty of $\pm$ 28% for production rates. Average annual sediment production rate is calculated independently for the northwest and southeast regions (see Table 29) by multiplying the measured rate for each stream order by the drainage density of that order in sixth-order basins (see Fig. 4). An additional 0.3 km/km^2 of fifth- and sixth-order streams were not sampled, since no undisturbed fifth-order basins remain in the central Clearwater drainage. Despite the high variation in rates between basins and stream orders, the average rate agrees closely for the two regions: to the

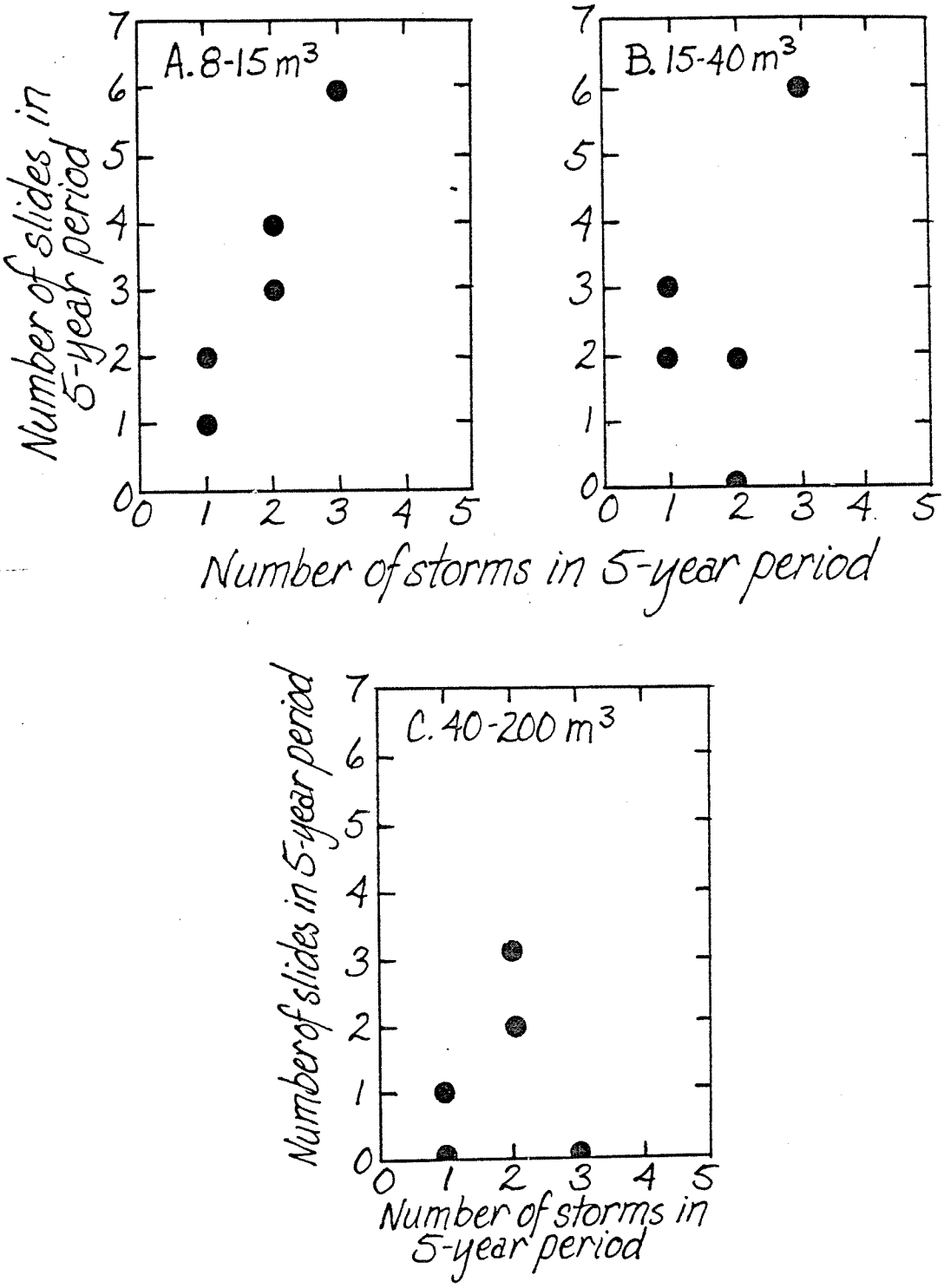

Figure 52. Number of natural landslides of various sizes versus number of storms of intensity greater than 250 mm/4 days in successive 5-year periods.

Table 28. Sediment production rates from natural landslides, classified by region, stream order, and size.

Stream order	Slide volume category (m^3)	Mapped channel length (km)	Number of slides*	Total volume of slides (m^3)	Sediment production by channel order* (m^3/channel-km/yr)
A. Northwest Clearwater basin (typified by Christmas Creek drainage).					
I	0 - 8	3.50	5	15	0.9
	8 - 40	3.50	4	75	1.1
	≥ 40	3.50	3	198	1.1
	Total	3.50	12	288	3.1
II	0 - 8	2.39	4	14	1.1
	8 - 40	2.39	12	174	3.7
	≥ 40	2.39	2	96	0.8
	Total	2.39	18	284	5.6
III	0 - 8	1.13	3	7	1.2
	8 - 40	1.13	2	25	1.1
	≥ 40	1.13	0	0	0
	Total	1.13	5	32	2.3
IV	0 - 8	0.47	0	0	0
	8 - 40	0.47	3	26	2.8
	≥ 40	0.47	0	0	0
	Total	0.47	3	26	2.8
B. Southeast Clearwater basin (typified by Stequaleho Creek drainage).					
I	0 - 8	1.38	1	1	0.2
	8 - 40	2.00	0	0	0
	≥ 40	2.00	2	185	1.8
	Total				2.0
II	0 - 8	1.32	0	0	0
	8 - 40	1.32	2	18	0.7
	≥ 40	1.32	2	360	5.4
	Total	1.32	4	378	6.1
III	0 - 8	0.24	0	0	0
	8 - 40	0.24	0	0	0
	≥ 40	0.24	1	41	3.4
	Total	0.24	1	41	3.4
IV	0 - 8	0.44	0	0	0
	8 - 40	0.44	4	56	6.4
	≥ 40	0.44	1	130	5.9
	Total	0.44	5	186	12.3

*Landslides considered are those with ages falling within the estimated recognition period for the landslide size category (see text for explanation): 0 - 8 m^3 --5 years; 8 - 40 m^3 -- 20 years; ≥ 40 m^3 -- 50 years.

Table 29. Total sediment production from landslides in undisturbed basins.

Region	Channel order	Length of order in 6th-order basin (km/km^2)	Number slides per channel-km	Volume mobilized by landslides (m^3/km^2-yr)	Volume delivered to streams (m^3/km^2-yr)
Northwest Clearwater	I	5.3	6.9	16	14
	II	2.2	9.6	12	11
	III	1.0	8.8	2.3	2.0
	IV	.5	12.8	1.4	1.2
	V	.2	-		
	VI	.1	-		
				32*	28*
Southeast Clearwater	I	5.3	3.9	.11	8.6
	II	2.2	4.5	13	11
	III	1.0	4.2	3.4	2.7
	IV	.5	13.6	6.2	5.1
	V	.2	-		
	VI	.1	-		
				34*	27*

*Values represent production only from the 9.0 km/km^2 of first-through fourth-order streams in a sixth-order basin; the remaining 0.3 km/km^2 of fifth- and sixth-order streams are not represented. Average mobilization and delivery rates are thus 3.6 and 3.0 m^3/channel-km/yr in the northwest Clearwater and 3.8 and 3.0 m^3/channel-km/yr in the southeast Clearwater.

northwest an average average of 3.6 m^3/channel-km/yr is produced by landsliding into the 9.0 km/km^2 of first-through fourth-order streams in a sixth-order basin while in the southeast 3.8 m^3/channel-km/yr is contributed.

Some proportion of the landslide material remains on the hillslope beyond the time that the slide can be recognized and is reincorporated

into the colluvial mantle. Contribution of sediment to the stream after this time would be by processes such as treethrow or bank erosion and would be mapped as such. The volume of debris remaining in a still-recognizable landslide scar is difficult to measure because regrowth is fast and because the thickness of deposits generally can not be measured accurately, but evidence of the presence of stored material was noted in 47 of the landslides and was not present in 16; the remaining 19 cases were indeterminate. Volume measurements could be made in five cases and estimates made for an additional twelve. The proportion of sediment remaining in storage of course depends on proximity to the stream, the size of the landslide, and the length of time since failure. A large valley-wall slide may permanently deflect a stream, while sediment from a small landslide caused by stream undercutting may be washed away within a few years.

Storage volume in eight of the thirteen slides larger than 40 m^3 could be measured or estimated. Four of these landslides originated in drainage depressions and four on valley walls; one of the latter was apparently initiated by undercutting and was the only one of these landslides to show no storage (see Fig. 53). None of the other slides stored less than 17% of the failed material. Data are too sparse to warrant similar analyses for smaller slides. The smaller landslides, however, are more likely to be initiated by direct undercutting of valley walls; and, as mentioned above, their smaller volumes could more easily be removed completely by the streams. Of the landslides smaller than 40 m^3, 35% showed no storage.

Although the uncertainty inherent in the data is extreme, the measured storage proportions may be used as guidelines for computations. The point of intersection of the storage curve fit by eye to Fig. 53a and the 50-year landslide age selected as the end of the resolution period for landslides greater than 40 m^3 was selected as the percentage of volume left in permanent storage; this value is equal to 20%. I will thus assume that on average 20% of the debris of all landslides greater than 40 m^3 is reincorporated into the soil mantle. Of the smaller landslides, 35% contributed all material, and the remaining 65% are assumed to store 20% of their original debris. This percentage is an estimator of the amount of material left in the landslide scar or on the slope below at the time that the landslide ceases to be recognizable.

Applying this storage percentage to the landslide sediment production rates in Table 28 produces the amount of sediment introduced into the stream for each order from landslides of the various size classes during the recognition period of the landslide (see Table 29). Average net production is 3.0 m^3/channel-km/yr for first-through fourth-order streams in regions, and uncertainty in the calculations is about $\pm$ 35%, based on uncertainties in dating, volume measurements, and storage estimates.

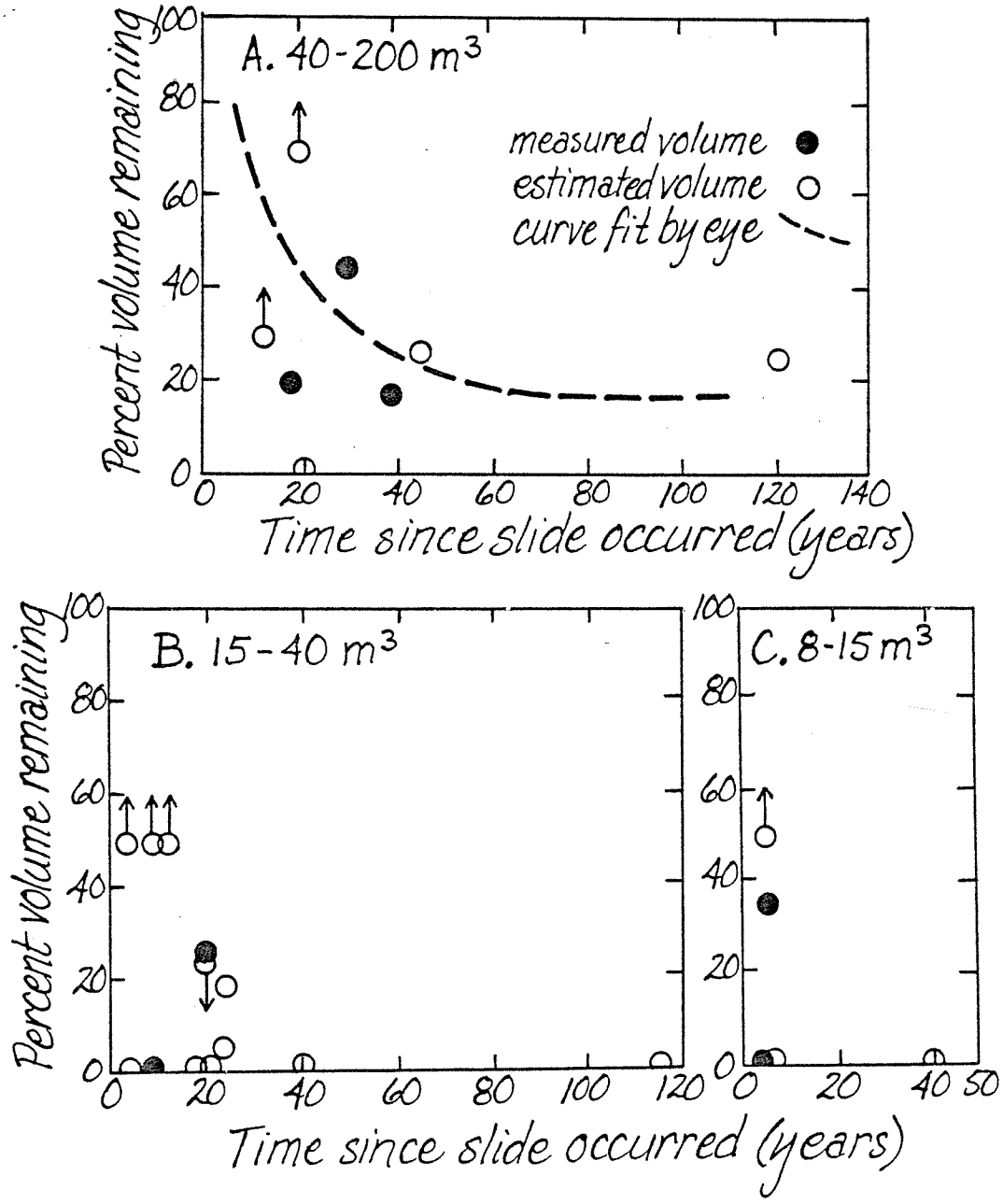

Figure 53. Proportion of total landslide debris remaining in storage on natural landslide scars.

Bank Erosion

Material from landslides or treethrows that enters long-term storage is gradually carried down-slope along with the rest of the soil profile by a series of processes referred to as soil creep. Although the transport rate is quite slow (estimated to be less than 2 mm/yr averaged over a 50-cm soil depth in coastal Oregon based on compilation in Dietrich and Dunne 1978) every slope is affected, so the amount of sediment transported is tremendous. Wherever a slope is in contact with a channel, creep transport of the soil profile causes the channel bank to encroach continuously, but very slowly, upon the channel. Soil exposed in the steep bank face tends to dry out, lose strength, and ravel; disaggregation and loosening of the soil by rootlets of mosses and herbs colonizing the bank face can result in the spalling of blankets of moss still clinging to as much as 2 cm of soil.

The rate of sediment loss due to such small-scale bank erosion processes has never been measured in small basins, nor were such measurements made during the present study. Field observations, however, allow an assessment of the order of importance of this sediment source. The significance of bank erosion was estimated by measuring the areal extent of raw banks along 2.0 km of first-through fourth-order channels (see Appendix Table H-3). Mapping was carried out during the low-flow season, but in most cases the mapped areas of devegetated bank would be subject to inundation only under the highest flows. Although the variations in the areas of eroding bank in stream segments of the same order were extreme (varying between 0 and 503 m^2/km for first-order streams), when the values are averaged by order the results are more consistent: areas of raw bank averaged between 134 and 280 m^2/km for first- through fourth-order channels at the time the basins were mapped in late summer (see Table 30).

Observations of damp, shaded road-cuts and of recent treethrow scars show that moss and algae can recolonize stabilized scars within a year. This observation indicates that some material has been lost from each raw section during the previous year. In some places the thickness of material lost could be measured directly: in four instances moss clumps with soil still attached were found below recent spalls; the average soil thickness was 12 mm (see Table 31). Experiments in pulling moss from intact banks resulted in exactly the same average, with failure occurring just beyond the ends of the rootlets. The agreement of average thicknesses suggests that the failure plane represents a plane of relative weakness between the compact interior soil and the soil laterally reinforced by rootlets. The actual failures may be initiated by frost action or perhaps merely by the increasing weight of the mosses on the bank face acting in a cantilever fashion. Four measurements of net retreat made by determining the lengths of exposed roots and thickness of scarps left after spalling average 19 mm, but the period of time over which the scars have been actively producing sediment is unknown.

Table 30. Total area affected by bank erosion.

Channel order	Measured area of bank erosion (m^2)	Mapped length of channel (km)	Average area (m^2/km)	Length of 6^{th}-order in 6^{th}-order basin (km/km^2)	Area of bank erosion in 6^{th}-order basin
I	108	.81	130	5.3	710
II	47	.33	140	2.2	310
III	79	.28	280	1.0	280
IV	81	.53	150	.5	76
V				.2	30*
VI				.1	15*
				9.3	1,420

* Values calculated using average measured area of eroding bank per channel kilometer for other channel orders.

Table 31. Proxy measurements of stream bank retreat.

Soil thickness attached to spalled moss (mm)	Soil thickness attached to moss pulled off by hand (mm)	Depth of scarps; exposure of roots (mm)
10	8	20
20	20	25
5	5	10
12	8	20
	20	
mean 12	12	19

Once the moss layer has fallen from the wall, the free face becomes susceptible to the activity of other erosion processes; it is possible that continued ravelling of the face might leave it unstable and unvegetated for several years. During most of the period of ravelling, the active erosional processes are the same as those active on cut-banks of roads, for which erosion pin measurements indicate a retreat rate of 16 (±3) mm/yr. This rate is expected to be lower for the damper stream banks. Infrequent inundation may also play a role in eroding the banks, as may undercutting at lower stages. In general, however, only the relatively infrequent areas of constant undercutting exhibit undercuts of greater than five centimeters, and this amount of erosion had undoubtedly occurred over a length of time greater than a year.

If an average erosion rate of between 1 and 3 cm/yr is assumed for bank erosion; if the measured areas of raw bank are assumed to be typical for the various stream orders at a given time; and if stabilized erosion scars are assumed to be revegetated within a year; then first- through fourth-order channels would be contributing sediment at a rate of 1.6 to 4.6 m^3/channel-km/yr by bank erosion.

It is evident that these figures provide a mere estimate; full treatment of the problem would require intensive monitoring of bank erosion processes.

Debris Flows

Because debris flows are infrequent, their evaluation in undisturbed basins poses major difficulties. The steep valley walls and dense forest canopy conspire to make evaluation by aerial photograph interpretation impossible, so an attempt was made to determine their frequency by field mapping.

Two atypical debris flows were encountered in the 1.1 km^2 of basin mapped. One of these was a one- to two-year-old flow mobilizing only 40 m^3 of valley-wall sediment, while the second was a flow showing evidence of about five recurrences over a 50-year period, as determined from ages of vegetation on successive fans. This flow was responsible for removing about 200 m^3 of sediment from valley walls. The period of time during which a moderate-sized flow would be recognizable on the basis of channel and failure characteristics is estimated to be 20 years. This age is based on the resolution period of 8 to 15 m^3 landslides, which are the size nearest the scale of valley-wall disturbances caused by debris flows.

The sample set can be enlarged further by considering road maintenance history. If a road intersects a first-order basin near its mouth a debris flow in that basin will damage the road and so be remembered by road maintenance personnel, yet the road itself will not have influenced the original failure or the initiation of the flow. During a 5-year

period three such flows occurred in a possible contributing area of 6.0 km^2.

Averaging these sources of data provides a mean incidence of 0.95 debris flows per square kilometer in 10 years. Sediment production from erosion of valley walls by eight debris flows mapped in clearcuts averages 111 m^3/flow. If this volume is assumed to apply also to debris flows in unlogged basins, then average sediment production from debris flows in undisturbed basins is about 10 $m^3/km^2/yr$, of which 100% is delivered to the stream. Both of the methods described consider debris flows only in basins of fourth order or smaller, since debris flows are not initiated in channels of higher order. The calculated rate is thus that per unit area of fourth-order basin. Uncertainty is estimated to be ±50%.

Animal Burrows

The mountain beaver (Aplodontia rufa) is common in the lower, northwest part of the Clearwater basin. These rodents live in extensive tunnel networks adjacent to streams. Several of the holes accessing each network have debris cones at their mouths, and these cones are occasionally built out into stream channels. Burrowing activity is most common in the spring and summer months as young animals disperse and excavate their permanent nest holes and as feeding tunnels and established nest holes are enlarged. Excavation is not carried on during winter months (Hooven 1977; Martin 1971; Scheffer 1929).

During late summer, mapping of 7.9 km of undisturbed channels in the northwest part of the Clearwater basin disclosed 27 new mountain beaver cones built partially within the high-water channel margins (see Appendix Table H-4). In the steeper southeast portion of the basin, however, mountain beaver holes were very rarely encountered, and only one was seen to disgorge sediment directly to a stream along the 1.8 km of channels mapped. Volumes of 15 debris cones were measured, providing an average of 0.13 m^3 and a range of 0.02 to 0.48 m^3. If this volume is applied to the mapped density of in-channel debris cones and if all the sediment introduced into the channel is assumed eventually to be washed away, then mountain beaver debris cones account for 0.44 m^3/channel-km of sediment introduced to streams from fourth-order basins in the northwest part of the basin. The confidence interval for this value is estimated to be ±30%, based on uncertainties in volume and distance measurements. In the southeast part of the basin the production rate from this source is very small.

An additional quantity of sediment is introduced by drainage emitted from mountain beaver tunnels. During the driest part of the year discharges of several milliliters per second were observed to flow from the mouths of three burrows per channel kilometer. In most cases the flow was turbid and its path marked by ponded silt. Net production due to this source, however, is unknown.

Total Sediment Production Rate in Undisturbed Catchments

A compilation of measurements and estimates of sediment production rates from the five natural sources considered results in a total sediment production rate of 79 ± 33 $m^3/km^2/yr$ for sixth-order basins (see Table 32), where the indicated uncertainty is estimated as the sum of

Table 32. Sediment production in undisturbed sixth-order basins.

Source	Sediment production to 1st through 4th order streams (m^3/channel-km/yr)	Sediment production in 6th order basin ($m^3/km^2/yr$)
Treethrow	0.96 ± 35%	8.9 ± 3.1
Landslides	3.0 ± 35%	28 ± 9.8
Bank erosion	3.1 ± 50%	29 ± 14
Burrows	0.44 ± 30%	4.1 ± 1.2
Debris flows		9.7 ± 4.8
		79 ± 33

*Values are calculated for all but debris flows by multiplying production rates per channel kilometer by drainage density of 9.3 km/km^2 for sixth-order basins. Debris flow value is calculated from the rate of 10 $m^3/km^2/yr$ measured in fourth-order basins by multiplying this value by the 97% of the area of sixth-order basins which drains into first- through fourth-order streams. Debris flows are not initiated in the 3% of the basin draining directly into high-order channels.

the component uncertainties. Rates of sediment production along fifth- and sixth-order channels are assumed to be equal to those measured along lower-order streams, except in the case of debris flows. Because debris flows occur only in basins of less than fourth order, their contribution was originally calculated on a per-area basis applicable to the sixth-order basin as a whole.

The distribution of soils in the region may again be used to estimate the proportion of the contributed sediment that is immediately available for transport by suspension. Textural analyses of all soils in Christmas basin (not just those involved in road-related landsliding, as calculated above) indicate that 35% ± 9% of the total soil mass is composed of particles less than 2 mm in diameter, while for Stequaleho basin the equivalent percentage is 26% ± 12%. The confidence intervals

given for soil textures represent the reported range in values. In the steady state condition of the undisturbed basins, however, the breakdown rate of larger clasts becomes of critical importance, and these textural values provide only a minimum estimate of suspended sediment yield. The proportion of total load removed as bedload has been measured in several undisturbed basins in the Pacific Northwest. Twenty-five reported values average 0.41 (see Fig. 54a and Table 34). In each case, however, values are based on infill rates of catch basins and undoubtedly include some proportion of suspended material, so such values necessarily represent maximum ratios of bedload to total load. Measurements of bedload during transport, on the other hand, provide more accurate determinations of bedload yield, but such measurements have not been made in undisturbed basins of the Pacific Northwest. Extensive sampling in the Rocky Mountain region indicates that in that area bedload comprises only 1% to 10% of the total sediment yield from undisturbed catchments (D. Rosgen, U.S. Forest Service, Arapaho-Roosevelt National Forest, personal communication). If this range is assumed to apply to the Pacific Northwest also, then about 90% of the bedload-sized material eventually must break down to fragments of suspendible size. This value would result in a predicted total suspended sediment yield of 74 $m^3/km^2/yr$ in undisturbed sixth-order basins. Measured average suspended sediment yields from undisturbed basins in the Pacific Northwest range between 3 and 79 $t/km^2/yr$ for basins monitored longer than a year (see Table 34 and Fig. 54b), but in many cases measurements are made at the mouths of catch basins and so represent minimum yields.

Measurements of Sediment Yield in Undisturbed Basins

Relatively few measurements of whole-basin sediment yields have been made in undisturbed basins in the Pacific Northwest, and periods of record are in most cases relatively short. The reported values, however, may be used to provide an independent check on the magnitude of the total sediment production rate calculated for undisturbed basins during the present study (for compilations of sediment yield data see Flaxman and High 1955 and Larson and Sidle 1980).

The records selected for comparison are limited to those from basins smaller than 30 km^2 which have climates and vegetation similar to those of the Clearwater basin. Sediment yields calculated from measurements of total sediment load are available for 46 measurement years for seven basins in Oregon and California (see Table 34 and Fig. 54c). In each case total yields are calculated as the sum of the yearly sediment accumulation in a settling basin and the yield computed from suspended sediment measurements immediately below the sediment trap. Measured yields from 1965 and 1966 were abnormally high as a result of the 1964 flood (see Anderson 1968), and because no storm of this magnitude occurred in the Clearwater basin, these data were excluded from the analysis. Averaging the 46 measurements provides a mean yield of 70 $t/km^2/yr$. Of these seven basins, however, only five are located in

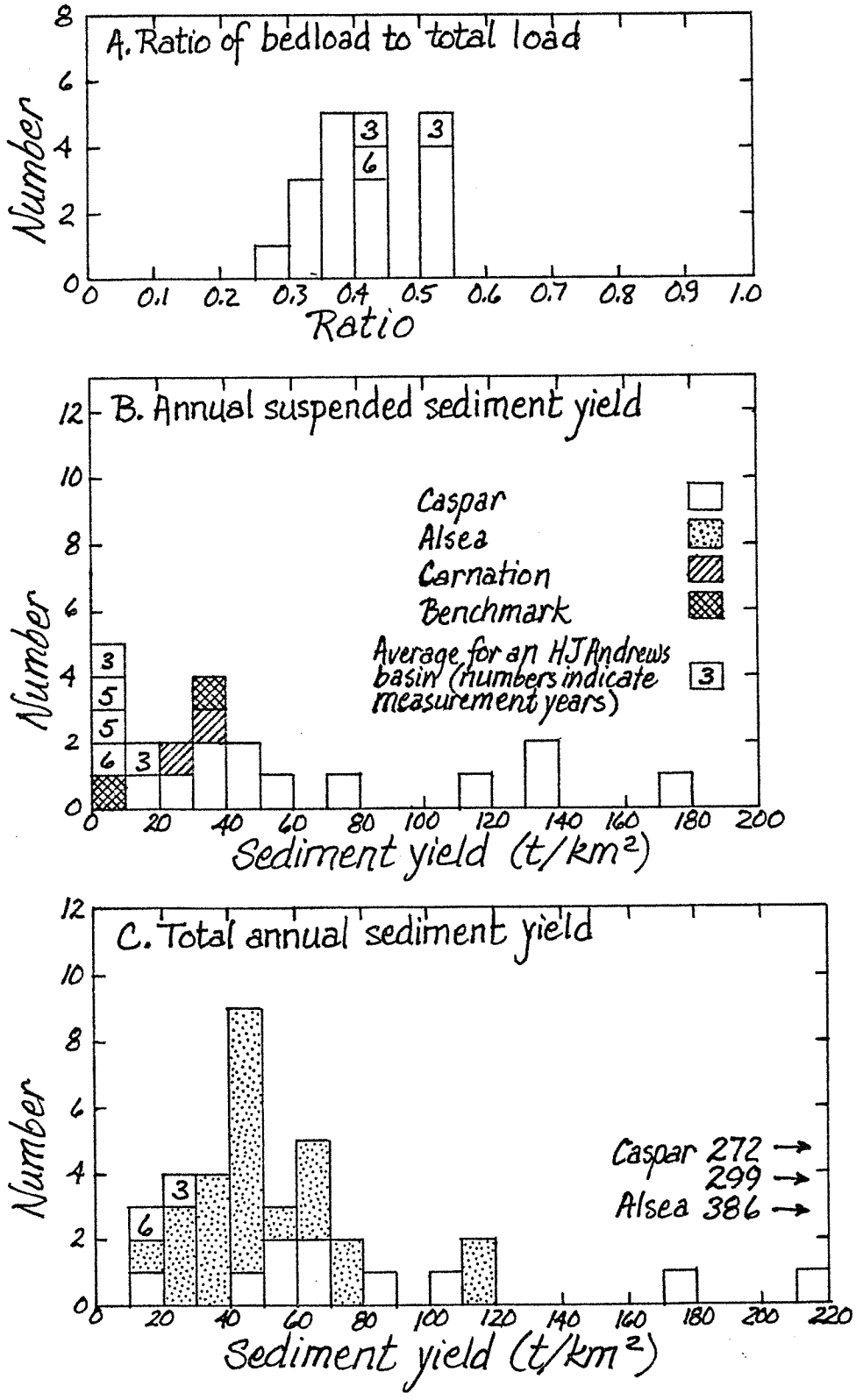

Figure 54. Measured sediment yields in undisturbed basins of the Pacific Northwest. See Table 33 for description of basins and references.

Table 33. Monitored undisturbed basins in the Pacific Northwest.

Study	Location	Rainfall (mm)	Bedrock	Sampling Methods	Basin	Area (km^2)	Data*	Record
H.J. Andrews[1]	Oregon Cascades	2300 snow	tuff,volcanic breccia, basalt	pump sampler, settling basin	Watershed 1	.96	s,b	57-62
					Watershed 2	.60	"	60-62
					Watershed 3	1.01	"	57-59
					Watershed 9	.09	s	69-73
					Watershed 10	.11	"	69-73
Caspar Creek[2]	California Coast Range	1000	sandstone, shale	hand-held and pump samplers, settling basin	North Fork	5.08	s,b	63-73**
					South Fork	4.25	"	63-67**
Alsea Basin[3]	Oregon Coast Range	2500	sandstone	hand-held sampler settling basin	Flynn	2.02	t	59-73**
					Deer	3.03	"	59-65**
					Needle	.70	"	59-65**
Carnation Cr.[4]	Vancouver Is., Canada	3200	volcanics	pump sampler, settling basin	Carnation	10.10	s	3/73-3/75
Benchmark[5]	Olympic Mts., Washington	3300	sandstone, siltstone	pump sampler	Rock	2.4	"	10/78-10/79
					Tower	2.6	"	10/78-10/79

*Data: s - suspended load, b - bedload, t - total load
**Data from two years following 1964 storm not included in averages
[1]Fredriksen 1970, Swanson et al. in press
[2]Rice et al. 1978
[3]Brown and Krygier 1971, Larson and Sidle 1980
[4]Canada Inland Water Directorate 1976a, 1976b, 1977
[5]Unpublished data from University of Washington Forest Hydrology Group

Table 34. Summary of sediment yield measurements in undisturbed basins (for description of basins and sources of data see Table 33).

Basin	Area (km^2)	Number of Samples	Proportion of bedload to total load	Suspended load ($t/km^2/yr$)	Total load ($t/km^2/yr$)
H.J. Andrews					
Watershed 1	.96	6	0.44	7.8	13.9
Watershed 2	.60	3	0.52	5.6	
Watershed 3	1.01	3	0.42	13.0	22.5
Watershed 9	.09	5		3.1	
Watershed 10	.11	5		9.0	
Average			0.46	7.4	16.8
Caspar Cr.**					
North Fork	5.08	11*	0.43	78.9	133.1
South Fork	4.25	5*	0.32	57.4	85.5
Average			0.40	73.5	121.2
Carnation Cr.	10.10	2		30.5	
Benchmark					
Rock	2.4	1		34.5	
Tower	2.6	1		8.2	
Average				21.4	
Alsea**					
Flynn	2.02	13			75.6
Needle	3.03	6			42.5
Deer	.70	6			59.3
Average					63.7
Grand Average					
Bedload/total		27	0.42		
Suspended load		38		30.2	
Total load		46			69.5

*Data from two years following 1964 storm not included in sediment yield calculations.

**Basins with sedimentary bedrock similar to that of the Clearwater area. Averaging the 37 measurements of total load from these basins provides an expected yield of 82.3 $t/km^2/yr$.

sedimentary terranes similar to that of the Clearwater area and are subjected to minimal snowfall. If only the 37 measurements from these basins are considered, then the resulting average sediment yield is 82 ($\pm$14) t/km^2/yr; this value is expected to more closely represent the sediment yield from the Clearwater basin than that calculated above.

The average annual sediment production rate of 79 $\pm$ 33 t/km^2 calculated for the natural sources considered in this study thus appears to be reasonable for the Clearwater basin; an estimated 95% of this value represents suspended sediment. Because the undisturbed basin may be assumed to approximate a steady state condition, the average total sediment yield must directly reflect the rate of sediment production from hillslope to stream channel.

Comparison of Road-Related and Natural Sediment Production Rates

The previous calculations of road-related sediment production allow a direct comparison between sediment production in roaded and undisturbed basins. A drainage basin with the same road density and history of road development and use as Christmas basin but without any clearcuts would be expected to have an average annual total sediment production of 269 m^3/km^2, of which 190 m^3/km^2 is from road-related sources evaluated during this study (see Table 35). Production from sediment sources not related to roads may be assumed to equal that of an undisturbed basin, 79 $\pm$ 33 m^3/km^2; and production from road-related sources not considered in the study would raise the total to an even higher value. The presence and use of roads is thus responsible for increasing the rate of sediment production by at least a factor of 3.4 over natural conditions. The same calculation for Stequaleho basin produces an expected production rate of 387 m^3/km^2, an increase by a factor of 4.9. Because many road-related sediment sources selectively yield fine-grained sediment, in a basin similar to Christmas basin the production rate of sediment smaller than 2 mm in diameter would increase from 28 m^3/km^2/yr to 125 m^3/km^2/yr (as measured upon entry into streams), an increase by a factor of 4.5. In a basin such as Stequaleho, production of fine sediment would increase from 21 to 151 m^3/km^2/yr, a 7.2-fold increase.

Measurements of Suspended Sediment Yield in Disturbed Basins

Suspended sediment measurements were made in both Christmas and Stequaleho basins during the 1973-1974 water year by the University of Washington Forest Hydrology Group. Calculated yields are 211 t/km^2 in Christmas basin and 146 t/km^2 in Stequaleho. Most samples were taken with an automatic pump sampler and the precise location of the intake is unknown, so values should be assumed to represent only a general magnitude of suspended sediment yield. Precipitation during the year was

Table 35. Calculated road-related and background sediment production in hypothetical 10 km^2 basins located in the northwest and southeast parts of the Clearwater drainage. Road density in each basin is 2.5 km/km^2, and roads are subjected to an average distribution of road uses.* Basins are considered to be otherwise undisturbed. Totals are subject to rounding error.

	Basin in northwest ($t/km^2/yr$)		Basin in southeast ($t/km^2/yr$)	
Source	Total	<2 mm	Total	<2 mm
Road-related				
Landslides	115	32	194	47
Debris flows	11	3.1	41	10
Gullies	0.9	0.3	1.6	0.4
Sidecast erosion	2.2	2.2	3.4	3.4
Secondary erosion	8.5	8.5	14	14
Rills	2.3	2.3	4.2	4.2
Backcuts**	(4.0)	(4.0)	(4.0)	(4.0)
Road surface and backcut				
Heavy use	36	36	36	36
Temporary non-use	5.2	5.2	5.2	5.2
Moderate use	5.2	5.2	5.2	5.2
Light use	3.7	3.7	3.7	3.7
Non-use	0.6	0.6	0.6	0.6
Total	190	99	308	130
Natural				
Landslides	28	9.9	28	7.2
Debris flows	9.7	3.4	9.7	2.5
Bank erosion	29	10	29	7.5
Treethrow	8.9	3.1	8.9	2.3
Burrows	4.1	1.4	4.1	1.1
Total	79	28	79	21
Grand total	269	127	387	151

*Average use: 6% heavy, 5% moderate, 39% light, 50% abandoned.

**Backcut contribution is included with road-surface sediment production but is listed separately here to allow comparison.

3978 mm at the Clearwater gauge, 29% above average. Reconstructions of road development and use in Stequaleho basin make possible the calculation of road-related sediment production for this year, and precipitation records permit the adjustment of road surface sediment yield to reflect the higher-than-average precipitation (see Table 17). Sediment yields for roads not heavily used are assumed to increase by the same proportion as yields from heavy-use surfaces, which have been calculated directly from measurements of storm precipitation. These values are listed in Table 36. Total sediment production from road-related sources

Table 36. Sediment production from road-related sources in Stequaleho basin during the 1973-1974 water year.

Source	Road length (km)	Total sediment production ($t/km^2/yr$)	Production of sediment <2 mm ($t/km^2/yr$)
Landslides		101	25
Debris flows		21	5.2
Gullies		0.9	0.2
Sidecast erosion		1.7	1.7
Secondary erosion		7.3	7.3
Rills		2.2	2.2
Backcuts*		(2.1)	(2.1)
Road surface and backcut			
Heavy use	0.7	12	12
Temporary non-use	0.7	1.7	1.7
Moderate use	14.6	3.8	3.8
Light use	1.3	3.7	3.7
Non-use	16.3	0.5	0.5
	32.9	154	63

*Backcut contribution is included with road-surface production but is listed separately to allow comparison.

is calculated to be 154 t/km^2 for Stequaleho basin. If the breakdown of newly-contributed coarse sediment during transport is assumed to be small for the first 10 years after development began in the basin, and the proportion of fine sediment lost to storage is assumed to be small,

then the suspended sediment yield is approximately equal to the proportion of fines in the sediment contributed. This value produces an expected suspended sediment yield of 63 t/km^2 for Stequaleho basin during the 1973-74 water year. At this time the basin was 21% clearcut and had a road density of 1.3 km/km^2, but road use for this year was lower than average.

Natural sediment sources in the 79% of the basin that had not yet been cleacut would have accounted for at least an additional 62 t/km^2 of sediment. Because of the lag-time between the contribution of sediment to a stream and its removal from a basin, however, the quantity of sediment attributable to natural sources would actually be much higher. Coarse sediment contributed to streams before disturbance would require several years of slow bedload transport in order to break down to a size more readily transported, and sediment in rootwads and landslide deposits dating from before clearcutting may remain in storage for decades. Thus a high proportion of the sediment yield during a year is actually from sources active in the past, and recent changes in the distribution of sediment sources would require several years before their effects were noticeable. In Stequaleho basin the actual sediment yield from natural sources during the 1973-74 year was thus probably close to the pre-disturbance value. If breakdown rate for sediment from natural sources is assumed to be the same as before disturbance, expected suspended sediment yield is 75 t/km^2 from natural sources during the 1973-74 water year.

The road-related sediment sources considered in this study could account for about 43% of the measured suspended sediment yield of 146 t/km^2 for the 1973-74 water year. The 62 to 75 t/km^2 from natural sources would comprise an additional 42% to 51% of the yield, and the remaining 8 to 21 t/km^2 would have originated from sources related directly to clearcutting or from the additional road-related sources not considered during the study. Because breakdown rates, changes in the volume of sediment in storage, and the effects of the above-average precipitation on mass movements were not measured, this calculation should be considered only as an indication of the relative magnitude of various sediment contributions. A full analysis of the relative importance of different sediment sources would also require an independent evaluation of sediment production rates in clearcuts, and fieldwork toward this end was carried out during the study. These sources will be discussed in a separate report.

Conclusions

This study has attempted to identify, to measure sediment production rates from, and to determine the significance of various sediment sources related to the presence of gravel-surfaced roads. The following points raised during the investigation are of particular interest:

1. The approach taken was to analyze each type of source independently and to calculate total sediment production by summing the contributions of the various sources. This approach is here demonstrated to be feasible and is seen to be quite flexible in allowing sediment yields to be calculated for different basin conditions.

2. Unit hydrographs are constructed for drainage from various road surfaces and allow the construction of continuous discharge hydrographs from records of rainfall intensity. The lag to peak for runoff from 5.5°, 250-m long, in-use gravel road surfaces is on the order of 8 minutes. Hydrograph peaks on abandoned roads, on the other hand, are attenuated, showing a lag to peak of over 16 minutes.

3. Infiltration capacity on in-use gravel road surfaces is between 0.4 and 0.6 mm/hr and is estimated to be approximately 1.0 mm/hr on abandoned roads.

4. Sediment rating curves can be used to characterize sediment transport from road surfaces of different types. When combined with runoff hydrographs for a typical year, rating curves demonstrate a 1125-fold difference between sediment yields from heavily-used and abandoned road surfaces.

5. Paving a heavily-used road surface decreases sediment yield from that road segment by a factor of 236, as measured at the mouth of the culvert draining the segment. The sediment transported from paved segments is generated by erosion of backcuts.

6. Erosion pins demonstrate a backcut erosion rate of 16 ($\pm$3) mm during a typical year. Sixteen measurements of root exposure on dateable backcut vegetation indicate a long-term erosion rate of 15 ($\pm$2) mm/yr over 5- to 16-year periods.

7. Combination of the sediment rating curve from paved road segments and the infiltration capacity from in-use gravel road surfaces provides an estimate of sediment yield from road backcuts. On a typical heavily-used road segment, only 0.4% of the sediment yield at the culvert mouth is derived from the backcut, while on a lightly-used segment this component comprises 55% of the yield.

8. After road use ends, sediment yield from the road surface decreases quickly. Sediment yield from heavily-used road segments after one and two days of no use has decreased by a factor of 7.5.

9. Landslides related to roads and associated erosion, including gullying, rilling, and surface erosion of both landslide scars and sidecast material, produced an average of 51 t/yr per kilometer of road in Christmas basin during the first 11 years after development began. In Stequaleho basin such landslides produced an average of 87 t/road-km-yr over a 13-year period.

10. Debris flows related to roads produced 4.5 t/road-km-yr in Christmas basin over the same time period, while in Stequaleho basin the rate was 16 t/road-km-yr.

11. Most of the sediment produced by road-related mass movements came from a few large landslides and debris flows. In Christmas basin 36% of the sediment production due to road-related landslides and 25% of that due to debris flows are from single disturbances. In Stequaleho the equivalent percentages are 34% for landslides and 29% for debris flows.

12. As much as 38% of the production of sediment smaller than 2 mm in diameter from sources associated with road-related landslides and gullies may be due to surface erosion and rilling of the scars after the disturbance has occurred.

13. Of the landslides scars observed in the field, 40% are currently sites onto which road surface runoff drains over low road-side berms. Whether such drainage played a role in the destabilization of the sites is unknown.

14. Although the total volume of sediment eroded from valley walls by debris flows is relatively small, debris flows are very important to sediment production in that they were responsible for delivering 34% of the landslide-derived sediment into streams.

15. If total sediment production from roads is considered, landslides are seen to be the dominant source. Road-induced landslides are responsible for 59% of the total sediment production from the road-related sediment sources considered in Christmas basin, while sediment transport from road surfaces accounts for an additional 28%. In Stequaleho 58% of the production is from landslides and 19% from road surfaces.

16. If only that sediment less than 2 mm in diameter is considered, road surface erosion becomes the most important source. Road surface erosion contributes 49% and landslides 31% of the total suspendible sediment from the road-related sources considered in Christmas basin. In Stequaleho basin, 43% of the fines are from road-surface erosion and 32% from landslide-related sources. In both cases secondary erosion of landslide scars will increase the significance of landslide-related sediment production.

17. Independent measurements of sediment production rates from natural sources in the Clearwater basin indicate an average annual production rate of 79 ± 33 t/km^2. Approximately 35% of this total is contributed by landslides, 36% by bank erosion, 12% by debris flows, 11% by treethrow, and 5% by animal burrowing. Measurements of total sediment yield in five similar basins in Oregon and California indicate an average annual yield of 82 t/km^2.

18. The presence of 2.5 km/km^2 of roads undergoing a typical road-use distribution in an otherwise undisturbed basin would increase sediment production by a factor of 3.4 in the northwest part of Clearwater basin and by a factor of 4.9 in the southeast area.

19. Comparison of the suspended sediment yield measured in Stequaleho basin during the 1973-74 water year and the calculated sediment production from roads for the same year suggests that approximately 42% to 51% of the yield was derived from natural sources and 43% from road-related sources.

Gravel-surfaced forest roads are thus demonstrated to be an important source of sediment in logged basins in the Pacific Northwest. Most of the sediment derived from roads is a result of landslides, road surface erosion related to heavy road use, and debris flows; and road surface erosion is seen to be particularly significant as a source of fine sediment.

Suggestions for Further Work

In many respects the present study provides only a preliminary indication of the relative importance of various sources of sediment. The results suggest other studies that could be conducted to understand the influence of these sediment sources on sediment yields and channel morphology:

1. The transfer of sediment into and out of fluvial storage elements must be measured if sediment production measurements are to be directly linked to sediment yields and if changes in sediment loading along a channel are to be understood.

2. Rates of sediment transport and residence time in various storage elements must be measured in order to determine the lag time between the occurrence of a disturbance and the time at which its effects are felt elsewhere in the basin. This information is also necessary to determine the length of time over which impact from a disturbance will be felt.

3. Rates of breakdown of coarse material during transport must be determined in order to understand the relationship between total sediment production and the production of fine-grained sediment in a basin.

4. The importance of other road-related sediment sources such as landslides triggered by road-induced changes in basin hydrology, increased bank erosion by the same mechanism, disturbances caused by the actual construction of roads, and treethrow along road rights-of-way must be evaluated.

Many refinements are possible in the determination of sediment production rates from the road-related sources considered in this study:

5. The number of monitored road segments should be increased.

6. The effects of road gradient and segment length on road-surface sediment transport rates should be determined directly and the results applied to the actual distribution of road gradients and lengths in the basins.

7. Additional years of continuous rainfall records should be used in direct calculations of sediment yield from road surfaces of various types.

8. Dating of road-related landslides should be made more precise by dating vegetation on the scars in order to recognize temporal patterns in landslide distribution with respect to road age.

9. Precise records of dates of landslides may allow the recognition of relationships between landslide frequency and the magnitude of hydrologic events.

10. Landslide distribution should be examined with respect to site factors such as hillslope gradient, bedrock type, wedge distribution, and drainage in order to define sediment production rates from landslides as a function of the distribution of the factors controlling the occurrence of the landslides.

11. The length of time over which erosion may occur on landslide scars must be determined in order to more closely evaluate the importance of secondary erosion on landslide scars.

12. Delivery ratio from the landslides should be more closely defined.

Finally, a more accurate comparison of road-related and natural sediment sources demands a more accurate determination of sediment production from natural sources.

13. Sediment production rates should be measured along undisturbed fifth- and sixth-order channels.

14. A larger area should be examined in order to increase the sample size for various sources. The frequency of debris flows in natural basins is particularly poorly defined.

15. Creep rate and rates of other hillslope transport processes should be measured in shallow soils on undisturbed, forested slopes.

16. Bank erosion rates should be measured directly.

17. As with road-related landslides, production rates from various sources should be related directly to controlling variables and site characteristics such as hillslope gradient and form, drainage, location on a slope, and bedrock type.

LITERATURE CITED

Abercrombie, W. B., J. M. Hunt, and A. G. Larson. 1978. Hydrologic data summary Clearwater River basin water year 1976-1977. Univ. Washington, Coll. For. Resour. 24 pp.

Abercrombie, W. B., J. M. Hunt, and A. G. Larson. 1979. Hydrologic data summary Clearwater River basin water year 1977-1978. Univ. Washington, Coll. For. Resour. 24 pp.

American Association of State Highway Officials. 1966. Standard specifications for highway materials and methods of sampling and testing. Part II. Amer. Assoc. State Highway Officials, 9th ed.

Anderson, H. W. 1954. Suspended sediment discharge as related to stream flow, topography, soil and land use. Trans. Amer. Geophys. Union 35:268-281.

Anderson, H. W. 1957. Relating sediment yield to watershed variables. Trans. Amer. Geophys. Union 38:921-924.

Anderson, H. W. 1968. Major flood effect on subsequent suspended sediment discharge. EOS, Trans. Amer. Geophys. Union 49:175.

Anderson, H. W. 1970. Principal components analysis of watershed variables affecting suspended sediment discharge after a major flood. Pages 404-416 in Proc. Int. Sympos. Results of research on representative and experimental basins. Int. Assoc. Sci. Hydrol. Pub. 96.

Anderson, H. W. 1971. Relative contribution of sediment from source areas, and transport processes. Pages 55-63 in J. Morris, ed. Proc. Sympos.: Forest land uses and stream environment. Oregon State Univ., Corvallis.

Anderson, H. W., and R. L. Hobba. 1959. Forests and floods in the northwestern United States. Int. Assoc. Sci. Hydrol. Publ. 48:30-39.

Anderson, H. W., and J. R. Wallis. 1965. Some interpretations of sediment sources and causes, Pacific coastal basins, Oregon and California. Proc. Fed. Interagency Sedimentation Conf. 1963; USDA Misc. Publ. 970.

Ateshian, J. K. H. 1974. Estimation of rainfall erosion index. J. Irrigation and Drainage Div., Amer. Soc. Civ. Eng. 100(IR3):293-307.

Aubertin, G. M., and J. H. Patric. 1974. Water quality after clear-cutting a small watershed in West Virginia. J. Environ. Qual. 3(3):243-249.

Beschta, R. L. 1978. Long term patterns of sediment production following road construction of logging in the Oregon Coast Range. Water Resour. Res. 14(6):1011-1016.

Bethlahmy, N., and W. J. Kidd. 1966. Controlling soil movement from steep road fills. USDA For. Serv. Res. Note INT-45. 4 pp.

Bishop, D. M., and M. E. Stevens. 1964. Landslides on logged areas in southeast Alaska. USDA For. Serv. Res. Pap. NOR-1. 18 pp.

Brown, G. W., and J. T. Krygier. 1971. Clear-cut logging and sediment production in the Oregon Coast Range. Water Resour. Res. 7(5):1189-1198.

Burroughs, E. R., Jr., G. R. Chalfant, and M. A. Townsend. 1976. Slope stability in road construction: a guide to the construction of stable roads in western Oregon and northern California. U.S. Dep. Interior, Bur. Land Mgmt., Oregon State Office. 102 pp.

Canada Inland Waters Directorate. 1976. Sediment Data Canadian Rivers. 1973. Inland waters directorate, Water Resources Branch, Dep. Fish. and Environ. Ottawa, Canada. 364 pp.

Canada Inland Waters Directorate. 1976. Sediment Data Canadian Rivers. 1974. Inland waters directorate, Water Resources Branch, Dep. Fish. and Environ. Ottawa, Canada. 432 pp.

Canada Inland Waters Directorate. 1977. Sediment Data Canadian Rivers. 1975. Inland waters directorate, Water Resources Branch, Dep. Fish. and Environ. Ottawa, Canada. 364 pp.

Carson, M. A., C. H. Taylor, and B. J. Grey. 1973. Sediment production in a small Appalachian watershed during spring runoff: the Eaton Basin 1970-1972. Canad. J. Earth Sci. 10(12):1707-1734.

Cederholm, C. J., L. M. Reid, and E. O. Salo. In press. Cumulative effects of logging road sediment on salmonid populations in the Clearwater River, Jefferson County, Washington. In Proceedings of a conference on Salmon-Spawning Gravel: a renewable resource in the Pacific Northwest? Seattle, WA. October 6-7, 1980.

Cederholm, C. J., and E. O. Salo. 1979. The effects of logging road landslide siltation on the salmon and trout spawning gravels of Stequaleho Creek and the Clearwater River basin, Jefferson County, Washington 1972-1978. Univ. Washington, Fish. Res. Inst., Final Report Part III, FRI-UW-7915. 99 pp.

Collins, W. T. 1939. Runoff distribution graphs from precipitation occurring in more than one time unit. Civ. Eng. 9:559-561.

Cordone, A. J., and D. W. Kelley. 1961. The influence of inorganic sediment on the aquatic life of streams. Calif. Fish Game 47(2): 189-228.

Crandell, D. R. 1964. Pleistocene glaciations of the southwest Olympic Peninsula. U.S. Geol. Survey Prof. Paper 501-B. Pp. 135-139.

Croft, A. R., and J. A. Adams. 1950. Landslides and sedimentation in the North Fork of Ogden River. USDA For. Serv. Res. Pap. INT-21. 4 pp.

Day, N. F., and W. F. Megahan. 1975. Landslide occurrence on the Clearwater National Forest. Geol. Soc. Amer. Abstr. with Prog. 7:602-603.

Denny, C. S., and J. C. Goodlett. 1956. Micro-relief resulting from fallen trees. Pages 59-66 in Surficial geology of Potter County, Pennsylvania. U.S. Geol. Survey Prof. Pap. 288.

Dietrich, W. E., and T. Dunne. 1978. Sediment budget for a small catchment in mountainous terrain. Zeit. Geomorph. Suppl. Bd. 29:191-206.

Dietrich, W. E., T. Dunne, N. Humphrey, and L. M. Reid. In press. Construction of sediment budgets for catchments. In Proc. Sympos. on sediment budgets and routing in forest catchments, 1979. Oregon State Univ., Corvallis.

Diseker, E. G., and E. C. Richardson. 1962. Erosion rates and control methods on highway cuts. Trans. Amer. Soc. Agr. Eng. 5:153-155.

Dissmeyer, G. E. 1973. Evaluating the impact of individual forest management practices on suspended sediment. Plants, Animals and Man: Proc. 28th Annual Meeting, Soil Conserv. Soc. Amer., Hot Springs, Ark. Pp. 258-264.

Dissmeyer, G. E. 1976. Erosion and sediment from forest land uses, management practices, and disturbances in the southeastern United States. Proc. 3rd Fed. Interagency Sedimentation Conf. 1976. Pp. I-140 to I-148.

Dunne, T., and W. E. Dietrich. 1980. Experimental investigation of Horton overland flow on tropical hillslopes 2. Hydraulic characteristics and hillslope hydrographs. Zeit. Geomorph. Suppl. Bd. 35:60-80.

Dunne, T., and L. B. Leopold. 1978. Water in environmental planning. W. H. Freeman & Co., San Francisco. 818 pp.

Dyrness, C. T. 1967. Mass soil movements in the H. J. Andrews Experimental Forest. USDA For. Serv. Res. Pap. PNW-42. 12 pp.

Dyrness, C. T. 1970. Stabilization of newly constructed road backslopes by mulch and grass-legume treatments. USDA For. Serv. Res. Note PNW-123.

Dyrness, C. T. 1975. Grass-legume mixtures for erosion control along forest roads in western Oregon. J. Soil Wat. Conserv. 30:169-173.

Farmer, E. E., and J. E. Fletcher. 1977. Highway erosion control systems: an evaluation based on the universal soil loss equation. In Soil erosion: prediction and control. Proc. Nat. Conf. Soil Erosion. Purdue Univ., Indiana. Soil Conserv. Serv., Special Publ. 21.

Fiksdal, A. J. 1973. A landslide survey of the upper Clearwater and Solleks River areas, Jefferson County. Unpubl. report for the Geol. and Earth Resour. Div. of State of Washington Dep. Natural Resour.

Fiksdal, A. J. 1974. A landslide survey of the Stequaleho Creek watershed. Suppl. Rep. in Cederholm, C. J., and L. C. Lestelle, Observations on the effect of landslide siltaton on salmon and trout resources of the Clearwater River. Univ. Washington, Fish. Res. Inst. FRI-UW-7404.

Fiksdal, A. J. No date. A landslide survey of the Stequaleho Creek watershed and upper Clearwater River area. Mimeo.

Flaxman, E. M., and R. D. High. 1955. Sedimentation in drainage basins of the Pacific coast states. U.S. Soil. Conserv. Serv. Portland, OR.

Fredriksen, R. L. 1963. A case history of a mud and rock slide on an experimental watershed. USDA For. Serv. Res. Note PNW-1. 4 pp.

Fredriksen, R. L. 1965. Sedimentation after logging road construction in a small western Oregon watershed. Proc. Fed. Interagency Sedimentation Conf. 1963. USDA Misc. Publication 970.

Fredriksen, R. L. 1970. Erosion and sedimentation following road construction and timber harvest on unstable soils in three small western Oregon watersheds. USDA For. Serv. Res. Pap. PNW-104. 15 pp.

Gibbons, D. R., and E. O. Salo. 1973. An annotated bibliography of the effects of logging on fish of the western United States and Canada. USDA For. Serv. Gen. Tech. Rep. PNW-10. 145 pp.

Gilmour, D. A. 1971. Effects of logging on streamflow and sedimentation in a North Queensland rainforest catchment. Commonwealth For. Res. Note 50(143):38-48.

Gonsior, M. J., and R. B. Gardner. 1971. Investigation of slope failures in the Idaho Batholith. U.S. For. Ser. Res. Pap. INT-97. 34 pp.

Gresswell, S., D. Heller, and D. N. Swanston. 1979. Mass movement response to forest management in the central Oregon Coast Ranges. USDA For. Serv. Res. Bull. PNW-84. 26 pp.

Guy, H. P. 1969. Laboratory theory and methods for sediment analysis. Water Resource Inventory, Book 5, Chap. C-1. U.S. Geol. Surv. 58 pp.

Hafley, W. L. 1975. Rural road systems as a source of sediment pollution - a case study. Pages 393-405 in Watershed Management. Proc. Sympos., Irrigation and Drainage Div., Amer. Soc. Civ. Eng., Logan, Utah Aug. 11-13, 1975.

Hammer, T. R. 1972. Stream channel enlargement due to urbanization. Water Resour. Res. 8(6):1530-1537.

Harr, R. D., R. L. Fredriksen, and J. Rothacher. 1979. Changes in streamflow following timber harvest in southwest Oregon. USDA For. Serv. Res. Pap. PNW-249. 22 pp.

Harr, R. D., W. C. Harper, J. T. Krygier, and F. S. Hsieh. 1975. Changes in storm hydrographs after roadbuilding and clearcutting in the Oregon Coast Range. Water Resour. Res. 11:436-444.

Haupt, H. F. 1959. A method for controlling sediment from logging roads. Intermontaine For. and Range Exp. Sta. Misc. Publ. 22. 22 pp.

Haupt, H. F. 1959. Road and slope characteristics affecting sediment movement from logging roads. J. For. 57:329-332.

Haupt, H. F. 1965. Good logging practices reduce sedimentation in central Idaho. J. For. 63:664-670.

Heusser, C. J. 1978. Palynology of Quaternary deposits of the lower Bogachiel River area, Olympic Peninsula, Washington. Canad. J. Earth Sci. 15(10):1568-1578.

Hooven, E. F. 1977. The mountain beaver in Oregon: its life history and control. Oregon State Univ. For. Res. Lab., Res. Pap. 30.

Hoover, M. D. 1945. Careless skidding reduced benefits of forest cover for watershed protection. J. For. 43:765-766.

Hoover, M. D. 1952. Water and timber management. J. Soil Wat. Conserv. 7(2):75-78.

Hornbeck, J. W., and K. G. Reinhart. 1964. Water quality and soil erosion as affected by logging in steep terrain. J. Soil Wat. Conserv. 19:23-27.

Imeson, A. C. 1976. Some effects of burrowing animals on slope processes in the Luxembourg Ardennes. Part 1: The excavation of animal mounds in experimental plots. Geografiska Annaler Series A 58(1-2):115-125.

Imeson, A. C., and P. D. Jungerius. 1977. The widening of valley incisions by soil fall in a forested Keuper area - Luxembourg. Earth Surface Processes 2(2-3):141-152.

Imeson, A. C., and F. J. P. M. Kwaad. 1976. Some effects of burrowing animals on slope processes in the Luxembourg Ardennes. Part 2: The erosion of animal mounds by splash under forest. Geografiska Annaler Series A 58(4):317-328.

Kidd, W. J. 1963. Soil erosion control structures on skid trails. USDA For. Serv. Res. Pap. INT-1. 8 pp.

Kidd, W. J., and J. N. Kochenderfer. 1973. Managing steep land. 5. Soil constraints on logging road construction on steep land east and west. J. For. 71(5):284-286.

Kochenderfer, J. N. 1977. Area in roads after logging in the central Appalachians. J. For. 75(8):507-508.

Koski, K. V. 1975. The survival and fitness of two stocks of chum salmon (Oncorhynchus keta) from egg deposition to emergence in a controlled stream environment at Big Beef Creek. Ph.D. Dissertation, Univ. Washington, Seattle. 212 pp.

Kotarba, A. 1970. The morphogenetic role of foehn wind in the Tatra Mountains. Studia Geomorphologica Carpatho - Balcanica 4:171-186.

Krammes, J. S., and D. M. Burns. 1973. Road construction on Caspar Creek watersheds. Ten year report on impact. USDA For. Serv. Res. Pap. PSW-93.

Larse, R. W. 1971. Prevention and control of erosion and stream sedimentation from forest roads. Pages 76-83 in J. Morris, ed. Proc. Sympos. Forest land uses and stream environment. Oregon State Univ., Corvallis.

Larson, A. G., and H. J. Jacoby. 1976. Hydrologic data summary Clearwater River basin water year 1974-75. Univ. Washington, Coll. For. Resour. 34 pp.

Larson, A. G., and J. J. Jacoby. 1977. Hydrologic data summary Clearwater River basin water year 1975-1976. Univ. Washington, Coll. For. Resour. 24 pp.

Larson, K. R., and R. C. Sidle. 1980. Erosion and sedimentation data catalog of the Pacific Northwest. USDA For. Serv., Pac. Northwest Region. R6-WM-050-1981.

Leaf, C. F. 1974. A model for predicting erosion of sediment yield from secondary forest road construction. USDA For. Serv. Res. Note. RM-274.

Lehre, A. K. in press. Sediment budget of a small mountain catchment in north-central California. In Proc. Symp. on sediment budgets and routing in forest catchments, 1979. Oregon State Univ., Corvallis.

Leopold, L. B. 1968. Hydrology for urban land planning--a guide book on the hydrologic effects of urban land use. U.S. Geol. Survey, Circ. 554. 18 pp.

Leopold, L. B., W. W. Emmett, and R. M. Myrick. 1966. Channel and hillslope processes in a semiarid area, New Mexico. U.S. Geol. Survey Prof. Pap. 352-G. Pp. 193-253.

Lieberman, J. A., and M. D. Hoover. 1948. Protecting quality of streamflow by better logging. South. Lumberman. 177(2225):236-240.

Lund, J. W. No date. Surfacing loss study. USDA For. Serv. Region 6. 9 pp.

Madej, M. A. 1978. Response of a stream channel to an increase in sediment load. M.S. Thesis, Univ. Washington, Seattle. 111 pp.

Madej, M. A. In press. Sediment routing and channel changes in an aggrading stream, Puget Lowland, Washington. In Proc. Symp. on sediment budgets and routing in forest catchments, 1979. Oregon State Univ., Corvallis.

Martin, P. 1971. Movements and activities of the mountain beaver (Aplodontia rufa). J. Mammalogy 52:717-723.

McCreary, F. R. 1975. Soil survey of Jefferson County area, Washington. USDA Soil Conserv. Serv. 100 pp.

Megahan, W. F. 1967. Summary of research on mass stability by the Intermountain Forest and Range Experimental Station soil stabilization project, Boise, Idaho. In Unpubl. Proc., USDA For. Serv. Berkeley Mass Erosion Conference, October, 1967.

Megahan, W. F. 1972. Subsurface flow interception by a logging road in mountains of central Idaho. Pages 350-356 in Nat. Symp. on watersheds in transition. Colorado State Univ., Fort Collins, CO.

Megahan, W. F. 1974. Erosion over time on severely disturbed granite soils: a model. USDA For. Serv. Res. Pap. INT-156. 14 pp.

Megahan, W. F. 1975. Sedimentation in relation to logging activities in the mountains of central Idaho. Pages 74-82 in Present prospective technology for predicting sediment yields and sources; Proc. Sediment Yield Workshop, USDA Sedimentation Lab., U.S. Agric. Res. Serv., ARS-S-40.

Megahan, W. F. 1978. Erosion processes on steep granitic road fills in central Idaho. Proc. Soil Sci. Soc. Amer. 2:350-357.

Megahan, W. F. 1980. Erosion from roadcuts in granitic slopes of the Idaho batholith. Abstract. Cordilleran section of the Geol. Soc. Amer., 76th Annual Meeting, Oregon State Univ., Corvallis.

Megahan, W. F., and W. J. Kidd, Jr. 1972a. Effects of logging roads on sediment production rates in the Idaho batholith. U.S. For. Serv. Res. Pap. INT-123. 14 pp.

Megahan, W. F., and W. J. Kidd, Jr. 1972b. Effects of logging and logging roads on erosion and sediment deposition from steep terrain. J. For. 70:136-141.

Meyer, L. D., C. B. Johnson, and G. R. Foster. 1972. Stone and woodchip mulches for erosion control on construction sites. J. Soil Wat. Conserv. 27:264.

Mitchell, W. C., and G. R. Trimble, Jr. 1959. How much land is needed for the logging transport system? J. For. 57(1):10-11.

National Oceanic and Atmospheric Administration (NOAA). 1973. Precipitation-frequency atlas of the western United States. Vol. IX. U.S. Dep. Comm., NOAA, Nat. Weather Serv., Silver Springs, MD.

Noggle, C. C. 1978. Behavioral, physiological, and lethal effects of suspended sediment on juvenile salmonids. M.S. Thesis, Univ. Washington, Seattle. 87 pp.

O'Loughlin, C. L. 1972. A preliminary study of landslides in the coast mountains of southwest British Columbia. Pages 101-111 in O. Slaymaker, and McPherson, eds. Mountain Geomorphology. Tantalus Res. Ltd., Vancouver, B.C.

Packer, P. E. 1967. Forest treatment effects on water quality. Pages 687-699 in W. E. Sopper and H. W. Lull, eds. Internat. Sympos. For. Hydrology.

Packer, P. E. 1967. Criteria for designing and locating logging roads to control sediment. For. Sci. 13(1):2-18.

Patric, J. H. 1976. Soil erosion in the eastern forest. J. For. 74(10):671-677.

Patric, J. H., and J. L. Gorman. 1978. Soil disturbance caused by skyline cable logging on steep slopes in West Virginia. J. Soil Wat. Conserv. 33(1):32-35.

Phillips, E. L., and W. R. Donaldson. 1972. Washington climate for these counties: Clallam, Grays Harbor, Jefferson, Pacific, Wahkiakum. Coop. Extension Serv., Coll. Agric., Washington State Univ., Pullman. 88 pp.

Pierson, T. C. 1977. Factors controlling debris flow initiation on forested hillslopes in the Oregon Coast Range. Ph.D. Dissertation, Univ. Washington, Seattle. 166 pp.

Price, L. W. 1971. Geomorphic effect of the arctic ground squirrel in an Alpine environment. Geografiska Annaler Ser. A. 53:100-106.

Rice, R. M., J. S. Rothacher, and W. R. Megahan. 1972. Erosional consequences of timber harvesting: an appraisal. Pages 321-329 in Proc. Nat. Symp. on watersheds in transition.

Rice, R. M., F. B. Tilley, and P. A. Datzman. 1979. A watershed's response to logging and roads: South Fork of Caspar Creek, California, 1967-1976. USDA For. Serv. Res. Pap. PSW-146. 12 pp.

Rothacher, J. 1973. Does harvest in west slope Douglas fir increase peak flow in small forest streams? USDA For. Serv. Res. Pap. PNW-163. 13 pp.

Santantonio, D., R. K. Hermann, and W. S. Overton. 1977. Root biomass studies in forest ecosystems. Pedobiologia Bd. 17. S. 1. Pp. 1-31.

Scheffer, T. H. 1929. Mountain beavers in the Pacific Northwest: their habits, economic status, and control. USDA Farmer's Bull. 1598. 18 pp.

Shapley, S., S. Phillip, and D. M. Bishop. 1965. Sedimentation in a salmon stream. J. Fish. Res. Board Can. 22(4):919-928.

Streeter, V. L., and E. B. Wylie. 1979. Fluid mechanics. 7th ed. McGraw-Hill, New York. 562 pp.

Swanson, F. J., and C. T. Dyrness. 1975. Impact of clearcutting and road construction on soil erosion by landslides in the western Cascade Range, Oregon. Geology 3:392-396.

Swanson, F. J., R. L. Fredriksen, and F. M. McCorison. in press. Material transfer in a western Oregon forested watershed in Synthesis Volume, U.S. Internat. Biol. Prog. Coniferous For. Biome.

Swanston, D. N. 1967a. Debris avalanching in thin soils derived from bedrock. USDA For. Serv. Res. Note PNW-64. 7 pp.

Swanston, D. N. 1967b. Soil water piezometry in a southeast Alaska landslide area. USDA For. Serv. Res. Note PNW-68. 17 pp.

Swanston, D. N. 1970. Mechanics of debris avalanching in shallow till soils of southeast Alaska. USDA For. Serv. Res. Pap. PNW-103. 17 pp.

Swanston, D. N. 1974. Slope stability problems associated with timber harvesting in mountainous regions of western United States. USDA For. Serv. General Tech. Rep. PNW-21. 14 pp.

Swanston, D. N., and F. J. Swanson. 1976. Timber harvesting, mass erosion, and steepland forest geomorphology in the Pacific Northwest. Pages 199-221 in D. R. Coates, ed. Geomorphology and Engineering. Dowden, Hutchinson and Ross, Stroudsburg, PA.

Tabor, R. W., and W. M. Cady. 1978. Geologic map of the Olympic Peninsula, Washington. U.S. Geol. Survey, Miscellaneous Investigations Series, Map I-994.

Tagart, J. V. 1976. The survival from egg deposition to emergence of coho salmon in the Clearwater River, Jefferson County. M.S. Thesis, Univ. Washington, Seattle. 101 pp.

Thorn, C. E. 1978. A preliminary assessment of the geomorphic role of pocket gophers in the alpine zone of the Colorado Front Range. Geografiska Annaler Series A. 60A(3-4):181-187.

Trimble, G. R., and R. S. Sartz. 1957. How far from a stream should a logging road be located? J. For. 55:339-341.

Trimble, G. R., and S. Weitzman. 1953. Soil erosion on logging roads. Soil Sci. Soc. Amer. Proc. 17:152-154.

U.S. Environmental Data Service. (monthly.) Climatological data Washington. U.S. Dep. Comm. Nat. Oceanic and Atmospheric Administration.

U.S. Soil Conservation Service (USSCS). 1975. Procedure for computing sheet and rill erosion on project areas. U.S. Soil Conserv. Serv. Tech. Rel. No. 51. 15 pp.

Wald, A. R. 1975. Impact of truck traffic and road maintenance on suspended sediment yield from 14′ standard forest roads. M.S. Thesis, Univ. Washington, Seattle. 38 pp.

Wallis, J. R., and H. W. Anderson. 1965. An application of multivariate analysis to sediment network design. Int. Assoc. Sci. Hydrol. Publ. 67. Pp. 357-378.

Washington Forest Practice Board. 1976. Washington forest practice rules and regulations. Wash. For. Prac. Bd., Olympia, WA. 83 pp.

Weitzman, S., and G. R. Trimble, Jr. 1952. Skid-road erosion can be reduced. J. Soil Wat. Conserv. 7(3):122-124.

Weitzman, S., and G. R. Trimble, Jr. 1955. Integrating timber and watershed management in mountain areas. J. Soil Wat. Conserv. 10(2):70-75.

Wilson, R. L. 1963. Source of erosion on newly constructed logging roads in the H. J. Andrews experimental forest. Unpubl. Rep. BLM. Forest Resources Library, Univ. Washington, Seattle. 21 pp.

Wischmeier, W. H., C. B. Johnson, and B. V. Cross. 1971. A soil erodibility nomograph for farmland and construction sites. J. Soil Wat. Conserv. 26(5):189-192.

Wischmeier, W. H., and L. D. Meyer. 1973. Soil erosion: causes, mechanisms, prevention, and control. Highway Res. Bd. Spec. Rep. 135.

Wischmeier, W. H., and D. D. Smith. 1965. Predicting rainfall-erosion losses from cropland east of the Rocky Mountains. U.S. Dep. Agric. Agriculture Handbook No. 282.

Wooldridge, D. D. 1979a. Suspended sediment transport and forest road construction, Wildhorse Creek, Kalama River Basin. For. Practices Water Quality Mgt. Plan, App. 1. Washington State Dep. Ecol. 40 pp.

Wooldridge, D. D. 1979b. Forest road construction and suspended sediment, Campbell Creek, Skagit River basin. For. Practices Water Quality Mgt. Plan, App. 2. Washington State Dep. Ecol. 27 pp.

Wooldridge, D. D. 1979c. Suspended sediment from truck traffic on forest roads, Meadow and Coal Creeks. For. Practices Water Quality Mgt. Plan, App. 3. Washington State Dep. Ecol. 33 pp.

Wooldridge, D. D., A. G. Larson, and A. R. Wald. 1975. Hydrologic data summary Clearwater River basin water year 1973-1974. Univ. Washington, Coll. For. Resour. 66 pp.

Yair, A. 1974. Sources of runoff and sediment supplied by the slopes of a first order drainage basin in an arid environment (Northern Negev). Page 5 in R. Gerson, and M. Inbar, eds. The field study program of the Jerusalem-Elat Symposium. Zeit. fur Geomorphol. Suppl. Bd. 29.

Yee, C. S., and R. D. Harr. 1977a. Effect of wetting mode on shear strength of two aggregated soils. USDA For. Serv. Res. Note PNW-303. 9 pp.

Yee, C. S., and R. D. Harr. 1977b. Influence of soil aggregation on slope stability in the Oregon Coast Ranges. Environ. Geol. 1:367-377.

APPENDICES

APPENDIX A. HYDROGRAPH PEAKS USED IN CONSTRUCTION OF UNIT HYDROGRAPHS

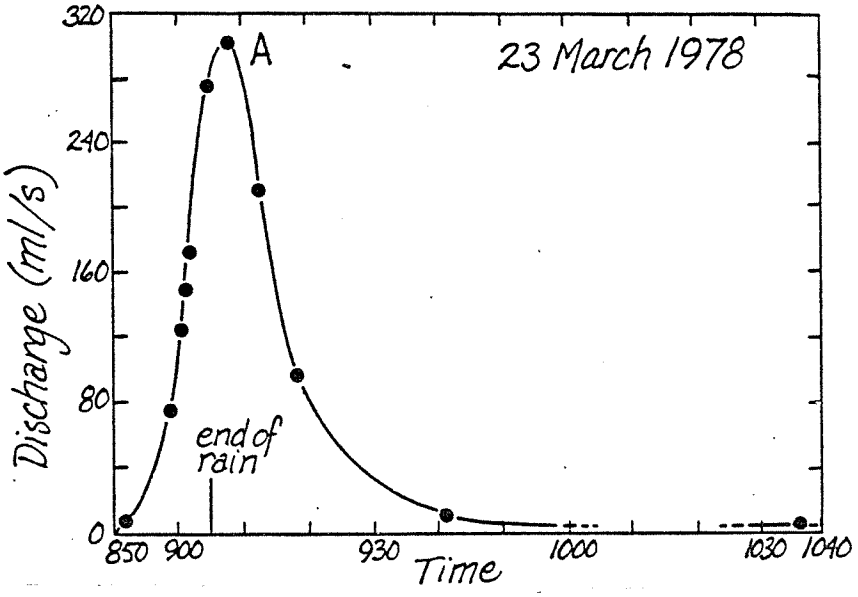

Figure A-1. Hydrograph peak CMI-1-A, heavy-use road.

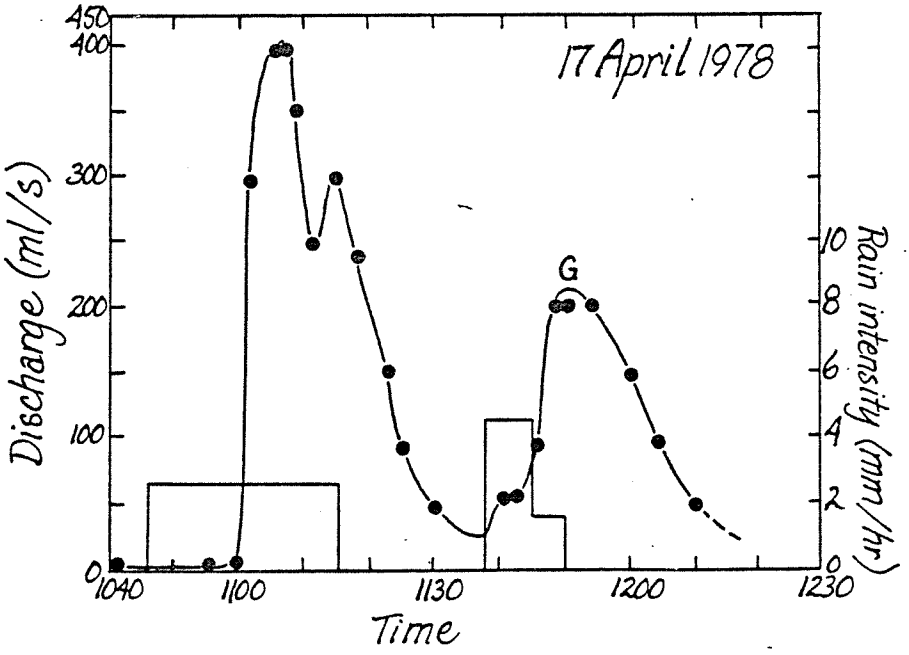

Figure A-2. Hydrograph peak CMI-1-G, heavy-use road.

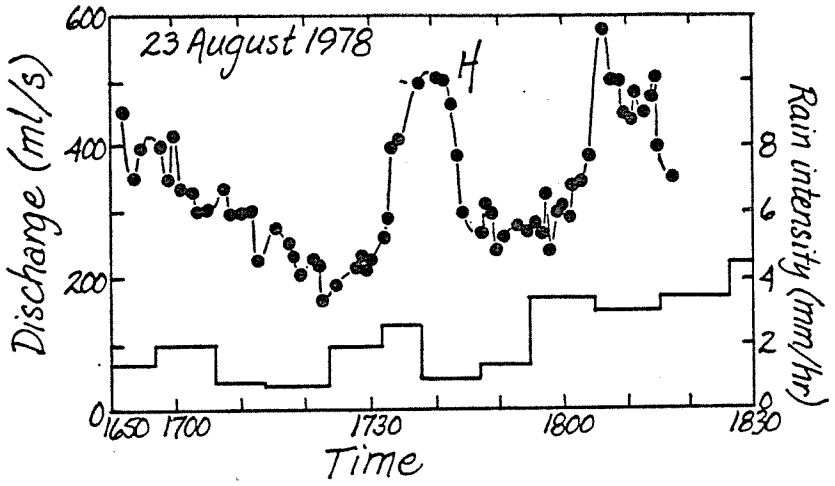

Figure A-3. Hydrograph peak CMI-1-H, heavy-use road.

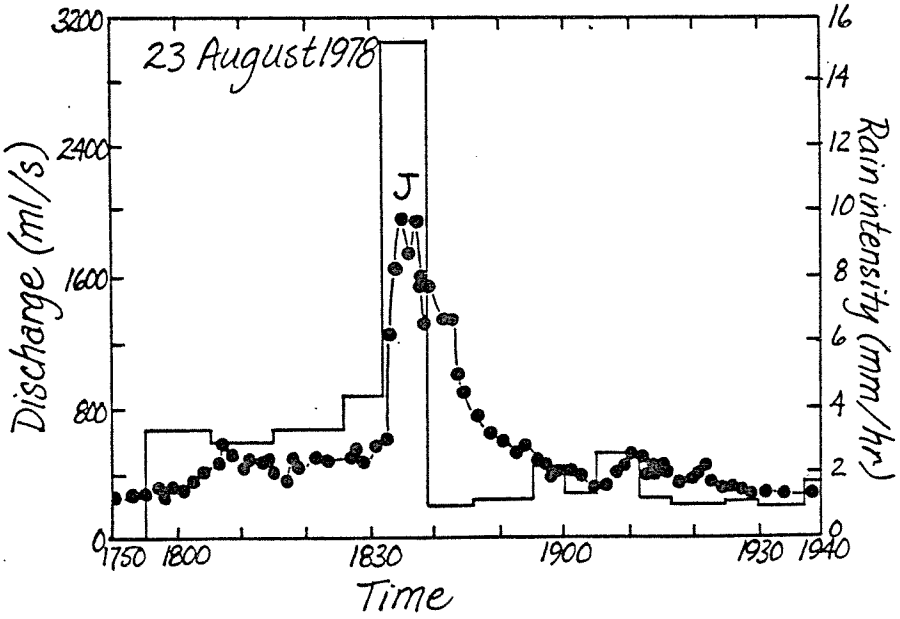

Figure A-4. Hydrograph peak CMI-1-J, heavy-use road.

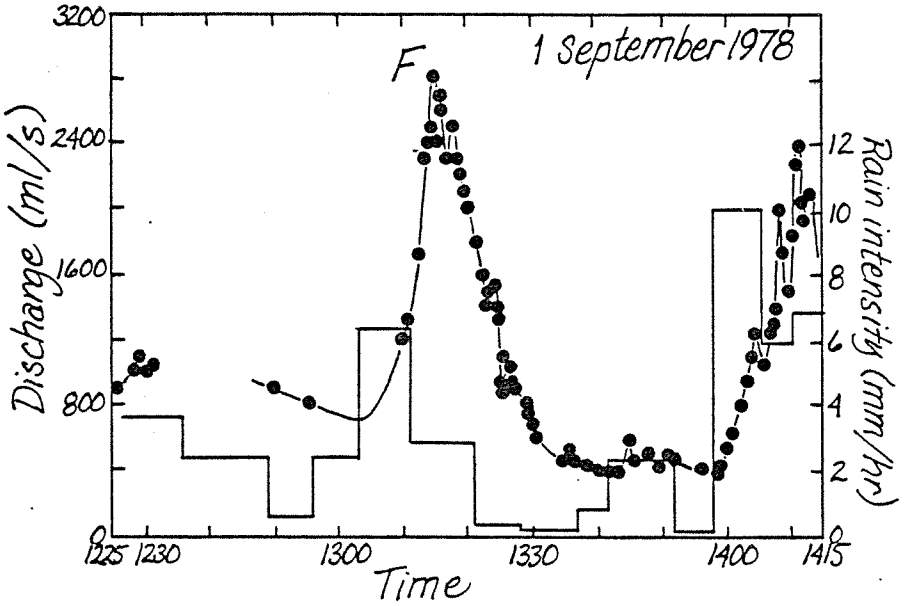

Figure A-5. Hydrograph peak CMI-4-F, light- to heavy-use road.

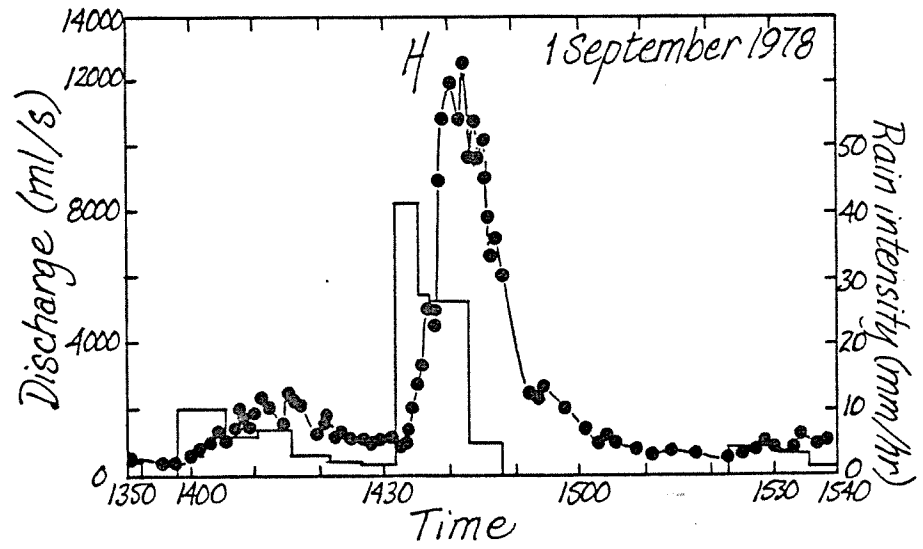

Figure A-6. Hydrograph peak CMI-4-H, light- to heavy-use road.

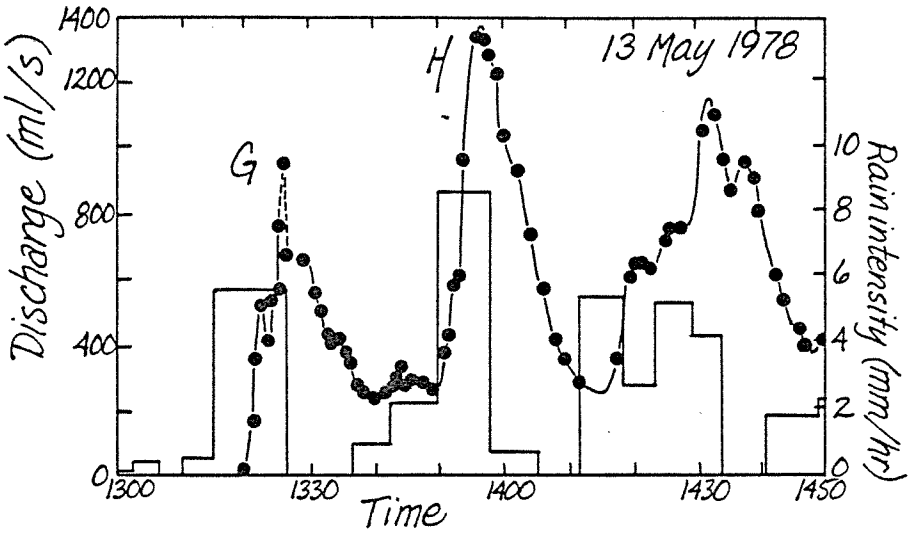

Figure A-7. Hydrograph peaks CSQ-5-G and CSQ-5-H, temporary non-use road.

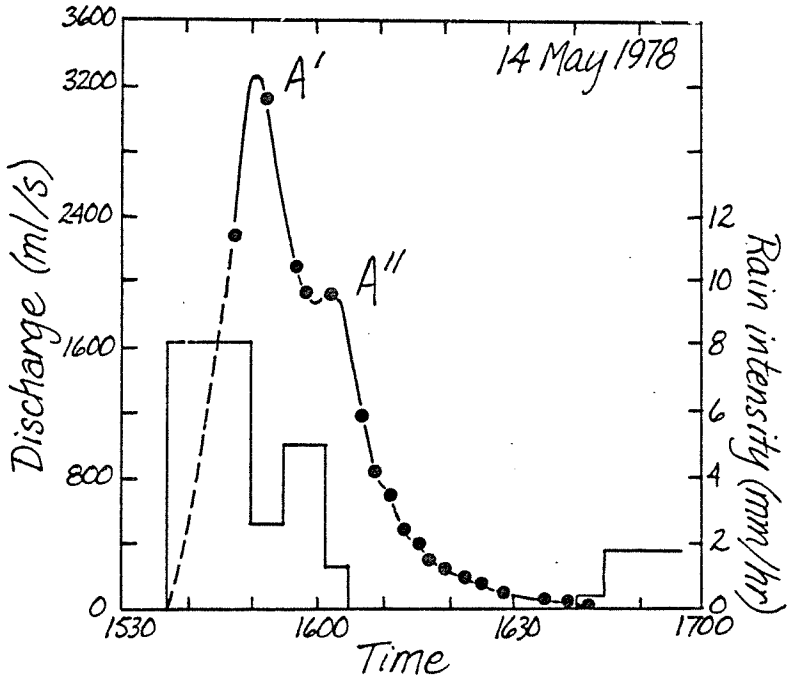

Figure A-8. Hydrograph peaks CSQ-6-A' and CSQ-6-A", paved road.

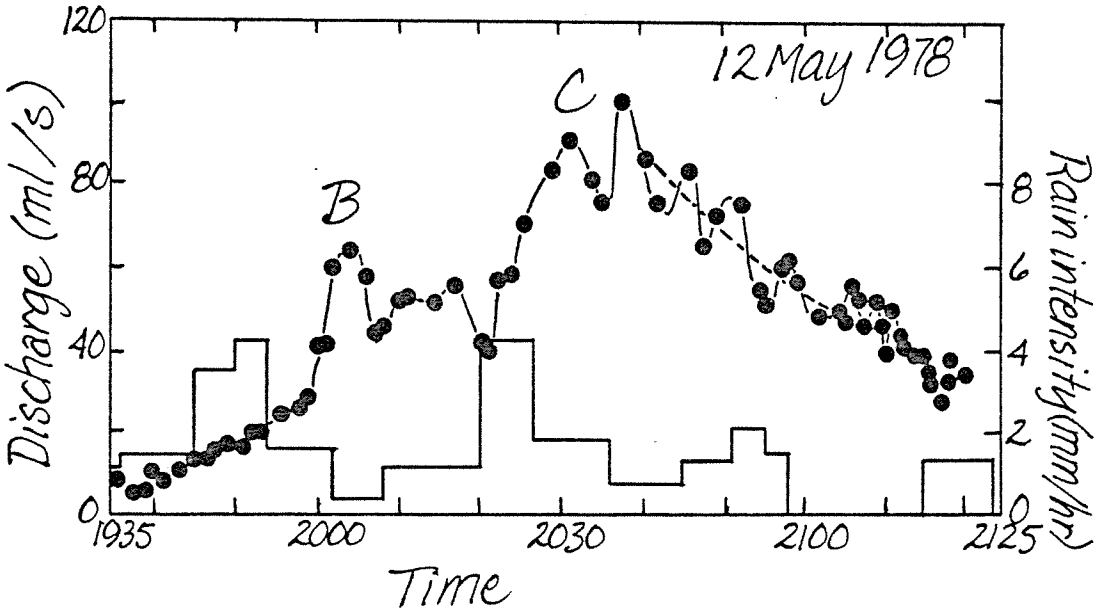

Figure A-9. Hydrograph peaks CSQ-2-B and CSQ-2-C, abandoned road.

APPENDIX B. UNIT HYDROGRAPHS FOR VARIOUS ROAD SEGMENTS

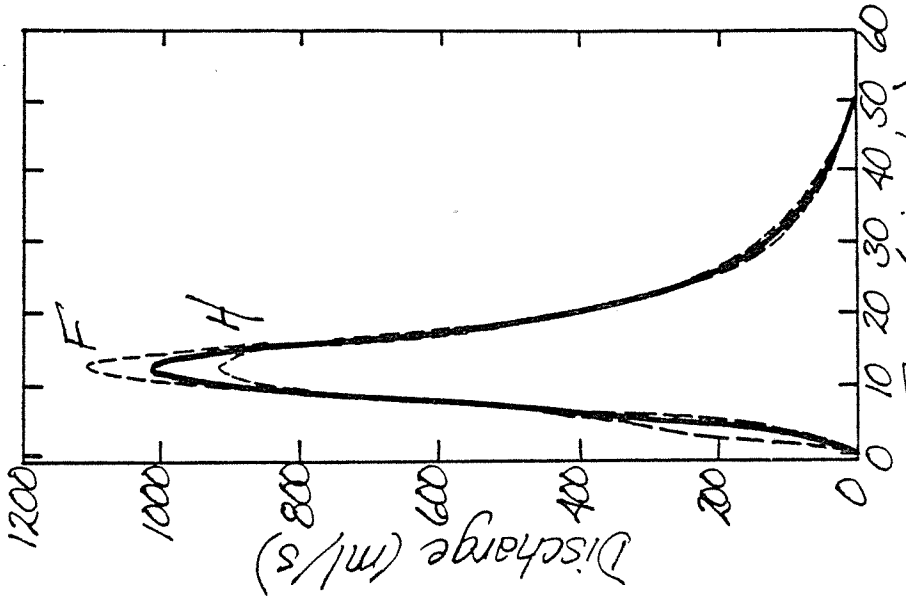

Figure B-2. Measured and average (solid line) unit hydrographs for CMI-4, light- to heavy-use road.

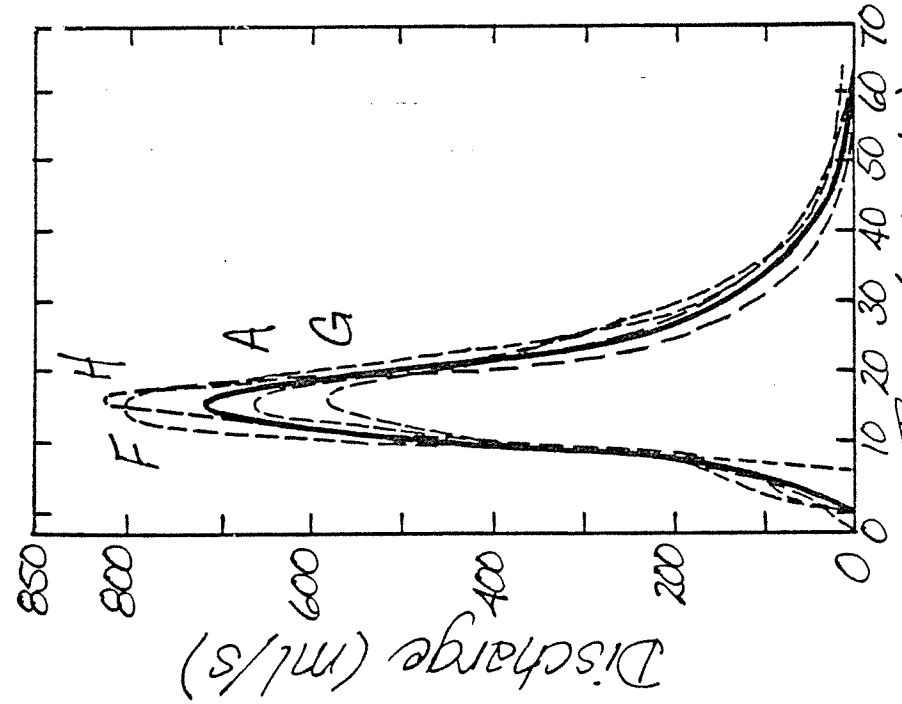

Figure B-1. Measured and average (solid line) unit hydrographs for CMI-1, heavy-use road.

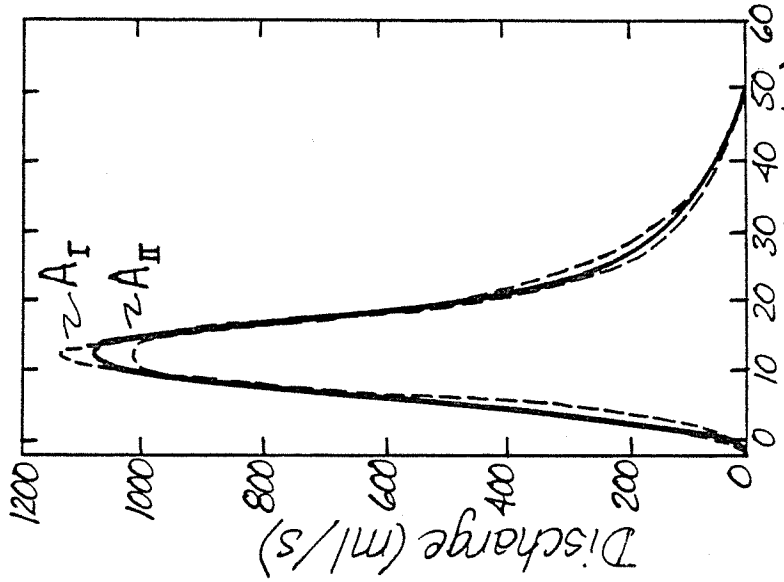

Figure B-4. Measured and average (solid line) unit hydrographs for CSQ-6, paved road.

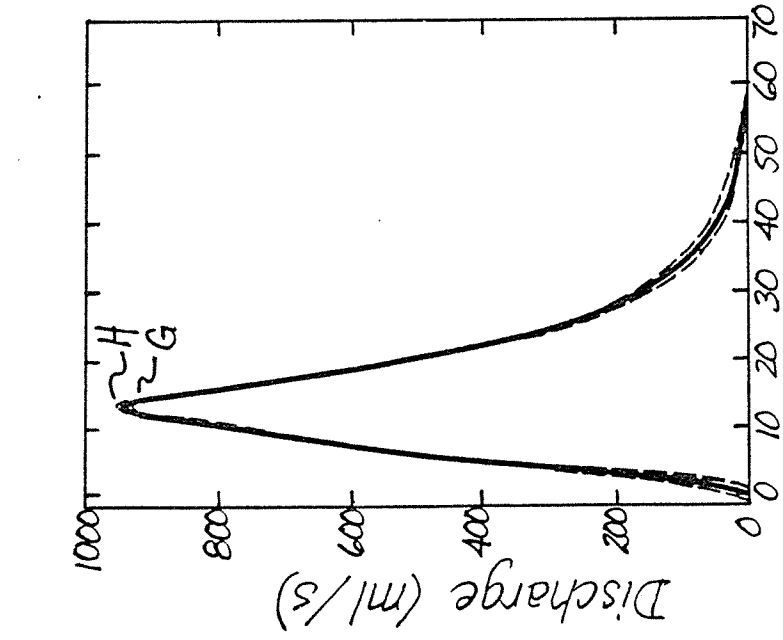

Figure B-3. Measured and average (solid line) unit hydrographs for CSQ-5, temporary non-use road.

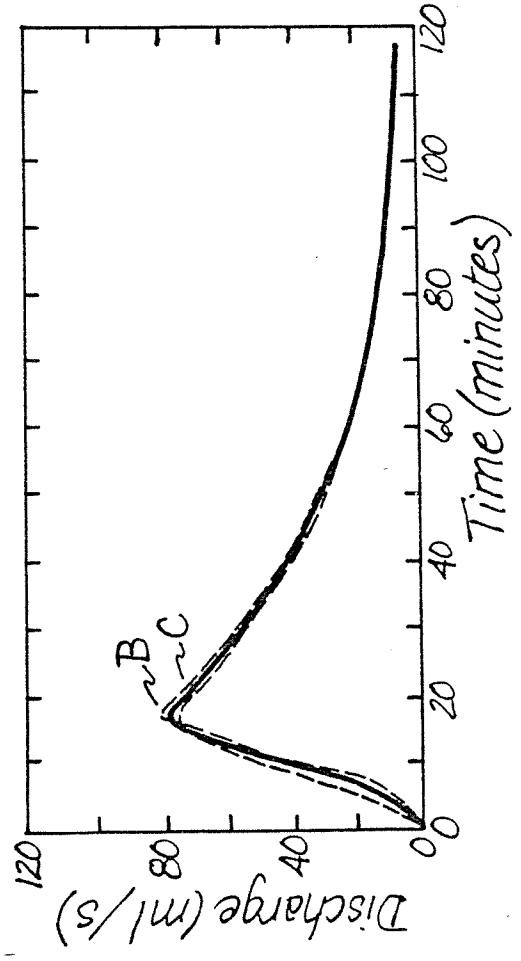

Figure B-5. Measured and average (solid line) unit hydrographs for CSQ-2, abandoned road.

APPENDIX C. SEDIMENT CONCENTRATION VERSUS DISCHARGE CURVES FOR ROADS OF VARIOUS USE-LEVELS

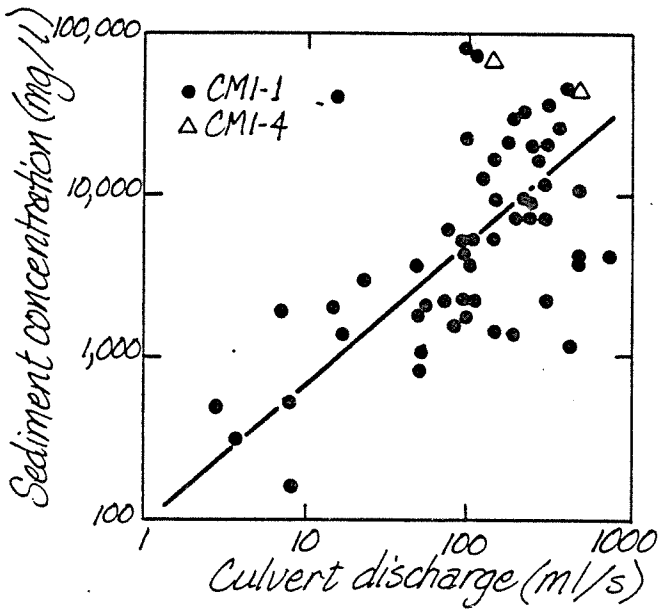

Figure C-1. Sediment concentration versus discharge curve for heavy-use roads.

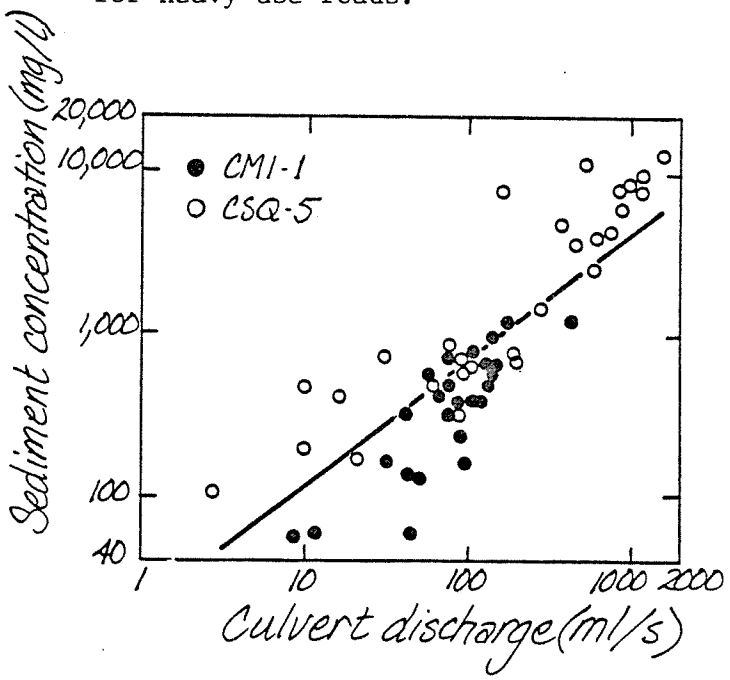

Figure C-2. Sediment concentration versus discharge curve for temporary non-use roads.

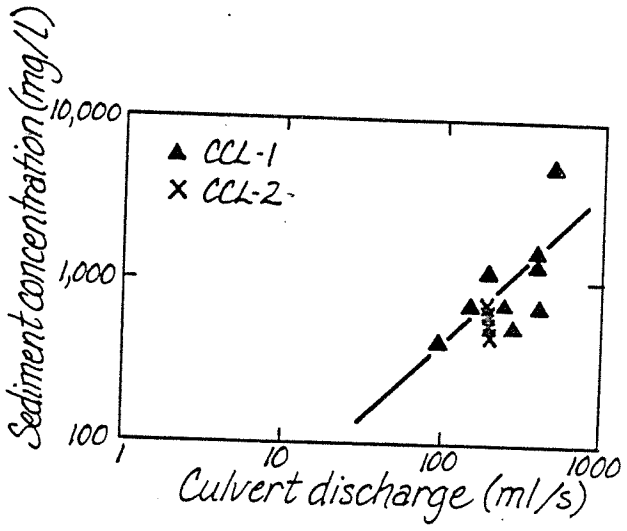

Figure C-3. Sediment concentration versus discharge curve for moderate-use roads.

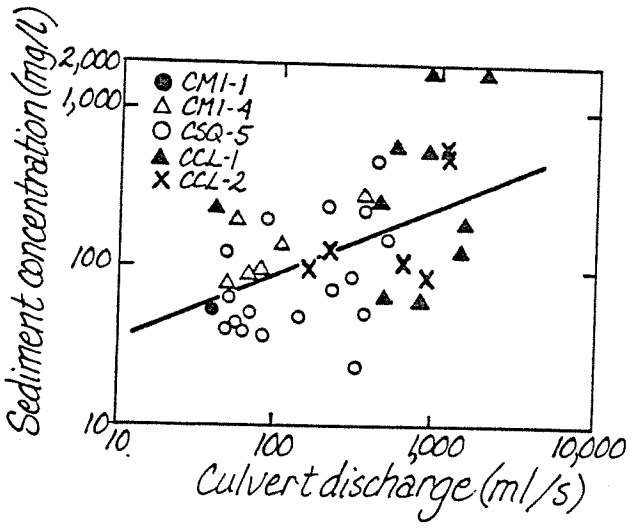

Figure C-4. Sediment concentration versus discharge curve for light-use roads.

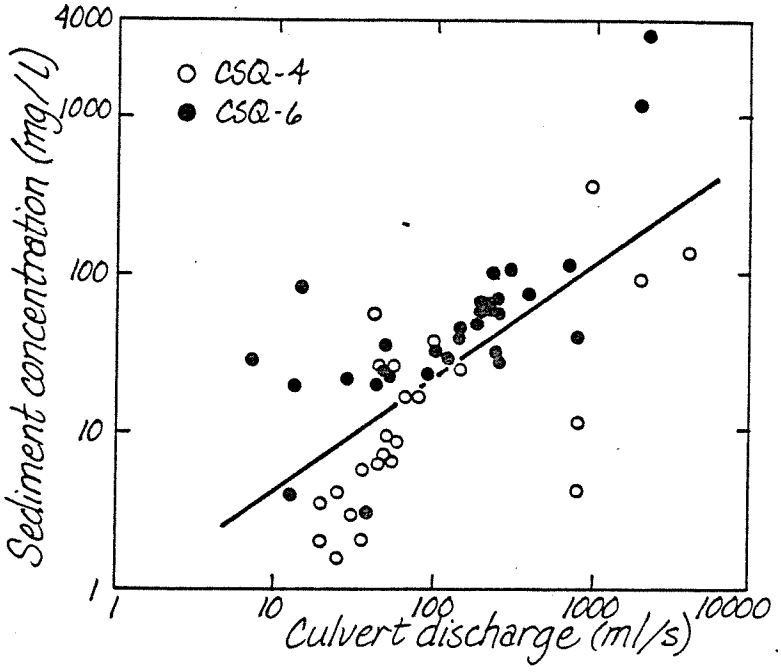

Figure C-5. Sediment concentration versus discharge curve for paved roads.

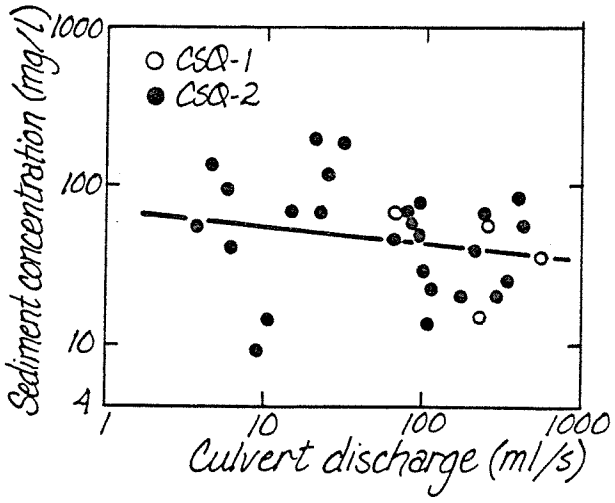

Figure C-6. Sediment concentration versus discharge curve for abandoned roads.

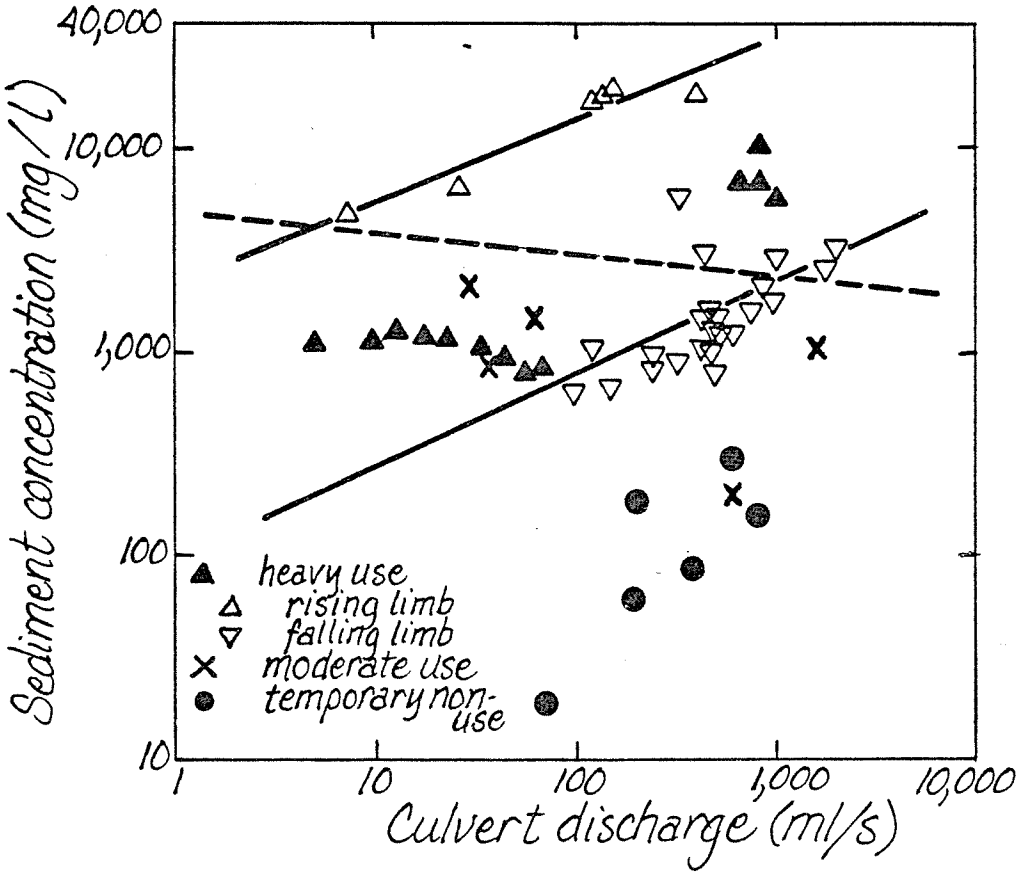

Figure C-7. Sediment concentration versus discharge for gravel mainline road (CSQ-3) under three use levels. Solid lines represent regressed curves for rising and falling limbs under heavy-use conditions, while dashed line indicates regression for grouped heavy-use data.

APPENDIX D. SEDIMENT CONCENTRATION VERSUS DISCHARGE CURVES FOR CULVERT AND SURFACE FLOWS ON VARIOUS ROAD SEGMENTS

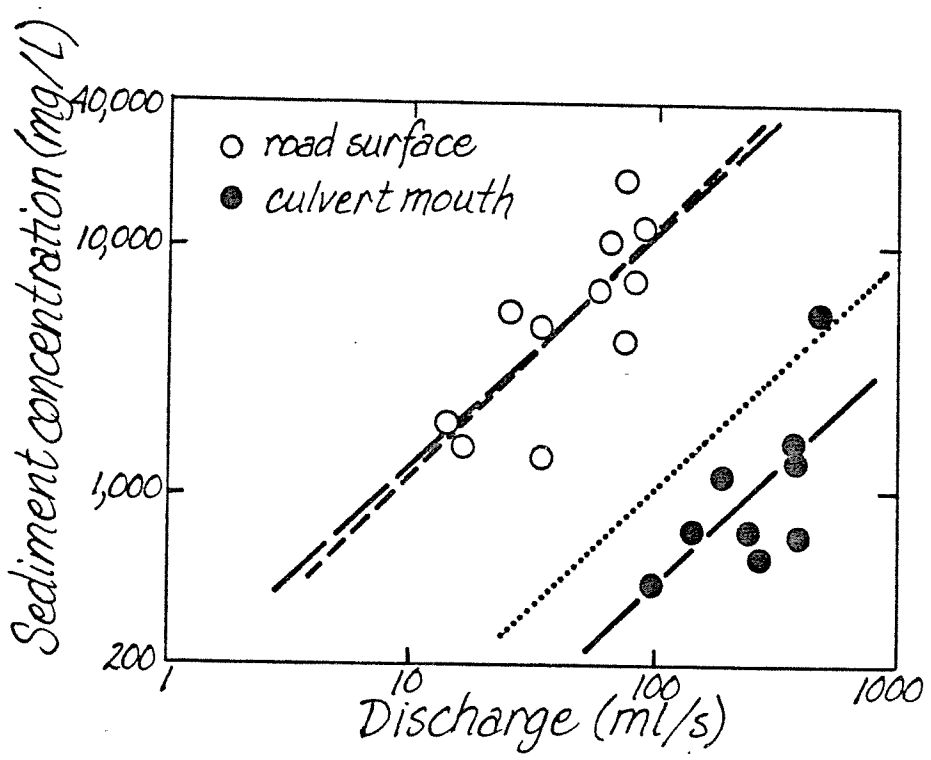

Figure D-1. Sediment concentration versus discharge curve for culvert and surface flows on moderately-used road, CCL-1, during winter storms. The solid line indicates the regressed curve for culvert measurements, while the dotted line is the corresponding curve predicted from road surface measurements. The short-dashed line is regressed directly from road surface measurements, while the slope of the long-dashed line has been constrained to equal that of the regressed curve for culvert measurements.

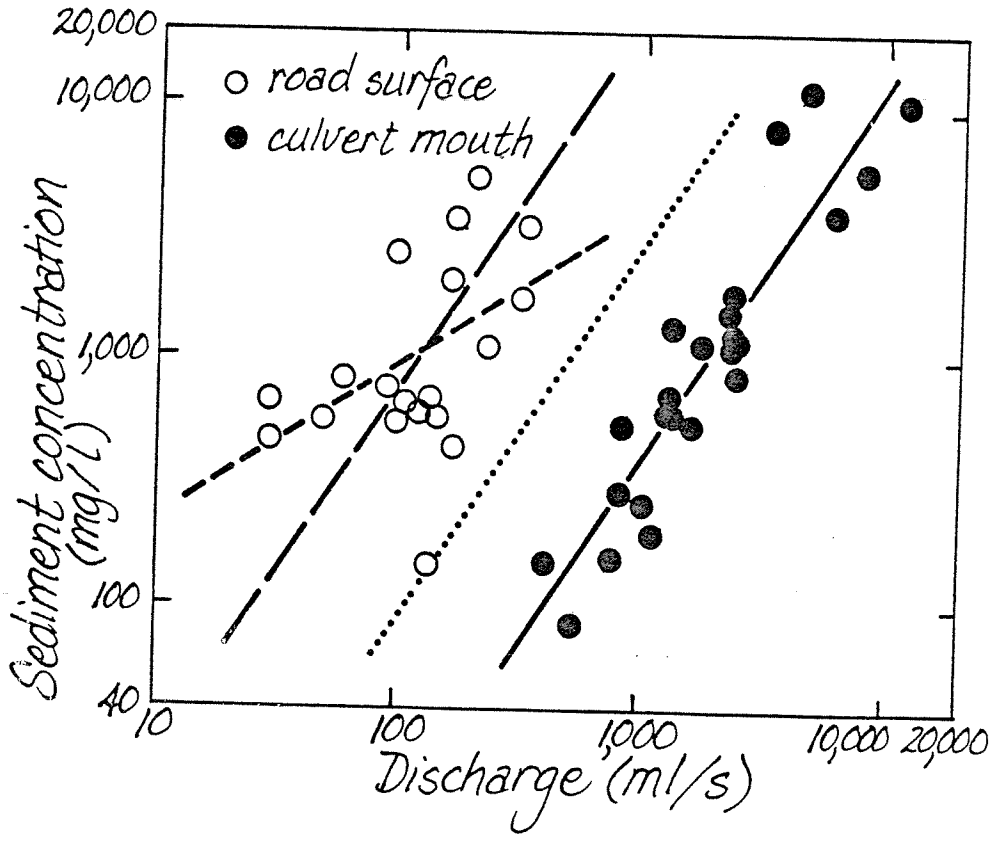

Figure D-2. Sediment concentration versus discharge curve for culvert and surface flows on lightly-used road, CMI-4, during summer storms. The solid line indicates the regressed curve for culvert measurements, while the dotted line is the corresponding curve predicted from road surface measurements. The short-dashed line is regressed directly from road surface measurements, while the slope of the long-dashed line has been constrained to equal that of the regressed curve for culvert measurements.

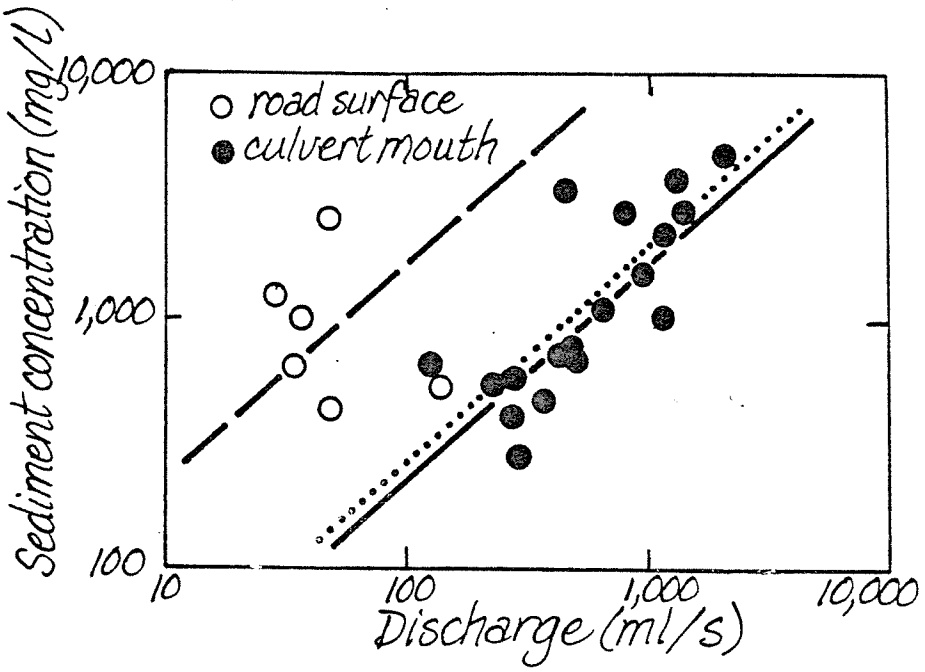

Figure D-3. Sediment concentration versus discharge curve for culvert and surface flows on heavily-used road, CMI-1, during summer storms. The solid line indicates the regressed curve for culvert measurements, while the dotted line is the corresponding curve predicted from road surface measurements. The dashed line is the regressed curve for road surface measurements, with slope constrained to equal that of the relation for culvert measurements.

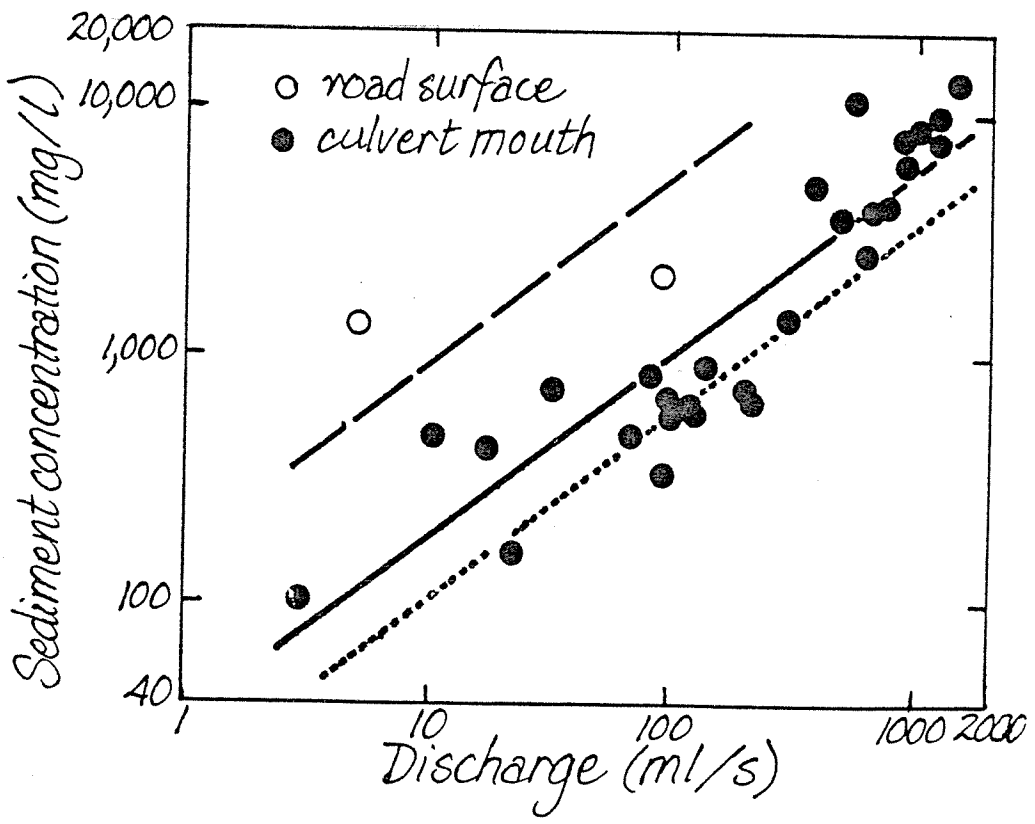

Figure D-4. Sediment concentration versus discharge curve for culvert and surface flows on temporarily non-used road, CSQ-5, during winter storms. The solid line indicates the regressed curve for culvert measurements, while the dotted line is the corresponding curve predicted from road surface measurements. The dashed line is the regressed curve for road surface measurements, with slope constrained to equal that of the relation for culvert measurements.

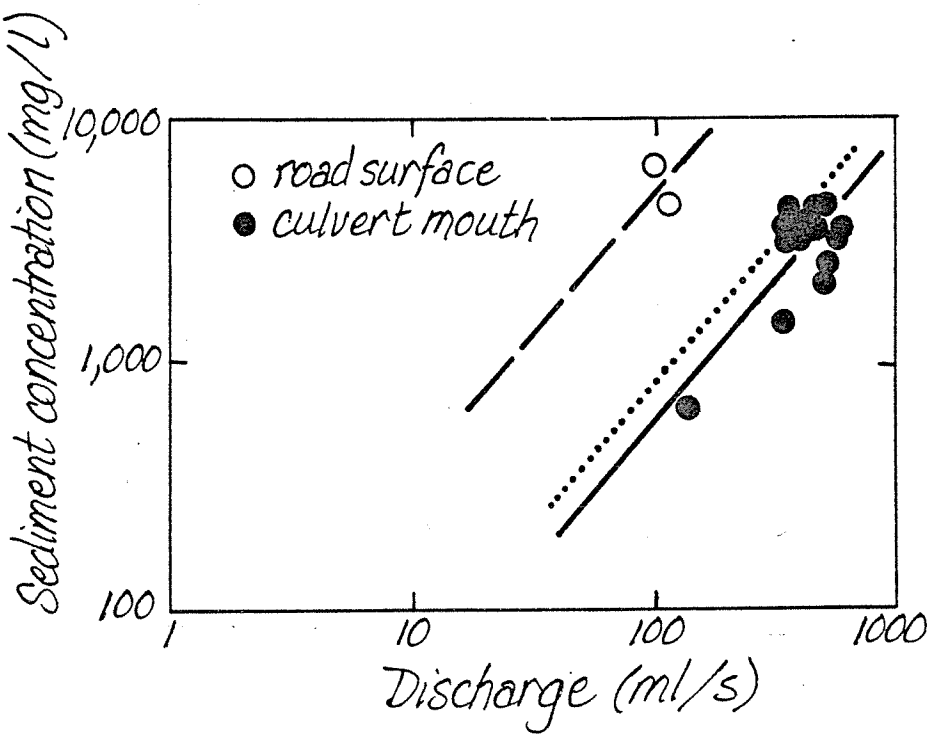

Figure D-5. Sediment concentration versus discharge curve for culvert and surface flows on heavy-use road, CMI-4, during summer storms. The solid line indicates the regressed curve for culvert measurements, while the dotted line is the corresponding curve predicted from road surface measurements. The dashed line is the regressed curve for road surface measurements, with slope constrained to equal that of the relation for culvert measurements.

APPENDIX E. EROSION PIN DATA

The following tables are those used to calculate monthly erosion rates on backcuts. Data were collected from erosion pin networks at uneven intervals, and many of the networks were destroyed before a year's record was complete. The data from individual erosion pins are thus averaged over shorter periods defined by the dates of measurements. This approach tends to mask abrupt changes in erosion rates because the results are in the form of a running average. Most of the measurements are averaged over a period of longer than a month. In the following tables these multiple-month averages are indicated by ties between months.

Table E-1. Monthly erosion pin data from cut-faces (A = aggradation; no symbol = erosion. Measurements are in millimeters.).

Month:	Oct	Nov	Dec	Jan	Feb	Mar	Apr	May	June	July	Aug	Sept
	---3.8	4.6----4.6----4.6			0	0------0------0				12.3	3.8-----3.8---	
	---3.3	0------0------0			2.1	A0.2---A0.2---A0.2				5.4	3.3-----3.3---	
	--A0.5	4.3----4.3----4.3			0.9	0------0------0				16.6	A0.5----A0.5---	
	---0.7	0.5----0.5----0.5			3.4	A0.2---A0.2---A0.2				7.5	0.7-----0.7---	
	---3.6	1.8----1.8----1.8			0	0.4----0.4----0.4				4.3	3.6-----0.6---	
	---2.2	4.7----4.7		0------0		1.6----1.6----1.6				13.4	2.2-----2.2---	
	---1.3	0------0		0.3----0.3		5	4.3	14.2----14.2		6.4	1.3-----1.3---	
	A4.4	A0.2---A0.2		0.5----0.5		0.7	2.9	1.6-----1.6				
	0	A0.2---A0.2		2------2		9.3	2.9	3.1-----3.1				
	2			1.5----1.5		A1.4	A5.7	2.3-----2.3				
	0.4----0.4----0.4----0.4----0.4						A2.9	0.5-----0.5				
	A10	3.7----3.7----3.7----3.7					2.9	A2.3----A2.3				
	2	1.4----1.4----1.4----1.4						5.7-----5.7				
	5	A0.5---A0.5---A0.5---A0.5										
	2	A0.5---A0.5---A0.5---A0.5										
	5			5.5----5.5								
	6			A2.2---A2.2								
	0			A0.5---A0.5								
				1.4----1.4								
				9.5----9.5								
				A4.4---A4.4								
				2.7----2.7								
					2.1							
Samples	18	14	14	22	23	10	12	13	7	7	7	7
Mean	1.2	1.4	1.4	1.5	1.3	1.5	0.5	2.0	3.6	9.4	2.1	2.1
Standard error ±	0.9	0.5	0.5	0.6	0.6	1.0	0.8	1.1	2.0	1.8	0.6	0.6

Table E-2. Monthly erosion pin data from debris mantles below 1 to 3 m cut-face (A = aggradation, no symbol = erosion. Measurements are in millimeters. Asterisk indicates measurement not used.).

Month:	Oct	Nov	Dec	Jan	Feb	Mar	Apr	May	June	July	Aug	Sept
			A1.6---A1.6	A6-----A6	A1.4----A1.4	A0.4---A0.4	A10.2---A10.2	A0.4---A0.4	A0.4	A0.4		
			2.6----2.6	4.4----4.4	A3.3----A3.3	A0.7---A0.7	A4.8----A4.8	A0.7---A0.7	A0.7	A0.7		
			A1.6---A1.6	A1.4---A1.4	A4.3	1.3----1.3	A0.4---A0.4	A0.4---A0.4				
			3.8----3.8	A5.5---A5.5	A0.9	26.5*	A0.7---A0.7	A0.7---A0.7				
			1.6----1.6	A5.5---A5.5	1.3	1.8	A1.8----A1.8	A1.8----A1.8				
			1.6----1.6	A4.6---A4.6	A3.8	A77.3*	A3.6----A3.6	A3.6----A3.6				
			A1.6---A1.6	A1.9---A1.9	5.6	4.6	2.4-----2.4	2.4-----2.4				
				4.4----4.4	0.9	A11.5	0.6-----0.6	0.6-----0.6				
				A4.4---A4.4	A6-----A6	A6.9	0-------0	0-------0				
				A3.8---A3.8	4.4----4.4	A9.7	1.8-----1.8	1.8-----1.8				
				A2.7---A2.7	A1.4---A1.4	A7.1	1.2-----1.2	1.2-----1.2				
					A5.5---A5.5	1.8	0.6-----0.6	0.6-----0.6				
					A5.5---A5.5	0	0.6-----0.6	0.6-----0.6				
					A4.6---A4.6	0	2.4-----2.4	2.4-----2.4				
					A1.9---A1.9	0	A3------A3	A3------A3				
					4.4----4.4	0	5.4-----5.4	5.4-----5.4				
					A4.4---A4.4		A7.8----A7.8	A7.8----A7.8				
					A3.8---A3.8		0.6-----0.6	0.6-----0.6				
					A2.7---A2.7		A4.2----A4.2	A4.2----A4.2				
							A4.2----A4.2					
Samples			7	18	19	16	22	21	2	2		
Mean			0.6	A1.3	A1.7	A0.1	A1.0	A1.1	A0.6	A0.6		
Standard error ±			0.8	0.4	0.4	1.1	0.3	0.4				

Table E-3. Monthly erosion pin data from debris mantles below 3 to 5 m cut-faces (A = aggradation, no symbol = erosion. Measurements are in millimeters, and ties indicate multi-month averages.).

Month:	Oct	Nov	Dec	Jan	Feb	Mar	Apr	May	June	July	Aug	Sept
	27.2	0------0		0.8----0.8		4.2	3------3					
	3.3	6.3----6.3		4------4		1.7	A1.2---A1.2					
	0	1.8----1.8		2------2		A5.8	3.8	3.4				
	0	A0.8---A0.8		1------1		4.2	A4.7	1.7				
	3.3	A1.1---A1.1		0.8----0.8		A5	A3.8					
	16.7	3.7----3.7		1------1		0.8	A8.4					
		A2.1---A2.1		0------0		A3.3	A1.9					
		3.7----3.7		2.3----2.3		0.9	17.1					
		A2.1---A2.1		0.5----0.5		A1.1---A1.1						
		A2.4---A2.4		1.3----1.3		3.6----3.6						
		A4.7---A4.7		2------2		A0.5---A0.5						
		1.3----1.3			A4.3	A0.7---A0.7						
		A6.3---A6.3			A7.7	A8.3	A17.8					
		11-----11			A7.7	A13.3	A16.9					
		4------4			A3	A16.7						
		A2.8---A2.8			0.9	A1.7						
		1.9----1.9			A1.3	A5						
		5.4----5.4			A6.6	A5						
		11-----11			0.9	A3.4						
		3.3----3.3			A2.8	0						
		A4.7---A4.7			3.3	0						
		A4.7---A4.7				A11.7						
		1.6----1.6				0						
						A1.7						
						0						
						A1.7						
Samples	6	23	23	11	21	26	14	4				
Mean	8.4	1.0	1.0	1.4	A0.6	A2.7	A2.1	1.7				
Standard error ±	5.1	0.4	0.4	0.2	0.3	0.4	1.4	2.3				

Table E-4. Monthly erosion pin data from backcut toeslopes (A = aggradation; no symbol = erosion. Measurements are in millimeters.).

Month:	Oct	Nov	Dec	Jan	Feb	Mar	Apr	May	June	July	Aug	Sept
					A27.0	A9.2	A12.8	A5.9---A5.9		A12.7---A12.7		
					A25.7	A11.7	A11.7	A5.6---A5.6		A11.6---A11.6		
					A43.7	A8.3	1.1	A7.8---A7.8		A11.4---A11.4		
					A16.3	A25	A0.4	A8.6---A8.6		A11.1---A11.1		
					A22.3	A9.3	A5.6					
					A15.0	A20.7	A6.4					
					A12.1	A33.6	A3.4					
					A7.7		A4.4					
							A6.7					
Samples					8	7	9	4	4	4	4	
Mean					A21.2	A16.8	A5.6	A7.0	A7.0	A11.7	A11.7	
Standard error ±					3.5	3.6	1.2	1.6	1.6	0.8	0.8	

Table E-5. Monthly erosion pin data from ditches below 1 to 3 m cut-faces.

Month:	Feb	Mar	Apr	May	June	July	Aug
	A1.7		A18.6---A18.6				
	A2.6		A2.1----A2.1				
	19.7		A19.5---A19.5				
	1.3		4.2-----4.2				
	A0.9			A13.8---A13.8			
	A0.9			A17.1---A17.1			
	A0.7			3.7-----3.7			
Samples	7		4	7	3		
Mean	2.0		A9.0	A9.0	A9.1		
Standard error ±	2.9		12.8	3.9	47.3		

Table E-6. Monthly erosion pin data from ditches below 3 to 5 m cut-faces.

Month:	Feb	Mar	Apr	May	June	July	Aug
	1	1.4	A71.1	A1.2---A1.2		A23.6---A23.6	
	A6.3	A21.4	A61.1	A1.5---A1.5		A24.6---A24.6	
		A35.6	A6.7	13.5---13.5			
		A31.1	A14.5	A7.7---A7.7			
		A23.1		0.6----0.6			
		A9.4		A9.5---A9.5			
				A19.6--A19.6			
				A17.8--A17.8			
				A4.9---A4.9			
				A6.7---A6.7			
				A10.7--A10.7			
				A17.1--A17.1			
				A11.3--A11.3			
Samples	2	6	4	13	13	2	2
Mean	A2.6	A19.9	A38.4	A7.2	A7.2	A24.1	A24.1
Standard error ±		6.4	34.9	1.5	1.5		

APPENDIX F. ROAD-RELATED LANDSLIDES

Table F-1. Road-related landslides of Christmas basin which contribute sediment to streams (for locations of slides see Appendix Figure F-1).

Slide	Year first seen	Field check	Type of slide	Slide depth (m)	Hillslope gradient (degrees)	Slide area (m^2)	Slide volume (m^3)	Proportion delivered to stream	Volume delivered (m^3)	Number of rills	Volume of rills (m^3)
1	1977	x	F	0.4	43	260	100	.5	51	0	
2	1977	x	S2	0.3*	43	220	65	0-.25	8	0	
3	1977	x	0,(S3)	0.25	43	260	77	0	0	0	
4	1977	x	F,DT	0.75	43	2,420	1,810	.9**	1,630	0	
5	1977	x	S3	0.25	36	590	150	.4	55	4	3.9
6	1971	x	S2	0.3	36	700	210	.5	100	0	
7	1971	x	D	0.9*	36	150	130	.75	99	0	
8	1971	x	S3	0.3	47	100	30	0-.25	4	0	
9	1971	x	0,(S3)	0.2	40	280	56	0	0	0	
10	1977	x	S3	0.3	42	650	200	.5-.75	120	4	2.9
11	1971	x	S3	0.3	49	320	95	M	44	0	
12	1977	x	S3	0.3*	49	250	75	M	35	1	.5
13	1977	x	F	0.4	46	38	15	.75	11	1	.1
14	1977	x	S1	0.25	40	200	40	0-.25	5	0	
15a	1975	x	F,DT	1.35	40	300	400	.8	330	1	.8
15b	1977	x	S2	0.3*	40	660	130	0-.25	16	2	1.8
16	1977	x	R,(S2)[1]	0.2	40	73	15	0	rill	1	.9
17	1977	x	S2	0.2	40	96	19	.6	12	3	3.5

Table F-1. Road-related landslides of Christmas basin which contribute sediment to streams (for locations of slides see Appendix Figure F-1) - continued.

Slide	Year first seen	Field check	Type of slide	Slide depth (m)	Hillslope gradient (degrees)	Slide area (m^2)	Slide volume (m^3)	Proportion delivered to stream	Volume delivered (m^3)	Number of rills	Volume of rills (m^3)
18	1977		D,DT	0.9*	54*	740*	670	H	440		
19	1977		D	0.9*	48*	330*	300	L	21		
20a	1977	x	O,(S2)		34	390	120	0	0	0	
20b	1977	x	O,(D)		34	240	220	0	0	0	
20c	1977	x	R,(F)	1.0	34	140	140	0	rill	3	2.4
20d	1977	x	R,(D)	0.5	34	60	54	0	rill	1	1.0
20e	1977	x	O,(F)	1.5	34	160	240	0	0	0	
20f	1977	x	G	0.6	34	50[3]	29	.5	15		
21a	1977	x	R,(S2)	0.25	40	26	8	0	rill	2	.3
21b	1977	x	O,(S2)		40	9	3	0	0	0	
21c	1977	x	O,(S2)		40	9	3	0	0	0	
21d	1977	x	O,(S2)	0.25	40	14	4	0	0	0	
22	1971	x	D	0.9*	39	570*	510	L	36	1	2.0
23	1977		S	0.3*	43*	450*	140	L	10		
24	1977		S	0.3*	46*	740*	220	M	100		
25	1971		S	0.3*	46*	170*	50	H	32		
26	1971		D	0.9*	46*	210*	190	H	120		
27	1977		S	0.3*	48*	93*	28	M	13		

Table F-1. Road-related landslides of Christmas basin which contribute sediment to streams (for locations of slides see Appendix Figure F-1) - continued.

Slide	Year first seen	Field check	Type of slide	Slide depth (m)	Hillslope gradient (degrees)	Slide area (m^2)	Slide volume (m^3)	Proportion delivered to stream	Volume delivered (m^3)	Number of rills	Volume of rills (m^3)
28	1977		S	0.3*	48*	200*	60	M	28		
29[2]	1971		S	0.3*	45*	320*	97	M	45		
30[2]	1971		D	0.9*	48*	730*	660	L	47		
31	1971		S	0.3*	51*	260*	79	L	6		
32	1971		D	0.9*	51*	280*	250	H	160		
33	1977		D	0.9*	48*	120*	110	M	52		
34	1971		D	0.9*	48*	330*	300	H	190		
35	1977	x	F	1.25	38	76	88	.8	69	1	.9
36	1977	x	F	0.5	40	350	170	0-.25	22	0	
37	1977	x	S3	0.3*	40	540	160	0-.25	20	0	
38a	1977	x	S2	0.25	48	510	130	.25-.5	48	2	8.4
38b	1977	x	D	0.3	48	35	10	.25	3	1	.8
39a	1977	x	S3	0.5	39	30	15	.7	10	1	.4
39b	1977	x	F	0.85	39	45	39	.6	17	0	
40	1977		S	0.3*	48	100	31	L	2		
41	1977	x	O,(S3)		48	120	34	O	0		
42	1975	x	S1	0.4	37	100	37	.5	20	0	
43	1975	x	S3	0.3	29	49	15	.2	3	0	
44a	1975	x	S2	0.3*		65	16	.3	5	0	

Table F-1. Road-related landslides of Christmas basin which contribute sediment to streams (for locations of slides see Appendix Figure F-1) - continued.

Slide	Year first seen	Field check	Type of slide	Slide depth (m)	Hillslope gradient (degrees)	Slide area (m^2)	Slide volume (m^3)	Proportion delivered to stream	Volume delivered (m^3)	Number of rills	Volume of rills (m^3)
44b	1975	x	G	1.0		16	16	.3	5	0	
45	1975	x	F	1.0		360	360	.1	36	0	
46	1977		D	0.9*	48*	170*	150	M	69	1	.5
47	1975		S	0.3*	43	490*	150	M	68		
48	1975		S	0.3*	43	490*	150	M	68		
49	1975		S	0.3*	43	490*	150	M	68		
50	1975		S	0.3*	34*	110*	34	L	2		
51	1975		D,DT	0.9*	40	880*	790	H	510		
52	1975		S,DT	0.3*	40	1,290*	390	H	250		
53	1977		D	0.9*	43*	580*	520	H	340		
54	1975		S	0.3*	43*	190*	57	L	4		
55	1977	x	O,(S3)			310	92	O	0		
56	1971		D	0.9*	52*	730*	660	H	430		
57	1971		S	0.3*	52*	580*	180	H	110		
58	1971		S	0.3*	52*	610*	180	L	13		
59	1977		D	0.9*	48*	290*	260	L	18		
60	1975		D,DT	0.9*	48*	540*	490	H	320		
61	1971		D,DT	1.0**	51*	6,930*	6,930	H	4,500		
62	1971		S	0.3*	48*	1,350*	400	L	29		

Table F-1. Road-related landslides of Christmas basin which contribute sediment to streams (for locations of slides see Appendix Figure F-1) - continued.

Slide	Year first seen	Field check	Type of slide	Slide depth (m)	Hillslope gradient (degrees)	Slide area (m^2)	Slide volume (m^3)	Proportion delivered to stream	Volume delivered (m^3)	Number of rills	Volume of rills (m^3)
63a	1971	x	F	0.75	37	40	30	.25-.5	11	0	
63b	1971	x	S3	0.3	38	330	99	.25-.5	38	2	1.2
64	1977	x	F,DT	0.75	41	300	220	M	100	0	
65a	1977	x	S2,DT	0.3*	41	640	190	H	120	0	
65b	1977	x	D,DT	0.5	41	24	12	H	8	1	.6
66	1977	x	D	0.75	38	400	300	0-.25	38	3	9.9
67	1971	x	G	1.0	38	12	12	1.0	12	0	
68a	1971	x	S3	0.3*	38*	110	56	.5-.75	35	1	4.5
68b	1971	x	S2	0.3*	38*	180	45	0-.25	6	0	
69	1971	x	F,DT	1.67	36	810	1,220	.5	610	4	12.6
70	1977	x	S1	0.3*	37	400	120	H	79	6	20.6
71	1977	x	S2	0.3*		150	45	0-.25	6	0	
72	1977		S	0.3*	46*	860*	260	H	170		
73a	1975	x	S2	0.3*	46*	360	110	H	71	0	
73b	1975	x	S3	0.3*	46*	720	220	.75	160	4	9.9
74	1975	x	O,(S3)			270	81	0	0		

Table F-1. Road-related landslides of Christmas basin which contribute sediment to streams (for locations of slides see Appendix Figure F-1) - continued.

D - deep failure (identified from photo)
F - landslide involving fill (identified in field)
G - gully
DT -landslide debris involved in debris flow
O - field work shows no delivery
R - delivery only by rills
S - shallow failure (identified from photo)
S1 - shallow disturbance without failure
S2 - shallow disturbance, mode indeterminate
S3 - shallow failure (identified in field)
* - value measured from map if gradient or assumed if depth
** - value approximate, from surface reconstruction
()[1]- parenthetic designation is type of landslide present
2 - landslides identified from early photographs only
3 - disturbance superimposed on catalogued landslides

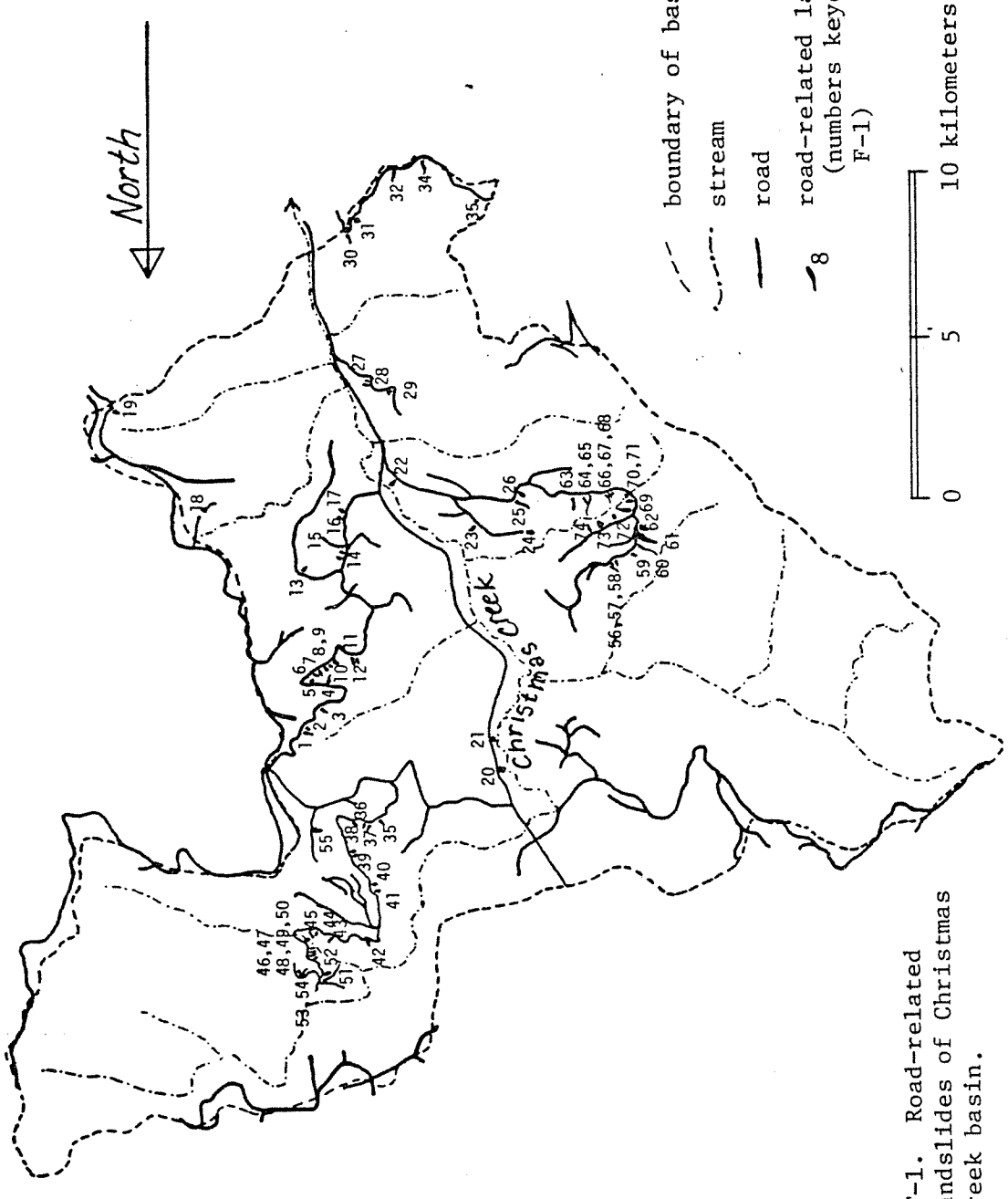

Figure F-1. Road-related landslides of Christmas Creek basin.

Table F-2. Road-related landslides and associated disturbances in Stequaleho basin, as mapped from aerial photographs (for locations of slides see Appendix Figure F-2).

Slide	Type	Thickness (m)	Hillslope gradient (degrees)	Area (m^2)	Volume (m^3)	Delivery	Volume delivered (m^3)
1	D,DT	.9	45	2,060	1,850	H	1,200
2	S	.3	45	160	50	L	4
3	S	.3	55	410	120	L	9
4	S	.3	48	870	260	L	19
5	S	.3	43	420	130	L	9
6	S	.3	52	230	70	L	5
7	S	.3	45	540	160	L	11
8	S	.3	45	160	50	L	4
9	D	.9	45	170	160	M	73
10	S	.3	45	82	25	L	2
11	D,DT	.9	45	1,110	1,000	M	460
12	S	.3	48	300	92	L	7
13	D,DT	.9	48	220	200	H	130
14	S	.3	48	440	130	L	9
15	S	.3	48	100	30	H	19
16	D,DT	.9	45	380	340	M	160
17	D,DT	.9	45	1,180	1,070	M	500
18	D,DT	.9	45	310	280	H	180
19	D,DT	.9	54	910	820	H	530
20	S,DT	.3	45	2,060	620	H	400
21	S	.3	48	1,740	520	L	37
22	S,DT	.3	45	1,540	560	M	220
23	S	.3	45	440	130	L	10
24	D,DT	.9	48	860	780	M	360
25	D,DT	.9	45	160	150	H	97
26	D,DT	.9	45	540	490	H	320
27	D,DT	.9	45	100	93	H	60
28	S,DT	.3	45	400	120	H	77

Table F-2. Road-related landslides and associated disturbances in Stequaleho basin, as mapped from aerial photographs (for locations of slides see Appendix Figure F-2) - continued.

Slide	Type	Thickness (m)	Hillslope gradient (degrees)	Area (m^2)	Volume (m^3)	Delivery	Volume delivered (m^3)
29	D	.9	55	410	370	L	26
30	S	.3	48	410	120	L	9
31	D	.9	45	150	130	L	9
32	D,DT	.9	52	2,800	2,520	H	1,640
33	D,DT	.9	52	1,460	1,310	H	850
34	S	.3	45	120	37	L	3
35	S	.3	45	49	15	L	1
36	S	.3	45	930	280	L	20
37	D,DT	.9	50	690	620	H	400
38	S	.3	50	1,220	360	H	240
39	S	.3	43	1,060	320	H	210
40	D	.9	43	1,060	960	H	620
41	D	.9	59	500	450	M	210
42	D	.9	59	330	290	M	140
43	D	.9	52	640	580	L	41
44	D,DT	.9	55	13,800	12,500	H	8,080
45	S	.3	59	1,140	340	L	24
46	S	.3	59	910	270	L	19
47	D	.9	48	350	310	M	150
48	S	.3	57	1,290	390	L	27
49	D	.9	57	47	42	M	20
50	S	.3	57	170	51	H	33
51	S	.3	52	250	76	L	5
52	D	.9	52	190	170	L	12
53	S	.3	57	2,790	840	M	390
54	S	.3	55	300	92	L	7
55	S	.3	55	260	77	L	5
56	S	.3	50	180	54	L	4

Table F-2. Road-related landslides and associated disturbances in Stequaleho basin, as mapped from aerial photographs (for locations of slides see Appendix Figure F-2) - continued.

Slide	Type	Thickness (m)	Hillslope gradient (degrees)	Area (m^2)	Volume (m^3)	Delivery	Volume delivered (m^3)
57	S	.3	57	1,340	400	L	29
58	S	.3	54	88	26	M	12
59	S	.3	54	700	210	H	140
60	S	.3	54	700	210	L	15
61	D,DT	.9	54	970	880	H	570
62	D	.9	50	1,010	910	L	65
63	S	.3	41	1,240	370	M	170
64	S	.3	45	3,050	910	M	420
65	S	.3	48	390	120	H	77
66	S	.3	48	390	120	L	8
67	S	.3	48	510	150	L	11
68	S	.3	47	1,120	340	H	220
69	S	.3	54	200	59	M	27
70	S	.3	52	1,280	380	L	27
71	S	.3	38	260	79	L	6
72	S	.3	38	88	26	L	2
73	S	.3	38	550	160	L	12
74	S	.3	38	180	55	L	4
75	D,DT	.9	57	760	680	M	320
76	D	.9	59	880	790	L	56
77	D	.9	48	490	410	L	29
78	S	.3	36	140	43	M	20
79	D	.9	34	490	440	L	31
80	S	.3	43	390	120	L	8
81	S	.3	40	850	260	L	18
82	S	.3	40	680	200	L	14
83	S	.3	32	620	180	L	13

Table F-2. Road-related landslides and associated disturbances in Stequaleho basin, as mapped from aerial photographs (for locations of slides see Appendix Figure F-2) - continued.

Slide	Type	Thickness (m)	Hillslope gradient (degrees)	Area (m^2)	Volume (m^3)	Delivery	Volume delivered (m^3)
84	S	.3	55	280	83	L	6
85	S	.3	54	730	220	M	100
86	S	.3	54	290	88	M	41
87	D	.9	48	1,220	1,100	H	710
88	S,DT	.3	48	870	260	H	170
89	S	.3	48	920	280	H	180
90	D,DT	.9	48	440	390	H	250
91	D,DT	.9	55	610	550	H	360
92	D,DT	.9	45	1,240	1,110	H	720
93	S	.3	38	730	220	M	100
94	D	.9	32	290	260	H	170
95	D	.9	32	260	230	H	150
96	D,DT	.9	54	220	200	H	130

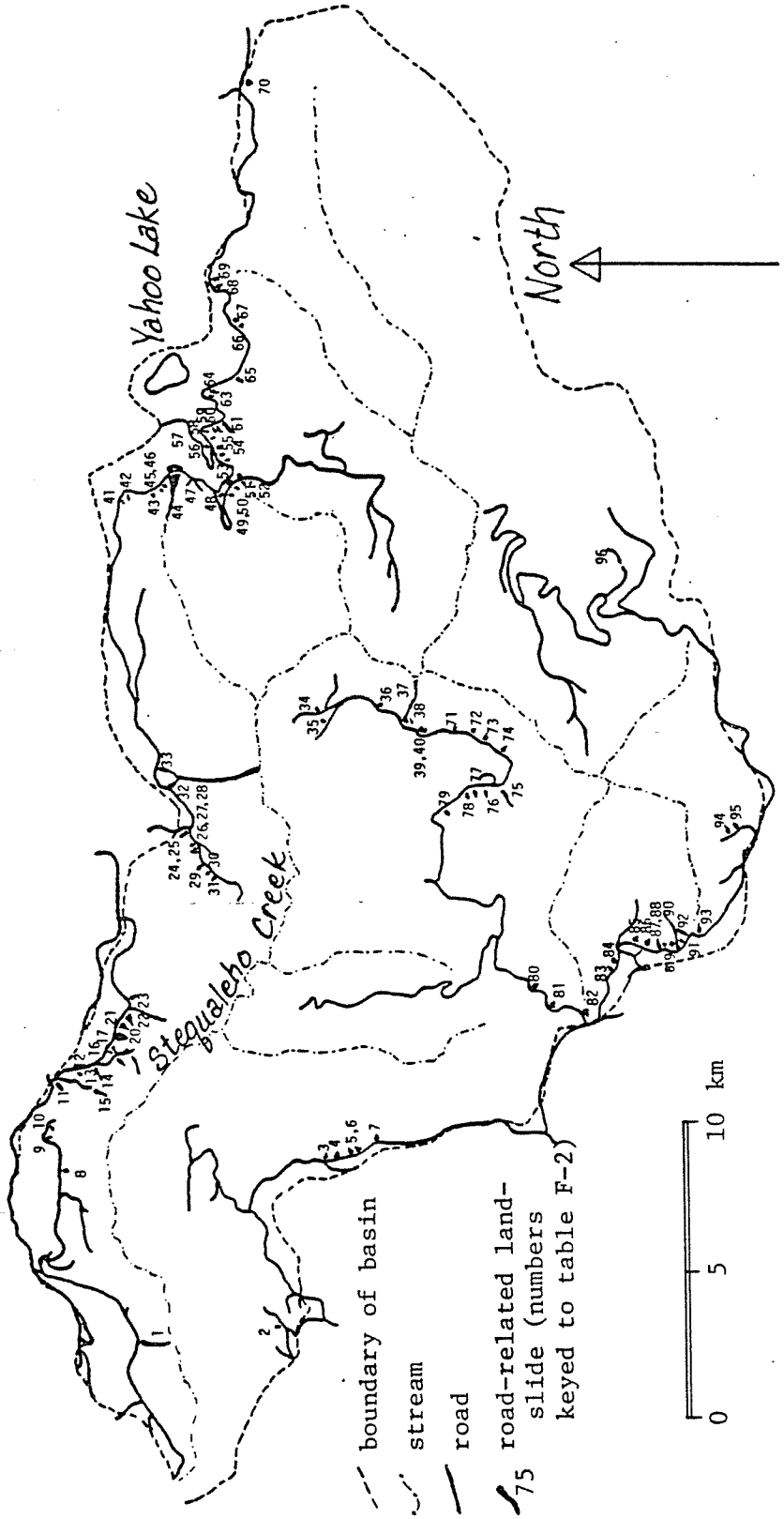

Figure F-2. Road-related landslides of Stequaleho Creek basin.

Table F-3. Rills on road-related landslide scars, Christmas basin (for landslide locations see Appendix Figure F-1).

Slide	Slide area (m^2)	Number of rills			Volume of rills (m^3)	
		None	Non-road*	Road**	Non-road*	Road**
1	260	x				
2	220	x				
3	260	x				
4	2,420	x				
5	590		2	2	1.9	2.0
6	700	x				
7	150	x				
8	100	x				
9	280	x				
10	650		1	3	.4	2.5
11	320	x				
12	250			1		.5
13	38			1		.1
14	200	x				
15a	300			1		.8
15b	660			2		1.8
16	73			1		.9
17	96			3		3.5
20a	390	x				
20b	240	x				
20c	140		1	2	.4	2.0
20d	60		1		1.0	
20e	160	x				
21a	26			2		.3
21b	9	x				
21c	9	x				
21d	14	x				
22	570			1		2.0
35	76			1		.9

Table F-3. Rills on road-related landslide scars, Christmas basin (for landslide locations see Appendix Figure F-1) - continued.

Slide	Slide area (m^2)	Number of rills			Volume of rills (m^3)	
		None	Non-road*	Road**	Non-road*	Road**
36	350	x				
37	540	x				
38a	510			2		8.4
38b	35			1		.8
39a	30			1		.4
39b	45	x				
42	100	x				
43	49	x				
44a	65	x				
44b	16	x				
45	360	x				
46	170			1		5.0
63a	40	x				
63b	330		1	1	.8	.4
64	300	x				
65a	640	x				
65b	24			1		.6
66	400		2	1	2.4	7.5
67	12	x				
68a	110			1		4.5
68b	180	x				
69	810		3	1	6.1	6.5
70	400			6		20.6
71	150	x				
73a	360	x				
73b	720		4		9.9	
55	16,020	31	15	36	22.9	72.0

*Non-road - Rill does not originate at point of entry of road-surface drainage onto landslide scar.

**Road - Road-surface drainage feeds directly into head of rill.

Table F-4. Debris flows in Christmas and Stequaleho basins.

Basin	Debris flow	Slide	First year shown	Channel gradient (degrees)	Flow length (m)	Flow track wall width (m)	Area affected (m^2)	Volume of sediment removed (m^3)
Christmas	T1	4	1977	15	48	7.0	520	91
	T2	15a	1975	20	95	3.5	520	91
	T3	18	1977	27	48	5.9	440	77
	T4	51,52	1975	19	84	8.2	1,070	190
	T5	60	1975	26	95	5.9	870	150
	T6	61	1971	25	60	16.6	1,550	270
	T7	64	1971	27	48	3.5	260	46
	T8	65	1971	23	89	5.9	820	140
	T9	69	1971	23	24	5.9	220	39
Stequaleho	T1	1	1971	29	110	2.3	390	68
	T2	11	1971	29	36	7.1	400	450
	T3	13	1971	33	66	3.5	360	63
	T4	16,17,18	1971	28	200	2.3	730	130
	T5	19	1975	28	96	4.7	700	120
	T6	20	1971	25	130	2.3	470	83
	T7	22	1971	28	120	2.3	430	75
	T8	24	1971	26	160	4.7	1,140	200
	T9	25,26, 27,28	1971	27	130	2.3	450	79
	T10	32	1971	22	500	9.5	7,460	1,310
	T11	33	1971	23	130	4.7	960	170
	T12	37	1975	23	260	7.1	2,920	510
	T13	44	1971	25	310	9.5	4,630	810
	T14	61	1977	29	38	9.5	560	98
	T15	75	1975	35	90	1.1	150	27
	T16	88	1971	27	180	5.9	1,650	290
	T17	90	1971	31	180	4.7	1,320	230
	T18	91	1971	33	42	4.7	310	54
	T19	92	1971	28	60	2.3	220	38
	T20	96	1977	29	72	3.5	390	69

APPENDIX G. CALCULATED SEDIMENT PRODUCTION FROM ROAD-RELATED SOURCES

Table G-1. Calculated sediment production from road-related sources in Christmas basin during selected years (values in metric tons; totals subject to rounding error).

Source	1967	1971	1975	1977
Landslides*	96	1,140	1,640	1,730
Debris flows	9	110	160	170
Gullies	1	9	13	14
Sidecast erosion	2	21	31	32
Secondary erosion	7	85	120	130
Rills	2	23	33	35
Backcut erosion**	(3)	(40)	(57)	(60)
Road surface and backcut				
Heavy use	-	530	710	320
Temporary non-use	-	76	100	46
Moderate use	-	56	-	-
Light use	-	18	28	26
Non-use	1	7	12	13
	120	2,070	2,850	2,510

*Shallow disturbances of indeterminate origin are included in landslide value.

**Backcut contribution is included with road-surface production but is listed separately for purposes of comparison.

Table G-2. Calculated sediment production from road-related sources in Stequaleho basin (values in metric tons; totals subject to rounding error).

Source	1964	1965	1966	1967	1968	1969	1970	1971	1972	1973	1974	1975	1976	1977
Landslides	55	200	560	840	890	1,060	1,350	1,630	2,070	2,370	2,550	2,880	3,200	3,680
Debris flow	12	41	120	180	190	220	280	340	430	500	540	600	670	770
Gullies	1	2	5	7	8	9	11	14	18	20	22	24	27	31
Sidecast erosion	1	3	10	15	15	18	23	28	36	41	44	50	55	64
Secondary erosion	4	14	40	61	64	77	98	120	150	170	180	210	230	270
Rills	1	4	12	18	19	23	29	36	45	52	56	63	70	80
Backcuts***	(1)	(4)	(11)	(17)	(18)	(22)	(28)	(34)	(43)	(49)	(53)	(59)	(66)	(76)
Road surface and backcut														
Heavy use	86	160	400	250	48	-	-	1,640	820	340	-	800	-	750
Temporary non-use	12	22	58	37	7	-	-	240	120	50	-	120	-	110
Moderate use	4	13	53	1	1	69	69	69	110	6	100	100	59	59
Light use	4	10	25	24	15	23	20	35	72	95	51	43	65	77
Paved	-	-	-	-	-	-	-	-	-	-	-	-	6	6
Non-use	-	-	tr	2	3	3	5	2	2	5	8	9	9	8
	180	470	1,280	1,440	1,260	1,500	1,880	4,150	3,870	3,650	3,550	4,900	4,390	5,900

*Values for all years but 1977 are calculated using average road lengths present during the year (the road lengths present at the beginning and end of the year are averaged). Measurements were made during the summer of 1977, so the length of road present at that time was used in sediment production calculations for the 1977 year.

**Shallow disturbances of indeterminate origin are included in landslide value.

***Backcut contribution is included with road-surface sediment production but is listed separately to allow comparison.

Table G-3. Calculated production of fine-grained sediment from road-related sources in Christmas basin during selected years (values in metric tons; totals subject to rounding error).

Source	1967	1971	1975	1977
Landslides*	27	320	460	480
Debris flows	3	31	45	47
Gullies	tr	3	4	4
Sidecast erosion	2	21	31	32
Secondary erosion	7	85	120	130
Rills	2	23	33	35
Backcut erosion**	(3)	(40)	(57)	(60)
Road surface and backcut				
Heavy use	-	530	710	320
Temporary non-use	-	76	100	46
Moderate use	-	56	-	-
Light use	-	18	28	26
Non-use	1	7	12	13
	41	1,170	1,540	1,130

*Shallow disturbances of indeterminate origin are included in landslide value.

**Backcut contribution is included with road-surface production but is listed separately to allow comparison.

Table G-4. Calculated production of fine-grained sediment from road-related sources in Stequaleho basin (values in metric tons; totals subject to rounding error).

Source	1964	1965	1966	1967	1968	1969	1970	1971	1972	1973	1974	1975	1976	1977*
Landslides**	14	48	140	210	220	260	330	400	510	580	620	700	780	900
Debris flows	3	10	28	43	46	54	69	84	110	120	130	150	160	190
Gullies	tr	1	1	2	2	2	3	3	4	5	5	6	7	8
Sidecast erosion	1	3	10	15	15	18	23	28	36	41	44	50	55	64
Secondary erosion	4	14	40	61	64	77	98	120	150	170	180	210	230	270
Rills	1	4	12	18	19	23	29	36	45	52	56	63	70	80
Backcuts***	(1)	(4)	(11)	(17)	(18)	(22)	(28)	(34)	(43)	(49)	(53)	(59)	(66)	(76)
Road surface and backcut														
Heavy use	86	160	400	250	48	-	-	1,640	820	340	-	800	-	750
Temporary non-use	12	22	58	37	7	-	-	240	120	50	-	120	-	110
Moderate use	4	13	53	1	1	69	69	69	110	6	100	100	59	59
Light use	4	10	25	24	15	23	20	35	72	95	51	43	65	77
Paved	-	-	-	-	-	-	-	-	-	-	-	-	6	6
Non-use	-	-	tr	2	3	3	5	2	2	5	8	9	9	8
	130	280	770	660	440	530	650	2,660	1,980	1,460	1,190	2,250	1,440	2,520

*Values for all years but 1977 are calculated using average road lengths present during the year (the road lengths present at the beginning and end of the year are averaged). Measurements were made during the summer of 1977, so the length of road present at that time was used in sediment production calculations for the 1977 year.

**Shallow disturbances of indeterminate origin are included in landslide value.

***Backcut contribution is included with road-surface production but is listed separately to allow comparison.

APPENDIX H. SEDIMENT PRODUCTION IN UNDISTURBED BASINS

Table H-1. Treefalls mapped along undisturbed channels (for descriptions of basins see Table 25).

Basin	Channel order	Length of channel mapped (km)	Number of treefalls	Number of treefalls in channel	Number of falls adjacent to channel
Nick	1	1.35	31	10	12
	2	.46	22	4	9
	3	.37	8	1	6
Creak I	1	1.12	61	12	19
	2	.57	5	0	2
	3	.15	11	1	3
Palm	1	1.35	75	20	24
	2	.49	16	0	8
	3	.21	7	0	6
Arm	4	.27	29	2	12
Creak II	1	.03*	6	3	2
	4	.20	12	0	6
Verti	1	.85	13	0	0
	2	.22	4	0	2
Vertitoo I	2	.09	3	1	0
Vertitoo II	3	.24	4	0	2
	4	.44	8	2	3
Tree	1	.15*	6	2	3
	2	.45*	26	1	7
	3	.21*	9	0	5
		9.22	356	59	131

*Treefalls were not mapped along part of the channel length included in Table 25.

Table H-2. Mapped landslides in undisturbed basins (for descriptions of basins see Table 25).

Basin	Slide	Stream order	Slide volume (m^3)	Age (yrs)	Dating method*	Site type*	Volume of sediment in storage (m^3)*
Blacktarp	A	1	80	19	h	d	s
Green	A	1	10	20	h	d	21
	B	2	8	20	h	v	s
	C	2	200	14-68	h,h	v	34
	D	2	21	14-30	a,c	v,f,uc	-
	E	2	3	14-30	a,c	v,f,uc	-
	F	2	10	17	h	uc	s
	G	2	160	30	h	v	?
Collapse	C	1	22	30-70	l	v,uc	s
	D	1	24	5-15	c,e	v,uc	s
	E	2	9	5-10	c,e	uc	-
	F	2	18	5	nv	uc	-
	G	2	15	5	nv	uc	-
	G'	2	11	5	nv	v,t,f	-
	H	2	16	5-20	c,e	v	?
	I	1	98	10-80	f,c	d	25
	J	1	56	80	l	d	s
	K	2	10	10-30	c,e	v,uc,f	-
Nick	A	2	20	3	f	d	5
	B	1	16	2-5	l,f	d,t	tr
	C	1	15	2-5	f	v	s
	D	1	4	5	c,nv	v,uc	s
	E	1	.7	5	m,c	uc,v	-
	F	1	.7	5	m,c	uc,v	-
	G	1	20	2-5	f	d	5
	H	3	2.5	5	f	uc,v	.3
	H'	3	5	10	f	uc,t,sl,v	2
	I	1	16	117	h	uc,v	tr
	I'	1	1.6	5	c	v,uc	-

Table H-2. Mapped landslides in undisturbed basins (for descriptions of basins see Table 25) - continued.

Basin	Slide	Stream order	Slide volume (m^3)	Age (yrs)	Dating method*	Site type*	Volume of sediment in storage (m^3)*
	J	1	2.2	5	c	v,uc	tr
	K	1	5	5	c	v,uc	s
	L	2	.9	3	f	v,uc	s
	M	2	89	122	h	d	22
Nick	N	1	1.2	?	-	v	s
	O	1	6	5	f	v,s,uc	s
	P	1	1.2	5	c	v,s,uc	s
	Q	1	1.2	5	c	uc	-
	R	1	3.7	5	f	v,s,uc	s
	S	2	10	2-5	f	v,uc	s
Palm	A	2	55	14	h	d	18
	B	2	22	9	sf	v,t,uc	14
	C	1	60	32	h	v	27
	D	2	24	13	h	d	3-6
	E	3	4	5-12	sb,c	v,t	3
	F	1	3.5	?	-	v,s	s
	H	1	4.2	5	f	v,uc	s
	I	2	2	?	-	v	?
	J	2	5	?	-	v	?
	K	1	2	?	-	v,uc	?
	M	2	2	?	-	v	?
Creak	A	1	40	10-30	f,e	v,s	26
Creak II	A	4	1.5	8	t	v	s
	B	4	8	5-20	c,e	v,uc	s
Arm	A	4	25	25	h	v,uc,t	8
	B	4	9	25-50	c,e	v,uc	-
	C	4	9	12	sf	v,t	6
	D	4	9	7	t	v,uc	s

Table H-2. Mapped landslides in undisturbed basins (for descriptions of basins see Table 25) - continued.

Basin	Slide	Stream order	Slide volume (m^3)	Age (yrs)	Dating method*	Site type*	Volume of sediment in storage (m^3)*
Verti	C	1	.2	5	t	v	-
	D	1	5	7	d	c	s
	E	1	1.2	5	f,c	v,uc	-
	F	1	3.3	16	h	v	?
Vertitoo I	A	3	41	5-15	f,e	d,t	?
Vertitoo II	A	4	36	62	h	v,uc	?
	B	4	24	8	t	v,uc	s
	C	4	10	5	t	v	7
	D	4	130	30-70	l	v,cu,t	s
	E	4	10	19	c	v	?
Vertitoo II	F	4	12	19	ald	v,uc	-
Tree	A	2	9	5	e	v,uc	-
	B	3	13	10	sf	v,t	s
	C	3	26	30-50	l	v,t	s
	D	3	5.4	?	-	v,uc	?
	E	3	2.5	2	c	v,t	?
	F	3	1.8	2	c	v	?
	G	3	12	2	l	v,t	s
	H	3	1.5	5	c	v,uc	?
	I	2	3.6	3	f	v,uc	?
	J	2	.5	?	-	v,uc	s
	K	2	6	6	h	v,uc	?
	L	2	10	4	l,f	v,uc	?
	M	2	3	5	c	v,uc	?
	N	2	41	5-15	c,e	v,uc	?

*Symbols:
Dating method; a
ald - alder
c - comparison
e - estimate

Table H-2. Mapped landslides in undisturbed basins (for descriptions of basins see Table 25) - continued.

*Symbols:

Dating method; - continued
- f - fern
- h - hemlock
- l - log
- m - moss
- nv - no vegetation
- sb - salmonberry
- sf - shelf fungus
- t - tree associated

Site type;
- d - drainage depression
- s - slump
- t - treefall
- uc - undercut
- v - valley wall

Storage;
- s - sediment present, volume unknown.

Table H-3. Area undergoing bank erosion along streams of various orders (for description of basins see Table 25).

Basin	Order	Tributary	Length (km)	Area of wall erosion[1] (m^3)	Area of terrace erosion[2] (m^3)	Indeterminate; terrace or wall erosion[3] (m^3)	Indeterminate; wall, terrace, or floodplain erosion[4] (m^3)	Area (m^2) / km
Arm	4	A	.32	-	-	36.6	15.8	140
Creak II	4	A	.20	-	-	36.0	-	180
Nick	3	A	.28	39.2	8.9	17.8	21.2	280
	2	A	.16	21.4	-	1.5	1.5	140
	2	B	.18	19.0	-	1.2	6.5	130
	1	A	.08	3.3	-	-	-	40
	1	C	.08	42.8	-	-	-	500
	1	D	.06	-	-	-	-	0
	1	E	.14	28.4	-	.7	.2	210
	1	M	.09	4.9	-	-	-	52
	1	O	.06	4.0	-	-	-	62
	1	N	.05	-	-	-	-	0
	1	S	.12	18.0	-	-	1.0	150
	1	P	.02	-	-	-	-	0
	1	T	.06	3.6	-	-	2.0	73
	1	V	.03	1.2	-	-	-	37

[1]Sediment is produced directly from the soil mantle of the valley wall.
[2]Sediment is produced from erosion of glacio-fluvial terraces.
[3]Source not distinguished, but since sediment is derived either from valley wall or glacio-fluvial terrace, total value is considered in calculations.
[4]Source not distinguished. Sediment may have been derived from floodplains or other secondary sources, so half of total is considered in calculations.

Table H-4. Mountain beaver burrows adjacent to streams in undisturbed, forested basins (for descriptions of basins see Table 25).

Basin	Area (ha)	Channel length (km)	Number of burrows	Number of cones in channel	Number of drain holes	Measured volumes of cones (m^3)
Nick	16	2.18	27	0	5	.016 .21 .056 .108 .17 .088
Creak I	12	1.84	21	1	6	.48 .048
Palm	17	2.05	39	5	7	.14 .09 .09 .09 .09 .16 .17
Arm	2	.27	0	0	0	
Creak II	5	.67	68	8	1	
Verti	8	1.07	3	1	0	
Vertitoo I	2	.33	0	0	0	
Vertitoo II	2	.44	0	0	0	
Tree	10	.88	76	13	4	
		9.73	234	28	23	